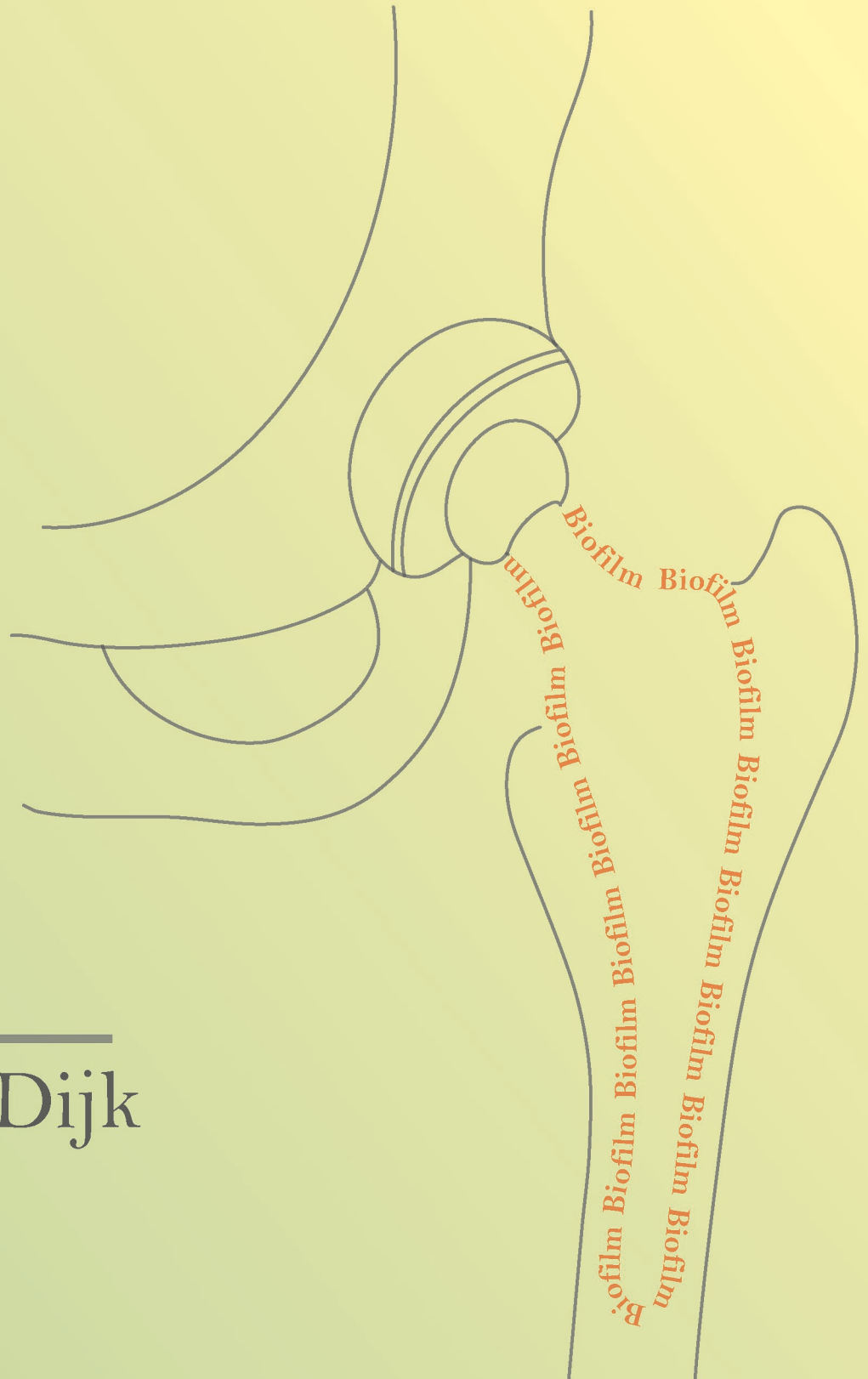


Periprosthetic joint infection

Development of new therapies



Bruce van Dijk



Periprosthetic joint infections

Development of new therapies

Bruce van Dijk



Periprosthetic joint infections; Development of new therapies

Colofon

ISBN: 978-90-393-7705-5
Author: Bruce van Dijk
Cover design: Bruce van Dijk
Layout: Bruce van Dijk
Printing: 24drukwerk

© 2024, Bruce van Dijk. All rights reserved. No part of this book may be reproduced or transmitted in any form or by any means, without permission of the author.

The research and publication of this thesis was supported by:
Health Holland, financed by the Netherlands Organization for Scientific Research (NWO)



Periprosthetic joint infections

Development of new therapies

Prothese infecties

Ontwikkeling van nieuwe behandelopties

(met een samenvatting in het Nederlands)

Proefschrift

ter verkrijging van de graad van doctor aan de
Universiteit Utrecht
op gezag van de
rector magnificus, prof. dr. H.R.B.M. Kummeling,
ingevolge het besluit van het College voor Promoties
in het openbaar te verdedigen op

woensdag 26 juni 2024 des middags te 4.15 uur

door

Bruce van Dijk

geboren op 6 oktober 1986
te Soest



Promotoren:

Prof. dr. ir. H. Weinans
Prof. dr. S.H.M. Rooijackers

Copromotoren:

Dr. B.C.H. van der Wal
Dr. H.C. Vogely

Beoordelingscommissie:

Prof. dr. M.G.J. de Boer
Prof. dr. L.C. Heyligers
Prof. dr. P.A. de Jong (voorzitter)
Prof. dr. J.A.J.W. Kluijtmans
Prof. dr. J.J. Verlaan



Table of Contents

Chapter 1.	General introduction and outline of this thesis	8
Current treatment of periprosthetic joint infection		
Chapter 2.	One-year infection control rates of a DAIR (debridement, antibiotics and implant retention) procedure after primary and prosthetic-joint-infection-related revision arthroplasty - a retrospective cohort study	20
Chapter 3.	A mean 4-year evaluation of infection control rates of hip and knee prosthetic joint infection-related revision arthroplasty: an observational study	32
Visualizing <i>Staphylococcus aureus</i> biofilm in vivo		
Chapter 4.	Human monoclonal antibodies against <i>Staphylococcus aureus</i> surface antigens recognize in vitro and in vivo biofilm	50
Chapter 5.	Evaluating the targeting of <i>Staphylococcus aureus</i> -infected implant with a radiolabeled antibody as a prelude to radioimmunotherapy of infection in mice	90
Alternative treatment options for implant infections		
Chapter 6.	Treating infections with ionizing radiation: a historical perspective and emerging techniques	104
Chapter 7.	Radioimmunotherapy of methicillin-resistant <i>Staphylococcus aureus</i> in planktonic state and biofilms	124
Chapter 8.	Photoimmunotherapy of <i>Staphylococcus aureus</i> implant infection in mice	136
Chapter 9.	General discussion and Future Perspectives	148
Appendices	Dutch summary/Nederlandse Samenvatting	158
	List of Publications	
	List of Abbreviations and Definitions	
	Acknowledgement	
	Curriculum Vitae	



General introduction and outline of this thesis



General Introduction

Implants and infections

Human enhancement in the form of implants have been around for centuries and can improve quality of life greatly. A prime example are orthopedic implants that replace joints such as those of hip or knee. The post-surgical satisfaction is high as these implants reduce pain and improve function^{1,2}. Unfortunately, as with any foreign body, there is a chance of an infection where bacteria can colonize the implant with potentially disastrous consequences. Periprosthetic joint infection (PJI) is such a devastating complication after primary joint arthroplasty with an incidence ranging from 1% to 2.5%^{3,4}. The incidence of PJI after revision arthroplasty is even much higher and can reach up to 6-16%⁵. In 2019, an estimated total of around 60.000 total hip- and knee arthroplasties were performed in the Netherlands⁶. In the United States of America, there were approximately 1,5 million hip and knee procedures and the predicted total annual count is increasing to 2,8 million in 2030 and 4,8 million in 2040^{7,8}. On top of that, the increased expected lifespan puts more patients at risk of late PJI⁹, as well as a higher chance of a revision procedure.

Staphylococcus aureus and their biofilm

The most common bacteria that causes healthcare infections is *Staphylococcus aureus*.^{10,11} *S. aureus* is responsible for high morbidity and mortality, especially after medical procedures involving prosthetic implants such as that of the hip and knee. The bacteria sustain itself by colonizing the implant and reproduce. In this process a biofilm is formed on the prosthetic material and is made of extracellular polymeric substance consisting of polysaccharides, proteins and extracellular DNA.^{12,13} This biofilm hinders the host immune system and is a barrier for many antimicrobial agents.^{12,14} Bacteria in a biofilm have different gene expression and are therefore phenotypically different when compared to free-floating bacteria.¹⁵ In addition, bacteria in a biofilm are mostly in a metabolically inactive (dormant) state and therefore not susceptible to most antibiotics.¹⁶ Bacteria can also penetrate in the bone tissue and hide in a dormant state within the canalicular network. Dormant bacteria can remain on an implant surface or in the bone tissue for several years before they can become active again and cause an (re)infection resulting in failure of the prosthesis. On top of that, these bacteria potentially increase antibiotic resistance even further in the case they were treated with antibiotics in the past. Due to the reduced accessibility and decreased susceptibility to the antibiotics, treatment can be complicated (Figure 1) and even after ‘successful’ treatment an infection might re-occur even after many years.



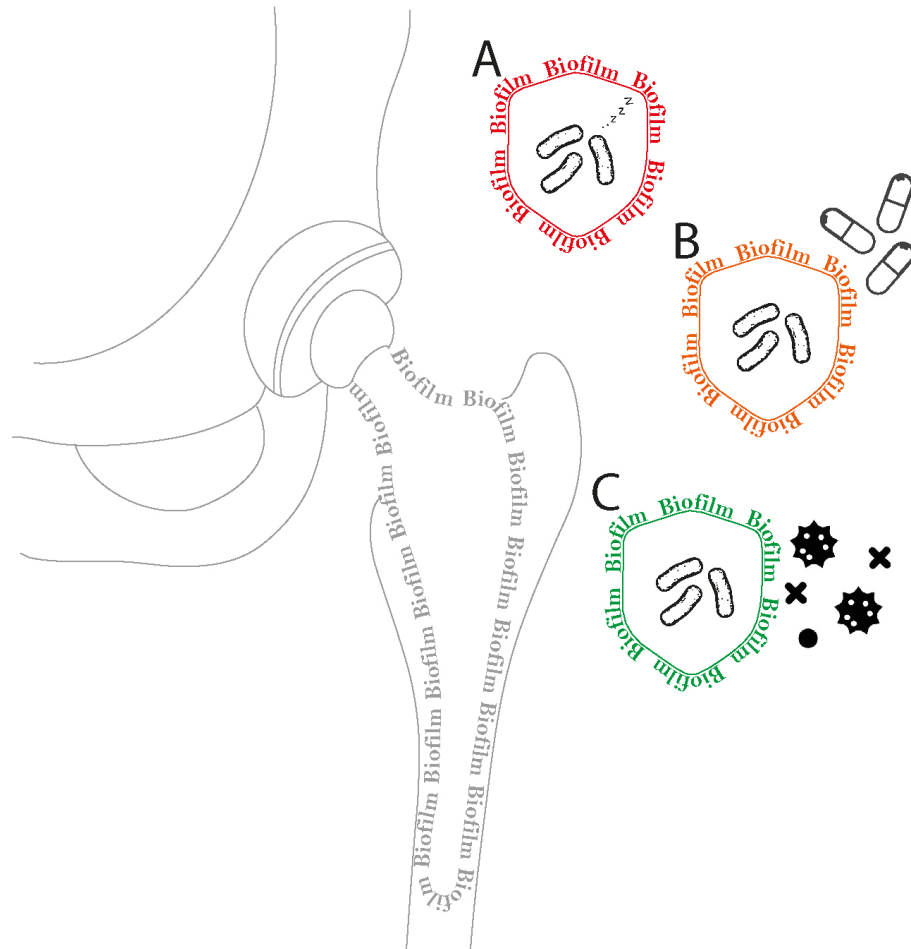


Figure 1. Chronic periprosthetic joint infection with a biofilm on the prosthesis complicating treatment due to e.g. (A) dormant bacteria, (B) antibiotic resistance and (C) barrier for immune cells and antibiotics.

Classification and Current treatment of PJI

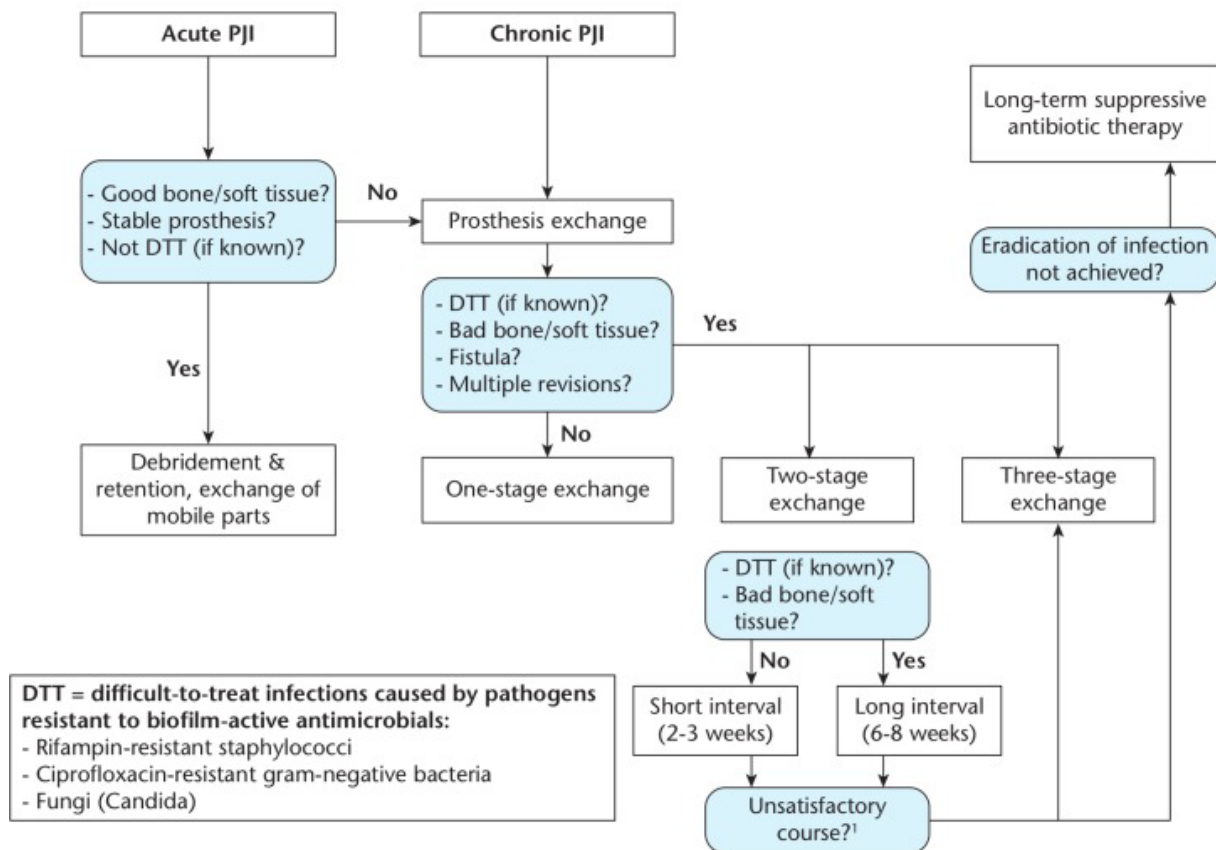
There are multiple classifications for PJI such as described by Cierny¹⁷, McPherson¹⁸, Tsukayama,¹⁹ or Zimmerli²⁰ where time of onset plays an important role²¹. When we only take time as a factor, PJI can be categorized in early (e.g. <3 months), delayed (e.g. 3-24 months) or late onset (e.g. >24 months) as we do in the UMC Utrecht. However, there is no consensus about the length of each category as the infection occurs as a continuum over time. Therefore a clear time-dependent cut-off for 'early', 'delayed' or 'late' cannot be defined²². The route of infection however is different as early and delayed onset PJI are associated with bacterial contamination during surgery when the prosthesis is implanted, whereas late hematogenous infection is considered secondary to e.g. dental, respiratory tract, skin, or urinary tract infections²⁰, where bacteria traveled via the blood to the implant and surrounding tissue causing an infection.

The treatment of choice in acute PJI or an acute-onset late hematogenous infection, is one or two debridement, antibiotics and implant retention (DAIR) procedures. In this procedure the joint and surrounding tissue is meticulously cleaned/debrided. The mobile parts are removed to clean hard to reach places e.g., behind a hip implant or in small gaps between implant parts, after which these parts are replaced (figure 3). Treatment of chronic PJI (Figure 2) often involves revision of the implant in a one- or two stages combined with long-term use of antibiotics. In a one-stage revision procedure (Figure 3), the infected implant is removed after



which the joint space is debrided and irrigated, followed by reimplantation of a new (revision) hip or knee prosthesis during the same procedure. In a two-stage revision procedure (Figure 4), revision of the final prosthesis is done in two separate surgical interventions. In the first stage the implant is removed, subsequently the infected area is debrided and irrigated and a local antibiotic carrier such as an antibiotic-loaded spacer can be implanted. Such a spacer consists of an implant made of antibiotic-impregnated/antibiotic-eluting bone cement that slowly releases antibiotics to the surrounding tissue for a period of 2 to 8 weeks, enabling high local concentrations of antimicrobial agents^{23,24}. Subsequently a second procedure is performed where the antibiotic-loaded spacer is removed before implantation of the final hip- or knee prosthesis.

TREATMENT ALGORITHM



¹ Clinical signs of infection, elevated CRP, intra-operative pus, compromised tissue

Figure 2. Treatment algorithm for PJI. Image from: Izakovicova P, Borens O, Trampuz A. Periprosthetic joint infection: current concepts and outlook. *EFORT Open Rev.* 2019 Jul 29;4(7):482-494 published with permission of first author.



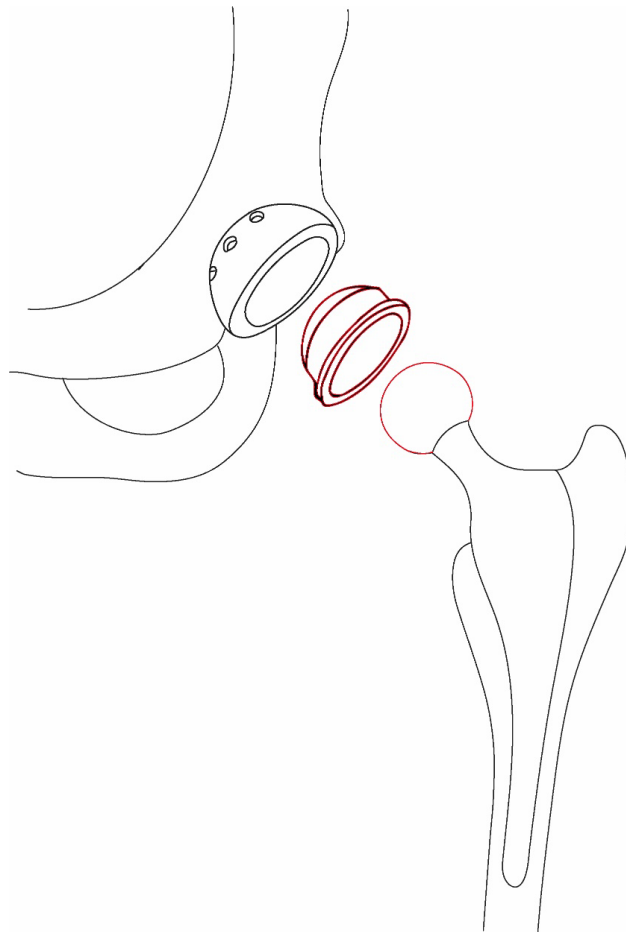


Figure 3. The parts of a hip prosthesis are 1. femoral stem, 2. femoral head, 3. liner, 4. acetabular cup. The mobile parts that are replaced during a DAIR procedure to treat a periprosthetic hip joint infection are the femoral head and liner (in red).

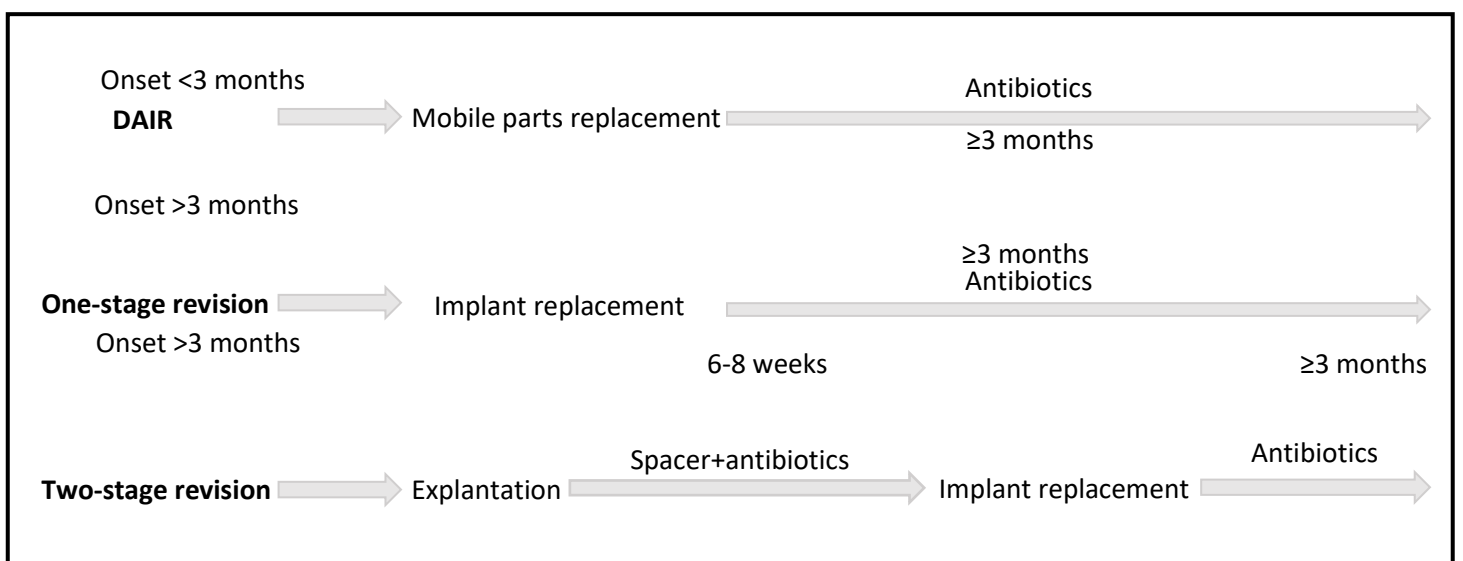


Figure 4. Comparison of DAIR, one- and two stage revision surgery for periprosthetic joint infections of the hip and knee in the UMCU.



Patient population

Outcomes of PJI treatment are still unpredictable despite intensive treatment with prolonged antibiotics often combined with multiple invasive debridement and irrigation surgeries with- or without implant exchange. On top of that, the (often) elderly PJI population usually has multiple comorbidities. The mortality after one year in patient with PJI range from 2.6-10.6%^{25,26} with an average of around 4%^{25,27} and increases to around 21%^{25,27} after 5 years. After two-stage revision surgery for chronic periprosthetic hip and knee infection the 5 year overall mortality rate was 40.72%²⁸ and 33.05%²⁹ respectively. The 5-year mortality rate of PJI even exceed that of most forms of melanoma, breast- and prostate cancer³⁰. Even more worrisome, the 10-year mortality rate is higher than the combined 10-year mortality rate for all cancers in the United States of America (44% versus 39%)²⁷. In this regard, PJI patients are not dissimilar to oncology patients, with comparably high morbidity- and mortality rates. As a matter of course, the absolute number of patients that are deceased as a result of PJI is much lower than that of cancer as it is a leading cause of death worldwide, accounting for nearly 10 million deaths in 2020³¹. Other similarities between patient with PJI and cancer is that there are cells that grow uncontrollably and spread to other parts of the body and to be eradicated in order to cure the patients. This raises the question if PJI patients could benefit from certain therapies that are used in oncology.

Alternative treatment options

Over a century ago, Paul Ehrlich described a theory in which a ‘Zauberkegel’ or ‘magic bullet’ could selectively kill pathogens or cells without harming healthy tissue³². Technology advanced tremendously over the years and the possibilities seem endless. For example, Ehrlich’s magic bullets could nowadays refer to monoclonal antibodies (mAb) that target specific cells and can act either as a treatment by directly activating the immune system or they can be used as a vehicle to bring other molecules such as radionuclides, photosensitizers or enzymes. to a target. In oncology, radioimmunotherapy and photoimmunotherapy is currently introduced to treat multiple types of cancer such as leukemias, lymphomas, and head- and neck tumours³³⁻³⁵. The same strategies could potentially be used to treat PJI as well, especially in patients with PJI that have no other treatment options left, e.g. with long-term chronic biofilm, and/or antibiotic resistance.

In radioimmunotherapy, antibodies are conjugated to radionuclides that emit ionizing radiation³⁴. The radioantibody is intravenously injected and is directed towards the target as it specifically binds to the target cells or tissue. The target cell is destroyed by the ionizing radiation as this directly breaks down the DNA structure. Due to the relative short penetration depth of specific radionuclides, they are capable of destroying the target cells while causing very limited damage to the surrounding (non-targeted) healthy tissue. Obviously, this requires very specific binding of the antibody to the target tissue.

Photoimmunotherapy is when antibodies are conjugated to photosensitizers. Photosensitizers are light-activated non-toxic dyes that release large amount of reactive oxygen species (ROS) when illuminated using near infrared light. ROS can kill pathogens directly by causing oxidative damage to DNA and specific bacteria such as *S. aureus* are very sensitive to ROS. The same process of oxidative damage is also used by different cells of the immune system such as phagocytes as a deadly weapon against bacterial cells.

In theory, implant infections such as PJI could be treated with antibodies alone that target *S. aureus* to eliminate bacteria directly by signaling or flag bacterial cells and help the immune system to eliminate the bacteria. However, bacteria in a biofilm are protected by a physical



layer, therefore signaling alone is probably not sufficient and additional (potential) antibacterial molecules need to be coupled to the antibodies. For example, radioimmunotherapy or photoimmuno-antibacterial therapy in combination with antibiotics could be a powerful combination in the treatment of PJI.

Outline of the thesis

The focus of this thesis is to explore alternative (immune-based) therapies to treat *S. aureus* implant infections and specifically PJIs. First the patient population is identified who could benefit from new therapies by investigating the success rate of current treatment of acute (**see chapter 2**) and chronic (**see chapter 3**) PJI. Second, immunotherapy starts with selecting an antibody that is specific to *S. aureus in vitro* and *in vivo*. A subcutaneous implant infection mouse model is used to visualize and quantify the antibodies specificity for *S. aureus* biofilm using SPECT-CT (**see chapter 4**). Another important issue is the biodistribution of the antibody (**see chapter 5**). It is not only important to be specific, but non-specific binding or accumulation in other host tissues could in fact be dangerous when treating patients with potential harmful molecules

such as radionuclides that are potential bactericidal but can also harm healthy tissue. To use ionizing radiation, one must learn from the mistakes made in history, e.g. high doses, non-specific targeting, type of radiation etcetera. Therefore, an extensive systematic review (**see chapter 6**) is conducted when treating infections with ionizing radiation. In vitro studies (**see chapter 7**) must be conducted to validate which potential radionuclides are suitable for infection treatment before transferring these too *in vivo* experiments and the clinic. Finally, photosensitizers are proven safe when not activated, but lethal to cancers cells when activated. Therefore, the potential bactericidal effect of photo-immunotherapy for eradication biofilm is studied *in vitro* and *in vivo* (**see chapter 8**).



REFERENCES

1. Bourne RB, Chesworth BM, Davis AM, Mahomed NN, Charron KDJ. Patient satisfaction after total knee arthroplasty: Who is satisfied and who is not? *Clin Orthop Relat Res*. 2010;468(1):57-63.
2. Mancuso CA, Salvati EA, Johanson NA, Peterson MGE, Charlson ME. Patients' expectations and satisfaction with total hip arthroplasty. *J Arthroplasty*. 1997;12(4):387-396.
3. Izakovicova P, Borens O, Trampuz A. Periprosthetic joint infection: current concepts and outlook. *EFORT open Rev*. 2019;4(7):482-494.
4. Kurtz SM, Lau E, Watson H, Schmier JK, Parvizi J. Economic burden of periprosthetic joint infection in the United States. *J Arthroplasty*. 2012;27(8 Suppl 1):61-5.e1.
5. Goud AL, Harlianto NI, Ezzafzafi S, Veltman ES, Bekkers JEJ, van der Wal BCH. Reinfection rates after one- and two-stage revision surgery for hip and knee arthroplasty: a systematic review and meta-analysis. *Arch Orthop Trauma Surg*. 2021;143(2):829-838.
6. Dutch Arthroplasty Register (LROI). Online LROI annual report 2019. Lroi. 2019;(June):57-62. <https://www.lroi-rapportage.nl/>
7. American Joint Replacement Registry (AJRR): 2021 Annual Report. Rosemont, IL: American Academy of Orthopaedic Surgeons (AAOS), 2021.
8. Singh JA, Yu S, Chen L, Cleveland JD. Rates of total joint replacement in the United States: Future projections to 2020-2040 using the national inpatient sample. *J Rheumatol*. 2019;46(9):1134-1140.
9. Huotari K, Peltola M, Jamsen E. The incidence of late prosthetic joint infections: a registry-based study of 112,708 primary hip and knee replacements. *Acta Orthop*. 2015;86(3):321-325.
10. Lowy FD. Medical progress: Staphylococcus aureus infections. *N Engl J Med*. 1998;339(8):520-532.
11. Tong SYC, Davis JS, Eichenberger E, Holland TL, Fowler VG. Staphylococcus aureus infections: Epidemiology, pathophysiology, clinical manifestations, and management. *Clin Microbiol Rev*. 2015;28(3):603-661.
12. Otto M. Staphylococcal Biofilms. *Microbiol Spectr*. 2018;6(4).
13. Miller RJ, Crosby HA, Schilcher K, Wang Y, Ortines RV, Mazhar M, Dikeman DA, Pinsker BL, Brown ID, Joyce DP, Zhang J, Archer NK, Liu H, Alphonse MP, Czupryna J, Anderson WR, Bernthal NM, Fortuno-Miranda L, Bulte JWM, Francis KP, Horswill AR, Miller LS. Development of a Staphylococcus aureus reporter strain with click beetle red luciferase for enhanced in vivo imaging of experimental bacteremia and mixed infections. *Sci Rep*. 2019 Nov 13;9(1):16663.
14. de Vor L, Rooijackers SHM, van Strijp JAG. Staphylococci evade the innate immune response by disarming neutrophils and forming biofilms. *FEBS Lett*. Published online 2020.
15. Beenken KE, Dunman PM, McAleese F, Macapagal D, Murphy E, Projan SJ, Blevins JS, Smeltzer MS. Global gene expression in Staphylococcus aureus biofilms. *J Bacteriol*. 2004 Jul;186(14):4665-84.
16. Resch A, Rosenstein R, Nerz C, Götz F. Differential gene expression profiling of Staphylococcus aureus cultivated under biofilm and planktonic conditions. *Appl Environ Microbiol*. 2005;71(5):2663-2676
17. Cierny G, Dipasquale D. Periprosthetic Total Joint Infections. *Clin Orthopaedics Relat Res*. 2002;(403):23-28.
18. Mcpherson EJ, Woodson C, Holtom P, Roidis N, Shufelt C. Outcomes Using a Staging System. *Clin Orthop Relat Res*. 2002;(403):8-15.
19. Tsukayama DT, Goldberg VM, Kyle R. Diagnosis and management of infection after total knee arthroplasty. *J Bone Joint Surg Am*. 2003;85-A Suppl 1:S75-80.
20. Zimmerli W, Trampuz a, Ochsner PE. Prosthetic-joint infections. *N Engl J Med*. 2004;351(16):1645-1654.
21. Tande AJ, Patel R. Prosthetic joint infection. *Clin Microbiol Rev*. 2014 Apr;27(2):302-45.



22. McNally M, Sousa R, Wouthuyzen-Bakker M, Chen AF, Soriano A, Vogely HC, Clauss M, Higuera CA, Trebše R. The EBJIS definition of periprosthetic joint infection. *Bone Joint J.* 2021 Jan;103-B(1):18-25.
23. Craig A, King SW, van Duren BH, Veysi VT, Jain S, Palan J. Articular spacers in two-stage revision arthroplasty for prosthetic joint infection of the hip and the knee. *EFORT Open Rev.* 2022;7(2):137-152.
24. Izakovicova P, Borens O, Trampuz A. Periprosthetic joint infection: current concepts and outlook. *EFORT Open Rev.* 2019;4(7):482-494.
25. Natsuhara KM, Shelton TJ, Meehan JP, Lum ZC. Mortality During Total Hip Periprosthetic Joint Infection. *J Arthroplasty.* 2019 Jul;34(7S):S337-S342.
26. Thompson O, W-Dahl A, Stefánsdóttir A. Increased short- and long-term mortality amongst patients with early periprosthetic knee joint infection. *BMC Musculoskelet Disord.* 2022;23(1):1-7.
27. Wildeman P, Rolfson O, Söderquist B, Wretenberg P, Lindgren V. What Are the Long-term Outcomes of Mortality, Quality of Life, and Hip Function after Prosthetic Joint Infection of the Hip? A 10-year Follow-up from Sweden. *Clin Orthop Relat Res.* 2021;479(10):2203-2213.
28. Kildow BJ, Springer BD, Brown TS, Lyden E, Fehring TK, Garvin KL. Long Term Results of Two-Stage Revision for Chronic Periprosthetic Hip Infection: A Multicenter Study. *J Clin Med.* 2022;11(6).
29. Kildow BJ, Springer BD, Brown TS, Lyden ER, Fehring TK, Garvin KL. Long Term Results of Two-Stage Revision for Chronic Periprosthetic Knee Infection: A Multicenter Study. *J Arthroplasty.* 2022 Jun;37(6S):S327-S332.
30. Zmistowski B, Karam JA, Durinka JB, Casper DS, Parvizi J. Periprosthetic joint infection increases the risk of one-year mortality. *J Bone Joint Surg Am.* 2013 Dec 18;95(24):2177-84.
31. Ferlay J, Ervik M, Lam F, Colombet M, Mery L, Piñeros M, Znaor A, Soerjomataram I, Bray F (2020). Global Cancer Observatory: Cancer Today. Lyon, France: International Agency for Research on Cancer. Available from: <https://gco.iarc.fr/today>, accessed [Dec 2022].
32. Strebhardt K, Ullrich A. Paul Ehrlich's magic bullet concept: 100 years of progress. *Nat Rev Cancer.* 2008 Jun;8(6):473-80.
33. Cognetti DM, Johnson JM, Curry JM, Kochuparambil ST, McDonald D, Mott F, Fidler MJ, Stenson K, Vasan NR, Razaq MA, Campana J, Ha P, Mann G, Ishida K, Garcia-Guzman M, Biel M, Gillenwater AM. Phase 1/2a, open-label, multicenter study of RM-1929 photoimmunotherapy in patients with locoregional, recurrent head and neck squamous cell carcinoma. *Head Neck.* 2021 Dec;43(12):3875-3887.
34. Larson SM, Carrasquillo JA, Cheung NK PO. Radioimmunotherapy of human tumours. *Nat Rev Cancer* 2015 Jun;15(6)347-60.
35. Stein, Paul D., Fowler, Sarah E. G. 131I-Tositumomab Therapy as Initial Treatment for Follicular Lymphoma. *N Engl J Med.* 2006;355:11-20.



Current treatment of periprosthetic joint infection





**One-year infection control rates of a DAIR (debridement, antibiotics and implant retention) procedure after primary and prosthetic-joint-infection-related revision arthroplasty
- a retrospective cohort study**

Based on: | Nurmohamed FRHA | van Dijk B | Veltman ES | Hoekstra M | Rentenaar RJ | Weinans | Vogely HC | van der Wal BCH | *One-year infection control rates of a DAIR (debridement, antibiotics and implant retention) procedure after primary and prosthetic-joint-infection-related revision arthroplasty – a retrospective cohort study*. J. Bone Joint Infect., 6, 91–97, 2021.



ABSTRACT

Introduction: Debridement, antibiotics, and implant retention (DAIR) procedures are effective treatments for acute postoperative or acute hematogenous periprosthetic joint infections. However, literature reporting on the effectiveness of DAIR procedures performed after a one or two stage revision because of a PJI (PJI-related revision arthroplasty) is scarce. The aim of this study is to retrospectively evaluate the infection control after one year of a DAIR procedure in case of an early postoperative infection either after primary arthroplasty or after PJI-related revision arthroplasty

Materials and methods: All patients treated with a DAIR procedure within 3 months after onset of PJI between 2009 and 2017 were retrospectively included. Data were collected on patient- and infection characteristics. All infections were confirmed by applying MSIS-2014 criteria. The primary outcome was successful control of infection at one year after a DAIR procedure which was defined as the absence of clinical signs such as pain, swelling and erythema, radiological signs, such as prostheses loosening, or laboratory signs, such as CRP (<10) with no use of antibiotic therapy.

Results: 67 patients were treated with a DAIR procedure (41 hips and 26 knees). Successful infection control rates of a DAIR procedure after primary arthroplasty (n=51) and after prior PJI-related revision arthroplasty (n=16) were 69% and 56% respectively (p 0.38). The successful infection control rates of a DAIR procedure after an early acute infection (n=35) and after a hematogenous infection (n=16) following primary arthroplasty were both 69% (p 1.00).

Conclusion: In this limited study population no statistical significant difference is found after one year in infection control between DAIR procedures after primary arthroplasty and PJI-related revision arthroplasty.



INTRODUCTION

Prosthetic joint infection (PJI) is a devastating complication following total hip and knee arthroplasty. The incidences of PJI in the Western countries are reported to range up to 4% for primary total hip and knee arthroplasty, and even as high as 20% following revision arthroplasty^{1,2}.

The most common clinical signs of acute and hematogenous PJI include acute pain, erythema and fever^{3,4}. A debridement, antibiotics and implant retention (DAIR) procedure is the treatment of choice for acute PJI of the hip and knee⁵⁻⁷. A recent systematic review and meta-analysis reported a wide range of success percentages for DAIR procedures from 11% to 100%^{8,9}. Several studies have shown that the time between onset of symptoms and the DAIR procedure is strongly associated with the success rate of treatment^{8,10-12}. Nonetheless, even more than six weeks after the index arthroplasty an eradication rate of 60% can be achieved when performing DAIR¹³. The success rate of DAIR for early postoperative infection is better than for hematogenous infections^{7,14}. There is no place for DAIR in the treatment of chronic infections⁶. Prior infection in another prosthetic joint and prior two-stage exchange for PJI of the same joint are both reported to worsen the infection eradication rate of a repeated revision procedure compared to a first revision^{15,16}. However, the effectiveness of DAIR procedures after prior PJI-related revision arthroplasty is still up to debate.

The primary aim of this study is to retrospectively evaluate the infection control rate of DAIR procedures performed after a one or two stage revision because of a PJI (PJI-related revision arthroplasty) in comparison to DAIR procedures performed after primary arthroplasty. The secondary aim of this study is to evaluate if the infection control rate of a DAIR procedure after primary arthroplasty depends on whether an infection is early postoperative or hematogenous. We hypothesize that previous PJI-related revision arthroplasty has a negative effect on the infection control rate of subsequently performed DAIR procedures.

METHODS

For this observational study, ethical approval was waived by the local Medical Ethics Review Committee (METC), no: 17-284/C. After approval, we reviewed the records of all patients in our prospectively collected database who had an infection treatment of the hip or knee in our hospital between 2009 and 2017. We included all patients with one periprosthetic joint infection. All DAIR procedures were performed after placing a primary hip or knee prosthesis or after full reimplantation of a hip or knee prosthesis for infection revision surgery. In all patients, diagnosis of infection was affirmed according to the Musculoskeletal Infection Society criteria¹⁷. In our institution DAIR procedures are only performed within three months after the onset of symptoms.

We retrieved general patient- and infection characteristics, complications during treatment, and final outcomes from patients' records. Primary outcome was tier 1 infection control after DAIR treatment, based on the Outcome-Reporting tool suggested by the Musculoskeletal Infection Society workgroup¹⁸. The absence of clinical signs such as pain, swelling and erythema, radiological signs, such as prostheses loosening, or laboratory signs, such as CRP (<10) with no use of antibiotic therapy at the final follow-up 1 year after the first subsequent performed DAIR procedure was seen as a successful outcome. We used the presence of prior PJI-related revision procedure and type of infection (acute early or hematogenous) as variable to separately analyze whether the infection control rate was affected¹⁹.

Failure of treatment was defined as failed control of the periprosthetic infection. This includes tier 2 or higher based on the aforementioned Outcome-Reporting tool. Specifically, additional



surgeries such as resection arthroplasty, arthrodesis, or amputation of the limb or the administration of suppressive antibiotics prior to the final follow-up of one year postoperative was seen as a failed outcome. Only a third repeated DAIR was considered as failure of treatment.

Patient characteristics.

Characteristics such as age, sex, BMI, ASA, smoking or alcohol use, comorbidities and previous infection treatment were extracted from the medical charts. Previous PJI-related procedures were subdivided in (multiple) DAIR procedures, and (one- or two-stage) revision procedures.

Prosthetic joint infection characteristics

PJI characteristics included location of infection, type of infection and involvement of soft tissue. To determine the degree of compromise of the host and the infection site the McPherson staging system was used¹⁹. For early acute infections defined as onset of infection within 3 months after surgery, the time between primary or PJI-related revision arthroplasty and the DAIR procedure was used as the infection period. For acute hematogenous infections defined as infections spread from a distant infectious focus, the time from onset of symptoms until the DAIR procedure was calculated as the infection period.

The DAIR procedure

A debridement, antibiotics and implant retention procedure consist of several steps in consecutive order. First six synovial fluid- or tissue samples are collected for culture and a meticulous debridement of the joint is performed to remove all infected tissue. The interchangeable parts (insert of the knee and inlay and head of the hip) are removed to facilitate posterior joint debridement and are then replaced. During surgery the joint is extensively lavaged with six liters of NaCl 0.9%.

All patients were treated with cefazolin until culture results were available. When culture results were available the definite antibiotic strategy was determined according to the found pathogen and antibiotic susceptibility test results in close consultation with a medical microbiologist and an infectious disease specialist. Patients generally received three months of antibiotic treatment following DAIR.

Statistical analysis

Descriptive statistics, mean and range are used to represent the demographics of the patients. Fisher's exact test was used to assess the level of significance for differences between the infection control rates of the groups. A P value <0.05 was considered to be statistically significant. Calculations and statistical analyses were performed using Excel and SPSS software [27].



RESULTS

Between 2009 and 2017, 67 patients were treated for acute PJI with a DAIR procedure. Forty-one hip- and 26 knee surgeries were performed. General patient - and infection characteristics are shown in Figure 1 & 2 and Table 1 & 2. All patients had a follow-up of one year after the first DAIR procedure. Overall, the infection was eradicated in 44 out of 67 patients.

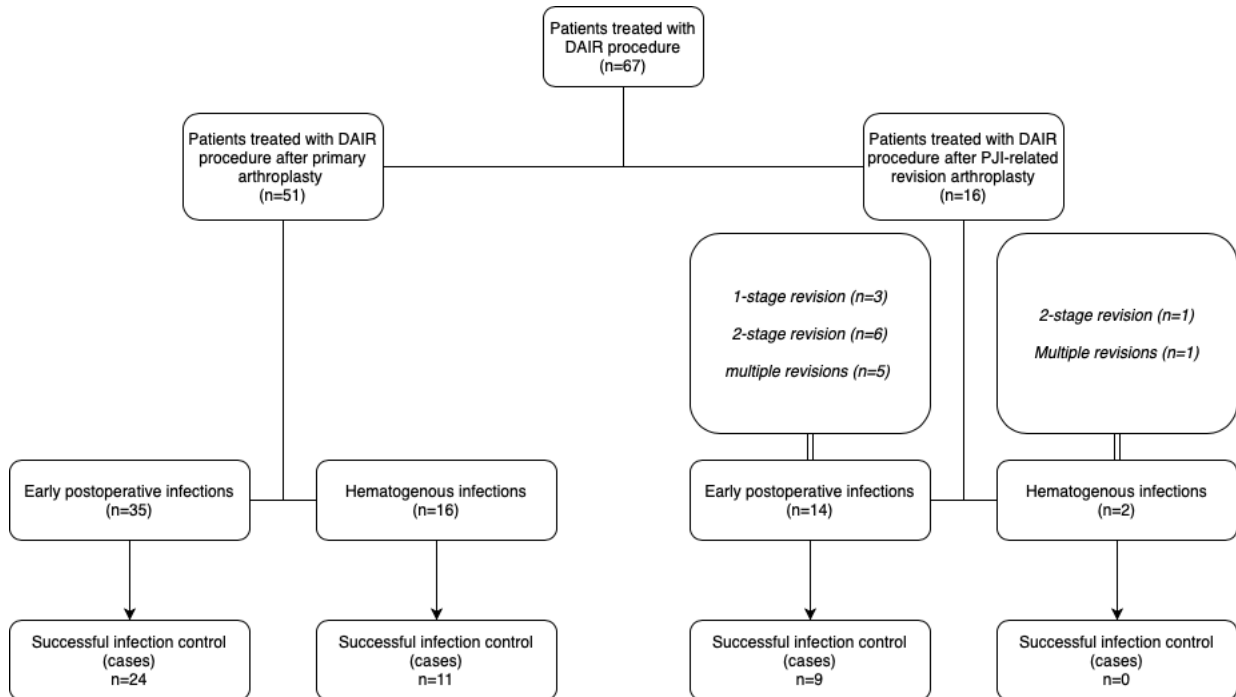


Figure 1. Flow diagram showing the infection characteristics, previous PJI-procedures and number of successfully controlled infections.

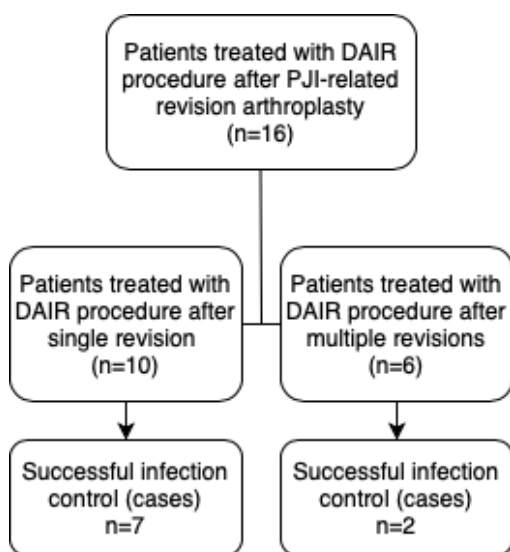


Figure 2. Flow diagram showing the numbers of patients with successfully controlled infections according to the frequency of previous PJI-related revision arthroplasty.



DAIR procedure after primary arthroplasty versus after previous PJI-related revision arthroplasty.

In 51 patients a DAIR procedure was performed after primary arthroplasty. In 16 patients a DAIR procedure was performed after previous PJI-related revision procedure. A flow diagram of included patients and type of PJI-related revision arthroplasty can be found in figure 1. For the two patients with a hematogenous infection after previous PJI-related revision arthroplasty, the interval between revision surgery and the onset of hematogenous infection were 215 and 722 days. The infection control rate of DAIR procedures performed after primary arthroplasty was 69% (35 out of 51 cases). For hip and knee cases, the infection control rate was 72% (21 out of 29 cases) and 64% (14 out of 22 cases) respectively. The infection control rate of DAIR procedures performed after PJI-related revision arthroplasty was 56% (9 out of 16 cases). For hip and knee cases, the infection control rate was 67% (8 out of 12 cases) and 25% (1 out of 4 cases) respectively. There was no statistically significant difference in the infection control rate between DAIR procedures performed after primary arthroplasty and after PJI-related revision arthroplasty (p 0.38).

DAIR after early acute versus hematogenous infections after primary arthroplasty.

In 35 patients a DAIR procedure was performed for an early acute infection following primary arthroplasty. In 16 patients a DAIR procedure was performed for an acute hematogenous infection (figure 1). The mean duration of symptoms was 12 days (0 days-83 days) for hematogenous infections. The infection control rate of DAIR procedures for early acute infections was 69% (24 out of 35 cases). For hip and knee cases, infection control rate was 74% (17 out of 23 cases) and 58% (7 out of 12 cases) respectively. The infection control rate of DAIR procedures performed for hematogenous infections was 69% (11 out of 16 cases). For hip and knee cases, the infection control rate was 67% (4 out of 6 cases) and 70% (7 out of 10 cases) respectively. There was no statistically significant difference in the infection control rate between these two groups (p 1.00).

Microbiology findings

The microbiology culture results of the tissue cultures taken during DAIR treatment can be found in table 2. Sixty-three cases had positive perioperative findings. No pathogen was identified in 4 cases. In two of these cases, preoperative antibiotic treatment was administered by the referring physician prior to surgery.



Table 1. Baseline patient characteristics

	Total (n)	Successful infection control (n)	Failed infection control (n)
Number of patients (%)	67	44 (66)	23 (34)
Hip (%)	41	29 (71)	12 (29)
Knee (%)	26	15 (58)	11 (42)
Mean age (range)	67 (18-92)	68 (18-92)	63 (35-78)
Gender M/F (%)	29/38	16 (55) / 28 (74)	13 (45) / 10 (26)
Mean BMI (range)	27 (19-45)	27 (19-44)	28 (19-45)
Mean duration of infection (days)	20	22	16
Risk factors			
Smoking (%)	12	7 (58)	5 (42)
Alcohol abuse (%)	7	6 (86)	1 (14)
ASA 1 / 2 / 3	6 / 37 / 24	4 / 23 / 17	2 / 14 / 7
Host-score (according to McPherson)			
Uncompromised (%)	19	9 (47)	10 (53)
Compromised (%)	44	32 (73)	12 (27)
Significantly compromised (%)	4	3 (75)	1 (25)
Local extremity grade (according to McPherson)			
Uncompromised (%)	58	41 (71)	17 (29)
Compromised (%)	9	3 (33)	6 (67)



Table 2. Microbiology findings

	Cases (n)	Successful infection control (n)
<i>Staphylococcus aureus</i>	13	8
<i>Staphylococcus epidermidis</i>	14	10
Other staphylococci ¹	5	5
<i>Betahaemolytic streptococci</i> ²	4	3
<i>Enterococci</i> ³	6	2
<i>Enterobacterales</i> ⁴	6	5
<i>Pseudomonas aeruginosa</i>	2	2
Other pathogens ⁵	7	4
Polymicrobial	6	2
No organism identified	4	3
Total	67	44

¹*S. capitis* (n=2), *S. warneri* (n= 1), *S. haemolyticus* (n= 1), *S. pseudointermedius* (n= 1).

²*S. dysgalactiae* (n=3), *S. agalactiae* (n=1)

³*E. faecalis* (n=3) *E. faecium* (n=3)

⁴*Escherichia coli* (n=2), *Klebsiella pneumoniae* (n= 2), *Enterobacter cloacae* complex (n= 1), *Serratia marcescens* (n= 1).

⁵*Corynebacterium striatum*(n= 1),*Corynebacterium tuberculostearium* (n= 1), *Anaerococcus hydrogenalis* (n= 1), *Cutibacterium acnes* (n= 3), *Ureaplasma parvum* (n= 1).



DISCUSSION

This study retrospectively evaluated the infection control rate of DAIR procedures performed for PJI after primary arthroplasty or after previous PJI-related revision arthroplasty of the hip and knee in a tertiary referral center. The infection control rate of DAIR procedures after primary arthroplasty was 69% (35 out of 51 cases) compared to 56% (9 out of 16 cases) for DAIR procedures after previous PJI-related revision arthroplasty. Our study population is too small to draw definite conclusions; however, these results show a trend that previous PJI treatment could have a negative effect on the infection control rate of DAIR procedures.

There seems to be a contrast between the infection control rates of DAIR performed after primary arthroplasty and DAIR after PJI-related revision arthroplasty. Even though the infection control rate for DAIR procedures after previous PJI-related revision arthroplasty is reduced, our data show that about 6 out of 10 infections can still be controlled without further major revision surgery. Furthermore, only 2 out of 6 DAIR procedures after multiple PJI-related revision arthroplasty were successful, whereas the infection was controlled in 7 out of 10 DAIR procedures after a single PJI-related revision procedure (p 0.30) (Figure 2). The infection control rate of DAIR treatment seems to further decline as the number of previously performed PJI-related revision arthroplasty increases.

Most of our infection control rates of DAIR procedures are comparable to the overall pooled success rate of 61,4% reported in a recent meta-analysis⁸. However, some other retrospective studies have reported higher infection control rates for DAIR procedures^{7,11,14,20}. The relatively large number of patients with ASA 3 and McPherson compromised host score (table 1) may cause a lower successful control rate in our population.

Literature on the results of DAIR procedures after revision surgery is scarce. Byren and colleagues reported a failure rate of 35% and a 3.1 times increase in hazard ratio for failure of DAIR if it is performed after revision arthroplasty compared to after primary arthroplasty²⁰. Shohat and colleagues found no significant difference in the success rate if DAIR was performed after primary or revision arthroplasty (p 0.182)²¹. Lastly, Wouthuyzen-Bakker and colleagues found an unadjusted and adjusted odds ratio of 1.65 (p 0.04) and 0.96 (p 0.90) for failure of a DAIR performed on revised prostheses with late prosthetic joint infections²². Considering that no significant difference is found in the infection control rate of DAIR procedures after PJI-related revision arthroplasty in two studies and that this study found an infection control rate of 56%, a DAIR procedure should still be a treatment option for PJI after revision arthroplasty. Nonetheless, the aforementioned studies show the same trend as reported in this study.

A limitation of this study is reflected by the retrospective design. The number of patients included in this study was relatively low, which was caused by the scarcity of PJI requiring DAIR. Logically, especially the number of patients with DAIR after revision surgery was low. Moreover, misclassification bias and risk factors that were present but not measured should also be accounted with. Heterogeneity of the groups can cause bias.

Our results show that even though the infection control rate may decrease after prior PJI-related revision arthroplasty, a subsequently performed DAIR procedure can retain the prosthesis in about 60% of the patients. These findings should be confirmed prospectively in a larger group of patients. We recommend performing a prospective multicenter evaluation of DAIR treatment to give a conclusive answer. Moreover, for patients with an infection after primary arthroplasty, we found no difference in infection control rate between early postoperative and acute hematogenous infections.



REFERENCES

1. Ahmed SS, Yaghmour KM, Haddad FS. The Changing Face of Infection, Diagnosis, and Management in the United Kingdom. *Orthop Clin North Am.* 2020;51(2):141-146.
2. Hosny HA, Keenan J. Management of prosthetic joint infection. *Surg (United Kingdom).* 2020;38(2):114-120.
3. Barrett L, Atkins B. The clinical presentation of prosthetic joint infection. *J Antimicrob Chemother.* 2014;69(SUPPL1):25-28.
4. Zimmerli W. Prosthetic-joint-associated infections. *Best Pract Res Clin Rheumatol.* 2006;20(6):1045-1063.
5. Chotanaphuti T, Courtney PM, Fram B, et al. Hip and Knee Section, Treatment, Algorithm: Proceedings of International Consensus on Orthopedic Infections. *J Arthroplasty.* 2019;34(2):S393-S397.
6. Sukeik M, Haddad FS. Periprosthetic joint infections after total hip replacement: an algorithmic approach. *SICOT-J.* 2019;5:5.
7. Wouthuyzen-Bakker M, Sebillotte M, Huotari K, et al. Lower Success Rate of Débridement and Implant Retention in Late Acute versus Early Acute Periprosthetic Joint Infection Caused by Staphylococcus spp. Results from a Matched Cohort Study. *Clin Orthop Relat Res.* 2020;478(6):1348-1355.
8. Kunutsor SK, Beswick AD, Whitehouse MR, Wylde V, Blom AW. Debridement, antibiotics and implant retention for periprosthetic joint infections: A systematic review and meta-analysis of treatment outcomes. *J Infect.* 2018;77(6):479-488.
9. Tsang SJ, Ting J, Simpson AHRW, Gaston P. Outcomes following debridement, antibiotics and implant retention in the management of periprosthetic infections of the hip: A review of cohort studies. *Bone Jt J.* 2017;99B(11):1458-1466.
10. Kuiper JWP, Vos SJ, Saouti R, et al. Prosthetic joint-associated infections treated with DAIR (debridement, antibiotics, irrigation, and retention). *Acta Orthop.* 2013;84(4):380-386.
11. Sendi P, Lötcher PO, Kessler B, Graber P, Zimmerli W, Clauss M. Debridement and implant retention in the management of hip periprosthetic joint infection. *Bone Jt J.* 2017;99B(3):330-336.
12. Karczewski D, Winkler T, Renz N, et al. A standardized interdisciplinary algorithm for the treatment of prosthetic joint infections. *Bone Joint J.* 2019;101-B(2):132-139.
13. Lowik CAM, Parvizi J, Jutte PC, et al. Debridement, antibiotics and implant retention is a viable treatment option for early periprosthetic joint infection presenting more than four weeks after index arthroplasty. *Clin Infect Dis.* Published online August 2019.
14. Volpin A, Sukeik M, Alazzawi S, Haddad FS. Aggressive Early Debridement in Treatment of Acute Periprosthetic Joint Infections After Hip and Knee Replacements. *Open Orthop J.* 2016;10:669-678.
15. Khan N, Parmar D, Ibrahim MS, Kayani B, Haddad FS. Outcomes of repeat two-stage exchange hip arthroplasty for prosthetic joint infection. *Bone Jt J.* 2019;101-B:110-115.
16. Chalmers BP, Weston JT, Osmon DR, Hanssen AD, Berry DJ, Abdel MP. Prior hip or knee prosthetic joint infection in another joint increases risk three-fold of prosthetic joint infection after primary total knee arthroplasty: A matched control study. *Bone Jt J.* 2019;101:91-97.
17. Parvizi J, Gehrke T. Definition of periprosthetic joint infection. *J Arthroplasty.* 2014;29(7):1331.
18. Fillingham YA, Della Valle CJ, Suleiman LI, et al. Definition of Successful Infection Management and Guidelines for Reporting of Outcomes after Surgical Treatment of Periprosthetic Joint Infection: From the Workgroup of the Musculoskeletal Infection Society (MSIS). *J Bone Jt Surg - Am Vol.* 2019;101(14):10-14.
19. Mcpherson EJ, Woodson C, Holtom P, Roidis N, Shufelt C. Outcomes Using a Staging System. *Clin Orthop Relat Res.* 2002;(403):8-15.
20. Byren I, Bejon P, Atkins BL, et al. One hundred and twelve infected arthroplasties treated with ‘ DAIR ’ (debridement , antibiotics and implant retention): antibiotic duration and outcome. *J Antimicrob Chemother.* 2009;63(6):1264-1271.



21. Shohat N, Goswami K, Tan TL, et al. 2020 Frank Stinchfield Award: Identifying who will fail following irrigation and debridement for prosthetic joint infection. *Bone Joint J.* 2020;102-B(7 B):11-19.
22. Wouthuyzen-Bakker M, Sebillotte M, Lomas J, et al. Clinical outcome and risk factors for failure in late acute prosthetic joint infections treated with debridement and implant retention. *J Infect.* 2019;78(1):40-47.



A mean 4-year evaluation of infection control rates of hip and knee prosthetic joint infection-related revision arthroplasty: an observational study

Based on: | van Dijk B | Nurmohamed | FRHA | Hooning van Duijvenbode JFF | Veltman ES | Rentenaar R J | Weinans | H | Vogely HC | van der Wal BCH | *A mean 4-year evaluation of infection control rates of hip and knee prosthetic joint infection-related revision arthroplasty: an observational study*. Acta Orthopaedica, 93, 652–657, 2021.



ABSTRACT

Introduction: The long-term results of the 1- or 2 stage revision procedure and infection-free prosthesis survival in tertiary referral center is unknown. In this retrospective observational study, the long-term results of infection control and infection-free prosthesis survival of the periprosthetic joint infection-related 1- and 2-stage revision procedure are evaluated. Furthermore, the merit of performing an antibiotic-free window in the 2-stage revision is evaluated.

Materials and methods: All patients that received a 1 or 2-stage revision procedure of the hip or knee between 2010 and 2017 were included. Data were collected on patient and infection characteristics. The primary treatment aim was successful infection control without the use of antibiotic therapy afterwards. Infection-free survival analysis was performed using the Kaplan-Meier method with type of periprosthetic joint infection-related revision as covariate. Within the group of 2-stage revisions, use of an antibiotic-free window was selected as covariate.

Results: 128 patients were treated for a periprosthetic joint infection-related revision procedure (81 hips and 47 knees). Successful infection control was achieved in 18 out of 21 cases for the 1-stage and 89 out of 107 cases for the 2-stage revision procedure (83%) respectively after a follow-up of more than 4 years. In addition, 2stage revision procedure infection control was achieved in 52 out of 60 cases with an antibiotic free interval and 37 out of 45 cases without such interval ($p=0.6$). The mean infection free survival of the 1-stage revision was 90 months (95% CI: 75-105) and 98 months (95% CI: 90-106) for the 2-stage revision procedure.

Conclusion: There seems to be no difference in infection control and infection-free survival between the 1- and 2-stage revision procedure. Second to that, an antibiotic-free window in case of a 2-stage revision did not seem to influence treatment outcome.

However, one must be cautious when interpreting these results due to confounding by indication and small study population. Therefore, no definite conclusion can be drawn.



INTRODUCTION

A devastating complication of joint arthroplasty is periprosthetic joint infection (PJI). The incidence of periprosthetic joint infection after primary arthroplasty ranges from 1-2%,¹. The outcome of PJI treatment is often not dichotomous but rather a gradient of outcomes that can be divided in four tiers,². Tier 1 is considered to be the most successful and describes an infection control with no antibiotic therapy. Tier 2 includes infection control with the patient being on suppressive antibiotic therapy. Tier 3 is where revision surgery or amputation is required after PJI treatment. Finally, tier 4 involves fatality. Surgical treatment options for chronic PJI revision arthroplasty include a 1- or 2-stage revision procedure. The 2-stage revision is the most frequently used treatment. However, the 1-stage revision procedure has increasingly been advocated because of the comparable outcomes with the 2-stage revision,^{3,4}. In a two stage revision procedure, there is no consensus on the proper length of antibiotic therapy and whether an antibiotic-free window may benefit treatment outcome,^{5,6}.

We evaluated the long-term results of PJI-related 1-stage and 2-stage revision procedures. The secondary aim is to evaluate whether the use of an antibiotic-free period in a 2-stage revision affects treatment outcome.

METHODS AND CHARACTERISTICS

In this retrospective cohort study, all patients treated with revision surgery of the hip or knee between January 2010 and January 2017 were included. Patients that complied with the MSIS criteria 2014 were considered to have a septic infection,⁷. This entails obtaining 2 positive cultures of the same microorganism or determining the existence of a communicating sinus tract. Elevated ESR, CRP, synovial leucocyte count, synovial neutrophils percentage and a single positive culture result were seen as minor criteria. Cases that did not comply with the aforementioned criteria were marked as MSIS-negative infections. The follow-up period was calculated as the time interval between the date of the definite revision procedure till failure of treatment, death or May 2020.

As suggested by the Musculoskeletal Infection Society workgroup, the primary treatment aim after revision for PJI was tier 1 infection control based on the outcome-reporting tool,². In this regard, no use of antibiotic therapy was considered as a successful outcome. Reasons to stop antibiotic therapy were, e.g. the absence of clinical signs such as pain, swelling and erythema and radiological signs such as loosening or laboratory signs such as CRP (>10 mg/L). Tier 2 or higher infection control based on the aforementioned outcome-reporting tool was considered as a failure of treatment.

Patient characteristics

Medical charts were examined for characteristics such as age, sex, BMI, ASA class, smoking or alcohol use, comorbidities and soft tissue involvement. Data on previous orthopedic treatments in the referring hospitals were retrieved from the referral letters.

Prosthesis and periprosthetic joint infection characteristics

PJI characteristics includes type of joint, type of revision procedure, type of infection (septic infection or MSIS-negative infection) and soft tissue involvement. The joint-age is defined as the time interval between primary arthroplasty and PJI-related revision procedure. The infection-free survival of the prosthesis was defined as the time between reimplantation of the prosthesis until the end of the follow-up period, without recurrence of infection. Type of



infection, grading of host and local infection site were evaluated according to Cierny, McPherson and Zimmerli classification systems,⁸⁻¹⁰.

Microbiology characteristics

Microbiology characteristics include tissue cultures for microbiological diagnostics. Special emphasis was made for difficult-to-treat microorganisms,^{1,11,12}. Length of antibiotic treatment within the interval of stages for a 2-stage revision and length of post-operative antibiotic treatment were calculated. Preoperative antibiotics were defined as therapeutic antibiotics continued during perioperative sampling.

Surgical treatment and procedure

A 1-stage revision consists of removing the infected prosthesis, meticulous debridement and irrigation of the joint space, followed by reimplantation of a hip or knee prosthesis during the same procedure. A 2-stage revision consist of two separate surgical interventions. During the first procedure, the infected prosthetic joint is removed along with all the material suspected to be infected, the joint is extensively debrided and irrigated and an antibiotic loaded spacer is implanted. The last stage of the 2-stage procedure is performed after 6 to 8 weeks. During this period, 45 patients were treated with antibiotics until reimplantation. In contrast to 60 patients that had an antibiotic-free period in the last 2 weeks of this interval. During the last stage of the 2-stage procedure the spacer is removed, the surgical site is again debrided and irrigated, and a hip or knee prosthesis is then reimplanted. Change of antibiotic protocol was practiced because the main consensus about the effectiveness of the antibiotic-free period was deemed to be questionable.

For both types of revision procedures, at least 5 intraoperative tissue, fluid and sonication fluid samples were taken for microbiological diagnostics. Vancomycin or Cefalozin was given as broad-spectrum antibiotic prophylaxis until the pathogen was identified and targeted antibiotic therapy could be started. The postoperative antibiotic treatment was determined in consultation with the microbiologist and adjusted, based on the perioperative culture results. The duration of antibiotic treatment after a second stage procedure was dependent on the outcome of the culture results. When the culture results were negative after reimplantation, an additional 6 weeks of antibiotic treatment were prescribed. When culture results returned positive, antibiotic treatment was prolonged until 3 months after reimplantation. The length of antibiotic treatment after a 1-stage revision was three months regardless of culture results. In addition, PJI with fungal pathogens were treated with antimycotic therapy for a duration of 1 year or lifelong according to hospital protocol.

The indication for the 1-stage or 2-stage revision procedure was set according to the consensus statement as composed by the Proceedings of the International Consensus on Periprosthetic Joint Infection,¹³.

Statistics

Descriptive statistics, mean and range are used to represent the demographics of the patient's procedure. Survival of prostheses was calculated using the Kaplan Meier method. Data management and analysis was performed using the Statistical Package for the Social Sciences (IBM Corp. Released 2017. IBM SPSS Statistics for Windows, Version 25.0. Armonk, NY: IBM Corp.)



RESULTS

128 PJI-related revision arthroplasty procedures were performed between 2010 and 2017. 3 of these patients died from non-PJI related reasons after the first step of the 2-stage revision procedure and were excluded in the analyses. A patient refused further treatment after the first step of the 2-stage revision procedure and was therefore excluded from all analyses (Figure 1). The mean follow-up period was 53 months (8 days - 115 months). Patient, prosthesis and periprosthetic joint infection characteristics are shown in table 1. The overall infection control rate for 1-stage and 2-stage revision procedures was 84% (107 out of 128 cases).

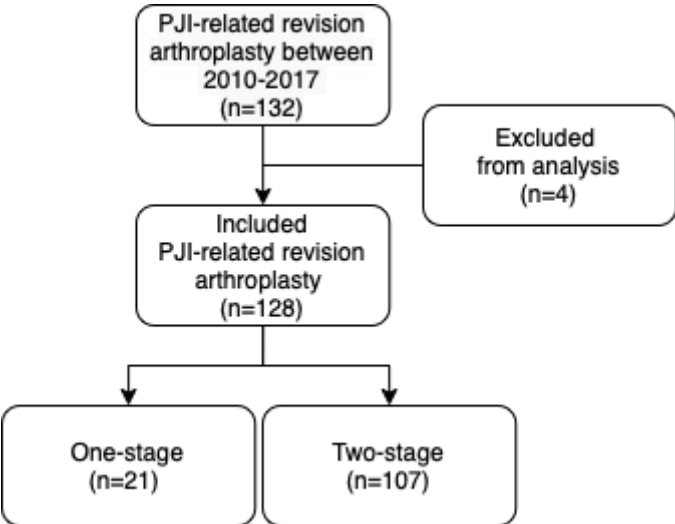


Figure 1. Flowchart of all included patients



Table 1	Total (n=128)	Two-stage revision procedure (n=107)	One-stage revision procedure (n=21)
Patient characteristics			
Infection control	107 (83.6%)	89 (83.2%)	18 (85.7%)
Age (range)	71 (44 - 92)	70.4 (44 - 92)	71.6 (55 -92)
Sex (M/F)	74/54	62 (57.9%) / 45 (42.1%)	12 (57.1%) / 9 (42.9%)
Mean BMI (range)	27.5 (17.5- 38.4)	27.7 (19.2 – 38.4)	26.2 (17.5 - 38.1)
ASA-1	15	13 (12.1%)	2 (9.5%)
ASA-2	84	72 (67.3%)	12 (57.1%)
ASA-3	28	22 (20.6%)	6 (28.6%)
ASA-4	1	0 (0.0%)	1 (4.8%)
Riskfactors			
Smoking	14	11 (10.3%)	3 (14.3%)
Alcohol abuse	15	11 (10.3%)	4 (19.0%)
Host-score according to McPherson			
Uncompromised	54	47 (43.9%)	7 (33.3%)
Compromised	69	56 (52.3%)	13 (61.9%)
Significantly compromised	5	4 (3.8%)	1 (4.8%)
Host-score according to Cierny			
Uncompromised	30	26 (24.3%)	4 (19.0%)
Local	4	4 (3.7%)	0 (0.0%)
Systemic	85	70 (65.4%)	15 (71.4%)
Local and systemic	9	7 (6.5%)	2 (9.5%)
Prosthesis and periprosthetic joint infection characteristics			
Total hip revisions	81	67 (62.6%)	14 (66.7%)
Total knee revisions	47	40 (37.4%)	7 (33.3%)
Indication index prosthesis			



Septic revision	107	91 (85.0%)	16 (76.2%)
-Two positive cultures of the same organism	81	70 (65.4%)	11 (52.4%)
-A sinus tract communicating with the joint	13	12 (11.2%)	1 (4.8%)
-Comply with at least a score of 6 of the minor criteria	13	9 (8.4%)	4 (19.0%)
MSIS-negative revision	21	16 (15.0%)	5 (23.8%)
Infection period			
Mean joint-age (months)	45.4 (0.0 - 341)	38.7 (0.0 – 283.0)	79.5 (1.0 – 341.0)
Soft tissue involvement			
Abscess or Fistula	22	18 (16.8 %)	4 (19.0%)
Infection score (McPherson)			
Early (< 4 weeks)	0	0 (0.0%)	0 (0.0%)
Late postoperative (>4 weeks)	128	107 (100.0%)	21 (100.0%)
Local score (McPherson)			
Uncompromised	5	5 (4.7%)	0 (0.0%)
Compromised	122	101 (94.4%)	21 (100.0%)
Significantly compromised	1	1 (0.9%)	0 (0.0%)
Infection type (Zimmerli)			
Early	11	10 (9.3%)	1 (4.8%)
Delayed	58	51 (47.7%)	7 (33.3%)
Late	59	46 (43.0%)	13 (61.9%)
Systemic antibiotics			
Preoperative	30	24 (22.4%)	6 (28.6%)

Table 1. Patient characteristics



Revision procedure

The infection control rate of the 1-stage revision procedure was 18 out of 21 cases; 12 out of 14 cases hips and 6 out of 7 cases knees. The infection control rate of the 2-stage revision procedure was 89 out of 107 cases (83%); 56 out of 67 hips and 33 out of 40 knees.

Infection-free survival analysis (Figures 2 and 3)

In 2 patients a girdle-stone procedure was done and were considered as a failed treatment for the infection control analysis but excluded from the prosthesis survival analysis because no implant could be placed. 126 of 128 patients were included for the infection-free prostheses survival analysis. The mean follow-up time of the 1-stage and 2-stage revision was 50 months (8 days to 104 months) and 52 months (9 days to 115 months) respectively. The cumulative infection-free survival of implanted prostheses was calculated at 0, 24, 48, 72 and 96 months. For the 1-stage revision this was 90%, 84%, 84%, 84% and 84% respectively and for the 2-stage revision, 87%, 85%, 81%, 77% and 77% respectively. The mean infection free survival of the implant was 90 months (95% CI: 75-105) after a 1-stage revision procedure and 98 months (95% CI: 90-106) after a 2-stage revision procedure.

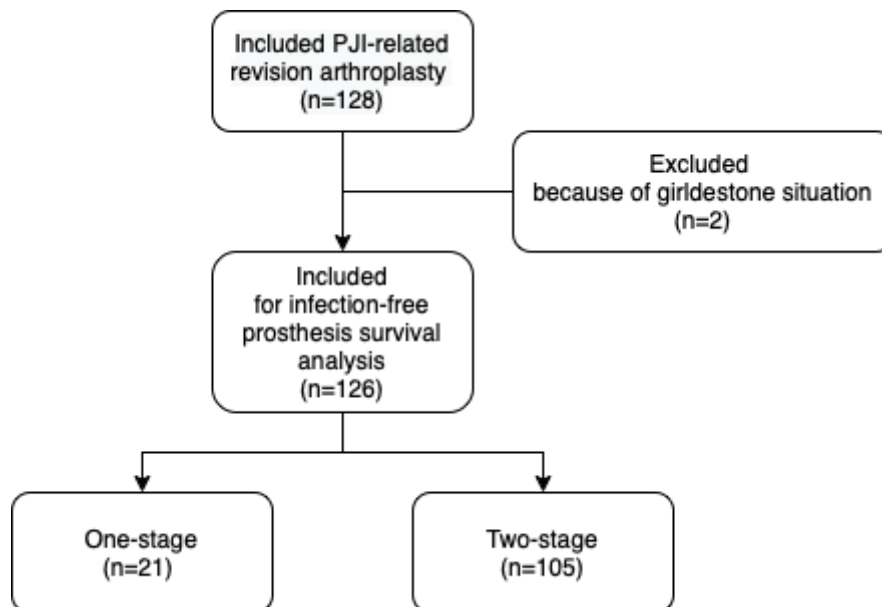


Figure 2: Flowchart of Patients included in the survival analysis of the PJI-related arthroplasty



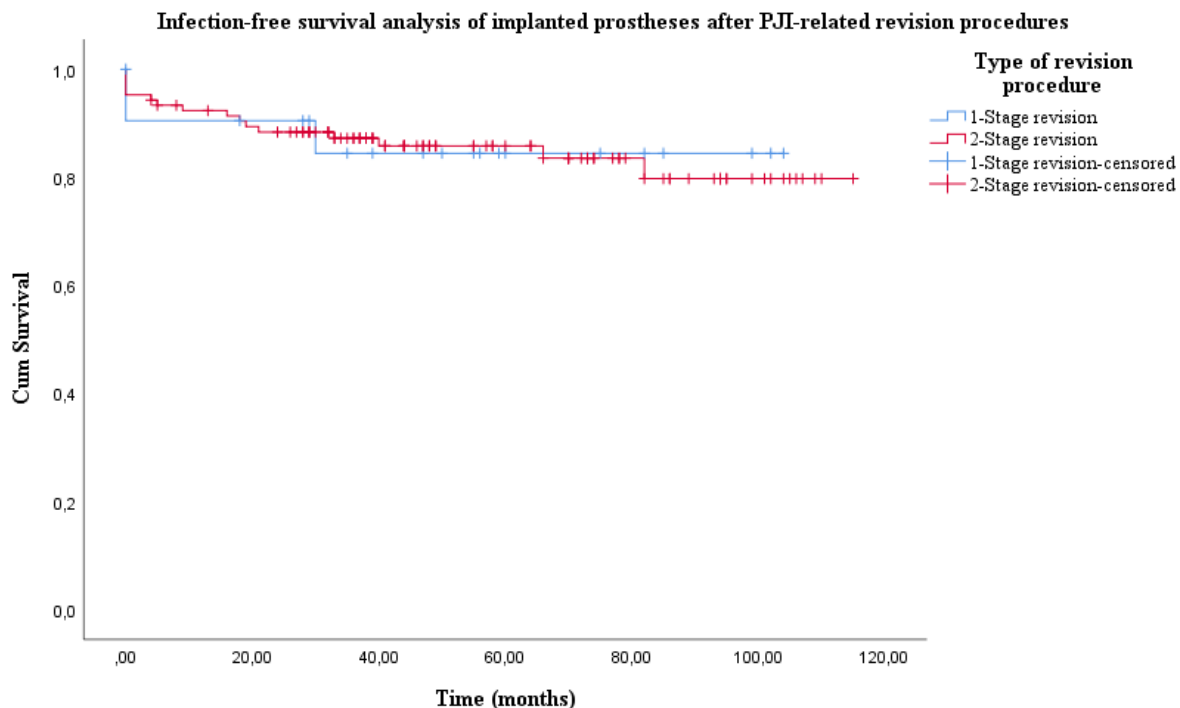


Figure 3. The survival analyses of the PJI-related revision arthroplasty using the Kaplan-Meier method

Antibiotic-free period for 2-stage PJI-related revision arthroplasty procedures

An antibiotic-free period was used with 2-stage revision in 60 cases, where antibiotics were continued until reimplantation in 45 cases. The infection control rates of the 2-stage revision procedure, with and without an antibiotic-free period, was 52 out of 60 cases and 37 out of 45 cases respectively. The infection control rates were 31 out of 37 hips and 21 out of 23 knees for patients with an antibiotic-free period and 25 out of 28 hips and 12 out of 17 knees for patients without an antibiotic-free period. We did not find a statistically significant difference in infection control rate between a 2-stage PJI-related revision arthroplasty with or without an antibiotic-free holiday ($p=0.6$).

Microbiological culture results (Table 2 and 3)

A positive perioperative culture was found in 98 cases. Polymicrobial infections were found in 31 cases. *Staphylococcus Aureus* was found in 14 cases that were all treated with a 2-stage revision procedure. Difficult-to-treat microorganisms were both found in the 1-stage and 2-stage revision procedure. Rifampicin-resistant staphylococci were found in 3 cases treated with a 1-stage revision procedure and in 6 cases treated with a 2-stage revision procedure. Ciprofloxacin-resistant gram-negative bacteria were found in 2 cases treated with a 2-stage revision procedure. Fungi were found in 1 case treated with a 1-stage revision procedure versus 2 cases treated with the 2-stage revision procedure. No vancomycin-resistant enterococci, quinolone-resistant gram-negative or enterococci were found in our study population. The infection control of the difficult-to-treat microorganisms can be found in table 3. Negative perioperative cultures were found in 30 cases. Out of these, 3 cases had a positive culture of pre-operatively obtained joint aspirate. In 4 of 21 cases of the 1-stage revision procedure and in 8 of 107 cases of the 2-stage revision procedure positive cultures of a pre-operatively obtained joint aspirate were found. No statistically significant difference was found in the incidence of pre-operative obtained bacteria between the 1-stage revision procedure and the 2-stage revision



procedure ($p= 0.1$).

A total of 30 patients received pre-operative antibiotics, of which 11 cases resulted in negative perioperative cultures. For cases with no pre-operative antibiotics, 19 out of 98 cases resulted in negative perioperative cultures ($p=0.08$).

The infection control rates of the 1-stage revision procedure, with and without the use of pre-operative antibiotics were 6 out of 6 cases and 12 out of 15 cases respectively. We found no statistically significant difference in infection control rate between a 1-stage PJI-related revision arthroplasty with and without use of pre-operative antibiotics ($p= 0.5$). The infection control rates of the 2-stage revision procedure, with and without use of pre-operative antibiotics were 22 out of 24 cases and 67 out of 83 cases respectively. We found no statistically significant difference in infection control rate between a 2-stage PJI-related revision arthroplasty with and without use of pre-operative antibiotics ($p=0.4$).

Furthermore, for the 2-stage revision procedures with an available last stage culture ($n=105$) an antibiotic-free period showed positive cultures at the last stage in 7 out of 60 cases. 2-stage revision procedures with no antibiotic-free period showed positive cultures in 5 out of 45 cases. No statistically significant difference was found in positive last-stage cultures of the 2-stage revision procedures with or without an antibiotic-free holiday ($p=1.0$).



	Successful infection control	Failed infection control	Total
Polymicrobial	27	4	31
<i>Staphylococcus epidermidis</i>	20	1	21
<i>Staphylococcus aureus</i>	9	5	14
<i>Staphylococcus capitis</i>	2	1	3
<i>Enterococcus faecalis</i>	2	1	3
<i>Enterobacter cloacae</i>	2	1	3
<i>Streptococcus dysgalactiae</i>	2	1	3
<i>Cutibacterium acnes</i>	2	1	3
<i>Staphylococcus lugdunensis</i>	1	1	2
<i>Corynebacterium striatum</i>	1	1	2
<i>Candida albicans</i>	0	1	1
None	29	1	30
Other ¹	10	2	12
Total	107	21	128
¹ Coagulase negative staphylococcus, <i>Enterococcus faecium</i> , <i>Escherichia coli</i> , <i>Haemophilus parainfluenzae</i> , <i>Bacillus cereus</i> complex, <i>Streptococcus anginosus</i> group, <i>Aggregatibacter</i> species, <i>Streptococcus mutans</i> , <i>Candida</i> species, <i>Granulicatella adiacens</i> and <i>Salmonella</i> species			

Table 2. Microbiology findings



	Successful infection control	Failed infection control	Total
Rifampicin-resistant staphylococci	8	1	9
Fungi	1	2	3
<i>Cutibacterium acnes</i>	2	1	3
Ciprofloxacin-resistant gram-negative bacteria	1	1	2
amoxicillin-resistant <i>Enterococcus faecium</i>	1	1	2
<i>Haemophilus parainfluenzae</i>	1	0	1
Salmonella species	1	0	1
Aggregatibacter species	1	0	1
<i>Escherichia coli</i>	1	0	1
Total	17	6	23

Table 3. Difficult-to-treat microorganisms

DISCUSSION

Performing a 2-stage revision procedure is the most frequently used procedure to treat chronic periprosthetic joint infections. However, the use of the 1-stage revision is gaining more and more support. In this study, the long-term results with a mean follow-up period of 53 months of PJI-related revision procedures are evaluated. Furthermore, the utilization of an antibiotic-free window within a 2-stage revision is evaluated.

The overall infection control rate was 84% (107 out of 128 cases) of which 18 out of 21 cases were successfully treated with a 1-stage revision procedure and 89 out of 107 cases (83%) treated with a 2-stage revision procedure. The infection control rates are similar between groups and similar to the rates found in literature,¹⁴⁻¹⁶. When functional outcome is also taken into account, a systemic review by Leonard et al. showed that 1-stage revision surgery was superior,¹⁵. However, one must be cautious when comparing 1- and 2 stage revision groups due to differences in indication for surgery. One-stage revision procedures are done in patients with better pre-operative conditions that fit specific selection criteria and consequently may lead to selection bias. Therefore, the choice of revision surgery should still be in concordance with consensus agreement as stated by Parvizi et al.¹³. Following the host scores according to Cierny and McPherson, our study population is compromised in 77% and 58% of all the cases respectively. Considering the specific selection criteria of the 1-stage revision procedure, we believe that an adequate infection control is still achieved with the 2-stage revision procedure,¹³

Infection control also includes infection-free implant survival. The mean infection free survival of the prostheses placed with the 1-stage revision was 90 months (95% CI: 75-105 months) and for the 2-stage revision procedure 98 months (95% CI: 90-106 months) with equal follow-up time. 2 patients were excluded from the survival analysis of the PJI-related revision arthroplasty due to a Girdlestone situation which means no new implant has been placed. However, patients



who died or had received a new prosthesis for non-PJI related causes within the follow-up time were still included in the analysis. This might give an overestimation of the infection-free survival time. However, with an infection-free survival of 90 and 97 months for both procedures, a good estimation can be made of the effectiveness of both procedures.

Performing an antibiotic-free window can help suppressed bacteria to be identified again in perioperative cultures, taken during the last stage of the 2-stage revision. Under those circumstances, the non-eradicated pathogen could be found after which a debridement of infection site can be performed to ensure successful treatment outcome. Considering the formation and self-preserving properties of a biofilm, performing an antibiotic-free window has no effect on eradicating a persistent pathogen before the last stage of the 2-stage revision procedure. However, performing a continued antibiotic treatment in the 2-stage revision procedure can increase the chance of successful treatment outcome by maintaining an offense against the pathogen concerned.⁵ We found no statistically significant difference in infection control rate by performing an antibiotic-free window. which is in line with the current literature^{5,6}.

No statistical significant difference (p 0.08) was found in obtaining negative culture results when using pre-operative antibiotics, which does not exclude that a lower culture yield can be observed with pre-operative use of antibiotics. However, as stated by Wouthuyzen-bakker et al., one must be cautious withholding pre-operative antibiotics as the risk of surgical site infection is decreased when antibiotic therapy is timely administered,¹⁷.

In our study population, 18% of all perioperative cultures found difficult-to-treat microorganisms. No definite conclusions on successful infection control could be made because of the low incidence of these difficult-to-treat microorganisms. To evaluate the effect of difficult-to-treat microorganisms on the successful outcome of PJI revision surgery, analyses in a larger patient population is necessary.¹²

Limitations of this study include a retrospective design with all its known forms of bias. However, the consecutive nature of this cohort of patients helps to avoid selection bias. Another limitation was the lack of data about functional outcome available for analysis.

In conclusion, we found in this retrospective study that after a mean follow-up of more than 4 years, similar successful infection control is seen between the 1-stage and 2-stage revision procedure, despite a patient population that is compromised, in 77% and 58% of all the cases respectively. Furthermore, performing an antibiotic-free window in the 2-stage PJI-related revision demonstrated no benefit to the treatment outcome.



REFERENCES

1. Izakovicova P, Borens O, Trampuz A. Periprosthetic joint infection: current concepts and outlook. *EFORT Open Rev.* 2019;4(7):482-494.
2. Fillingham YA, Della Valle CJ, Suleiman LI, et al. Definition of Successful Infection Management and Guidelines for Reporting of Outcomes after Surgical Treatment of Periprosthetic Joint Infection: From the Workgroup of the Musculoskeletal Infection Society (MSIS). *J Bone Jt Surg - Am Vol.* 2019;101(14):10-14.
3. Bori G, Navarro G, Morata L, Fernandez-Valencia JA, Soriano A, Gallart X. Preliminary Results After Changing From Two-Stage to One-Stage Revision Arthroplasty Protocol Using Cementless Arthroplasty for Chronic Infected Hip Replacements. *J Arthroplasty.* 2018;33(2):527-532.
4. Haddad FS, Sukeik M, Alazzawi S. Is Single-stage Revision According to a Strict Protocol Effective in Treatment of Chronic Knee Arthroplasty Infections? *Clin Orthop Relat Res.* 2015;473(1):8-14.
5. Castellani L, Daneman N, Mubareka S, Jenkinson R. Factors Associated with Choice and Success of One-Versus Two-Stage Revision Arthroplasty for Infected Hip and Knee Prostheses. *HSS J.* 2017;13(3):224-231.
6. Bejon P, Berendt A, Atkins BL, et al. Two-stage revision for prosthetic joint infection: predictors of outcome and the role of reimplantation microbiology. *J Antimicrob Chemother.* 2010;65(3):569-575.
7. Parvizi J, Gehrke T. Definition of periprosthetic joint infection. *J Arthroplasty.* 2014;29(7):1331.
8. Cierny G, Dipasquale D. Periprosthetic Total Joint Infections. *Clin Orthopaedics Relat Res.* 2002;(403):23-28.
9. Mcpherson EJ, Woodson C, Holtom P, Roidis N, Shufelt C. Outcomes Using a Staging System. *Clin Orthop Relat Res.* 2002;(403):8-15. doi:10.1097/01.bl0.0000030172.56585.c6
10. Zimmerli W, Trampuz a, Ochsner PE. Prosthetic-joint infections. *N Engl J Med.* 2004;351(16):1645-1654.
11. Ull C, Yilmaz E, Baecker H, Schildhauer T, Waydhas C, Hamsen U. Microbial findings and the role of difficult-to-treat pathogens in patients with periprosthetic infection admitted to the intensive care unit. *Orthop Rev (Pavia).* 2020;12(3):145-150.
12. Wimmer MD, Hischebeth GTR, Randau TM, et al. Difficult-to-treat pathogens significantly reduce infection resolution in periprosthetic joint infections. *Diagn Microbiol Infect Dis.* 2020;98(2).
13. Parvizi J, Gehrke T, Chen AF. Proceedings of the international consensus on periprosthetic joint infection. *Bone Jt J.* 2013;95 B(11):1450-1452.
14. Kunutsor SK, Whitehouse MR, Lenguerrand E, et al. Re-infection outcomes following one- and two-stage surgical revision of infected knee prosthesis: A systematic review and meta-analysis. *PLoS One.* 2016;11(3):1-15.
15. Leonard H a C, Liddle AD, Burke O, Murray DW, Pandit H. Single- or two-stage revision for infected total hip arthroplasty? A systematic review of the literature. *Clin Orthop Relat Res.* 2014;472(3):1036-1042.
16. Choi HR, Kwon YM, Freiberg AA, Malchau H. Comparison of one-stage revision with antibiotic cement versus two-stage revision results for infected total hip arthroplasty. *J Arthroplasty.* 2013;28(8 SUPPL):66-70.
17. Wouthuyzen-Bakker M, Benito N, Soriano A. The Effect of Preoperative Antimicrobial Prophylaxis on Intraoperative Culture Results in Patients with a Suspected or Confirmed Prosthetic Joint Infection: a Systematic Review. *J Clin Microbiol.* 2017;55(9):2765-2774.







Visualizing *Staphylococcus aureus* biofilm in vivo



Human monoclonal antibodies against *Staphylococcus aureus* surface antigens recognize in vitro and in vivo biofilm

Based on: | de Vor L* | van Dijk B* | van Kessel K | Kavanaugh JS | de Haas C | Aerts PC | Viveen MC | Boel EC | Fluit AC | Kwiecinski JM | Krijger GC | Ramakers RM | Beekman FJ | Dadachova E | Lam MGEH | Vogely HC | van der Wal BCH | van Strijp JA | Horswill AR | Weinans H | Rooijackers SH | *Human monoclonal antibodies against *Staphylococcus aureus* surface antigens recognize in vitro and in vivo biofilm*. Elife. 2022 Jan 6;11:e67301.

**authors contributed equally*



ABSTRACT

Implant-associated *Staphylococcus aureus* infections are difficult to treat because of biofilm formation. Bacteria in a biofilm are often insensitive to antibiotics and host immunity. Monoclonal antibodies (mAbs) could provide an alternative approach to improve the diagnosis and potential treatment of biofilm-related infections. Here, we show that mAbs targeting common surface components of *S. aureus* can recognize clinically relevant biofilm types. The mAbs were also shown to bind a collection of clinical isolates derived from different biofilm-associated infections (endocarditis, prosthetic joint, catheter). We identify two groups of antibodies: one group that uniquely binds *S. aureus* in biofilm state and one that recognizes *S. aureus* in both biofilm and planktonic state. Furthermore, we show that a mAb recognizing wall teichoic acid (clone 4497) specifically localizes to a subcutaneously implanted pre-colonized catheter in mice. In conclusion, we demonstrate the capacity of several human mAbs to detect *S. aureus* biofilms in vitro and in vivo.



INTRODUCTION

Implant-related infections are difficult to treat because of the ability of many bacterial species to form biofilm¹. Biofilms are bacterial communities that adhere to abiotic surfaces (such as medical implants) using a self-made extracellular polymeric substance (EPS), consisting of proteins, polysaccharides, and extracellular DNA^{2,3}. Bacteria in a biofilm are physically different from planktonic (free floating) bacteria and often more tolerant to antibiotics⁴. For instance, the EPS forms an important penetration barrier for many antimicrobial agents^{2,5}. In addition, most antibiotics cannot kill bacteria in a biofilm because they are in a metabolically inactive state⁶ and thus resistant to the antibiotics that act on active cellular processes (such as transcription/translation or cell wall formation⁷). Another complication is that biofilm infections often occur in areas of the body that are not easily accessible for treatment without invasive surgical procedures. Consequently, treatment consists of long-term antibiotic regimens or replacement of the infected implant. Specific and noninvasive laboratory tests for early detection are not yet available and the diagnosis is often made only at advanced stages. This failure to detect biofilms adds further complications to effective diagnosis and treatment of these infections.

The human pathogen *Staphylococcus aureus* is the leading cause of healthcare-associated infections^{8,9}. Today, 25% of healthcare-associated infections are related to medical implants such as heart valves, intravenous catheters, and prosthetic joints¹⁰. *S. aureus* causes one-third of all implant-related infections in Europe and the United States^{11,12} and is known for its ability to form biofilm¹. Due to the absence of a vaccine and the emergence of methicillin-resistant *S. aureus* (MRSA), there is a clear need for diagnostic tools and alternative therapies for *S. aureus* biofilm infections.

Antibody-based biologicals could provide an alternative approach to improve the diagnosis and/or treatment of *S. aureus* biofilm-related infections. Monoclonal antibodies (mAb) may be exploited as vehicles to specifically bring anti-biofilm agents (such as radionuclides, enzymes, or photosensitizers) to the site of infection¹³⁻²⁰. Furthermore, radioactively labeled mAbs could be used for early diagnosis of biofilm-related infections. At present, only one mAb recognizing *S. aureus* biofilm has been identified. This F598 antibody recognizes poly-*N*-acetyl glucosamine (PNAG)^{21,22} (also known as polysaccharide intercellular adhesion [PIA]^{23,24}, a highly positively charged polysaccharide that was first recognized as a major EPS component of *S. aureus* biofilm. However, PNAG is not the only component of *S. aureus* biofilms. Recently, it has become clear that *S. aureus* may also use cell wall anchored proteins and eDNA to facilitate initial attachment and intercellular adhesion²⁵⁻²⁸. In fact, deletion of the *icaADBC* locus (encoding PNAG) does not impair biofilm formation in multiple *S. aureus* strains^{4,28,29}. These biofilms, referred to as PNAG-negative, are phenotypically different from PNAG-positive biofilm³⁰⁻³⁵. Because both types of biofilm occur in the clinic, we here focus on identifying mAbs that recognize PNAG-positive and PNAG-negative biofilm. In this study, we show that previously identified mAbs against staphylococcal surface structures can recognize both PNAG-negative and PNAG-positive *S. aureus* biofilms. Importantly, we show that some of these mAbs recognize *S. aureus* in both biofilm and planktonic state, which is crucial because release and dissemination of planktonic cells from biofilm-infected implants lead to life-threatening complications³⁶. Finally, using SPECT/CT imaging, we show that radiolabeled mAbs have the potential to detect biofilm in vivo.



RESULTS

Production of mAbs and validation of S. aureus biofilms

In order to study the reactivity of mAbs with *S. aureus* biofilms, we selected mAbs that were previously found to recognize surface components of planktonic *S. aureus* cells^{14,37}. Specifically, we generated two antibodies recognizing cell wall teichoic acids (WTA) (4461-IgG and 4497-IgG)^{38,39}, one antibody against surface proteins of the SDR family (rF1-IgG)⁴⁰, one antibody against clumping factor A (ClfA) (T1-2-IgG), and one antibody of which the exact target is yet unknown (CR5132-IgG) (**Figure 1A**). As a positive control, we generated F598-IgG against PNAG²¹. As negative controls, we produced one antibody recognizing the hapten dinitrophenol (DNP) (G2a-2-IgG)⁴¹ and one recognizing HIV protein gp120 (b12-IgG)^{42,43}. The variable heavy and light chain sequences of all antibodies were obtained from different scientific and patent publications⁴⁴ (**Supplementary file 1**) and cloned into expression vectors to produce full-length human IgG1 (kappa) antibodies in EXPI293F cells.

Since we were interested in the reactivity of these mAbs with both PNAG-positive and PNAG-negative biofilms, we selected two *S. aureus* to serve as models for these different biofilm phenotypes. We used Wood46 as a model strain for PNAG-positive biofilm because strain Wood46 is known to produce PNAG⁴⁵ and known for its low surface expression of IgG binding staphylococcal protein A (SpA). This is an advantage in antibody binding assays because nonspecific binding of the IgG1 Fc domain to SpA complicates the detection of antibodies^{46,47}. As a model strain for PNAG-negative biofilms, we used LAC⁴⁸⁻⁵⁰, a member of the USA300 lineage that has emerged as the common cause of healthcare-associated MRSA infections, including implant infections⁵¹⁻⁵⁴. Previous studies have demonstrated that LAC is capable of forming robust biofilm with no detectable PNAG^{15,28,30,55,56}. Here, we used LAC Δ *spa* Δ *sbi*, a mutant that lacks both SpA and a second immunoglobulin-binding protein (Sbi). To confirm the EPS composition of Wood46 and LAC Δ *spa* Δ *sbi* biofilm, we treated biofilms with different EPS-degrading enzymes that degrade either PNAG (dispersin B [DspB]) or extracellular DNA (DNase I). As expected, LAC Δ *spa* Δ *sbi* biofilm (**Figure S1A**) was sensitive to DNase I but not DspB while Wood46 biofilm (**Figure S1B**) was sensitive to DspB but not DNase I. The fact that Wood46 was insensitive to DNase can be explained by shielding or DNA network stabilization by PNAG³⁰. At ultrastructural level, scanning electron microscopy (SEM) also verified the formation of phenotypically different biofilm by both strains (**Figure S1C,D**). Additionally, we verified that F598-IgG1, the only mAb in our panel that has been reported to bind biofilm²¹, indeed recognizes PNAG-positive biofilm of Wood46 (**Figure 1B**) but not PNAG-negative biofilm of LAC Δ *spa* Δ *sbi* (**Figure 1C**).



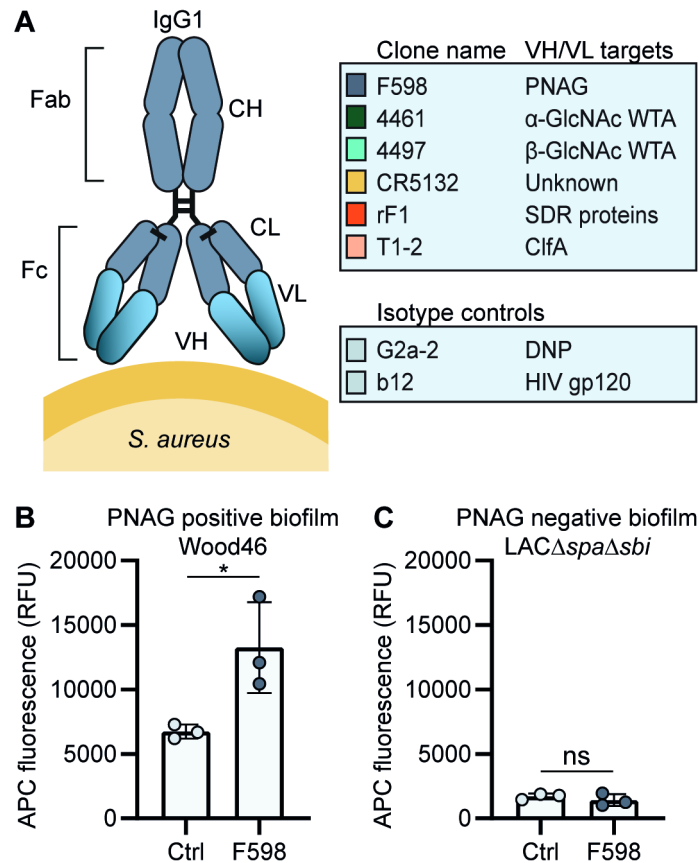


Figure 1. Production of monoclonal antibodies (mAbs) and validation of biofilm. (A) Human IgG1 antibodies are large (150 kDa) proteins, consisting of two functional domains. The fragment antigen binding (Fab) region confers antigen specificity, while the crystallizable fragment (Fc) region drives interactions with the immune system. Each IgG1 is composed of two identical heavy chains and two identical light chains, which all consist of a constant (CH, CL) and a variable (VH, VL) domain. A panel of six human IgG1 mAbs that recognize polysaccharide and protein components on the cell surface of *S. aureus* and two nonspecific isotype controls was produced. Variable heavy (VH) and light (VL) chain sequences obtained from different scientific and patent publications were cloned in homemade expression vectors containing human heavy chain (HC) and light chain (LC) constant regions, respectively. (B, C) Biofilms of Wood46 (B) and LAC Δ spa Δ sbi (C) were grown for 24 hr and incubated with 66 nM F598-IgG1 or ctrl-IgG1 (G2a-2). mAb binding was detected using APC-labeled anti-human IgG antibodies and a plate reader and plotted as fluorescence intensity per well. Data represent mean + SD of three independent experiments. A ratio paired *t*-test was performed to test for differences in antibody binding versus control and displayed only when significant as * $p \leq 0.05$, ** $p \leq 0.01$, *** $p \leq 0.001$, or **** $p \leq 0.0001$.

4461-IgG1 and 4497-IgG1 against WTA recognize PNAG-positive and PNAG-negative *S. aureus* biofilm.

Next, we tested the binding of other mAbs to *S. aureus* biofilms, starting with two well-defined antibodies recognizing WTA, the most abundant glycopolymer on the surface of *S. aureus*⁵⁷. mAbs 4461 and 4497 recognize different forms of WTA: while 4461 binds WTA with α -linked GlcNAc, 4497 recognizes β -linked GlcNAc^{38,39}. The extent to which WTA is modified with GlcNAc depends both on the presence of genes encoding enzymes responsible for α - or β -glycosylation⁵⁸ and the expression of these genes based on environmental conditions⁵⁹. First, we studied binding of 4461-IgG1 and 4497-IgG1 to exponential planktonic cultures of Wood46



and $LAC\Delta spa\Delta sbi$ (**Figure 2A**). In line with the fact that Wood46 is negative for the enzyme responsible for α -GlcNAc glycosylation of WTA (TarM; ⁵⁹), we observed no binding of 4461-IgG1 to planktonic Wood46. In contrast, 4461-IgG1 bound strongly to planktonic $LAC\Delta spa\Delta sbi$. For 4497-IgG, we observed that 4497-IgG1 bound strongly to planktonic Wood46 cells but very weakly to planktonic $LAC\Delta spa\Delta sbi$ (**Figure 2A**).

Upon studying binding of WTA-specific antibodies to biofilms, we observed that 4497-IgG1 strongly bound to PNAG-positive biofilm formed by Wood46 (**Figure 2B**). While F598-IgG1 exclusively binds PNAG-positive biofilms but not planktonic *S. aureus* (**Figure S2**), 4497-IgG1 can bind *S. aureus* Wood46 in both planktonic and biofilm states (Figure 2A and B). This is important because in the biofilm life cycle planktonic cells can be released from a biofilm and disseminate to other locations in the body ³⁶. Apart from recognizing PNAG-positive biofilms, 4497-IgG1 also bound the PNAG-negative biofilm formed by $LAC\Delta spa\Delta sbi$ (**Figure 2B**). This is remarkable because 4497-IgG1 did not potently bind planktonic $LAC\Delta spa\Delta sbi$ (**Figure 2A**). Finally, we observe that also 4461-IgG1 effectively recognizes PNAG-negative biofilms. In all, these data identify mAbs against WTA as potent binders of PNAG-positive (4497) and PNAG-negative (4461 and 4497) biofilms.

Because we observed background binding of control IgG1 to Wood46 biofilm compared to planktonic Wood46 (**Figure S2**), we wondered whether this could be explained by secreted SpA being incorporated in the biofilm matrix as Wood46 is unable to link secreted SpA to the surface due to a sortase defect ⁶⁰. To test this hypothesis, we performed a binding assay on planktonic versus biofilm Wood46 using nonspecific IgG1, nonspecific IgG3 (which is unable to bind to SpA via the Fc domain ⁶¹, and anti-SpA-IgG3 (binding SpA via the Fab-domain but not the Fc domain). Here, we observed high binding of anti-SpA-IgG3 to Wood46 biofilm (**Figure S3A**) but not planktonic (**Figure S3B**) bacteria. Thus, SpA is incorporated in Wood46 biofilm but is washed away in the planktonic binding assay.



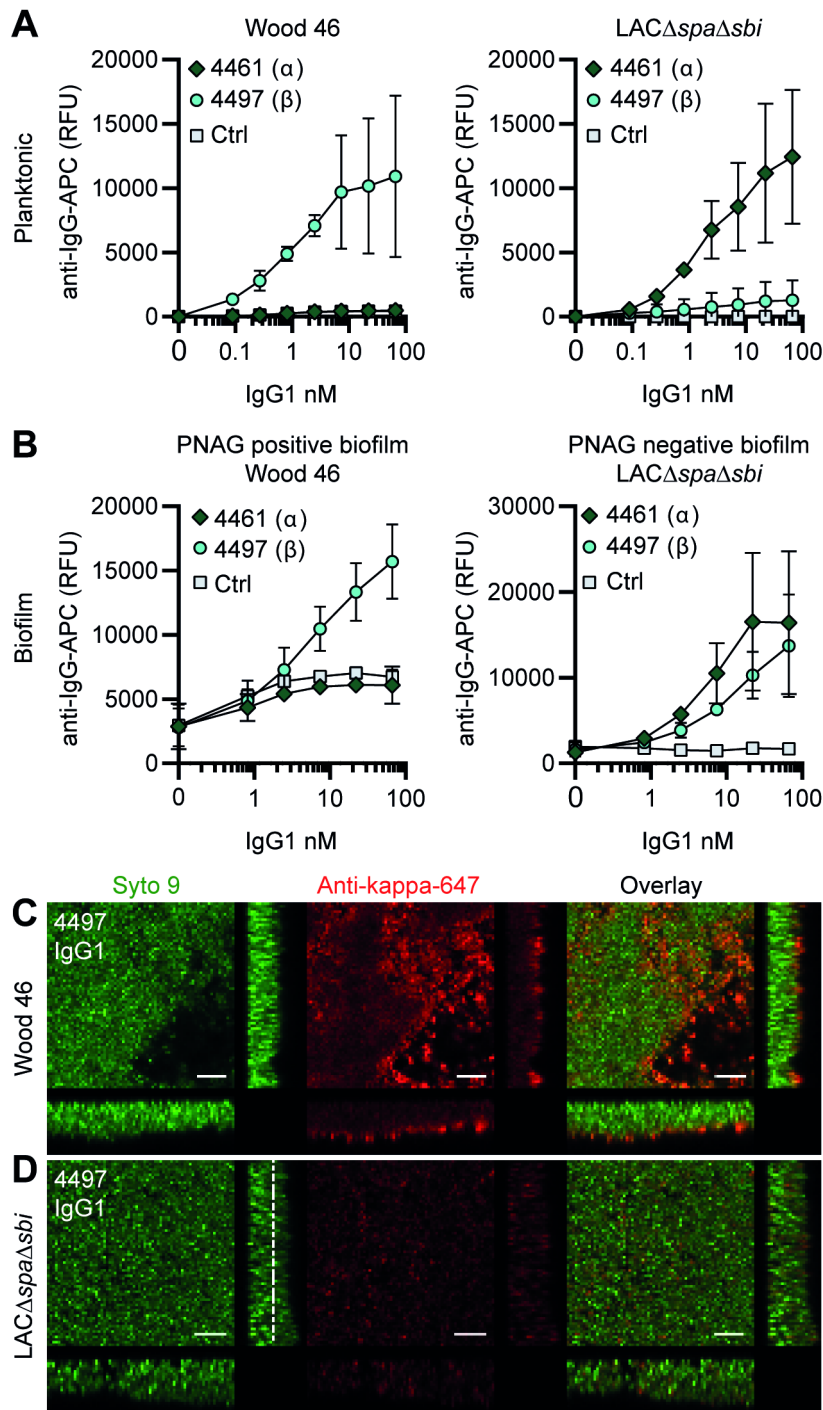


Figure 2. IgG1 monoclonal antibodies (mAbs) against wall teichoic acid (WTA) bind *S. aureus* in planktonic and biofilm mode. (A) Planktonic bacteria of Wood46 (left) and LAC Δ spa Δ sbi (right) were grown to exponential phase and incubated with a concentration range of 4461-IgG1 or 4497-IgG1. mAb binding was detected using APC-labeled anti-human IgG antibodies and flow cytometry and plotted as geoMFI of the bacterial population. (B) Biofilms of Wood46 (left) and LAC Δ spa Δ sbi (right) were grown for 24 hr and incubated with a concentration range of 4461-IgG1 or 4497-IgG1. mAb binding was detected using APC-labeled anti-human IgG antibodies and a plate reader and plotted as fluorescence intensity per well. Data represent mean + SD of three independent experiments. (C, D) Biofilm was grown for 24 hr and incubated with 66 nM IgG1 mAb. Bacteria were visualized by Syto9 (green), and mAb binding was detected by staining with Alexa Fluor 647-conjugated goat-anti-human-kappa F(ab')₂ antibody (red). Orthogonal views are representative for a total of three Z-stacks per condition and at least two independent experiments. Scale bars: 10 μ m.



Using confocal microscopy as an independent method, we confirmed binding of anti-WTA mAbs to in vitro biofilm. Biofilm was cultured in chambered microscopy slides and incubated with IgG1 mAbs or isotype controls (**Figure S4, S5**). Bound mAbs were detected by using AF647-labeled anti-human-kappa-antibodies; bacteria were visualized using DNA dye Syto9. A total of three Z-stacks were acquired at random locations in each chamber of the slide. Z-stacks were visualized as orthogonal views. Using this technique, we visualized binding of 4497-IgG1 to PNAG-positive (**Figure 2C**) and PNAG negative biofilm (**Figure 2D**) and binding of 4461-IgG1 to PNAG-negative biofilm (**Figure S4**). Importantly, isotype controls showed no binding (**Figure S4, S5**). In conclusion, we show that mAbs recognizing polysaccharides WTA α -GlcNAc and WTA β -GlcNAc are able to bind their targets when bacteria are growing in biofilm mode.

CR5132-IgG1 discriminates between planktonic bacteria and biofilm

mAb CR5132 was discovered through phage display libraries from human memory B cells (US 2012/0141493 A1) and was selected for binding to staphylococcal colonies scraped from plates. Since such colonies more closely resemble a surface attached biofilm than free-floating cells⁶², we were curious whether this mAb could recognize biofilm. Intriguingly, CR5132-IgG1 showed almost no detectable binding to exponential planktonic LAC Δ spa Δ sbi or Wood46 (**Figure 3A**), but it bound strongly to both PNAG-negative and PNAG-positive biofilms formed by these strains (**Figure 3B**). Confocal microscopy confirmed CR5132-IgG1 binding to PNAG-positive (**Figure 3C**) and PNAG-negative biofilms (**Figure 3D**). The ability of CR5132-IgG1 to target both types of *S. aureus* biofilms and to discriminate between planktonic bacteria and biofilm makes CR5132 a unique and interesting mAb. Because of the interesting binding phenotype of CR5132-IgG1, we performed experiments to identify its target. LTA was originally identified as one of the targets of CR5132 (US 2012/0141493 A1), but the quality of commercial LTA preparations varies greatly and often contains other components^{63,64}. Therefore, we first tested CR5132-IgG1 binding to *S. aureus* purified cell wall components LTA and peptidoglycan coated on ELISA plates. As a positive control, we used the established A120-IgG1, which is known to bind to LTA (EP2027155A2). Interestingly, we could not detect CR5132-IgG1 binding to LTA (**Figure S6A**) or peptidoglycan (**Figure S6B**), while A120-IgG1 showed detectable binding to LTA. Next, we tested CR5132-IgG1 binding to pure α -GlcNAc or β -GlcNAc WTA structures. To do this, we used magnetic beads that were artificially coated with the WTA backbone and then glycosylated by recombinant TarM, TarS, or TarP, resulting in pure β 1,4-GlcNAc, β 1,3- GlcNAc, or α 1,4-GlcNAc WTA structures in their natural conformation on a surface⁶⁵. This way, we identified WTA β -GlcNAc instead of LTA as one of the targets of CR5132 (**Figure S6C**).



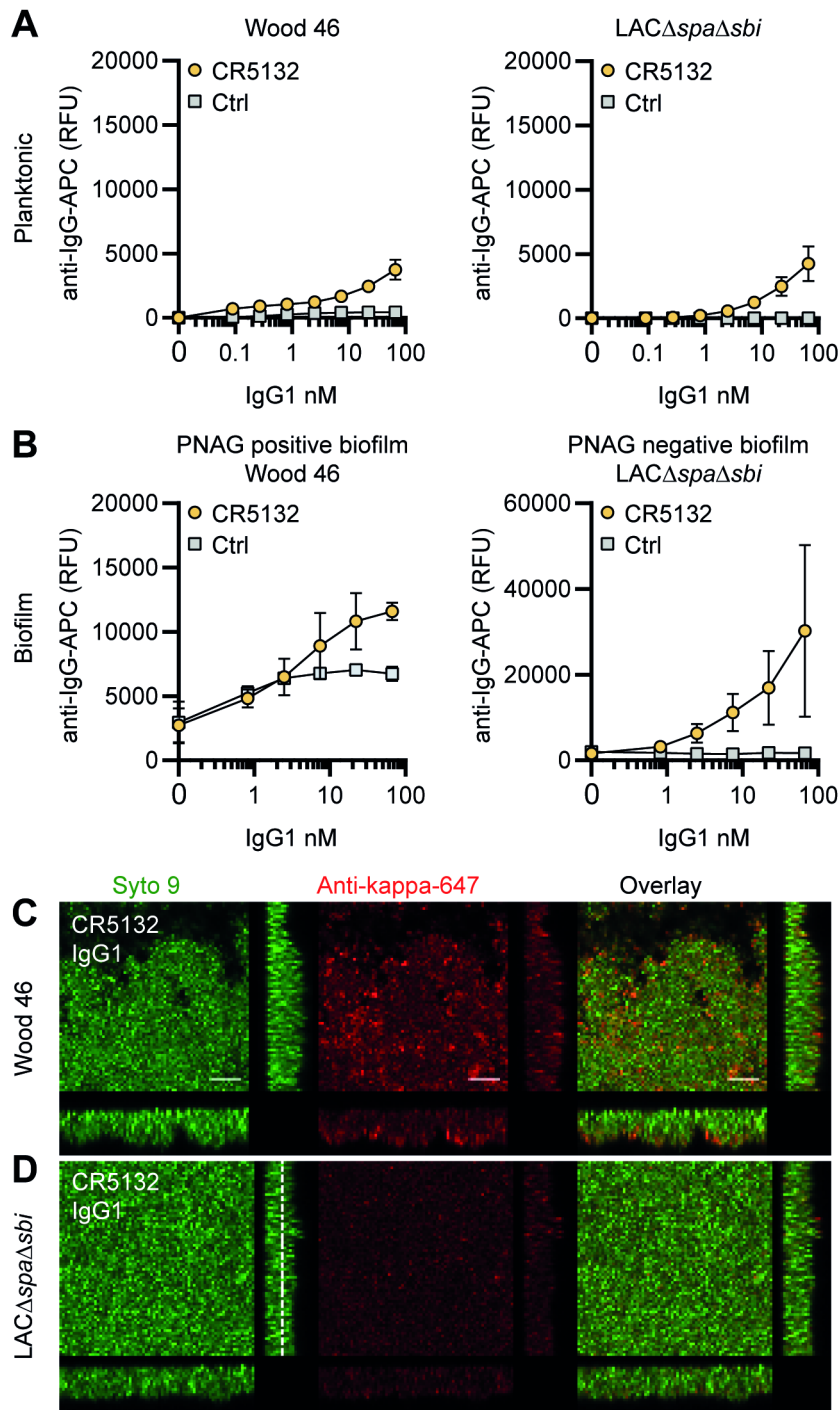


Figure 3. CR5132-IgG1 discriminates between planktonic bacteria and biofilm. (A) Planktonic bacteria of Wood46 (left) and LAC Δ spa Δ sbi (right) were grown to exponential phase and incubated with a concentration range of CR5132-IgG1. Monoclonal antibody (mAb) binding was detected using APC-labeled anti-human IgG antibodies and flow cytometry and plotted as geoMFI of the bacterial population. (B) Biofilms of Wood46 (left) and LAC Δ spa Δ sbi (right) were grown for 24 hr and incubated with a concentration range of CR5132-IgG1. mAb binding was detected using APC-labeled anti-human IgG antibodies and a plate reader and plotted as fluorescence intensity per well. Data represent mean + SD of at least three independent experiments. (C, D) Biofilm was grown for 24hr and incubated with 66 nM IgG1 mAb. Bacteria were visualized by Syto9 (green), and mAb binding was detected by staining with Alexa Fluor 647-conjugated goat-anti-human-kappa F(ab)₂ antibody (red). Orthogonal views are representative for a total of three Z-stacks per condition and at least two independent experiments. Scale bars: 10 μ m.



rF1-IgG1 against the SDR protein family binds S. aureus in planktonic and biofilm form

Finally, we tested whether mAbs recognizing proteins on the staphylococcal cell surface are able to bind *S. aureus* biofilm. mAb rF1 recognizes the SDR family of proteins, which is characterized by a large stretch of serine-aspartate dipeptide repeats (SDR) and includes *S. aureus* ClfA, clumping factor B (ClfB), and SDR proteins C, D, and E and three additional SDR proteins from *Staphylococcus epidermidis*⁶⁶. mAb rF1 recognizes glycosylated SDR repeats that are present in all members of this protein family. Additionally, the well-described mAb T1-2 recognizes SDR family member ClfA^{67,68}. We confirmed effective binding of rF1-IgG1 to exponential planktonic cultures of Wood46 and LAC Δ *spa* Δ *sbi* (**Figure 4A**). In addition, both PNAG-positive and PNAG-negative biofilms formed by these strains were bound by rF1-IgG1 (**Figure 4B**). T1-2-IgG1 binding to planktonic bacteria was only detectable in stationary LAC Δ *spa* Δ *sbi* cultures (**Figure S7**) and not in exponential cultures (**Figure 4A**) because ClfA is known to be expressed in the stationary phase⁶⁹. Furthermore, effective binding of T1-2-IgG1 to LAC Δ *spa* Δ *sbi* PNAG-negative biofilm was detected (**Figure 4B**). In contrast, we could not detect T1-2-IgG1 binding to Wood46 PNAG-positive biofilm (**Figure 4B**). This difference in binding might be explained by a greater abundance of ClfA in PNAG-negative biofilm than PNAG-positive biofilm or PNAG shielding ClfA from T1-2-IgG1 binding. In conclusion, we show that rF1-IgG1 and T1-2-IgG1 bind surface proteins on planktonic bacteria as well as biofilm formed by these bacteria. This means that besides *S. aureus* surface polysaccharides, surface proteins in a biofilm can also be recognized by mAbs.



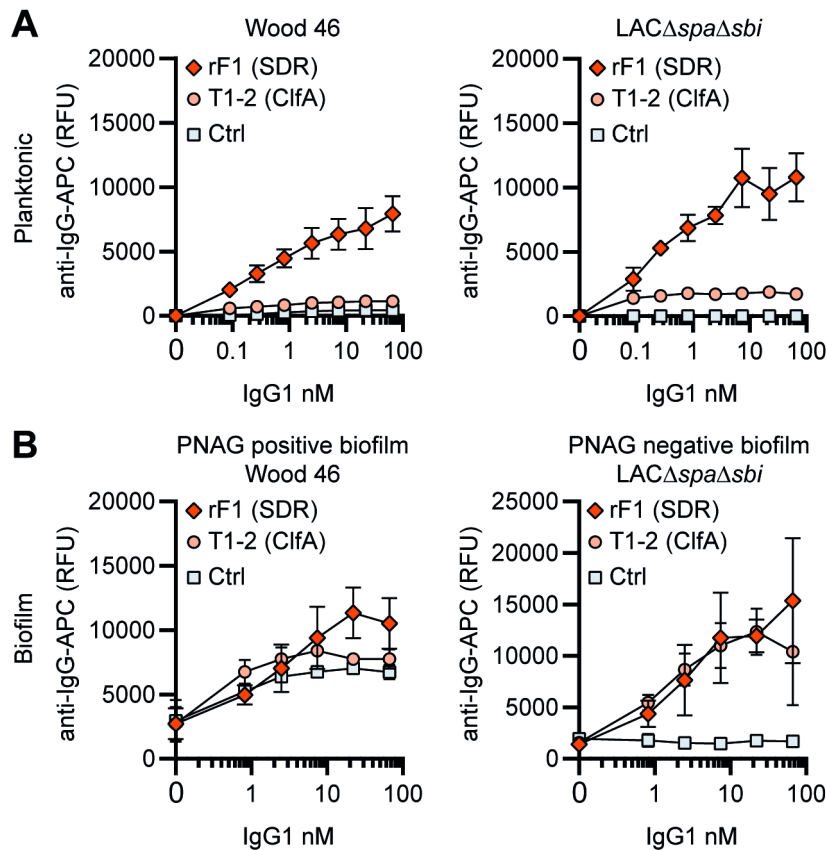


Figure 4. IgG1 monoclonal antibodies (mAbs) against protein components bind planktonic bacteria as well as biofilm. (A) Planktonic bacteria of Wood46 (left) and LACΔspaΔsbi (right) were grown to exponential phase and incubated with a concentration range of rF1-IgG1 or T1-2-IgG1. mAb binding was detected using APC-labeled anti-human IgG antibodies and flow cytometry and plotted as geoMFI of the bacterial population. (B) Biofilms of Wood46 (left) and LACΔspaΔsbi (right) were grown for 24 hr and incubated with a concentration range of rF1-IgG1 or T1-2-IgG1. mAb binding was detected using APC-labeled anti-human IgG antibodies and a plate reader and plotted as fluorescence intensity per well. Data represent mean + SD of three independent experiments.

Comparative binding of mAbs to *S. aureus* biofilm

A direct comparison of all biofilm-binding mAbs revealed 4497-IgG1 as the best binder to PNAG-positive biofilm (**Figure 5A**) and CR5132 as the best binder to PNAG-negative biofilm (**Figure 5B**). Furthermore, all mAbs that bind to exponential planktonic bacteria (**Figure S8**) were able to bind biofilm (**Figure 5**) formed by that strain. Additionally, some mAbs, that is, F598-IgG1 (anti-PNAG) and CR5132-IgG1 (anti-β-GlcNAc WTA), showed enhanced binding to biofilm compared to planktonic bacteria. Thus, we can identify two classes of mAbs: one class recognizing both planktonic bacteria and biofilm, and one class recognizing biofilm only (**Table 1**). Importantly, the mean AF647 fluorescence levels of Z-stacks acquired with the microscope (**Figure S9**) corresponded to our plate reader data (**Figure 5**). As most humans possess antibodies against *S. aureus*, we wondered whether preexisting antibodies might compete with the IgG1 mAbs for binding to epitopes. To test this possibility, biofilm cultures were incubated with AF647-labeled mAbs in the presence of excess IgG (mAb:IgG ratio 1:25) isolated from pooled human serum. This ratio was based on ongoing clinical trials for mAb therapy for *S. aureus* infections (**NCT02296320**), where 2 g and 5 g is administered to patients, reaching a 1:25 mAb:natural IgG ratio in the human circulation. Despite the excess IgG, the AF647-labeled mAbs retained, on average, approximately 60% of the fluorescence they had in



the absence of IgG (**Figure S10**). This indicates that the mAbs are able to recognize *S. aureus* biofilm in the presence of preexisting antibodies.

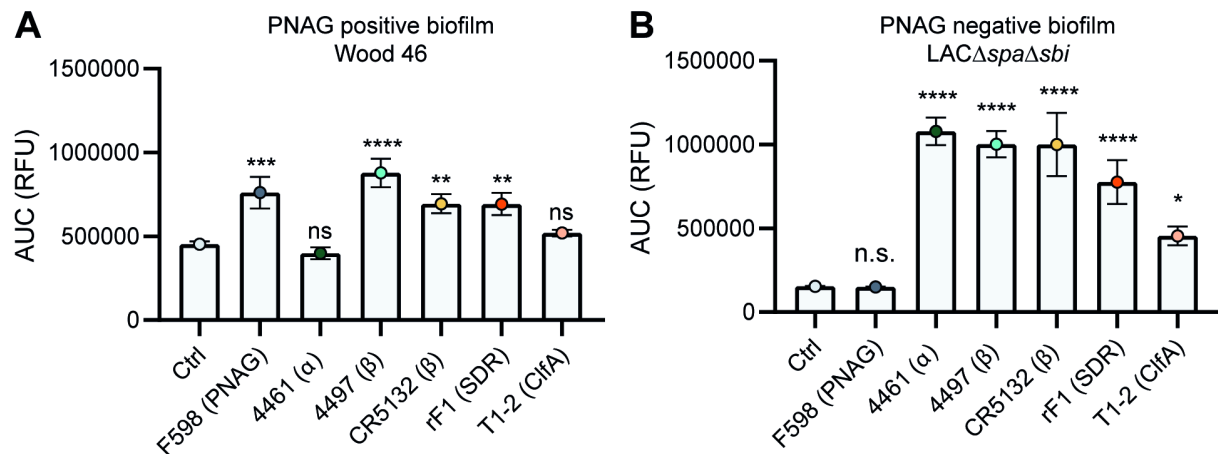


Figure 5. Comparative binding of IgG1 monoclonal antibodies (mAbs) to *S. aureus* biofilm. Biofilms of Wood46 (A) and LACΔspaΔsbi (B) were grown for 24 hr and incubated with a concentration range of IgG1 mAbs. mAb binding was detected using APC-labeled anti-human IgG antibodies and a plate reader. Data are expressed as area under the curve (AUC) of the binding curve (mean + SD) of three independent experiments. One-way ANOVA followed by Dunnett test was performed to test for differences in antibody binding versus control and displayed only when significant as * $p \leq 0.05$, ** $p \leq 0.01$, *** $p \leq 0.001$, or **** $p \leq 0.0001$.

The majority of mAbs recognize PNAG-positive and PNAG-negative biofilm formed by clinical isolates from biofilm-associated infections

Because clinical *S. aureus* isolates express SpA, we wanted to test mAb binding in the presence of this surface protein. To rule out nonspecific binding, we produced all mAbs in the IgG3 subclass, which is unable to bind SpA via the Fc domain⁶¹. Then, we compared our data acquired with LACΔspaΔsbi to the LAC WT strain. Binding of IgG3 mAbs to LAC WT in planktonic (**Figure S11A**) and biofilm (**Figure S11B**) was comparable to binding of IgG1 mAbs to planktonic (**Figure S8**) and biofilm (**Figure 5B**) LACΔspaΔsbi. Interestingly, we observed binding of 4497-IgG3 to LAC WT (**Figure S11**), suggesting that knocking out *spa* and *sbi* altered the WTA glycosylation pattern.

Next, we wanted to test if our data acquired on two model bacterial strains translated to clinical isolates from patients with biofilm-related infections. In literature, no correlation between *S. aureus* biofilm phenotypes (PNAG-positive and PNAG-negative) and the source of clinical biofilm infections has been described. Therefore, we collected a variety of *S. aureus* isolates from endocarditis (n = 4), prosthetic joint infections (PJIs) (n = 16), and catheter tip infections (n = 25). First, we determined whether these clinical isolates produced PNAG-positive or PNAG-negative biofilm by using a crystal violet assay and staining with F598-IgG3 (unable to bind SpA). We could detect significant F598-IgG3 binding to 1/4 endocarditis isolates, 5/25 catheter tip isolates, and 6/16 PJI isolates (**Figure 6A**). This indicates that production of PNAG is not a hallmark of one specific source of biofilm-related infections and that approximately one-third of isolates form PNAG-positive biofilm in vitro. This observation also underlines the importance of identifying mAbs that recognize both types of biofilm. As expected, there was a high variation in the amount of biofilm formation and the amount of PNAG produced (**Figure 6B**). These data show that our model bacterial strains Wood46 and LACΔspaΔsbi represent the different types of biofilm that is formed by clinical isolates. Next, we tested binding of the other anti-*S. aureus* IgG3 mAbs to six PNAG-positive clinical isolates and six PNAG-negative clinical isolates that were good biofilm formers (**Figure 6C**). Most importantly, we found that 4/6 mAbs (4497, CR5132, rF1, T1-2) recognize PNAG-positive and PNAG-negative biofilm



formed by all clinical isolates. Furthermore, we found that mAb 4461 (against α -GlcNAc WTA) recognizes 4 out of total 12 clinical isolates, in line with literature describing 35.7% of clinical isolates being TarM positive ⁷⁰.

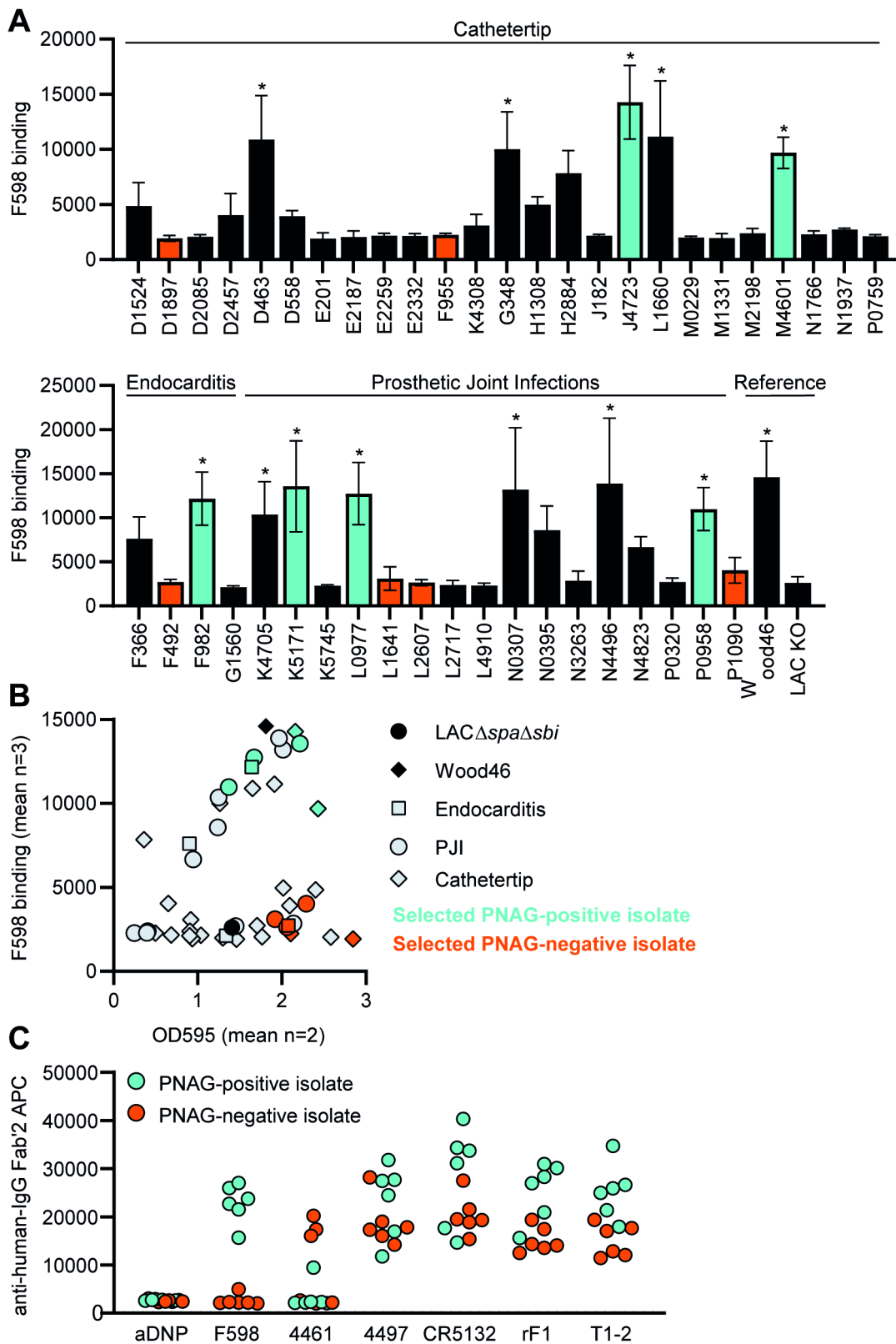


Figure 6. Binding of monoclonal antibodies (mAbs) to *S. aureus* clinical isolate biofilm. (A) Biofilm of clinical isolates derived from catheter tip, endocarditis, and prosthetic joint infections (PJIs) was grown



for 24 hr and incubated with 33 nM F598-IgG3. mAb binding was detected using APC-labeled anti-human IgG antibodies and a plate reader. (B) Scatter plot of F598-IgG3 binding to isolates and biofilm adherent biomass measured by crystal violet staining after mAb binding assay. Isolates selected for (C) are indicated. (C) Biofilms of clinical isolates was grown for 24 hr and incubated with 33 nM IgG3 mAbs. mAb binding was detected using APC-labeled anti-human IgG antibodies and a plate reader. Data (A) represent mean + SD of three independent experiments. One-way ANOVA followed by Dunnett test was performed to test for differences in antibody binding versus LAC KO and displayed only when significant as *. Data (B) represent mean two independent experiments.

Indium-111 labeled 4497-IgG1 localizes to subcutaneously implanted pre-colonized catheter in mice

Lastly, we studied whether mAbs against *S. aureus* biofilm could be used to localize in vivo to a subcutaneous implant pre-colonized with biofilm. Mice received a 5 mm catheter that was pre-colonized with *S. aureus* biofilm in one flank. As an internal control, a sterile catheter was inserted into the other flank. Pre-colonized catheters were generated by incubating catheters with *S. aureus* USA300 LAC (AH4802⁷¹) for 48 hr. Bacterial loads on the catheters before implantation were approximately 4.5×10^7 CFU (**Figure S12**). We selected 4497-IgG1 (against β -GlcNAc WTA) because it potently binds to LAC biofilm in vitro (**Figure 5**). To detect antibody localization in the mouse body, we radiolabeled 4497-IgG1 with indium-111 (¹¹¹In). Two days after implantation of the catheters, mice were injected intravenously with ¹¹¹In-labeled 4497-IgG1 and distribution of the radiolabel was visualized with total-body SPECT-CT scans at 24, 72, and 120 hr after injection. Maximum intensity projections of SPECT/CT scans showed typical distribution patterns for IgG distribution in mice^{72,73}. At 24 hr, activity was detected in blood-rich organs such as heart, lungs, and liver (**Figure 7A, S13**). In line with literature describing 2–3 days half-life of human IgG1 in mice⁷², antibodies were cleared from the circulation and blood-rich organs over time, while the specific activity of radiolabeled 4497-IgG1 around pre-colonized implants remained. Remaining activity that was detected at incision sites of the pre-colonized catheters was likely explained by nonspecific accumulation of antibodies at inflammatory sites.

To quantify the amount of antibody accumulating at pre-colonized and sterile implants, a volume of interest was drawn manually around the implants visible on SPECT-CT. The activity measured in the volume of interest was quantified as a percentage of the total body activity (**Figure 7B**). At all time points, 4497-IgG1 accumulated selectively at the pre-colonized catheter with a mean of 7.7% (24 hr), 8.1% (72 hr), and 6.4% (120 hr) of the total body activity in the region of interest around the pre-colonized implant compared to 1.1% (24 hr), 0.7% (72 hr), and 0.2% (120 hr) around the sterile implant. At each time point, we could detect a significant difference in 4497-IgG1 localization to pre-colonized implants compared to sterile implants. The same results were found in a similar pilot experiment with one mouse and less mAbs administered (**Figure S15**). At the end point (120 hr), thus 5 days after implantation of the catheter, CFU counts on implants (n = 3) were determined and a mean of $\sim 1.1 \times 10^6$ CFU were recovered from pre-colonized implants, whereas no bacteria were recovered from sterile controls (**Figure S12**). Interestingly, when a higher bacterial burden was recovered from a pre-colonized implant (n = 3) at the end point (**Figure S12**, each shape is one mouse), a higher 4497-IgG1 activity was measured at the implant (**Figure 7B**, 120 hr, see corresponding shapes), suggesting that a larger infection recruits more specific antibodies.

We used an SpA-expressing LAC USA300 strain in vivo because *S. aureus* clinical isolates express SpA. To control for nonspecific binding of mAbs via the IgG1 Fc tail, we used nonspecific ¹¹¹In-labeled palivizumab (an antiviral IgG1) in a different set of mice. In two out of four mice, we saw increased ¹¹¹In activity at the colonized implant compared to the sterile implant. ¹¹¹In-labeled palivizumab was detected at pre-colonized catheters with a mean of 5.0%



(24 hr), 5.2% (72 hr), and 2.9% (120 hr) of the total body radiolabel activity and at sterile catheters with 1.4% (24 hr), 0.4% (72 hr), and 0.2% (120 hr) (**Figure S14**). Because the mean ^{111}In -labeled 4497-IgG1 localization to colonized implants was higher than the mean ^{111}In -labeled palivizumab localization at each time point (6.4% vs. 2.9% at 120 hr), localization of ^{111}In -labeled 4497-IgG1 is likely a combination of specific and nonspecific binding at the colonized implant.

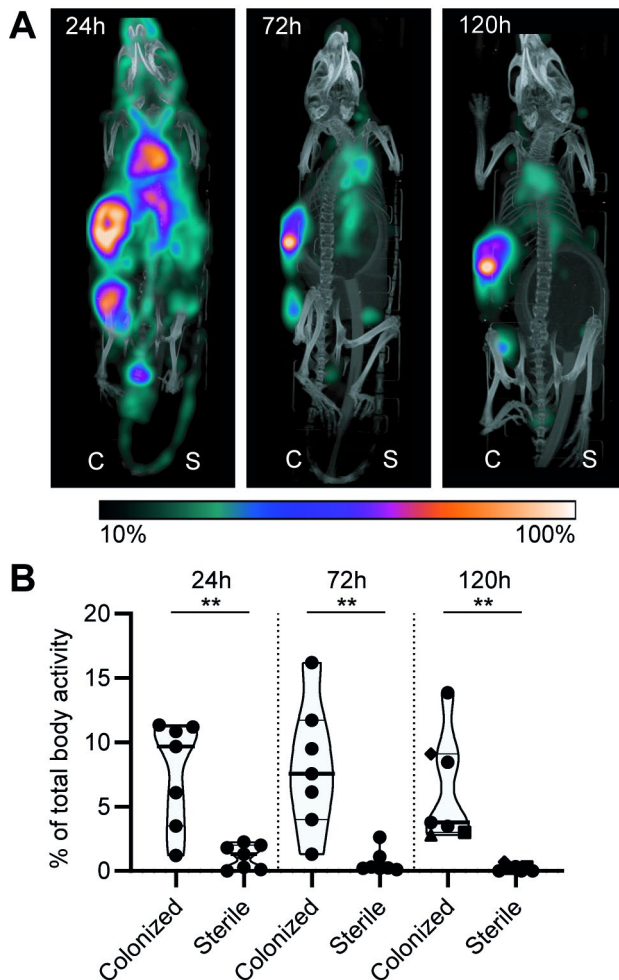


Figure 7. Localization of $[^{111}\text{In}]\text{In-4497-IgG1}$ to a subcutaneous implant pre-colonized with biofilm. Two days after implantation, mice were injected with 7.5 MBq $[^{111}\text{In}]\text{In-4497-IgG1}$ ($n = 7$) and imaged at 24 hr, 72 hr, and 120 hr after injection. (A) Maximum intensity projection (corrected for decay) of a mouse subcutaneously bearing pre-colonized (C; left flank) and sterile (S; right flank) catheter. Additional scans can be seen in the supplementary information (Figure S13). (B) The activity detected in regions of interests was expressed as a percentage of total body activity. Each data point represents one mouse. A two-tailed paired t -test was performed to test for differences in activity in sterile versus colonized implants displayed as $*p \leq 0.05$, $**p \leq 0.01$, $***p \leq 0.001$, or $****p \leq 0.0001$.

DISCUSSION

Identification of mAbs against *S. aureus* biofilms is a crucial starting point for the diagnosis of implant- or catheter-related infections. In this study, we show that previously identified mAbs against *S. aureus* surface structures have the capacity to bind *S. aureus* biofilm. At the start of this study, the only mAb known to react with *S. aureus* biofilm was the F598 antibody recognizing PNAG. F598 was selected to bind to planktonic *S. aureus* MN8m, which is a spontaneous PIA/PNAG-overproducing mutant of strain Mn8⁷⁴. Because numerous studies



have shown that *S. aureus* is capable of forming different biofilm matrices (PNAG-positive and PNAG-negative) ^{4,28,29}, we here focused on identifying antibodies recognizing different biofilm forms. Our study identified several mAbs (**Figures 5 and 6**) capable of binding both types of biofilm (4497-, CR5132-, and rF1-IgG1). This indicates that mAbs directed against WTA or the SDR protein family may be interesting candidates for targeting *S. aureus* biofilm infections. WTA comprises ~30% of the *S. aureus* bacterial surface, and therefore, it is an attractive mAb target ⁵⁷. However, WTA glycosylation can be strain specific and *S. aureus* can adapt WTA glycosylation upon environmental cues ⁵⁹. Indeed, we found that 4461-IgG1 (anti- α -GlcNAc WTA) and 4497-IgG1 (anti- β -GlcNAc WTA) recognized different *S. aureus* strains and their biofilm. Thus, mAbs targeting WTA may best be composed of a mix of mAbs recognizing both α - and β -glycosylated WTA.

Our study also shows that it is possible for antibodies to recognize both *S. aureus* biofilm and planktonic bacteria. This is crucial because during biofilm infection individual bacteria can disperse from the biofilm by secretion of various enzymes and surfactants to degrade the EPS ³⁶. These dispersed bacteria can then disseminate and colonize new body sites or develop into sepsis, which is the most serious complication of biofilm-associated infections. With antibodies recognizing both biofilms and planktonic bacteria (like mAbs recognizing WTA [4461, 4497]) and SDR protein family (rF1), it should be possible to target *S. aureus* bacteria in vivo throughout the entire infection cycle (**Table 1**). We also observed that some mAbs (F598 and CR5132) bind better to biofilm than the planktonic form of *S. aureus*. Such antibodies might be useful for the development of assays to discriminate between biofilm and planktonic cultures. Importantly, none of the mAbs in our panel bound planktonic *S. aureus* but not biofilm produced by the same strain. As our data suggest that the ability to form PNAG dependent biofilm is not a hallmark of certain infections, we think it is important to identify antibodies that recognize both phenotypes. Here, we show that 4497, CR5132, rF1, and T1-2 recognize a large set of clinical isolates derived from biofilm-related infections, being PNAG-dependent and -independent. Potentially, these results can be extended to other bacterial species such as *S. epidermidis*, which is the other main cause of implant-associated infections. Three mAbs in the panel (rF1⁴⁰, F598⁷⁴, CR5132 [US 2012/0141493 A1]) have been described to bind *S. epidermidis* in its planktonic state.

Table 1. MAb binding to biofilm and planktonic bacteria. Significant binding ($p < 0.05$) of IgG1 mAbs compared to control IgG1 s indicated with “+”, weak binding ($p > 0.05 - p < 0.99$) is indicated with “+/-“ and no significant binding ($p > 0.99$) is indicated with “-“.

Clone	Target	Biofilm		Planktonic	
		PNAG (+)	PNAG (-)	Wood46	LAC $\Delta spa \Delta sbi$
F598	PNAG	+	-	+/-	-
4461	WTA(α)	+/-	+	-	+
4497	WTA(β)	+	+	+	+/-
CR5132	WTA(β)	+	+	+/-	+
rF1	SDR proteins	+	+	+	+
T1-2	ClfA	+/-	+	+/-	+/-

Altogether, our in vitro data suggested that mAbs against *S. aureus* surface antigens may be suited to detect biofilms in vivo. As a proof of principle, we tested ¹¹¹In-labeled 4497-IgG1 localization to a subcutaneously implanted pre-colonized catheter in mice and found increased radiolabel around the colonized implant compared to the sterile implant within 24 hr after mAb injection, suggesting rapid localization of 4497-IgG1 to biofilm in vivo. The nonspecific localization of control-IgG1 to pre-colonized catheters at lower levels than specific IgG1 suggests that localization is a combination-specific binding to target antigens and nonspecific



binding to SpA expressed by *S. aureus*. Of note, we used a pre-colonized implant model and not an infection model where biofilm is developed in vivo. In the latter model, host factors such as fibrinogen will be incorporated in the in vivo biofilm EPS^{75–78}, which is why clinical biofilm is described as very heterogenic. Therefore, it is important to further test mAb binding in different in vivo models such as PJIs and osteomyelitis models.

We consider these results as a good starting point to further evaluate the diagnostic and therapeutic purposes of these mAbs. For advanced diagnostic purposes, specific mAbs could also be coupled to gamma- or positron-emitting radionuclides and then be used to detect the presence of *S. aureus* in a biofilm in a patient or during revision surgery. Alternatively, mAbs could be used in vitro to detect the presence of biofilm on explanted implants. For therapeutic purposes, mAbs that bind to biofilm could function as a delivery vehicle to specifically direct biofilm degrading enzymes, antibiotics, photosensitizers, or alpha-/beta-emitting radionuclides to the site of infection. Alternatively, biofilm-binding mAbs could be tested for their ability to induce the activation of the immune system via the Fc domain⁵. In all cases, the identification of mAbs recognizing *S. aureus* biofilm will have vast utility in the development of diagnostic and therapeutic tools for patients undergoing medical procedures.

METHODS

Expression and isolation of human mAbs

For human mAb expression, variable heavy (VH) and light (VL) chain sequences were cloned in homemade pcDNA3.4 expression vectors containing human heavy chain (HC) and light chain (LC) constant regions, respectively. To generate these homemade HC and LC constant region expression vectors, HC and LC constant regions from pFUSE-CHIg-hG1, pFUSE-CHIg-hG3, and pFUSE-CLIg-hk (Invivogen) were amplified by PCR and cloned separately into pcDNA3.4 (Thermo Fisher Scientific). All sequences used are shown in **Supplementary file 1**. VH and VL sequences were derived from antibodies previously described in scientific publications and patents listed in **Supplementary file 1**. Originally, all antibodies have been described as fully human, except for A120 was raised in mice by immunization with *S. aureus* LTA (EP2027155A2) and T1-2, which was raised in mice by immunization with ClfA⁷⁹ and later humanized to T1-2⁶⁸. CR5132 was discovered using ScFv phage libraries (US 2012/0141493 A1), and F598⁷⁴, 4461, 4497³⁸, and rF1⁴⁰ were cloned from human B cells derived from *S. aureus*-infected patients. For each VH and VL, human codon-optimized genes with an upstream KOZAK sequence and a HAVT20 signal peptide (MACPGFLWALVISTCLEFSMA) were ordered as gBlocks (Integrated DNA Technologies) and cloned into pcDNA3.4 HC and LC constant region expression vectors using Gibson assembly (BIOKE). TOP10F' *Escherichia coli* were used for propagation of the generated plasmids. After sequence verification, plasmids were isolated using NucleoBond Xtra Midi plasmid DNA purification (MACHEREY-NAGEL). For recombinant antibody expression, 2×10^6 cells/ml EXPI293F cells (Life Technologies) were transfected with 1 μ g DNA/ml cells in a 3:2 (LC:HC) ratio and transfected using polyethylenimine HCl MAX (Polysciences). EXPI293F cells were routinely screened negative for mycoplasma contamination. After 4–5 days of expression, IgG1 antibodies were isolated from cell supernatant using a HiTrap protein A column (GE Healthcare) and IgG3 antibodies were isolated with a HiTrap Protein G High Performance column (GE Healthcare) using the Äkta Pure protein chromatography system (GE Healthcare). Antibody fractions were dialyzed overnight in PBS and filter-sterilized through 0.22 μ m Spin-X filters. Antibodies were analyzed by size-exclusion chromatography (GE Healthcare) and separated for monomeric fraction in case aggregation levels were >5%. Antibody concentration was determined by measurement of the absorbance at 280 nm and stored at -20°C .



Bacterial strains and growth conditions

S. aureus strains Wood46 (ATCC 10832)^{46,47,60}, USA300 LAC (AH1263)²⁹, and USA300 LAC Δspa , *sbi::Tn* (AH4116) were used in this study. Strain USA300 LAC Δspa , *sbi::Tn* (AH4116) was constructed by transducing *sbi::Tn* from Nebraska Transposon Library⁸⁰ into USA300 LAC Δspa (AH3052)⁸¹ with phage 11. Strains were grown overnight on sheep blood agar (SBA) at 37°C and were cultured overnight in Tryptic Soy Broth (TSB) before each experiment. For exponential phase planktonic cultures, overnight cultures were sub cultured in fresh TSB for 2 hr. For stationary phase planktonic cultures, overnight cultures in TSB were used.

Biofilm culture

For PNAG-negative biofilm, overnight cultures of LAC or LAC Δspa *sbi::Tn* were diluted to an OD₆₀₀ of 1 and then diluted 1:1000 in fresh TSB containing 0.5% (wt/vol) glucose and 3% (wt/vol) NaCl. 200 μ L was transferred to wells in a flat-bottom 96-well plate (Corning Costar 3598, Tissue Culture treated) and incubated statically for 24 hr at 37°C. To facilitate attachment of PNAG-negative bacteria to the wells, plates were coated overnight at 4°C before inoculation. For experiments with EPS degrading enzymes, plates were coated with 20% human plasma (Sigma) in carbonate–bicarbonate buffer. For IgG1 binding assays, plates were coated with 20 μ g/mL human fibronectin (Sigma) in 0.1 M carbonate–bicarbonate buffer (pH 9.6). PNAG-positive Wood46 biofilms were grown similarly, except that no coating was used and growth medium was TSB supplemented with 0.5% (wt/vol) glucose.

Crystal violet assay

To determine the sensitivity of biofilms to DNase I, 1 mg/mL bovine DNase I (Roche) was added at the same time as inoculation and incubated during biofilm formation for 24 hr. To determine biofilm sensitivity to DspB, 30 nM DspB (MTA-Kane Biotech Inc) was added to 24 hr biofilm and incubated statically for 2 hr at 37°C. Biofilm adherence after treatment with DNase I or DspB compared to untreated controls was analyzed as follows. Wells were washed once with PBS, and adherent cells were fixed by drying plates at 60°C for 1 hr. Adherent material was stained with 0.1% crystal violet for 5 min, and excess stain was removed by washing with distilled water. Remaining dye was solubilized in 33% acetic acid, and biofilm formation was quantified by measuring the absorbance at 595 nm using a CLARIOstar plate reader (BMG LABTECH).

Scanning electron microscopy

Biofilms were grown as described above but on 12 mm round poly-L-lysine-coated glass coverslip (Corning). Coverslips were washed 1 \times with PBS and fixed for 24 hr at room temperature with 2% (v/v) formaldehyde, 0.5% (v/v) glutaraldehyde, and 0.15% (w/v) Ruthenium Red in 0.1 M phosphate buffer (pH 7.4). Coverslips were then rinsed two times with phosphate buffer and post-fixed for 2 hr at 4°C with 1% osmium tetroxide and 1.5% (w/v), potassium ferricyanide (K₃[Fe(CN)₆]) in 0.065 M phosphate buffer (pH 7.4). Coverslips were rinsed once in distilled water followed by a stepwise dehydration with ethanol (i.e., 50%, 70%, 80%, 95%, 2 \times 100%). Samples were then treated stepwise with hexamethyldisilazane (i.e., 50% HMDS/ethanol, 2 \times 100% HMDS) and air-dried overnight. The next day samples were mounted on 12 mm aluminum stubs for SEM using carbon adhesive discs (Agar Scientific), and additional conductive carbon tape (Agar Scientific) was placed over part of the sample to establish a conductive path to reduce charging effects. To further improve conductivity, the



surface of the samples was coated with a 6 nm layer of Au using a Quorum Q150R S sputter coater. Samples were imaged with a Scios FIB-SEM (Thermo Scientific) under high-vacuum conditions at an acceleration voltage of 20 kV and a current of 0.40 nA.

Antibody binding to planktonic cultures

To determine mAb binding capacity, planktonic bacterial cultures were suspended and washed in PBS containing 0.1% BSA (Serva) and mixed with a concentration range of IgG1-mAbs in a round-bottom 96-well plate in PBS-BSA. Each well contained 2.5×10^6 bacteria in a total volume of 55 μ L. Samples were incubated for 30 min at 4°C, shaking (~700 rpm), and washed once with PBS-BSA. Samples were further incubated for another 30 min at 4°C, shaking (~700 rpm), with APC-conjugated polyclonal goat-anti-human IgG F(ab')₂ antibody (Jackson ImmunoResearch, 1:500). After washing, samples were fixed for 30 min with cold 1% paraformaldehyde. APC fluorescence per bacterium was measured on a flow cytometer (FACSVerse, BD). Control bacteria were used to set proper FSC and SSC gate definitions to exclude debris and aggregated bacteria. Data were analyzed with FlowJo (version 10).

Antibody binding to biofilm cultures

To determine mAb binding capacity to biofilm, wells containing 24 hr biofilm were blocked for 30 min with 4% BSA in PBS. After washing with PBS, wells were incubated with a concentration range of IgG1-mAbs, or Fab fragments when indicated, in PBS-BSA (1%) for 1 hr at 4°C, statically. After washing two times with PBS, samples were further statically incubated for 1 hr at 4°C with APC-conjugated polyclonal goat-anti-human IgG F(ab')₂ antibody (Jackson ImmunoResearch, 1:500). Fab fragments were detected with Alexa Fluor 647-conjugated goat-anti-human-kappa F(ab')₂ antibody (Southern Biotech, 1:500). After washing, fluorescence per well was measured using a CLARIOstar plate reader (BMG LABTECH).

Peptidoglycan and LTA ELISA

Peptidoglycan from Wood46 was isolated as described in ⁸², and purified LTA was a kind gift from Sonja von Aulock and Siegfried Morath (University of Konstanz). We coated Maxisorb plates (Nunc) overnight at 4°C with 1 μ g/mL peptidoglycan or LTA. The plates were washed three times with PBS 0.05% Tween, blocked with PBS 4% BSA, and incubated 1 hr with a concentration range of CR5132-IgG1, A120-IgG1 (directed against LTA), or control IgG1. The plates were washed and incubated 1 hr with 1:6000 goat-fab'2-anti-human-kappa-HRP (Southern Biotech). Finally, the plates were washed and developed using 3,3',5,5'-tetramethylbenzidine (Thermo Fisher). The reaction was stopped by addition of 1 N H₂SO₄. Absorption at 450 nm was measured using a CLARIOstar plate reader (BMG LABTECH).

IgG1 binding to WTA glycosylated beads

Synthetic WTA (a kind gift of Jeroen Codee, Leiden University) was immobilized on magnetic beads as in van Dalen et al. ⁶⁵. Shortly, biotinylated RboP hexamers were enzymatically glycosylated by recombinant TarM, TarS, or TarP with UDP-GlcNAc (Merck) as substrate. After 2 hr incubation at room temperature, 5×10^7 pre-washed Dynabeads M280 Streptavidin (Thermo Fisher) were added and incubated for 15 min at room temperature. The coated beads were washed three times in PBS using a plate magnet, resuspended in PBS 0.1% BSA, and stored at 4°C. To determine CR5132 binding capacity, beads were suspended and washed in



PBS/0.05% Tween/0.1% BSA and mixed with a concentration range of CR5132-IgG1 or control IgG1 in a round-bottom 96-well plate in PBS/Tween/BSA. Each well contained 10^5 beads. Samples were incubated for 30 min at 4°C, shaking (~700 rpm), and washed once with PBS/Tween/BSA. Samples were further incubated for another 30 min at 4°C, shaking (~700 rpm), with APC-conjugated polyclonal goat-anti-human IgG F(ab')₂ antibody (Jackson ImmunoResearch, 1:500). After washing, APC fluorescence per bead was measured on a flow cytometer (FACSVerse, BD).

Antibody binding in the presence of human pooled IgG

MAB binding in the presence of human pooled IgG was assessed with mAbs that were directly fluorescently labeled. Briefly, mAbs were labeled with AF647 NHS ester (Thermo Fisher Scientific) by following the manufacturer's protocol. Labeled mAbs were buffer exchanged into PBS using desalting Zeba columns (Thermo Fisher Scientific), checked for degree of labeling (ranging from 2.9 to 4.5), and stored at 4°C. To isolate human pooled IgG, blood was drawn from 22 healthy volunteers and allowed to clot for 15 min at room temperature. After centrifugation for 10 min at $3220 \times g$ at 4°C, serum was collected, pooled, and subsequently stored at -80°C. IgG was isolated from pooled serum as described above. Biofilm cultures were prepared, washed, and incubated as described above. Samples were incubated with 10 µg/mL AF647-conjugated IgG1 mAbs in buffer or buffer containing 250 µg/mL pooled IgG. AF647 fluorescence per well was measured using a CLARIOstar plate reader (BMG LABTECH).

Confocal microscopy of static biofilm

Wood46 and LAC *Δspa sbi::Tn* biofilm were grown in glass-bottom cellVIEW slides (Greiner Bio-One [543079]) similarly as described above. cellVIEW slides were placed in a humid chamber during incubation to prevent evaporation of growth medium. After 24 hr, wells were gently washed with PBS and fixed for 30 min with cold 1% paraformaldehyde, followed by blocking with 4% BSA in PBS. After washing with PBS, wells were incubated with 66 nM IgG1-mAbs in PBS-BSA (1%) for 1 hr at 4°C, statically. After washing two times with PBS, samples were further statically incubated for 1 hr at 4°C with Alexa Fluor 647-conjugated goat-anti-human-kappa F(ab')₂ antibody (Southern Biotech, 1:300) and 6 µM Syto9 (Live/Dead BacLight Bacterial Viability Kit; Invitrogen). Z-stacks at three random locations per sample were collected at 0.42 µm intervals using a Leica SP5 confocal microscope with a HCX PL APO CS 63×/1.40–0.60 OIL objective (Leica Microsystems). Syto9 fluorescence was detected by excitation at 488 nm, and emission was collected between 495 nm and 570 nm. Alexa Fluor 647 fluorescence was detected by excitation at 633 nm, and emission was collected between 645 and 720 nm. Image acquisition and processing was performed using Leica LAS AF imaging software (Leica Microsystems).

Subcutaneous implantation of pre-colonized catheters in mice

To determine in vivo mAb localization to implant-associated biofilm, we subcutaneously implanted pre-colonized catheters in mice, as described in Kadurugamuwa et al.⁸³. Balb/cAnNCrl male mice weighing >20 g obtained from Charles River Laboratories were housed in our Laboratory Animal Facility. 1 hr before surgery, all mice were given 5 mg/kg carprofen. Anesthesia was induced with 5% isoflurane and maintained with 2% isoflurane. Their backs were shaved and the skin was disinfected with 70% ethanol. A 5 mm skin incision was made using scissors after which a 14 gauge piercing needle was carefully inserted subcutaneously at a distance of approximately 1–2 cm. A 5 mm segment of a 7 French



polyurethane catheter (Access Technologies) was inserted into the piercing needle and correctly positioned using a k-wire. The incision was closed using one or two sutures, and the skin was disinfected with 70% ethanol. Mice received one s.c. catheter in each flank. One catheter served as a sterile control, whereas the other was pre-colonized for 48 hr with an inoculum of $\sim 10^7$ CFU *S. aureus* LAC AH4802. Strain AH4802 is identical to AH4807 as reported in Miller et al. ⁷¹. The implantation of sterile and pre-colonized catheters in the left or the right flank was randomized. Before inoculation, the implants were sterilized with 70% ethanol and air dried. The inoculated implants were incubated at 37°C for 48 hr under agitation (200–300 RPM). New growth medium was added at 24 hr to maintain optimal growing conditions. Implants were washed three times with PBS to remove nonadherent bacteria and stored in PBS until implantation or used for determination of viable CFU counts. To this end, implants were placed in PBS and sonicated for 10 min in a Branson M2800E Ultrasonic Waterbath (Branson Ultrasonic Corporation). After sonication, total viable bacterial counts per implant were determined by serial dilution and plating.

Radionuclides and radiolabeling of antibodies

4497-IgG1 (anti- β -GlcNAc WTA) and control IgG1 antibody palivizumab (MedImmune) were labeled with indium-111 (¹¹¹In) using the bifunctional chelator CHXA" as described previously by Allen et al. ⁷². In short, antibodies were buffer exchanged into conjugation buffer and incubated at 37°C for 1.5 hr with a fivefold molar excess of bifunctional CHXA" (Macrocyclics, prepared less than 24 hr before use). The mAb-CHXA" conjugate was then exchanged into 0.15 M ammonium acetate buffer to remove unbound CHXA" and subsequently incubated with approximately 150 kBq ¹¹¹In (purchased as [¹¹¹In]InCl₃ from Curium Pharma) per μ g mAb. The reaction mixture was incubated for 60 min at 37°C after which free ¹¹¹In³⁺ was quenched by the addition of 0.05 M EDTA. Quality control was done by instant thin layer chromatography (iTLC) and confirmed radiolabeling at least 95% radiochemical purity of the antibodies.

USPECT-CT and CFU count

G*power 3.1.9.2 software was used to estimate group sizes for mouse experiments, aiming for a power of 0.95. A minimum of four mice per group was calculated based on the expected difference between 4497-IgG1 localization to sterile implants versus pre-colonized implants and experimental variation obtained in a pilot study. In the event that mAbs were incorrectly injected into the tail vein, mice were excluded from the analyses. Incorrect injection was determined by visual inspection during injection and with SPECT/CT scan, showing radioactivity in the tail tissue instead of the bloodstream.

Two days after subcutaneous implantation of catheters, 50 μ g radiolabeled antibody (7.5 MBq) was injected into the tail vein. Four mice were injected with [¹¹¹In]In-4497-IgG1 and four mice were injected with [¹¹¹In]In-palivizumab. At 24, 72, and 120 hr post injection, multimodality SPECT/CT imaging of mice was performed with a VECTOr⁶ CT scanner (MILabs, The Netherlands) using a MILabs HE-UHR-M mouse collimator with 162 pinholes (diameter, 0.75 mm) ⁸⁴. At 24 hr, a 30 min total-body SPECT-CT scan was conducted under anesthesia. Scanning duration at 72 and 120 hr was corrected for the decay of ¹¹¹In. Immediately after the last scan, mice were sacrificed by cervical dislocation while under anesthetics. The carcasses were stored at -20°C until radiation exposure levels were safe for further processing. Implants were aseptically removed, placed in PBS, and sonicated for 10 min in a Branson M2800E Ultrasonic Waterbath (Branson Ultrasonic Corporation). After sonication, total viable bacterial counts per implant were determined by serial dilution and plating.



Image visualization and SPECT/CT data analyses

The analyzing investigator was blinded for the injection of [^{111}In]-4497-IgG1 or [^{111}In]-palivizumab. Image processing and volume of interest analysis of the total-body SPECT scans were done using PMOD software (PMOD Technologies). SPECT image reconstruction was performed using Similarity Regulated OSEM⁸⁵, using 6 iterations and 128 subsets, and the total-body SPECT volumes were smoothed using a 3D Gaussian filter of 1.5 mm. To quantify the accumulation of ^{111}In around the catheters, regions of interest (ROIs) were delineated on SPECT/CT fusion scans as in Branderhorst et al.⁸⁶. 2D ROIs were manually drawn around the catheters and the full body on consecutive transversal slices that were reconstructed into a 3D volume of interest. Delineating the ROIs was done using an iso-contouring method with a threshold of 0.11. For each ROI, the reconstructed voxel intensity sums (total counts) were related to calibrator dose measurements (kBq). Accumulation of ^{111}In was defined as a percentage of total body activity, calculated as (total activity in the implant ROI/total activity in the body ROI) * 100. Reconstructed 3D body scans were visualized as maximum intensity projections, and the SPECT scale was adjusted by cutting 10% of the lower signal intensity to make the high-intensity regions readily visible.



REFERENCES

1. Arciola, C. R., Campoccia, D. & Montanaro, L. Implant infections: Adhesion, biofilm formation and immune evasion. *Nat. Rev. Microbiol.* **16**, 397–409 (2018).
2. Otto, M. Staphylococcal Biofilms. *Microbiol. Spectr.* **6**, (2018).
3. Schilcher, K. & Horswill, A. R. Staphylococcal Biofilm Development: Structure, Regulation, and Treatment Strategies. *Microbiol. Mol. Biol. Rev.* **84**, (2020).
4. Beenken, K. E. *et al.* Global Gene Expression in Staphylococcus aureus Biofilms. *Society* **186**, 4665–4684 (2004).
5. de Vor, L., Rooijackers, S. H. M. & van Strijp, J. A. G. Staphylococci evade the innate immune response by disarming neutrophils and forming biofilms. *FEBS Lett.* **594**, 2556–2569 (2020).
6. Resch, A., Rosenstein, R., Nerz, C. & Götz, F. Differential gene expression profiling of Staphylococcus aureus cultivated under biofilm and planktonic conditions. *Appl. Environ. Microbiol.* **71**, 2663–2676 (2005).
7. Mah, T. F. C. & O’Toole, G. A. Mechanisms of biofilm resistance to antimicrobial agents. *Trends in Microbiology* vol. 9 34–39 at [https://doi.org/10.1016/S0966-842X\(00\)01913-2](https://doi.org/10.1016/S0966-842X(00)01913-2) (2001).
8. Lowy, F. D. Staphylococcus aureus Infections. *N. Engl. J. Med.* **339**, 520–532 (1998).
9. Tong, S. Y. C., Davis, J. S., Eichenberger, E., Holland, T. L. & Fowler, V. G. Staphylococcus aureus infections: Epidemiology, pathophysiology, clinical manifestations, and management. *Clin. Microbiol. Rev.* **28**, 603–661 (2015).
10. Magill, S. S. *et al.* Multistate point-prevalence survey of health care-associated infections. *N. Engl. J. Med.* **370**, 1198–1208 (2014).
11. Aggarwal, V. K. *et al.* Organism profile in periprosthetic joint infection: pathogens differ at two arthroplasty infection referral centers in Europe and in the United States. *J. Knee Surg.* **27**, 399–406 (2014).
12. Arciola, C. R., An, Y. H., Campoccia, D., Donati, M. E. & Montanaro, L. Etiology of implant orthopedic infections: A survey on 1027 clinical isolates. *Int. J. Artif. Organs* **28**, 1091–1100 (2005).
13. Tursi, S. A. *et al.* Salmonella Typhimurium biofilm disruption by a human antibody that binds a pan-amyloid epitope on curli. *Nat. Commun.* **11**, 1–13 (2020).
14. Raafat, D., Otto, M., Reppschläger, K., Iqbal, J. & Holtfreter, S. Fighting Staphylococcus aureus Biofilms with Monoclonal Antibodies. *Trends Microbiol.* **27**, 303–322 (2019).
15. Lauderdale, K. J., Malone, C. L., Boles, B. R., Morcuende, J. & Horswill, A. R. Biofilm dispersal of community-associated methicillin-resistant Staphylococcus aureus on orthopedic implant material. *J. Orthop. Res.* **28**, 55–61 (2010).
16. Kaplan, J. B. *et al.* Recombinant human DNase i decreases biofilm and increases antimicrobial susceptibility in staphylococci. *J. Antibiot. (Tokyo)*. **65**, 73–77 (2012).
17. Goodman, S. D. *et al.* Biofilms can be dispersed by focusing the immune system on a common family of bacterial nucleoid-associated proteins. *Mucosal Immunol.* **4**, 625–637 (2011).
18. Brockson, M. E. *et al.* Evaluation of the kinetics and mechanism of action of anti-integration host factor-mediated disruption of bacterial biofilms. *Mol. Microbiol.* **93**, 1246–1258 (2014).
19. Estellés, A. *et al.* A high-affinity native human antibody disrupts biofilm from Staphylococcus aureus bacteria and potentiates antibiotic efficacy in a mouse implant infection model. *Antimicrob. Agents Chemother.* **60**, 2292–2301 (2016).
20. van Dijk, B. *et al.* Radioimmunotherapy of methicillin-resistant Staphylococcus aureus in planktonic state and biofilms. *PLoS One* **15**, e0233086 (2020).
21. Soliman, C. *et al.* Structural basis for antibody targeting of the broadly expressed microbial polysaccharide poly-N-acetylglucosamine. *J. Biol. Chem.* **293**, 5079–5089 (2018).
22. Soliman, C., Pier, G. B. & Ramsland, P. A. Antibody recognition of bacterial surfaces and extracellular polysaccharides. *Curr. Opin. Struct. Biol.* **62**, 48–55 (2020).
23. Maira-Litrán, T. *et al.* Immunochemical Properties of the Staphylococcal poly-N-acetylglucosamine Surface Polysaccharide. *Infect. Immun.* **70**, 4433–4440 (2002).



24. Mack, D. *et al.* The intercellular adhesin involved in biofilm accumulation of *Staphylococcus epidermidis* is a linear β -1,6-linked glucosaminoglycan: Purification and structural analysis. *J. Bacteriol.* **178**, 175–183 (1996).
25. Cucarella, C. *et al.* Bap, a *Staphylococcus aureus* surface protein involved in biofilm formation. *J. Bacteriol.* **183**, 2888–2896 (2001).
26. Corrigan, R. M., Rigby, D., Handley, P. & Foster, T. J. The role of *Staphylococcus aureus* surface protein SasG in adherence and biofilm formation. *Microbiology* **153**, 2435–2446 (2007).
27. O’Neill, E. *et al.* A novel *Staphylococcus aureus* biofilm phenotype mediated by the fibronectin-binding proteins, FnBPA and FnBPB. *J. Bacteriol.* **190**, 3835–3850 (2008).
28. D.E., M. *et al.* Temporal and Stochastic Control of *Staphylococcus aureus* Biofilm Development. *MBio* **5**, 1–12 (2014).
29. Boles, B. R., Thoendel, M., Roth, A. J. & Horswill, A. R. Identification of Genes Involved in Polysaccharide-Independent *Staphylococcus aureus* Biofilm Formation. *PLoS One* **5**, e10146 (2010).
30. Mlynek, K. D. *et al.* Genetic and biochemical analysis of cody-mediated cell aggregation in *staphylococcus aureus* reveals an interaction between extracellular DNA and polysaccharide in the extracellular matrix. *J. Bacteriol.* **202**, 1–21 (2020).
31. Rohde, H. *et al.* Polysaccharide intercellular adhesin or protein factors in biofilm accumulation of *Staphylococcus epidermidis* and *Staphylococcus aureus* isolated from prosthetic hip and knee joint infections. *Biomaterials* **28**, 1711–1720 (2007).
32. O’Neill, E. *et al.* Association between methicillin susceptibility and biofilm regulation in *Staphylococcus aureus* isolates from device-related infections. *J. Clin. Microbiol.* **45**, 1379–1388 (2007).
33. Sugimoto, S. *et al.* Broad impact of extracellular DNA on biofilm formation by clinically isolated Methicillin-resistant and -sensitive strains of *Staphylococcus aureus*. *Sci. Rep.* **8**, 2254 (2018).
34. McCarthy, H. *et al.* Methicillin resistance and the biofilm phenotype in *staphylococcus aureus*. *Front. Cell. Infect. Microbiol.* **5**, 1–9 (2015).
35. Fitzpatrick, F., Humphreys, H. & O’Gara, J. P. Evidence for *icaADBC*-independent biofilm development mechanism in methicillin-resistant *Staphylococcus aureus* clinical isolates. *J. Clin. Microbiol.* **43**, 1973–1976 (2005).
36. Lister, J. L. & Horswill, A. R. *Staphylococcus aureus* biofilms: recent developments in biofilm dispersal. *Front. Cell. Infect. Microbiol.* **4**, (2014).
37. Sause, W. E., Buckley, P. T., Strohl, W. R., Lynch, A. S. & Torres, V. J. Antibody-Based Biologics and Their Promise to Combat *Staphylococcus aureus* Infections. *Trends Pharmacol. Sci.* **37**, 231–241 (2016).
38. Lehar, S. M. *et al.* Novel antibody-antibiotic conjugate eliminates intracellular *S. aureus*. *Nature* **527**, 323–328 (2015).
39. Fong, R. *et al.* Structural investigation of human *S. aureus*-targeting antibodies that bind wall teichoic acid. *MAbs* **10**, 979–991 (2018).
40. Hazenbos, W. L. W. *et al.* Novel *Staphylococcal* Glycosyltransferases SdgA and SdgB Mediate Immunogenicity and Protection of Virulence-Associated Cell Wall Proteins. *PLoS Pathog.* **9**, e1003653 (2013).
41. Gonzalez, M. L., Frank, M. B., Ramsland, P. A., Hanas, J. S. & Waxman, F. J. Structural analysis of IgG2A monoclonal antibodies in relation to complement deposition and renal immune complex deposition. *Mol. Immunol.* **40**, 307–317 (2003).
42. Barbas, C. F. *et al.* Molecular profile of an antibody response to HIV-1 as probed by combinatorial libraries. *J. Mol. Biol.* **230**, 812–823 (1993).
43. Saphire, E. O. *et al.* Crystal structure of a neutralizing human IgG against HIV-1: A template for vaccine design. *Science (80-)*. **293**, 1155–1159 (2001).
44. Kabat, E. A., Wu, T. T., Perry, H. M., Gottesman, K. S. & Foeller, C. *Sequences of proteins of immunological interest. Analytical Biochemistry* vol. 138 (1984).
45. Cramton, S. E., Ulrich, M., Götz, F. & Döring, G. Anaerobic Conditions Induce Expression of Polysaccharide Intercellular Adhesin in *Staphylococcus aureus* and *Staphylococcus epidermidis*. *Infect. Immun.* **69**, 4079–4085 (2001).



46. Amend, A., Chhatwal, G. S., Schaeg, W. & Blobel, H. Characterization of immunoglobulin G binding to *Staphylococcus aureus* strain Wood 46. *Zentralblatt für Bakteriologie, Mikrobiologie und Hygiene - Abteilung 1 Original A* **258**, 472–479 (1984).
47. Balachandran, M., Riley, M. C., Bemis, D. A. & Kania, S. A. Complete Genome Sequence of *Staphylococcus aureus* Strain Wood 46. *Genome Announcements* **5**, (2017).
48. Kennedy, A. D. *et al.* Epidemic community-associated methicillin-resistant *Staphylococcus aureus*: Recent clonal expansion and diversification. *Proc. Natl. Acad. Sci. U. S. A.* **105**, 1327–1332 (2008).
49. Voyich, J. M. *et al.* Insights into Mechanisms Used by *Staphylococcus aureus* to Avoid Destruction by Human Neutrophils. *J. Immunol.* **175**, 3907–3919 (2005).
50. Montgomery, C. P. *et al.* Comparison of Virulence in Community-Associated Methicillin-Resistant *Staphylococcus aureus* Pulsotypes USA300 and USA400 in a Rat Model of Pneumonia. *J. Infect. Dis.* **198**, 561–570 (2008).
51. Seybold, U. *et al.* Emergence of Community-Associated Methicillin-Resistant *Staphylococcus aureus* USA300 Genotype as a Major Cause of Health Care--Associated Blood Stream Infections. *Clin. Infect. Dis.* **42**, 647–656 (2006).
52. Carrel, M., Perencevich, E. N. & David, M. Z. USA300 methicillin-resistant *Staphylococcus aureus*, United States, 2000–2013. *Emerg. Infect. Dis.* **21**, 1973–1980 (2015).
53. See, I. *et al.* Trends in Incidence of Methicillin-resistant *Staphylococcus aureus* Bloodstream Infections Differ by Strain Type and Healthcare Exposure, United States, 2005–2013. *Clin. Infect. Dis.* **70**, 19–25 (2020).
54. Haque, N. Z. *et al.* Infective endocarditis caused by USA300 methicillin-resistant *Staphylococcus aureus* (MRSA). *Int. J. Antimicrob. Agents* **30**, 72–77 (2007).
55. Lauderdale, K. J., Boles, B. R., Cheung, A. L. & Horswill, A. R. Interconnections between sigma b, agr, and proteolytic activity in *Staphylococcus aureus* biofilm maturation. *Infect. Immun.* **77**, 1623–1635 (2009).
56. Atwood, D. N. *et al.* Comparative impact of diverse regulatory loci on *Staphylococcus aureus* biofilm formation. *MicrobiologyOpen* **4**, 436–451 (2015).
57. Brown, S., Santa Maria, J. P. & Walker, S. Wall Teichoic Acids of Gram-Positive Bacteria. *Annu. Rev. Microbiol.* **67**, 313–336 (2013).
58. Li, X. *et al.* An accessory wall teichoic acid glycosyltransferase protects *Staphylococcus aureus* from the lytic activity of Podoviridae. *Sci. Rep.* **5**, 17219 (2015).
59. Mistretta, N. *et al.* Glycosylation of *Staphylococcus aureus* cell wall teichoic acid is influenced by environmental conditions. *Sci. Rep.* **9**, 1–11 (2019).
60. Balachandran, M., Giannone, R. J., Bemis, D. A. & Kania, S. A. Molecular basis of surface anchored protein A deficiency in the *Staphylococcus aureus* strain Wood 46. *PLoS One* **12**, e0183913 (2017).
61. Jendeborg, L. *et al.* Engineering of Fc1 and Fc3 from human immunoglobulin G to analyse subclass specificity for staphylococcal protein A. *J. Immunol. Methods* **201**, 25–34 (1997).
62. Serra, D. O., Klauck, G. & Hengge, R. Vertical stratification of matrix production is essential for physical integrity and architecture of macrocolony biofilms of *Escherichia coli*. *Environ. Microbiol.* **17**, 5073–88 (2015).
63. Morath, S., Geyer, A., Spreitzer, I., Hermann, C. & Hartung, T. Structural decomposition and heterogeneity of commercial lipoteichoic acid preparations. *Infect. Immun.* **70**, 938–944 (2002).
64. Morath, S., von Aulock, S. & Hartung, T. Structure/function relationships of lipoteichoic acids. *J. Endotoxin Res.* **11**, 348–356 (2005).
65. van Dalen, R. *et al.* Do not discard *Staphylococcus aureus* WTA as a vaccine antigen. *Nature* **572**, E1–E2 (2019).
66. Josefsson, E. *et al.* Three new members of the serine-aspartate repeat protein multigene family of *Staphylococcus aureus*. *Microbiology* **144**, 3387–3395 (1998).
67. Ganesh, V. K. *et al.* Lessons from the Crystal Structure of the *S. aureus* Surface Protein Clumping Factor A in Complex With Tefibazumab, an Inhibiting Monoclonal Antibody. *EBioMedicine* **13**, 328–338 (2016).



68. Domanski, P. J. *et al.* Characterization of a humanized monoclonal antibody recognizing clumping factor A expressed by *Staphylococcus aureus*. *Infect. Immun.* **73**, 5229–5232 (2005).
69. Wolz, C., Goerke, C., Landmann, R., Zimmerli, W. & Fluckiger, U. Transcription of clumping factor A in attached and unattached *Staphylococcus aureus* in vitro and during device-related infection. *Infect. Immun.* **70**, 2758–2762 (2002).
70. Winstel, V. *et al.* Wall Teichoic Acid Glycosylation Governs *Staphylococcus aureus* Nasal Colonization. *MBio* **6**, (2015).
71. Miller, R. J. *et al.* Development of a *Staphylococcus aureus* reporter strain with click beetle red luciferase for enhanced in vivo imaging of experimental bacteremia and mixed infections. *Sci. Rep.* **9**, (2019).
72. Allen, K., Jiao, R., Malo, M., Frank, C. & Dadachova, E. Biodistribution of a Radiolabeled Antibody in Mice as an Approach to Evaluating Antibody Pharmacokinetics. *Pharmaceutics* **10**, 262 (2018).
73. Yip, V. *et al.* Quantitative cumulative biodistribution of antibodies in mice: Effect of modulating binding affinity to the neonatal Fc receptor. *MAbs* **6**, 689–696 (2014).
74. Kelly-Quintos, C., Cavacini, L. A., Posner, M. R., Goldmann, D. & Pier, G. B. Characterization of the opsonic and protective activity against *Staphylococcus aureus* of fully human monoclonal antibodies specific for the bacterial surface polysaccharide poly-N-acetylglucosamine. *Infect. Immun.* **74**, 2742–2750 (2006).
75. Zapotoczna, M., McCarthy, H., Rudkin, J. K., O’Gara, J. P. & O’Neill, E. An Essential Role for Coagulase in *Staphylococcus aureus* Biofilm Development Reveals New Therapeutic Possibilities for Device-Related Infections. *J. Infect. Dis.* **212**, 1883–1893 (2015).
76. Kwiecinski, J., Kahlmeter, G. & Jin, T. Biofilm formation by *Staphylococcus aureus* isolates from skin and soft tissue infections. *Curr. Microbiol.* **70**, 698–703 (2015).
77. Kwiecinski, J. *et al.* Staphylokinase Control of *Staphylococcus aureus* Biofilm Formation and Detachment Through Host Plasminogen Activation. *J. Infect. Dis.* **213**, 139–48 (2016).
78. Nishitani, K. *et al.* Quantifying the natural history of biofilm formation in vivo during the establishment of chronic implant-associated *Staphylococcus aureus* osteomyelitis in mice to identify critical pathogen and host factors. *J. Orthop. Res.* **33**, 1311–1319 (2015).
79. Hall, A. E. *et al.* Characterization of a Protective Monoclonal Antibody Recognizing *Staphylococcus aureus* MSCRAMM Protein Clumping Factor A. *Infect. Immun.* **71**, 6864–6870 (2003).
80. Fey, P. D. *et al.* A Genetic Resource for Rapid and Comprehensive Phenotype Screening of Nonessential *Staphylococcus aureus* Genes. *MBio* **4**, (2013).
81. Ibberson, C. B. *et al.* *Staphylococcus aureus* hyaluronidase is a CodY-regulated virulence factor. *Infect. Immun.* **82**, 4253–4264 (2014).
82. Timmerman, C. P. *et al.* Induction of release of tumor necrosis factor from human monocytes by staphylococci and staphylococcal peptidoglycans. *Infect. Immun.* **61**, 4167–4172 (1993).
83. Kadurugamuwa, J. L. *et al.* Direct continuous method for monitoring biofilm infection in a mouse model. *Infect. Immun.* **71**, 882–90 (2003).
84. Goorden, M. C. *et al.* VECTor: A preclinical imaging system for simultaneous submillimeter SPECT and PET. *J. Nucl. Med.* **54**, 306–312 (2013).
85. Vaissier, P. E. B., Beekman, F. J. & Goorden, M. C. Similarity-regulation of OS-EM for accelerated SPECT reconstruction. *Phys. Med. Biol.* **61**, 4300–4315 (2016).
86. Branderhorst, W. *et al.* Three-Dimensional Histologic Validation of High-Resolution SPECT of Antibody Distributions Within Xenografts. *J. Nucl. Med.* **55**, 830–837 (2014).



Supplementary information for Chapter 5

Supplementary figures

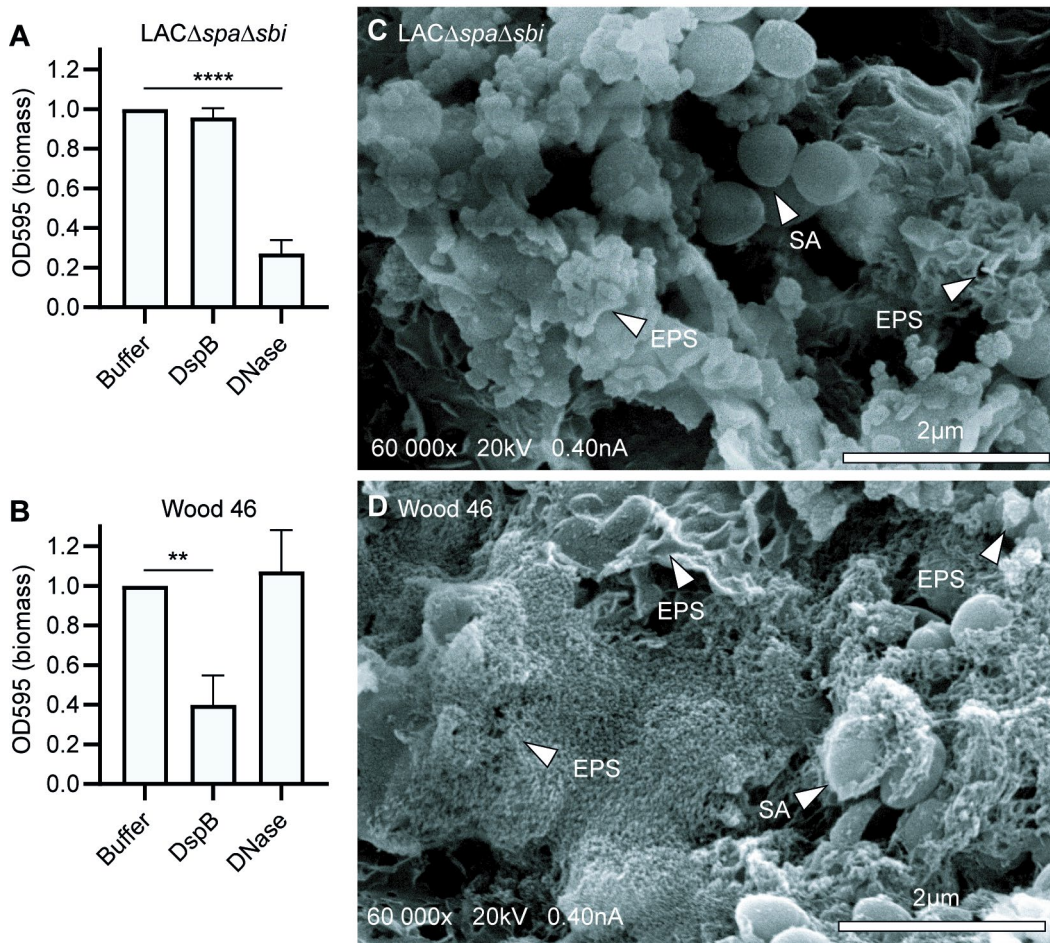


Figure S1. *S. aureus* strains LAC and Wood46 form different types of biofilm. (A, C) Biofilm of *S. aureus* strain LAC Δ spa Δ sbi (A) and Wood46 (C) was grown for 24 hr with buffer or DNase (1 mg/mL). DspB (30 nM) was added after 24 hr of biofilm formation. Adherent biofilm biomass was measured by crystal violet staining. Data represent mean + SD of three independent experiments. Triplicates were averaged and expressed as relative biomass by dividing the OD595 of treated samples by the OD595 of control samples. One-way ANOVA followed by Dunnett test was performed to test for differences in biofilm biomass and displayed only when significant as * $p \leq 0.05$, ** $p \leq 0.01$, *** $p \leq 0.001$, or **** $p \leq 0.0001$. (B, D) Representative scanning electron microscopy (SEM) images of LAC Δ spa Δ sbi (B) and Wood46 (D) biofilms established on glass coverslips following 24 hr incubation at 37°C. SA, *S. aureus*; EPS, extracellular polymeric substance structure.



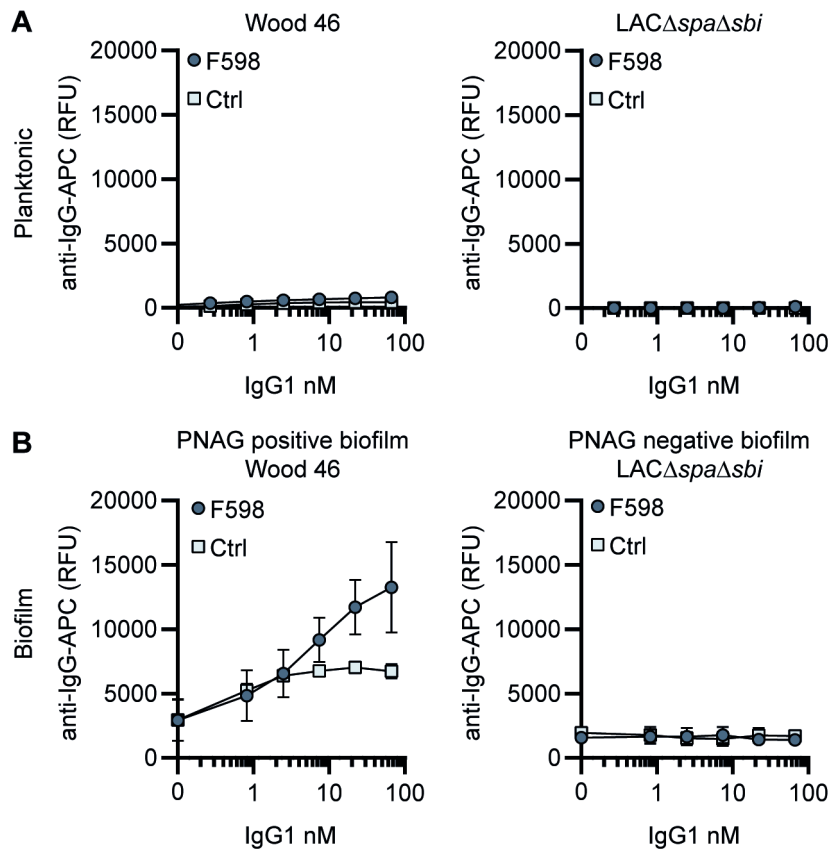


Figure S2. F598-IgG1 binds poly-N-acetyl glucosamine (PNAG)-dependent biofilms specifically. (A) Planktonic bacteria of LAC Δ spa Δ sbi (left) and Wood46 (right) were grown to exponential phase and incubated with a concentration range of F598-IgG1. MAb binding was detected using APC-labeled anti-human IgG antibodies and flow cytometry and plotted as geoMFI of the bacterial population. (B) Biofilm of Wood46 and LAC Δ spa Δ sbi were grown for 24 h and incubated with a concentration range of F598-IgG1. MAb binding was detected using APC-labeled anti-human IgG antibodies and a plate reader and plotted as fluorescence intensity per well. Data represent mean + SD of three independent experiments.

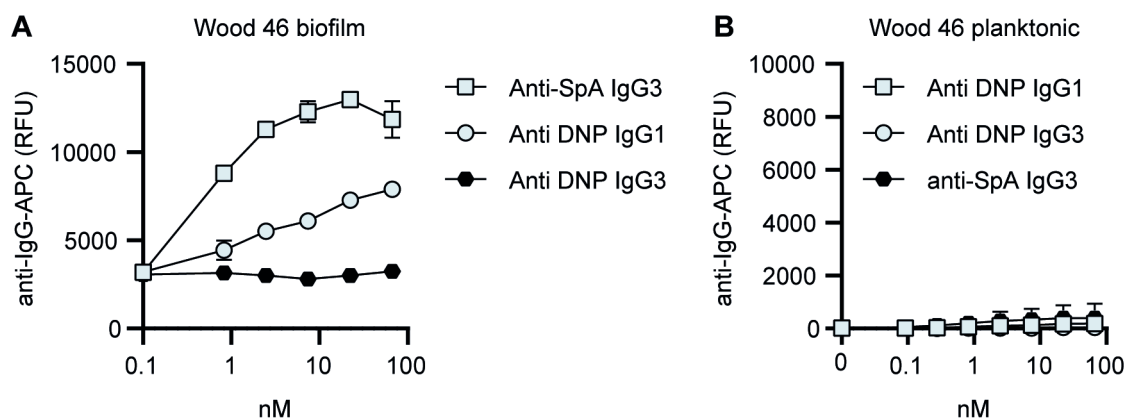


Figure S3. Background control monoclonal antibody (mAb) binding to Wood46 biofilm due to incorporation of secreted SpA in biofilm. (A) Wood46 biofilm was grown for 24 h and incubated with control IgG1, IgG3 and anti-SpA IgG3. MAb binding was detected using anti-human-kappa-AF647 antibodies and a plate reader. (B) Planktonic exponential Wood46 bacteria were incubated with control IgG1, IgG3 and anti-SpA IgG3. MAb binding was detected using anti-human-kappa-AF647 antibodies and flow cytometry. Data represent mean + SD of three independent experiments.



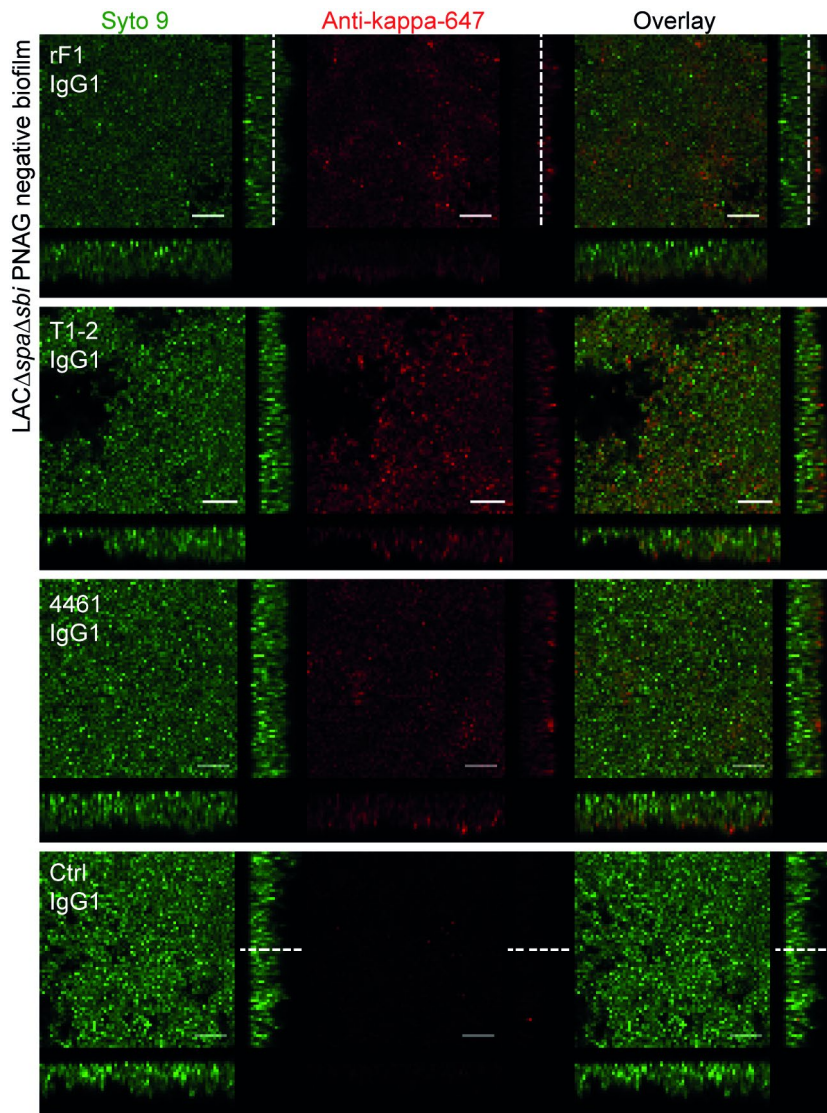


Figure S4. Orthogonal views of poly-*N*-acetyl glucosamine (PNAG)-negative biofilm incubated with IgG1 monoclonal antibodies (mAbs). Biofilm was grown for 24 h and incubated with 66 nM IgG1 mAbs or isotype controls. Bacteria were visualized by Syto 9 (green) and mAb binding was detected by staining with Alexa Fluor 647 conjugated goat-anti-human-kappa F(ab')₂ antibody (red). Syto 9 and AF647 were imaged using 488 and 633 nm lasers. Images are representative for a total of three Z-stacks per condition and two independent experiments. Scale bars: 10 μ m.



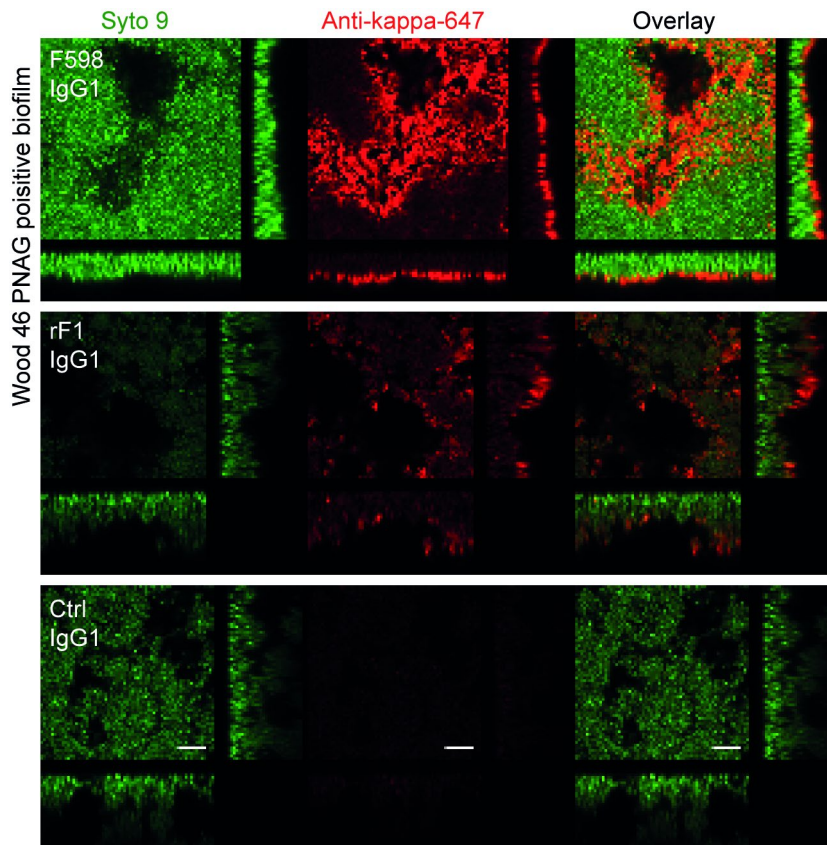


Figure S5. Orthogonal views of poly-N-acetyl glucosamine (PNAG)-positive biofilm incubated with IgG1 monoclonal antibodies (mAbs). Biofilm was grown for 24 h and incubated with 66 nM IgG1 mAbs or isotype controls. Bacteria were visualized by Syto 9 (green) and mAb binding was detected by staining with Alexa Fluor 647 conjugated goat-anti-human-kappa F(ab')₂ antibody (red). Syto 9 and AF647 were imaged using 488 and 633 nm lasers. Images are representative for a total of three Z-stacks per condition and two independent experiments. Scale bars: 10 μ m.



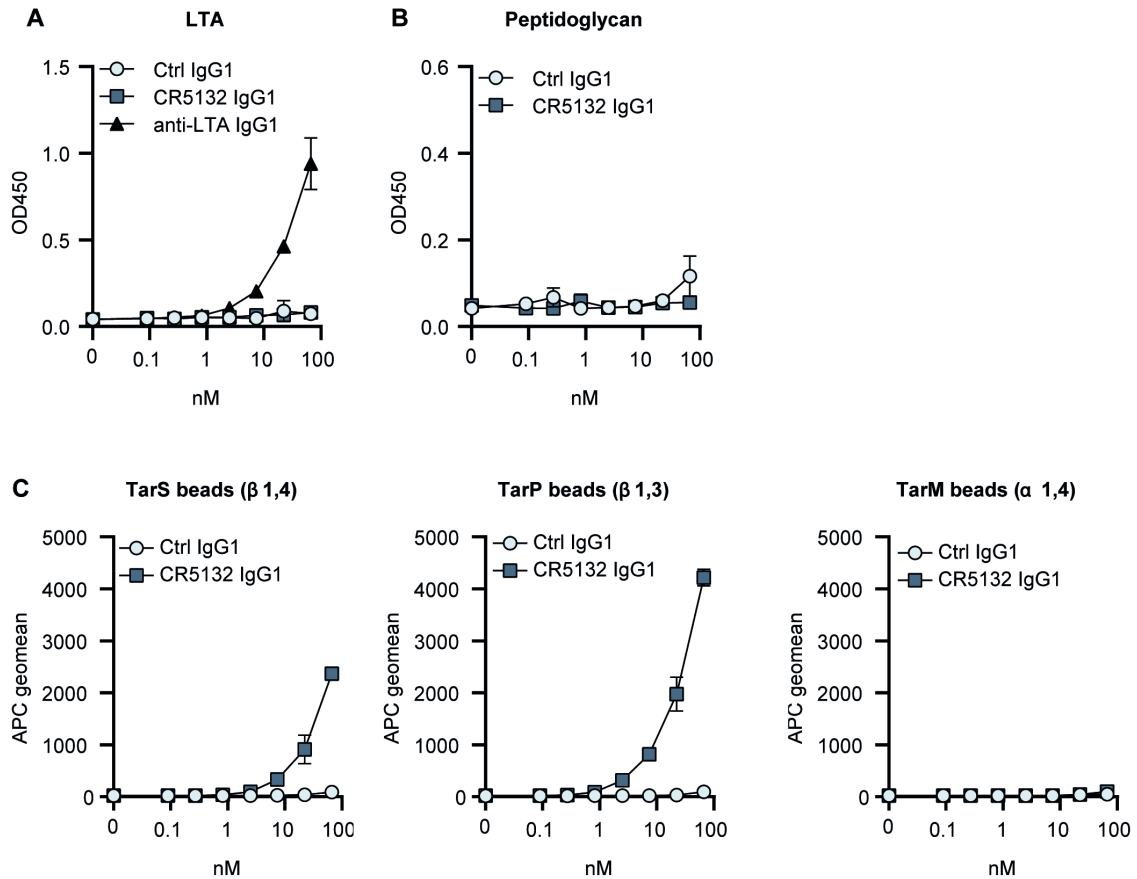


Figure S6. Target identification of CR5132. (A, B) ELISA plates were coated with purified peptidoglycan (A) and LTA (B). Plates were incubated with a concentration range of monoclonal antibodies (mAbs), and mAb binding was detected using anti-human kappa-HRP antibodies. (C) Wall teichoic acid (WTA)-coated beads were incubated with a concentration range of mAbs. mAb binding was detected using APC-labeled anti-human IgG antibodies and flow cytometry and plotted as geoMFI + SD of duplicates in one independent experiment (B, C).

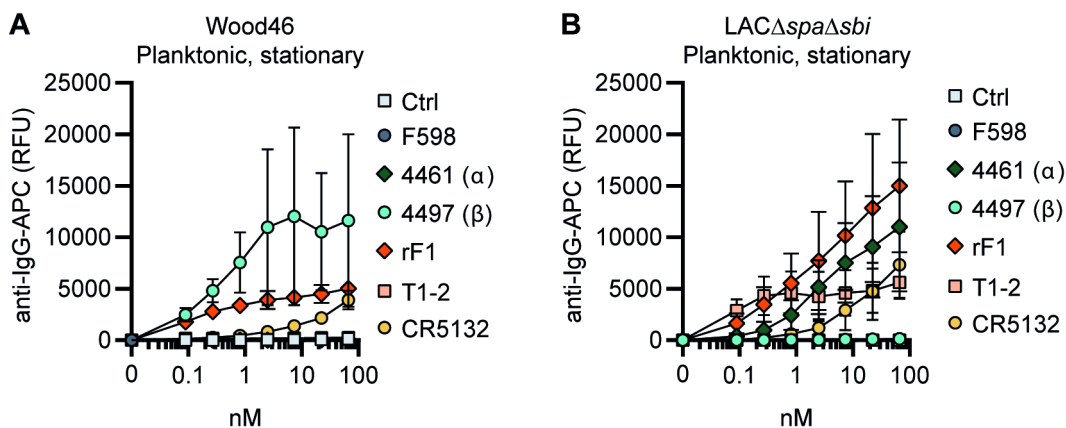


Figure S7. Binding of the monoclonal antibody (mAb) panel to stationary phase planktonic cultures. Planktonic bacteria of Wood46 (A) LAC Δ spa Δ sbi (B) were grown to stationary phase and incubated with a concentration range of mAbs. mAb binding was detected using APC-labeled anti-human IgG antibodies and flow cytometry and plotted as geoMFI of the bacterial population. Data represent mean + SD of three independent experiments.



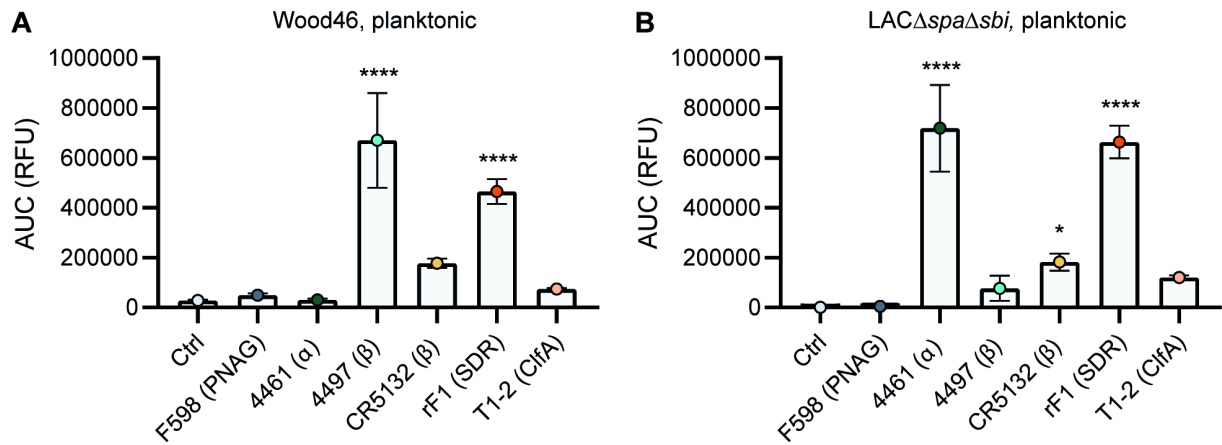


Figure S8. Comparative binding of IgG1 monoclonal antibodies (mAbs) to planktonic bacteria. Planktonic bacteria of Wood46 (A) and $LAC\Delta spa\Delta sbi$ (B) were grown to exponential phase and incubated with a concentration range of IgG1 mAbs. mAb binding was detected using APC-labeled anti-human IgG antibodies and flow cytometry. Data are expressed as area under the curve (AUC) of the binding curve (mean + SD) of three independent experiments. One-way ANOVA followed by Dunnett test was performed to test for differences in antibody binding versus control and displayed only when significant as $*p\leq 0.05$, $**p\leq 0.01$, $***p\leq 0.001$, or $****p\leq 0.0001$.

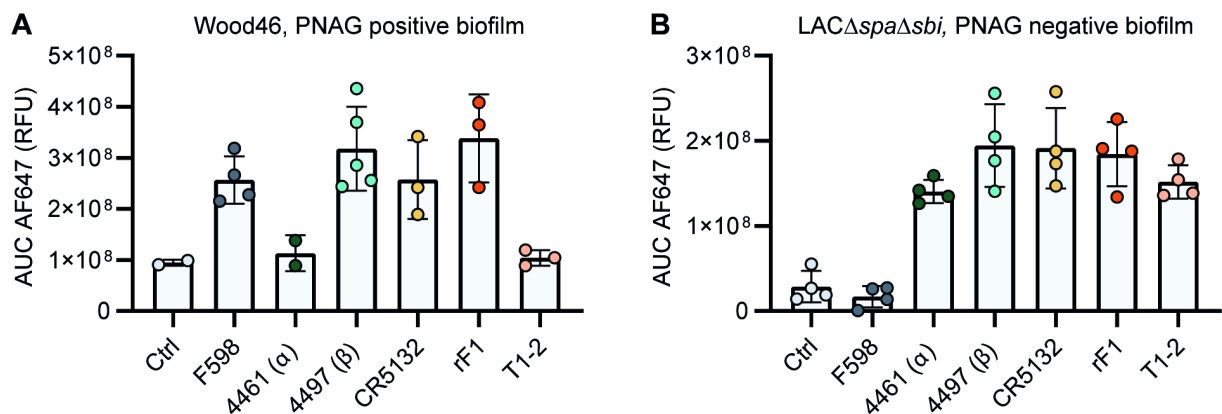


Figure S9. Mean total fluorescence per Z-stack corresponds to plate reader data. The total AF647 signal of obtained Z-stack profiles of biofilms Wood46 (A) and $LAC\Delta spa\Delta sbi$ (B) was calculated using Leica LAS AF imaging software. Data are representative for two independent experiments.

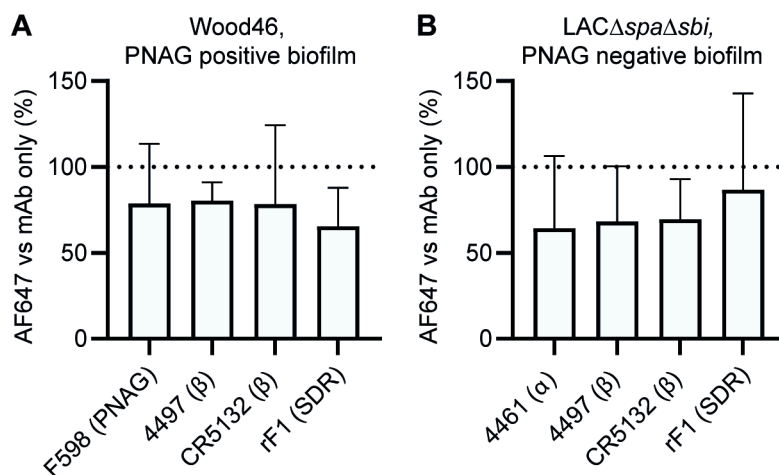


Figure S10. Binding in the presence of pooled serum IgG. Biofilm cultures of Wood46 (A) and LAC Δ spa Δ sbi (B) were incubated with 10 μ g/mL AF647-conjugated IgG1 monoclonal antibodies (mAbs) in buffer or buffer containing 250 μ g/mL pooled IgG. Data are expressed as % relative to mAb binding in buffer of three independent experiments performed in duplicate.

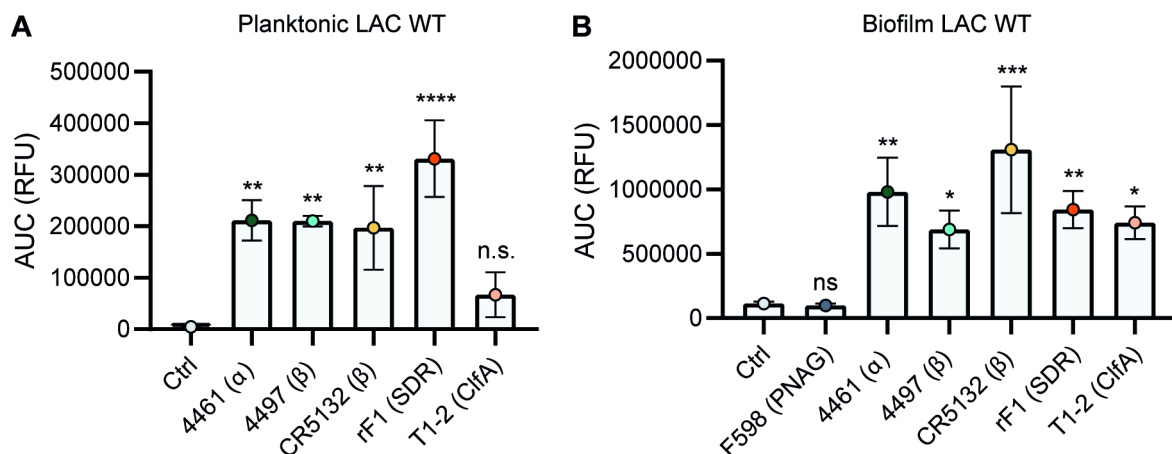


Figure S11. Binding of IgG3 monoclonal antibodies (mAbs) to planktonic and biofilm LAC wild type. (A) Planktonic bacteria of LAC WT (AH1263) were grown to exponential phase and incubated with a concentration range of IgG3 mAbs. mAb binding was detected using APC-labeled anti-human IgG antibodies and flow cytometry and plotted as geoMFI of the bacterial population. (B) LAC WT (AH1263) biofilm was grown for 24 hr and incubated with a concentration range of IgG3 mAbs. mAb binding was detected using APC-labeled anti-human IgG antibodies and a plate reader. Data represent mean + SD of three independent experiments. One-way ANOVA followed by Dunnett test was performed to test for differences in antibody binding versus control and displayed only when significant as * $p \leq 0.05$, ** $p \leq 0.01$, *** $p \leq 0.001$, or **** $p \leq 0.0001$.

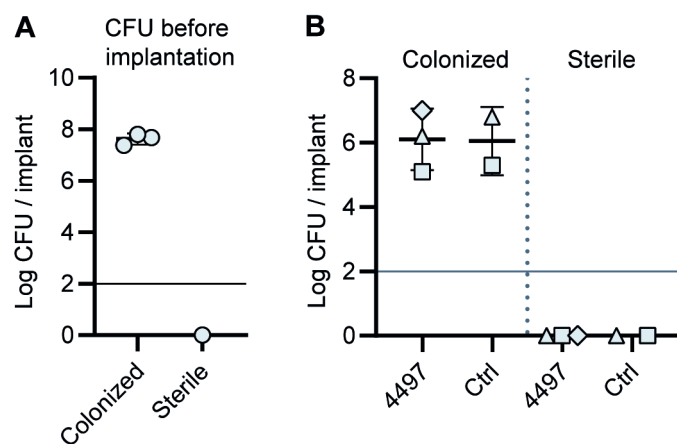


Figure S12. CFU count before implantation and after implantation. (A) 5 mm PU catheter segments were inoculated with *S. aureus* LAC. After 48 hr of incubation, catheters were washed and sonicated and viable CFU counts recovered were determined. Each data point represents an independent experiment. (B) Mice received subcutaneous pre-colonized and sterile catheters and 2 days later were injected with [111 In]In-4497-IgG1 ($n = 3$) or [111 In]In-palivizumab ($n = 2$). At time point 120 hr, mice were sacrificed and catheters were removed to determine CFU counts. Horizontal lines indicate detection limit.



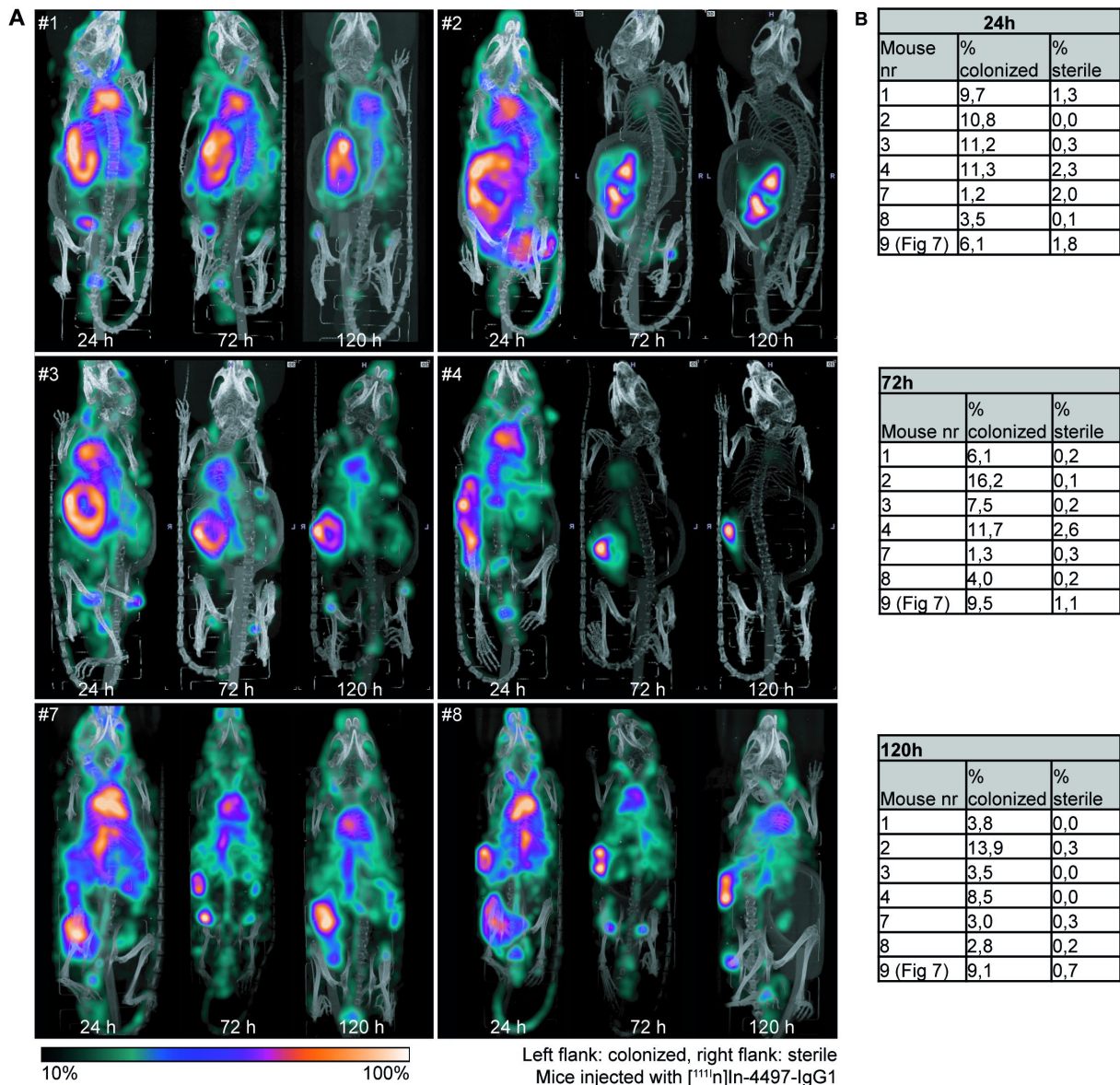
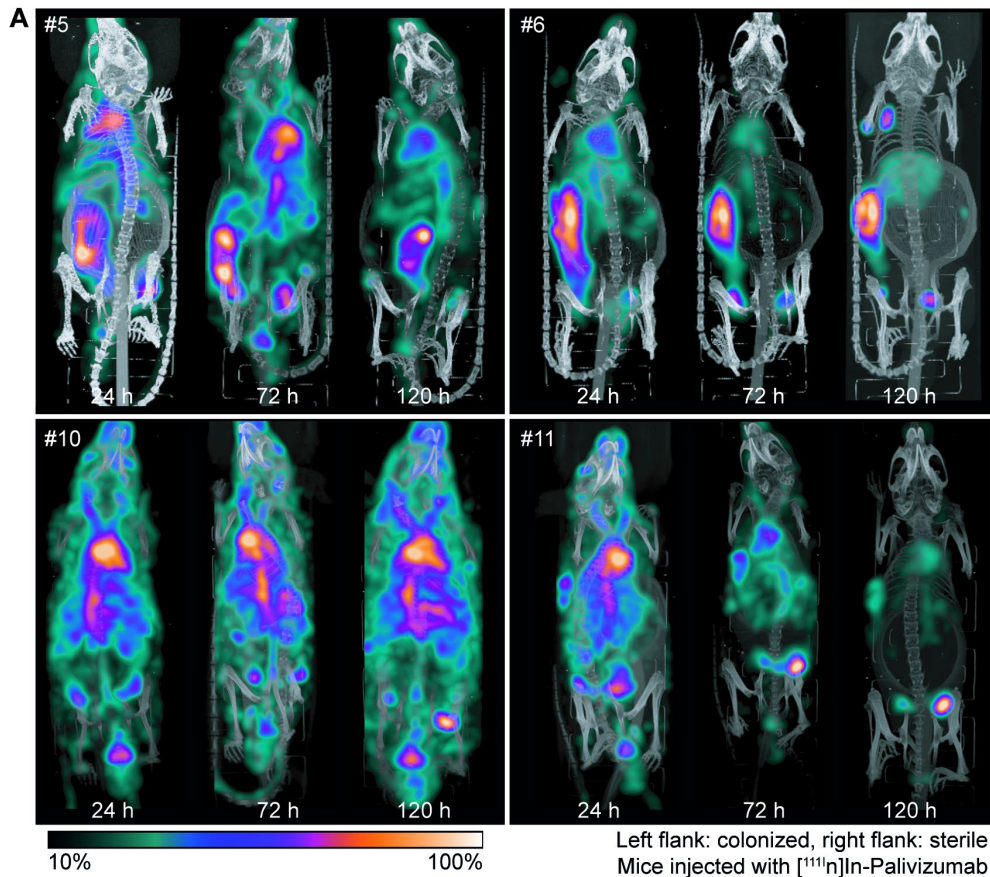


Figure S13. Localization of $[^{111}\text{In}]\text{In-4497-IgG1}$ to subcutaneous implant pre-colonized with biofilm in a mouse model. (A) Maximum intensity projections of $[^{111}\text{In}]\text{In-4497-IgG1}$ injected in mice subcutaneously bearing pre-colonized (left flank) and sterile (right flank) catheters. Implantation of colonized and sterile implants was randomized; however, for clarity, we here display all colonized implants on the left. (B) Corresponding percentages in regions of interest (ROIs) per mouse.





B

24h			72h			120h		
Mouse nr	% colonized	% sterile	Mouse nr	% colonized	% sterile	Mouse nr	% colonized	% sterile
5	5,9	0,5	5	4,0	0,5	5	2,9	0,0
6	11,2	3,1	6	13,7	0,0	6	7,3	0,0
10	2,0	1,3	10	1,6	0,2	10	0,7	0,2
11	0,9	0,8	11	1,8	0,8	11	1,3	0,7

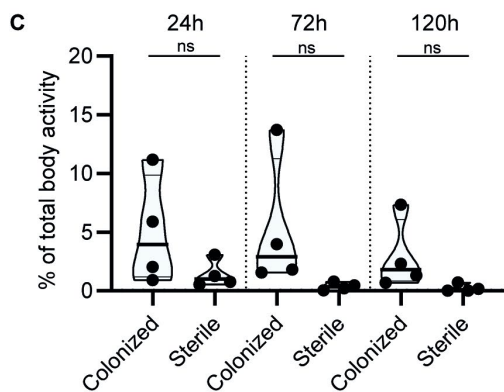


Figure S14. Localization of [¹¹¹In]In-palivizumab to a subcutaneous implant pre-colonized with biofilm. (A) Maximum intensity projections (corrected for decay) of mice subcutaneously bearing pre-colonized (left flank) and sterile (right flank) catheters. Two days after implantation, mice were injected with 7.5 MBq [¹¹¹In]In-palivizumab (n = 4) and imaged at 24 hr, 72 hr, and 120 hr after injection. Implantation of colonized and sterile implants was randomized, but for display all colonized implants are shown at the left flank. (B) Corresponding percentages in regions of interest (ROIs) per mouse. (C) The activity detected in regions of interests was expressed as a percentage of total body activity. Each data point represents one mouse. A two-tailed paired t-test was performed to test for differences in activity in sterile versus colonized implants.



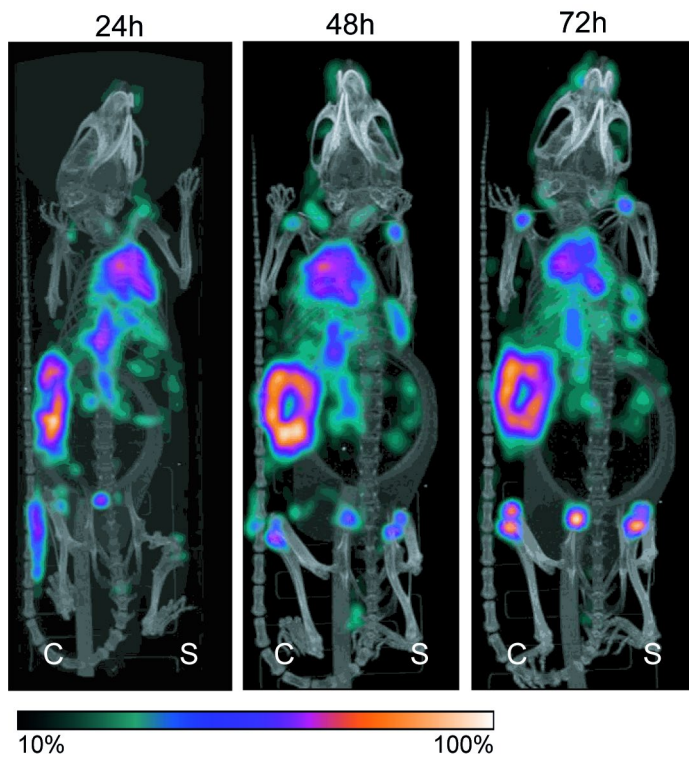


Figure S15. Pilot study for localization of $[^{111}\text{In}]\text{In-4497-IgG1}$ to subcutaneous implant-associated biofilm in a mouse model. One mouse received subcutaneous pre-colonized and sterile catheters and 2 days later was injected with 4 MBq $[^{111}\text{In}]\text{In-4497-IgG1}$. The same mouse was imaged at 24 hr, 48 hr, and 72 hr. Maximum intensity projections of $[^{111}\text{In}]\text{In-4497-IgG1}$ injected in mice subcutaneously pre-colonized (left flank) and sterile (right flank) catheters.



Supplementary information for Chapter 5

Supplementary table

Supplementary File 1. Protein sequences used for human monoclonal antibody production.

Clone, target	Sequence	Reference
VH variable heavy chain		
G2a2, <i>Anti-DNP</i>	DVRLQESGPGLVKPSQSLTCSVTGYSITNSYYWNWIRQFPGNKLEWM VYIGYDGSNNYNPSLKNRISITRDTSKNQFFLKLNSVTTEDTATYYCARA TYYGNYRGFAYWGQGLTVTSA	Gonzalez 2003 ⁴¹
B12, <i>Anti-gp120</i>	QVQLVQSGAEVKKPGASVKVSCQASGYRFSNFVIHWVRQAPGQRFWE MGWINPYNGNKEFSAKFQDRVTFTADTSANTAYMELRSLRSADTAVYY CARVGPYSWDDSPQDNYYMDVWGKGTIVVSS	Barbas 1993 ⁴² Saphire 2001 ⁴³
4461, <i>Anti-WTA(α)</i>	QVQLVQSGAEVRKPGASVKVSCASGYSFTDYMHVWRQAPGGGLEW MGWINPKSGGTNYAQRFGQGRVTMTGDTSSISAAYMDLASLTSDDTAVYY CVKDCGSGGLRDFWGGQGLTVTSS	WO/2014/193722 A1
4497, <i>Anti-WTA(β)</i>	EVQLVESGGGLVQPGGSLRLSCSASGFSFNSFWMHVWRQVPGKGLVWI SFTNNEGTTTAYADSVRGRFIISRDNKNTLYLEMNNLRGEDTAVYYCA RGDGGGLDDWGQGLTVTSS.	WO/2014/193722 A1 Lehar 2015 ³⁸ Fong 2018 ³⁹
CR5132	EVLESGGGLVQPGGSLRLSCSDSGFSFNYYWMTWVRQAPGKGLEWVA NINRDGSDKYHVDSVEGRFTISRDNKNSLYLQMNLRADDA VYFCARGGRITTSWYWRNWGGQGLTVTSS	US 2012/0141493 A1
F598, <i>Anti-PNAG</i>	QVQLQESGPGLVKPSSETLSLTCTVSGGSISGYYWSWIRQPPGKGLEWIGY IHYSRSTNSNPALKSRVTISSDTSKNQLSLRLSSVTAADTAVYYCARDTY YYDSGDYEDAFDIWGGQGLTMVTSS	US/2006/0115486 A1 Seq25 Kelly-Quintos 2006 ⁷⁴ Soliman 2018 ²¹
rF1, <i>Anti-GlcNac pan- SDR</i>	EVQLVESGGGLVQPGGSLRLSCAASGFTLSRFAMSWVRQAPGRGLEWV ASINSGNNPYARSVQYRFTVSRDVSQNTVSLQMNNLRAEDSATYFCAK DHPSSGWPTFDSWGPGLTVTSS	WO/2016/090040 Seq13 Hazebos 2013 ⁴⁰
T1-2, <i>Anti-CfA</i>	QVQLKESGPGLVAPSQSLITCAISGFSLSRYSVHWVRQPPGKGLEWLG IWGGGNTDYNALKSRSLISKDNKSKVFLKMNLSLQDDTAMYYCARK GEFYGYDGFVYWGQGLTVTSA	WO 02072600 A2
A120, <i>Anti-LTA</i>	EVMLVESGGGLVQPKGSLKLSAASGFTFNTYAMNWVRQAPGKGLEW VARIRKSNNYATYADSVKDRFTISRDDSQSMYLYLQMNNLKTEDTAM YYCVRGGKETDYAM DYWGQGTST VSS	WO 03/059259
10919 <i>Anti-SpA</i>	EVQLVQSGAEVKKPGASVKVSCASGYTFTSYMHVWRQAPGGGLEW MGIINPRVGSTSYAQKFQGRVTMTRDTSTSTVYMELSSLRSEDVAVYYC ARGRPLSGTGGHHYFDYWGGQGLTVTSS	US2018/0105584
VL variable light chain		
G2a2, <i>Anti-DNP</i>	DIRMTQTTSSLSASLGDRVTISCRASQDISNYLNWYQKPDGTVKLLIYY TSRLHSGVPSRFSGSGSGTDYSLTISNLEQEDIATYFCQQGNTLPWTFGGG TKLEIK	Gonzalez 2003 ⁴¹
B12, <i>Anti-gp120</i>	EIVLTQSPGTLSPGERATFSCRSSHSIRSRVAWYQHKPGQAPRLVIHG VSNRASGISDRFSGSGSGTDFLTITRVEPEDFALYYCQVYGASSYTFGQ GTKLERK	Barbas 1993 ⁴² Saphire 2001 ⁴³
4461, <i>Anti-WTA(α)</i>	DIQMTQSPDSLAVSLGERATINCKSSQSVLSRANNNYYVAWYQHKPGQP PKLLIYWASTREFGVPDRFSGSGSGTDFLTINSLQAEDVAVYYCQQYYT SRRTFGQGTKVEIK	WO/2014/193722 A1



4497, <i>Anti-WTA(β)</i>	DIQLTQSPDSLAVSLGERATINCKSSQSIFRTSRNKNLLNWWYQQRPGQPPR LLIHWASTRKSVPDRFSGSGFGTDFTLTITSLQAEDVAIYYCQQYFSPPY TFGQGTKLEIK	WO/2014/193722 A1 Lehar 2015 ³⁸ Fong 2018 ³⁹
CR5132	STDIQMTQSPSTLSASVGDRTVITCRASQSISSWLAWYQQKPGKAPKLLI YKASSLESQVPSRFSGSGGTEFTLTISLQPDFFATYYC QQYNSYPLTFGGGTKLEIK	US 2012/0141493 A1
F598, <i>Anti-PNAG</i>	QLVLTQSPSASASLGASVKLTCTLSSGHSNYAIAWHQQQPGKGPRLMK VNRDGSHIRGDGIPDRFSGSTSGAERYLTISLQSEDEADYYCQTWGAGI RVFGGGTKLTVLG	US/2006/0115486 A1 Seq 26 Kelly-Quintos 2006 ⁷⁴ Soliman 2018 ²¹
rF1, <i>Anti-GlcNac pan- SDR</i>	DIQLTQSPSALPASVGDRTVITCRASENVGDWLAWYRQKPGKAPNLLIY KTSILESGVPSRFSGSGGTEFTLTISLQPDFFATYYCQHMYMRFPYTFGQ GTKVEIK	WO/2016/090040_Seq1 4 Hazebos 2013 ⁴⁰
T1-2, <i>Anti-ClfA</i>	NIMMTQSPSSLAVSAGEKVTMSCKSSQSVLYSSNQKNYLAWYQQKPGQ SPKLLIYWASTRESGVPDRFTGSGGTDFTLTISLVQAEDLAVYYCHQYL SSYTFGGGTKLEIK	WO 02072600 A2
A120, <i>Anti-LTA</i>	DIVLSQSPAILSASPGEKVTMTCRASSVSVMHWYQQKPGSSPKPWYAT SNLASGVPARFSGSGGTSYSLTISRVEAEDAATYYCQQWSSNPPTFGGG TKLEIK	WO 03/059259
10919 <i>Anti-SpA</i>	EIVLTQSPATLSVSPGERATLSCQASQDISNYLNWYQQKPGQAPRLLIYD ASNLETGIPARFSGSGGTEFTLTISLQSEDFAVYYCQQVYALPPWTFGG GTKVEIK	US2018/0105584
HC constant regions		
IgG1	ASTKGPSVFPLAPSSKSTSGGTAALGCLVKDYFPEPVTVSWNSGALTSGV HTFPAVLQSSGLYSLSSVVTVPSSSLGTQTYICNVNHKPSNTKVDKKEP KSCDKHTHTCPCPAPELLGGPSVFLFPPKPKDTLMISRTPEVTCVVVDVSH EDPEVKFNWYVDGVEVHNAKTKPREEQYNSTYRVVSVLTVLHQDWLN GKEYKCKVSNKALPAPIEKTKAKAGQPREPQVYTLPPSREEMTKNQVSL TCLVKGFPYPSDIAVEWESNGQPENNYKTPPVLDSDGSFFLYSKLTVDKS RWQQGNVDFCSVMHEALHNHYTQKSLSLSPGK	Kabat 1991 ⁴⁴
IgG3	ASTKGPSVFPLAPCSRSTSGGTAALGCLVKDYFPEPVTVSWNSGALTSGV HTFPAVLQSSGLYSLSSVVTVPSSSLGTQTYTCNVNHKPSNTKVDKRVEL KTPPLGDTTHTCPRCPEPKSCTDTPPCPRCPEPKSCTDTPPCPRCPEPKSCTD PPPCPRCPAPELLGGPSVFLFPPKPKDTLMISRTPEVTCVVVDVSHEDPEV QFKWYVDGVEVHNAKTKPREEQYNSTFRVVSVLTVLHQDWLNGKEYK CKVSNKALPAPIEKTKAKAGQPREPQVYTLPPSREEMTKNQVSLTCLVK GFYPSDIAVEWESSGQPENNYNTTPPMLDSDGSFFLYSKLTVDKSRWQQ GNIFCSVMHEALHNRFQKSLSLSPGK	Derived from pFuse vector (Invivogen)
LC constant regions		
Kappa class	RTVAAPSVFIFPPSDEQLKSGTASVVCLLNNFYPREAKVQWKVDNALQS GNSQESVTEQDSKSTYLSSTLTLSKADYEEKHKVYACEVTHQGLSSPV TKSFNRGEC	Kabat 1991 ⁴⁴





Evaluating the Targeting of a Staphylococcus-aureus-Infected Implant with a Radiolabeled Antibody In Vivo

Based on: | van Dijk B | Hooning van Duijvenbode JFF | de Vor L | Nurmohamed | FRHA | Lam MGEH | Poot AJ | Ramakers RM | Koustoulidou S | Beekman FJ | van Strijp J | Rooijackers SHM | Dadachova E | Vogely HC | Weinans H | van der Wal BCH | *Evaluating the Targeting of a Staphylococcus-aureus-Infected Implant with a Radiolabeled Antibody In Vivo*. International Journal of Molecular Sciences. 2023; 24(5):4374.



ABSTRACT:

Implant infections caused by *Staphylococcus aureus* are difficult to treat due to biofilm formation, which complicates surgical and antibiotic treatment. We introduce an alternative approach using monoclonal antibodies (mAbs) targeting *S. aureus* and provide evidence of the specificity and biodistribution of *S.-aureus*-targeting antibodies in a mouse implant infection model. The monoclonal antibody 4497-IgG1 targeting wall teichoic acid in *S. aureus* was labeled with indium-111 using CHX-A"-DTPA as a chelator. Single Photon Emission Computed Tomography/computed tomographyscans were performed at 24, 72 and 120 h after administration of the ¹¹¹In-4497 mAb in Balb/cAnNCrl mice with a subcutaneous implant that was pre-colonized with *S. aureus* biofilm. The biodistribution of this labelled antibody over various organs was visualized and quantified using SPECT/CT imaging, and was compared to the uptake at the target tissue with the implanted infection. Uptake of the ¹¹¹In-4497 mAbs at the infected implant gradually increased from 8.34 %ID/cm³ at 24 h to 9.22 %ID/cm³ at 120 h. Uptake at the heart/blood pool decreased over time from 11.60 to 7.58 %ID/cm³, whereas the uptake in the other organs decreased from 7.26 to less than 4.66 %ID/cm³ at 120 h. The effective half-life of ¹¹¹In-4497 mAbs was determined to be 59 h. In conclusion, ¹¹¹In-4497 mAbs were found to specifically detect *S. aureus* and its biofilm with excellent and prolonged accumulation at the site of the colonized implant. Therefore, it has the potential to serve as a drug delivery system for the diagnostic and bactericidal treatment of biofilm.



INTRODUCTION

Healthcare-associated infections caused by *Staphylococcus aureus* are responsible for high morbidity and mortality, especially after medical procedures involving prosthetic implants^{1,2}. These infections are difficult to treat due to biofilm formation on the prosthetic material³. As a physical barrier, biofilms hinder the host immune system^{4,5} and can also prevent antibiotics from reaching the bacteria, thus increasing antibiotic resistance. In addition, the bacteria in a biofilm are mostly in a metabolically inactive state and therefore are not susceptible to most antibiotics⁶. These metabolically inactive bacteria can become active again, causing reinfection and potentially increasing antibiotic resistance even further. The treatment of (peri)prosthetic joint infection often involves the long-term use of antibiotics and surgery with or without removal of the implant. Despite this intensive treatment, the outcome is still unpredictable. In addition, older patients with prosthetic joint infection usually have multiple comorbidities, which requires multimodal treatment. Therefore, these patients bear resemblance to oncology patients, with comparably high morbidity and mortality rates. The 5-year mortality of prosthetic joint infections is even higher than that of most forms of breast, prostate and thyroid cancer^{7,8}. Consequently, alternative treatment options need to be explored, and knowledge on therapies applied in oncology could potentially be used to treat prosthetic infections.

Monoclonal antibodies (mAbs), as carriers for radiodiagnostic or radioimmunotherapeutic (RIT) isotopes, may provide an alternative approach to improve the diagnosis and treatment of *S. aureus* biofilm-related infections. Recent developments have seen the resurgent role of mAbs in the diagnosis of invasive fungal infections in patients, as well as in localizing HIV reservoirs in HIV-infected individuals^{9,10}. Radioimmunotherapy is used to treat multiple types of cancer and relies on the antigen-binding characteristics of the mAbs to deliver cytotoxic radiation to target malignant cell¹¹. Antibodies have been proposed as delivery vehicles for the radioimmunotherapy of infectious diseases¹², and a recent review highlights the multiple pre-clinical applications of RIT for therapy for various classes of infectious agents¹³. Theranostics is an emerging field in oncology that combines molecular imaging and specific targeted therapy in the same agent. When combined, non-invasive molecular imaging techniques, such as Single Photon Emission Computed Tomography (SPECT), could potentially elucidate the whole-body distribution of radiolabeled mAbs uptake in relation to the infected area and could predict its bactericidal effect. The key to a successful theranostic approach is a specific vehicle, e.g., proteins, nanobodies or peptides with high affinity and selectivity for the target cells. Furthermore, biodistribution and pharmacokinetics are fundamental aspects of understanding and predicting the efficacy and toxicity of potential theranostic agents.

The monoclonal antibody 4497-IgG1 (anti- β -GlcNAc WTA) specifically recognizes clinically relevant *S. aureus* biofilm types in vitro and targets *S. aureus* biofilm in vivo¹⁴. The antibody 4497-IgG1 targets wall teichoic acids (WTA)^{15,16}, which are found in both the bacterial cell wall and within the extracellular matrix of the biofilm, making it an ideal carrier for antibacterial and biofilm agents, such as enzymes, photosensitizers or therapeutic radionuclides against *S. aureus* biofilms. For example, previous in vitro results showed that this antibody charged with alpha-radiation emitting Bismuth-213 can selectively kill *S. aureus* cells in vitro in both planktonic and biofilm states¹⁷. The next step in the pre-clinical development of this potential radiodiagnostic and therapeutic *S. aureus* targeting antibody is determining its biodistribution throughout other organs. The aim of this study was to analyze the biodistribution and the whole-body clearance of 4497-IgG1 antibodies in a subcutaneous implant infection in mice. The antibody was radiolabeled with Indium-111 (¹¹¹In), after which visualization and quantification was performed using software analyses on SPECT/computed tomography (CT) images.



MATERIALS AND METHODS

S. aureus Targeting Antibodies and Radiolabeling

The 4497-IgG1 (anti- β -GlcNAc WTA) antibodies were synthesized as described before¹⁴, after which the antibodies were conjugated to the bifunctional chelator CHX-A''-DTPA before labeling with ¹¹¹In. CHX-A''-DTPA was chosen because it is a semi-rigid chelator that provides stable labeling at an ambient temperature¹⁸. The labeling of the antibodies with ¹¹¹In was performed as described previously¹⁴. In short, the antibodies were incubated at 37 °C for 1.5 h with a 5-fold molar excess of bifunctional CHX-A''-DTPA (Macrocyclics, Plano, TX, USA) in a conjugation buffer. In order to remove the unbound CHX-A''-DTPA, a mAb-CHX-A''-DTPA conjugate was exchanged into an ammonium acetate buffer using Amicon filters (Millipore, Burlington, MA, USA). The antibody conjugates were prepared less than 24 h before use. Radiolabeling with ¹¹¹In was performed in order to achieve a specific antibody activity of 150 kBq/ μ g. The reaction mixture was incubated for 60 min at 37 °C, after which free ¹¹¹In was bound by quenching the reaction with EDTA solution. The radiolabeling yield was measured by instant thin layer chromatography (iTLC) and confirmed the radiolabeling of at least 95% of the antibodies without the need for further purification.

Biofilm Culture and Subcutaneous Implant Infection Mouse Model

A group of 10 Balb/cAnNCrl male mice weighing >20 g obtained from Charles River Laboratories were used in this experiment. Each mouse received a biofilm infected implant in one flank and a sterile control in the other flank (the left and right side was randomized) as described previously¹⁴. In short, the implants were made by cutting a 5 mm segment of a 7 French polyurethane catheter (Access Technologies, Niles, MI, USA). The infected implants were pre-colonized with the biofilm of a luminescent strain of methicillin-resistant *S. aureus*, USA300 LAC (AH4802)¹⁹. An inoculum of $\sim 10^7$ CFU was used, after which the biofilms were grown for 48 h before implantation. The implantation was performed carefully using a 14-gauge guiding needle through which the catheter implants could be positioned correctly using a K-wire. The implantation of colonized and sterile implants was randomized to the left or right flank of the mouse. Seven mice were successfully injected intravenously in the tail with 50 μ g of radiolabeled antibody (7.5 MBq) two days after subcutaneous implantation. Incorrect injections were determined by SPECT/CT scans at 24 h. Three mice showed high uptake (>25% of total activity) in the tail, and thus were injected intramuscularly and were therefore excluded.

Biodistribution Quantification and Visualization Using SPECT-CT

The accumulation of radiolabeled antibody was visualized using multimodality SPECT/CT imaging (VECTor⁶ CT scanner, MILabs B.V., Houten, The Netherlands). The imaging of mice was performed at 24, 72 and 120 h post-injection using a mouse collimator (HE-UHR-M) with 162 pinholes (diameter 0.75 mm). The scanning time at 24 h was 30 min. Subsequently, scanning time was corrected for the decay of ¹¹¹In at 72 h (a 42 min scan time) and 120 h (a 60 min scan time). All the mice were sacrificed immediately after the last scan by cervical dislocation while under general anesthesia. SPECT image reconstruction was performed using Similarity Regulated OSEM²⁰ with 6 iterations and 128 subsets. PMOD Version 4.103 (PMOD Technologies Ltd., Zurich, Switzerland) was used for image processing and the volume of interest analysis. The SPECT scans were individually corrected for the decay of ¹¹¹In at each timepoint and were smoothed using a 1.5 mm 3D gaussian filter. The biodistribution of the 4497-¹¹¹In was analyzed by quantifying the accumulation of ¹¹¹In in multiple organs and was compared to the uptake at the pre-colonized and control implant sites, as well as their



corresponding incisions¹⁴. Quantification was performed by manually drawing a volume of interest (VOI) in the SPECT-CT-fused scans, outlining the bladder, brain, heart, implant, incision site, liver, lungs, kidneys and the full body. The heart and lungs are in close proximity to each other; therefore, the VOI of the lungs was first drawn to include the heart, after which the VOI of the heart was subtracted. The uptake in the kidneys was measured by outlining the kidney on the side of the control implant only. Due to the high uptake and the position of the infected implant, spillover effects could wrongfully increase the measured uptake in the underlying kidney. The accumulation of ¹¹¹In was defined as the percentage of the injected dose per cm³ (%ID/cm³), calculated as follows: (total activity in the organ or targeted area VOI (MBq)/(volume (cm³) × injected dose (MBq)) × 100%). The previously published data¹⁴ were converted from the percentage of total body activity to %ID/cm³, as this allowed for a more accurate comparison. Additionally, the uptake at the infection site was compared to that of the blood pool (i.e., muscle tissue) by analyzing the infection-to-muscle contrast ratio. The VOI of the muscles in the upper thigh was used as a reference. Finally, the effective and biological half-lives of 4497-¹¹¹In were determined. The effective decay of 4497-¹¹¹In was quantified by measuring the total body activity at 0, 24, 72 and 120 h using software analyses of SPECT-CT images, whereas the total body activity immediately after injection at 0 h represented the injected dose. The biological half-life was calculated using the following formula:

$$T_{effective} = \frac{T_{biological} \times T_{physical}}{T_{biological} + T_{physical}}$$

Statistical Analysis

Statistical analyses were performed using the Statistical Package for the Social Sciences (IBM Corp. Released 2017. IBM SPSS Statistics for Windows, version 25.0. Armonk, NY, USA) in order to determine significant differences between the uptake in different organs and the area of interest using one-way ANOVA followed by Bonferroni's post hoc test. A *p*-value of less than 0.05 was considered a significant difference between the organs and the target implant. The nonlinear regression analysis was performed using GraphPad Prism (GraphPad Software, GraphPad Prism for Windows, version 9.3.0, La Jolla, CA, USA).

RESULTS

The biodistribution of 4497-¹¹¹In was quantified in seven mice at 24, 72 and 120 h. The maximum intensity projections of the SPECT/CT scans showed increased uptake at the infected implant and heart (**Figure 1**). As shown previously¹⁴, 4497 accumulated specifically and continuously at the implant infection site. The uptake was 8.34 ± 2.25 %ID/cm³ around 24 h post-injection, after which the signal gradually increased to 9.15 ± 1.67 %ID/cm³ and 9.22 ± 2.86 %ID/cm³ at 72 h and 120 h, respectively. At all the timepoints, there was a significantly higher accumulation at the implant infection compared to the control implant in each mouse, with 3.9 ± 1.51 %ID/cm³ (24 h), 3.43 ± 0.91 %ID/cm³ (72 h) and 2.73 ± 0.64 %ID/cm³ (120 h). When comparing the uptake in the organs and targeted areas, statistical analyses showed a significantly higher uptake ($11.60 \pm 1.16\%$) in the heart compared to the other organs and the infected implant (*p* ≤ 0.01) at 24 h. Additionally, uptake at the infected implant at 24 h was significantly higher compared to the other organs except for the heart, liver and lungs. There was no significant difference between the uptake in the liver (6.25 ± 0.86 %ID/cm³, *p* = 0.125) and lungs (7.26 ± 0.51 %ID/cm³, *p* = 1.000) compared to the implant infection site. At 72 and



120 h, significantly higher uptake was seen at the implant infection site compared to all the other organs or targeted areas ($p \leq 0.001$), except for the heart with 8.86 ± 1.92 %ID/cm³, which showed no significant reduction relative to the target infection site ($p = 1.000$) with 7.58 ± 0.84 %ID/cm³ ($p = 0.960$), as shown in Figure 2. Additionally, the ratio between the infected implant and the blood pool (i.e., muscle) was 4.79:1 at 24 h, 5.35:1 at 72 h and 5.78:1 at 120 h. The data of individual mice and the results of the statistical analyses are available in the supporting information file.

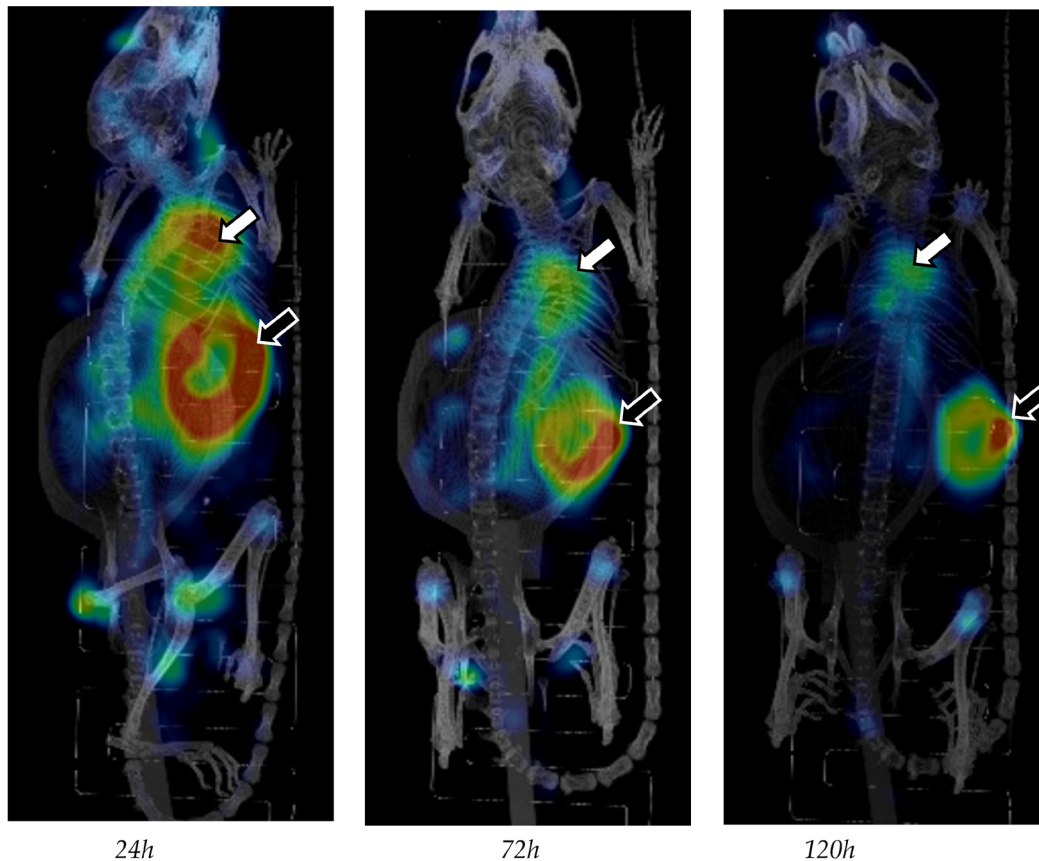


Figure 1. Reconstructed 3D body scans were visualized using maximum intensity projection at 24, 72 and 120 h, and the SPECT scale was adjusted by cutting 10% of the lower signal intensity to make the high-intensity regions readily visible. The white arrow points to the heart and the black arrow points to the infected implant. An increased signal is seen at the hips and knees probably due to detached ¹¹¹In.



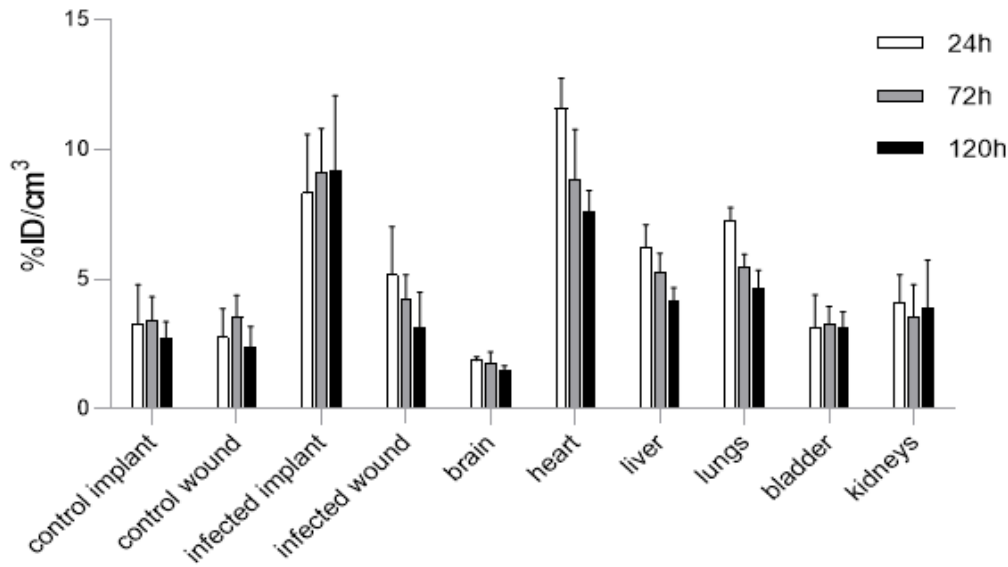


Figure 2. Biodistribution of ¹¹¹In-labeled 4497 antibody targeting *S. aureus* in seven BalB/C mice with a subcutaneous implant infection at multiple timepoints¹⁴. The bars represent 24, 72 and 120 h after IV administration. At 72 and 120 h, significantly higher uptake was seen at the implant infection site and the heart compared to all the other organs or targeted areas ($p \leq 0.002$).

The activity in each mouse decreased over time. This decrease was due to the effective half-life of 4497-¹¹¹In. The analyses showed an effective half-life of 59 h (Figure 3) for 4497-IgG1-CHX-A''-¹¹¹In. The physical half-life of ¹¹¹In is 67 h, resulting in a decay of 0.78 after 24 h, 0.48 after 72 h and 0.29 after 120 h after the time of injection. The biological half-life was calculated to be 522 h. The biological clearance as a percentage of the injected dose was 2.97 ± 2.23 , 4.56 ± 0.79 and $4.92 \pm 0.59\%$ at 24, 72 and 120 h, respectively. The biological decay reached a plateau phase between 24 and 72 h.

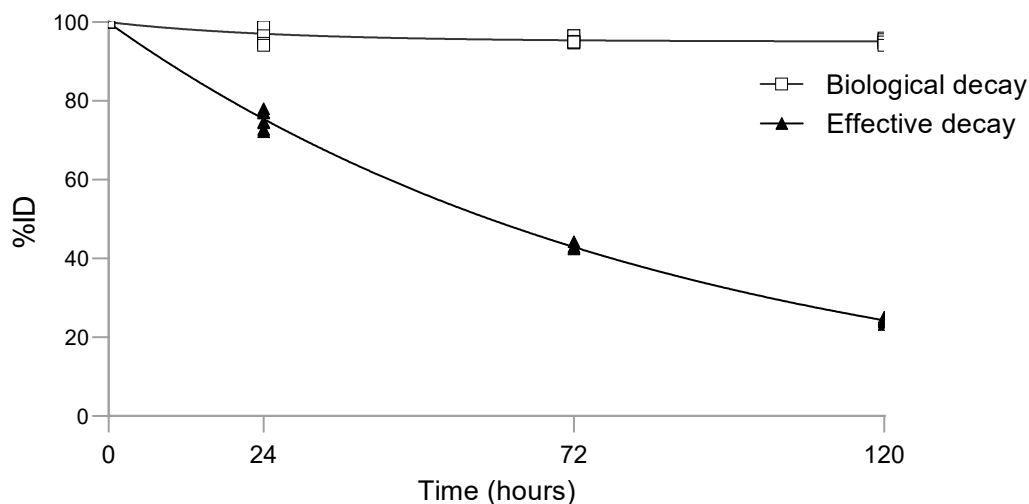


Figure 3. Whole body clearance of 4497-¹¹¹In in seven mice. Curve fitting using nonlinear regression analyses ($r^2 = 0.998$) showed that the effective half-life of 4497-¹¹¹In was 59 h.



DISCUSSION

This study analyzed the biodistribution of In¹¹¹-labeled 4497 IgG1 and its uptake at the target location, the infected implant. High uptake at the implant site at all the timepoints was accompanied by uptake in blood-rich organs, such as the heart, liver, lungs and kidneys, which is a typical biodistribution pattern for IgG in mice (Figure 1)^{21,22}. However, the increased liver uptake observed could be due to hepatic elimination and not solely because of its status as a blood-rich organ. In this respect, renal elimination is less likely as mAbs are too large to be filtered by the kidneys²³. High uptake in the heart was probably due to high activity in the blood, as similar uptake was seen in the aorta. In this regard, 4497-IgG1 showed high selectivity to the implant infection site over time with a favorable biodistribution pattern. However, due to a low elimination rate, prolonged exposure to high activity could pose a toxicity risk to healthy tissue if a long-lived radionuclide is considered for radioimmunotherapy. The specificity of 4497-¹¹¹In localization in the infected implant was confirmed by using a non-infected implant as a control. In addition, in a previous study¹⁴, the specificity of 4497-¹¹¹In for *S. aureus* infection in vivo was established using a palivizumab-¹¹¹In antibody to respiratory syncytial virus as an isotype matching control.

The rapid localization of the antibody to the infected implant is key for successful diagnostics and treatment. In this regard, the 4497 IgG1 antibody holds promise in a theranostic approach to deliver diagnostic and therapeutic radionuclides to the infection site. For example, antibodies labeled with ¹¹¹In or positron-emitting radioisotopes such as zirconium-89 could be a powerful diagnostic tool for SPECT and positron emission tomography (PET) imaging, where potentially even low-grade infection could be detected with high specificity and sensitivity. When combined with therapeutic radionuclides, a potential theranostic treatment might be possible. In this regard, retention of the antibody over time is important for long-lived radionuclides to employ their effects to the fullest extent.

Due to the retention of 4497 IgG1 at the infection site, long-lived radioisotopes, such as Actinium-225 (²²⁵Ac) (half-life 10 days, 5.9 MeV), are particularly interesting for our application in prosthetic joint infections. During its decay, ²²⁵Ac emits four α -particles and is therefore lethal at lower activities when compared to radioisotopes that emit only one α -particle, such as ²¹³Bi. Although a low dose (<10 kBq) of ²²⁵Ac did not have robust bactericidal properties compared to ²¹³Bi, higher doses could potentially be as destructive to bacteria and biofilm as ²¹³Bi.¹⁷ Alternatively, intermediate or high energy beta-emitting radioisotopes, such as Lutetium-177 or Rhenium-188, respectively, could be used, having the advantage of being readily available compared to alpha-emitting radionuclides as they are clinically used to treat prostate cancer and metastatic bone pain^{24,25}.

The long retention time may have been influenced by the slow elimination of the antibody, whereas the fast elimination of the radionuclides from healthy organs is important in order to minimize collateral damage. Diagnostics and treatment with radiation are always prone to safety concerns. Amongst others, bone marrow suppression is a feared complication. Due to high activity in the blood pool, bone marrow suppression might be expected. However, future toxicity studies need to confirm this.

The latest developments in infection imaging with radiopharmaceuticals have recently been highlighted²⁶. In order to improve the theranostic approach even further, smaller vehicles can be used, such as small proteins, nanobodies, such as heavy chain (VHH), or other single domain antibodies or peptides^{27,28}. In general, a smaller size leads to increased elimination of the potentially dangerous remaining unbound radioimmunoconjugates. Another advantage of smaller delivery molecules is increased penetration into tissue and presumably the biofilm²⁹. Other advantages include high stability, increased expression, solubility, specificity and



effective doses, as well reduced toxicity. Another approach to reduce the radiation dose to non-target tissues is the use of pre-targeting³⁰, where the antibody accumulates at the infection site, after which it is radiolabeled in vivo and most of the unbound antibody has cleared from the blood. For example, a patient with a periprosthetic joint infection, where the implant is colonized with bacteria and biofilm, could be diagnosed and treated with small targeting agents labeled with gamma- and alpha-emitters. When combined with a pre-targeting system, this could still be very effective and could minimize collateral damage.

Usually, biodistribution studies consist of administration of the targeting antibody in a relevant mouse model, followed by the harvesting organs or tissue samples at specific timepoints and measuring the radioactivity or subjecting them to more elaborate techniques, such as mass spectrometry. Measuring biodistribution using SPECT and calculating it using software is as accurate and requires fewer mice, as one mouse can be scanned at multiple timepoints. Another advantage is the easy identification of antibody accumulation anywhere in the body, and thus not being restricted to a predetermined focus on specific organs. For example, 4497 IgG1 targets both the dorsal knees and hips, although this targeting is not significant compared to that of other organs. This targeting is most likely due to lightly inflamed knee joints, which are commonly seen in young mice. Some concerns were expressed about the potential toxicity of long-lived alpha-emitters, such as ²²⁵Ac (with a physical half-life of 9.9 days) or ²²⁷Th (with a physical half-life of 18.7 days), in the radioimmunotherapy of cancer. However, phase 1/2 clinical trials with ²²⁵Ac- and ²²⁷Th-labeled antibodies have demonstrated acceptable safety profiles³¹⁻³⁴. We anticipate that the RIT of infections with long-lived alpha-emitters will reveal safety profiles that are similar to cancer RIT safety profiles.

Future studies that investigate the efficacy of a theranostic approach in the treatment of (implant) infections should include preclinical studies using radioimmunotherapy, such as using alpha- or beta-emitting radionuclides in the same subcutaneous implant infection mouse model or performing such experiments in an orthotopic model with an infected metal implant. If successful, a clinical study can be conducted starting with a small number of participants focusing on evaluating toxicity and adverse events. Eventually, radioimmunotherapy has the potential to reduce the high mortality and morbidity rates associated with implant infections, either as a standalone treatment or as an adjuvant therapy combined with antibiotics, with or without surgery.

Conclusion

The results of the in vivo nuclear imaging and biodistribution analyses of the 4497-IgG1 antibody showed that it specifically targets *S. aureus* and/or its biofilm in vivo. However, its low elimination rate could pose a risk to healthy tissue. Nevertheless, this antibody isotope formulation holds promise as a drug delivery system for diagnostics and as a bactericidal agent when using radioactive isotopes that can potentially eradicate the biofilm in (peri)prosthetic joint infections. These results indicate the need for further development of a preclinical treatment study in order to establish therapeutic efficacy and thereby paves the way for subsequent clinical trials.



REFERENCES

1. F. D. Lowy, "Medical progress: Staphylococcus aureus infections," *N. Engl. J. Med.*, vol. 339, no. 8, pp. 520–532, Aug. 1998.
2. S. Y. C. Tong, J. S. Davis, E. Eichenberger, T. L. Holland, and V. G. Fowler, "Staphylococcus aureus infections: Epidemiology, pathophysiology, clinical manifestations, and management," *Clin. Microbiol. Rev.*, vol. 28, no. 3, pp. 603–661, 2015.
3. C. R. Arciola, D. Campoccia, and L. Montanaro, "Implant infections: Adhesion, biofilm formation and immune evasion," *Nat. Rev. Microbiol.*, vol. 16, no. 7, pp. 397–409, 2018.
4. M. Otto, "Staphylococcal Biofilms," *Microbiol. Spectr.*, vol. 6, no. 4, Aug. 2018.
5. L. de Vor, S. H. M. Rooijackers, and J. A. G. van Strijp, "Staphylococci evade the innate immune response by disarming neutrophils and forming biofilms," *FEBS Letters*. Wiley Blackwell, 2020,
6. A. Resch, R. Rosenstein, C. Nerz, and F. Götz, "Differential gene expression profiling of Staphylococcus aureus cultivated under biofilm and planktonic conditions," *Appl. Environ. Microbiol.*, vol. 71, no. 5, pp. 2663–2676, May 2005.
7. B. Zmistowski and D. S. Casper, "Periprosthetic Joint Infection Increases the Risk," pp. 2177–2185, 2013.
8. R. L. Siegel, K. D. Miller, and A. Jemal, "Cancer statistics, 2019," *CA. Cancer J. Clin.*, vol. 69, no. 1, pp. 7–34, 2019.
9. J. Schwenck *et al.*, "Antibody-Guided Molecular Imaging of Aspergillus Lung Infections in Leukemia Patients," *J. Nucl. Med.*, vol. 63, no. 9, pp. 1450–1451, 2022.
10. D. R. Beckford-Vera *et al.*, "First-in-human immunoPET imaging of HIV-1 infection using 89Zr-labeled VRC01 broadly neutralizing antibody," *Nat. Commun.*, vol. 13, no. 1, 2022.
11. P. O. Larson SM, Carrasquillo JA, Cheung NK, "Radioimmunotherapy of human tumours," *Nat Rev Cancer*. 2015 Jun;15(6)347-60.
12. E. Dadachova and A. Casadevall, "Antibodies as delivery vehicles for radioimmunotherapy of infectious diseases," *Expert Opin. Drug Deliv.*, vol. 2, no. 6, pp. 1075–1084, Nov. 2005.
13. M. Helal and E. Dadachova, "Radioimmunotherapy as a Novel Approach in HIV , Bacterial , and Fungal Infectious Diseases," vol. 33, no. 8, pp. 1–6, 2018.
14. L. de Vor *et al.*, "Human monoclonal antibodies against Staphylococcus aureus surface antigens recognize in vitro and in vivo biofilm," *Elife*, vol. 11, pp. 1–25, 2022.
15. R. Fong *et al.*, "Structural investigation of human S. aureus-targeting antibodies that bind wall teichoic acid," *MAbs*, vol. 10, no. 7, pp. 979–991, 2018.
16. S. M. Lehar *et al.*, "Novel antibody-antibiotic conjugate eliminates intracellular S. aureus," *Nature*, vol. 527, no. 7578, pp. 323–328, 2015.
17. B. van Dijk *et al.*, "Radioimmunotherapy of methicillin-resistant Staphylococcus aureus in planktonic state and biofilms," *PLoS One*, vol. 15, no. 5, p. e0233086, 2020.
18. V. Tolmachev *et al.*, "Evaluation of a maleimido derivative of CHX-A" DTPA for sitespecific labeling of Affibody molecules," *Bioconjug Chem.*, vol. 19, no. 8, pp. 1579–1587, 2009.
19. R. J. Miller *et al.*, "Development of a Staphylococcus aureus reporter strain with click beetle red luciferase for enhanced in vivo imaging of experimental bacteremia and mixed infections," *Sci. Rep.*, vol. 9, no. 1, pp. 1–19, 2019.



20. P. E. B. Vaissier, F. J. Beekman, and M. C. Goorden, "Similarity-regulation of OS-EM for accelerated SPECT reconstruction," *Phys. Med. Biol.*, vol. 4300, p. 4300.
21. V. Yip *et al.*, "Quantitative cumulative biodistribution of antibodies in mice: Effect of modulating binding affinity to the neonatal Fc receptor," *MAbs*, vol. 6, no. 3, pp. 689–696, 2014.
22. K. J. H. Allen, R. Jiao, M. E. Malo, C. Frank, and E. Dadachova, "Biodistribution of a radiolabeled antibody in mice as an approach to evaluating antibody pharmacokinetics," *Pharmaceutics*, vol. 10, no. 4, 2018, doi: 10.3390/pharmaceutics10040262.
23. J. T. Ryman and B. Meibohm, "Pharmacokinetics of monoclonal antibodies," *CPT Pharmacometrics Syst. Pharmacol.*, vol. 6, no. 9, pp. 576–588, 2017, doi: 10.1002/psp4.12224.
24. S. T. Tagawa *et al.*, "Phase II study of lutetium-177-labeled anti-prostate-specific membrane antigen monoclonal antibody J591 for metastatic castration-resistant prostate cancer," *Clin. Cancer Res.*, vol. 19, no. 18, pp. 5182–5191, 2013, doi: 10.1158/1078-0432.CCR-13-0231.
25. I. Finlay, M. Mason, and M. Shelley, "Radioisotopes for the palliation of metastatic bone cancer: a systematic review," *Lancet Oncol.*, vol. 6, no. June, pp. 392–400, 2005, [Online]. Available: <http://www.sciencedirect.com/science/article/pii/S1470204505702060>.
26. E. Dadachova and D. E. N. Rangel, "Highlights of the Latest Developments in Radiopharmaceuticals for Infection Imaging and Future Perspectives," *Front. Med.*, vol. 9, no. February, pp. 1–7, 2022, doi: 10.3389/fmed.2022.819702.
27. S. Muyldermans, "Nanobodies: Natural single-domain antibodies," *Annu. Rev. Biochem.*, vol. 82, no. March, pp. 775–797, 2013, doi: 10.1146/annurev-biochem-063011-092449.
28. M. J. Hawkins, P. Soon-Shiong, and N. Desai, "Protein nanoparticles as drug carriers in clinical medicine," *Adv. Drug Deliv. Rev.*, vol. 60, no. 8, pp. 876–885, 2008, doi: 10.1016/j.addr.2007.08.044.
29. P. Bannas, J. Hambach, and F. Koch-Nolte, "Nanobodies and nanobody-based human heavy chain antibodies as antitumor therapeutics," *Front. Immunol.*, vol. 8, no. NOV, pp. 1–13, 2017.
30. B. M. Zeglis *et al.*, "A pretargeted PET imaging strategy based on bioorthogonal diels-alder click chemistry," *J. Nucl. Med.*, vol. 54, no. 8, pp. 1389–1396, 2013.
31. J. G. Jurcic, "Targeted Alpha-Particle Therapy for Hematologic Malignancies," *Semin. Nucl. Med.*, vol. 50, no. 2, pp. 152–161, 2020.
32. T. L. Rosenblat *et al.*, "Treatment of Patients with Acute Myeloid Leukemia with the Targeted Alpha-Particle Nanogenerator Actinium-225-Lintuzumab," *Clin. Cancer Res.*, vol. 28, no. 10, pp. 2030–2037, 2022.
33. J. G. Jurcic, "Ab therapy of AML: Native anti-CD33 Ab and drug conjugates," *Cytotherapy*, vol. 10, no. 1, pp. 7–12, 2008.
34. O. Lindén *et al.*, "227Th-Labeled Anti-CD22 Antibody (BAY 1862864) in Relapsed/Refractory CD22-Positive Non-Hodgkin Lymphoma: A First-in-Human, Phase I Study," *Cancer Biother. Radiopharm.*, vol. 36, no. 8, pp. 672–681, 2021.





Alternative treatment options for implant infections



Treating infections with ionizing radiation: a historical perspective and emerging techniques

Based on: | van Dijk B* | Lemans JVC* | Hoogendoorn RM | Dadachova E | de Klerk JMH | Vogely | HC | Weinans H | Lam MGEH | van der Wal BCH.
Treating Infections with Ionizing Radiation: A Historical Perspective and Emerging Techniques. Antimicrob Resist Infect Control. 2020; 9, 121. *authors contributed equally



ABSTRACT

Background: Widespread use and misuse of antibiotics have led to a dramatic increase in the emergence of antibiotic resistant bacteria, while the discovery and development of new antibiotics is declining. This has led to certain implant-associated infections such as periprosthetic joint infections, where a biofilm is formed, to become very difficult to treat. Alternative treatment modalities are needed to treat these types of infections in the future. One candidate that has been used extensively in the past, is the use of ionizing radiation. This review aims to provide a historical overview and future perspective of radiation therapy in infectious diseases with a focus on orthopedic infections.

Methods: A systematic search strategy was designed to select studies that used radiation as treatment for bacterial or fungal infections. A total of 216 potentially relevant full-text publications were independently reviewed, of which 182 focused on external radiation and 34 on internal radiation. Due to the large number of studies, several topics were chosen. The main advantages, disadvantages, limitations, and implications of radiation treatment for infections were discussed.

Results: In the pre-antibiotic era, high mortality rates were seen in different infections such as pneumonia, gas gangrene and otitis media. In some cases, external radiation therapy decreased the mortality significantly but long-term follow-up of the patients was often not performed so long term radiation effects, as well as potential increased risk of malignancies could not be investigated. Internal radiation using alpha and beta emitting radionuclides show great promise in treating fungal and bacterial infections when combined with selective targeting through antibodies, thus minimizing possible collateral damage to healthy tissue.

Conclusion: The novel prospects of radiation treatment strategies against planktonic and biofilm-related microbial infections seem feasible and are worth to investigate further. However, potential risks involving radiation treatment must be considered in each individual patient.



INTRODUCTION

For more than a century, radiation has been used as a treatment modality for a wide range of diseases. Its usefulness in diagnosis and oncological treatment is undisputed, but in the early 20th century, radiation was commonly employed to treat infections, especially due to a lack of alternative treatments and limited knowledge of possible side effects. In the 1940s, radiation treatment slowly became obsolete with the discovery and availability of antibiotics. However, the war against infections is still ongoing and widespread use and misuse of antibiotics have led to the emergence of antibiotic-resistant bacteria, while the discovery and development of new antibiotics is rapidly declining.¹

The field of orthopedic surgery is in dire need of novel treatments. Total joint replacements are a common, last-resort treatment for degenerative joint disease, but 1-4% of patients develop a periprosthetic joint infection (PJI).² PJI is difficult to treat as bacteria form a biofilm on the prosthetic material. This hinders the host immune system, but more importantly, the bacteria in a biofilm are mostly in a metabolic inactive or dormant state and therefore not susceptible to most antibiotics.³

Currently, patients with PJI get prolonged antibiotic treatment, occasionally combined with multiple irrigation and debridement surgeries with- or without implant exchange to combat the infection. Despite this intensive treatment, outcomes are still unpredictable. In addition, the (often) elderly PJI population usually has multiple comorbidities, which necessitates multimodality treatment. In this regard, PJI patients are not dissimilar to oncology patients, with comparably high morbidity- and mortality rates. The 5-year mortality of PJI even surpasses that of most forms of prostate-, breast- and thyroid cancer.^{4,5} Interestingly, like in these previously mentioned oncological conditions, ionizing radiation may start to play a role in treatment of infectious diseases.

Ionizing radiation therapies of the past, like x-ray- or radioactive iodine therapy, damaged a large area around the region of interest. However, recent advances in both external and internal radiation techniques make these therapies potentially more accurate. In external radiation treatment, these advances include intensity-modulated radiotherapy, as well as novel technologies like MR Linac.⁶ Similarly, in internal radiation treatment, radioimmunotherapy (RIT) has allowed the delivery of cytotoxic radiation to specific target cells, through the coupling of antibodies and radioisotopes.⁷ The same concept could be applied to treatment of infection, by coupling the radioisotopes to antibodies that targets bacterial cells or biofilm antigens.⁸ With these advances, a re-evaluation of their merits in infection treatments seems warranted. This article therefore aims to provide a historical overview as well as future perspective of radiation therapy in infectious diseases with a focus on orthopedic infections.

METHODS

A systematic search strategy was designed for three academic databases, Pubmed, Embase and Cochrane, to select studies that used radiation for treatment of bacterial or fungal infections (Appendix 1). Studies were independently screened in two stages: screening of titles and abstracts, followed by the retrieval and screening of full-text publications. Two reviewers used predetermined inclusion criteria as described in Table 1. Conflicts were solved by consensus, or through consultation of a third reviewer. Since most studies involving radiation treatment of infections were performed in the distant past, no restrictions were set on publication date. Reference screening and citation tracking of the included articles was performed. The included full-text publications were then divided into two main groups: studies investigating external radiation therapy and publications investigating internal radiation therapy. Since the included



publications differed strongly in scope, disease and patient populations, results were clustered by their organ system or disease group.

Table 1: Eligibility Criteria

External Radiation	
Inclusion Criteria	Exclusion Criteria
Investigates treatment of bacterial or fungal infection with radiation	Diagnostic studies
Human, clinical study	Indirect use of radiation
	In vitro research
	No abstract/full-text available
	No English/German/Dutch language
Internal Radiation	
Inclusion Criteria	Exclusion Criteria
Investigates treatment of bacterial or fungal infection with radiation	Diagnostic studies
	No abstract/full-text available
	No English/German/Dutch language

RESULTS

Of 16,302 studies, 216 potentially relevant full-text publications were reviewed and divided into two groups, external and internal radiation. In this review, external radiation is defined as a method for delivering a beam of x-rays to the infection site and internal radiation is defined as a systemic treatment, involving radioisotopes that deliver a cytotoxic level of radiation to an infected site. Through reference screening and citation tracking another 99 articles were found for a grand total of 216 articles in total (Figure 1). Due to the large number of studies, different articles in different topics were chosen that can directly or indirectly correlate to orthopaedic infections. Unfortunately, there were no suitable articles for radiation therapy on osteomyelitis that could be included. The following topics were chosen and are described in detail below: external radiation treatment for pneumonia, soft tissue application, otolaryngological application as external radiation therapies. For internal radiation treatment, bone tuberculosis, *Helicobacter pylori* and RIT for bacteria and fungus.



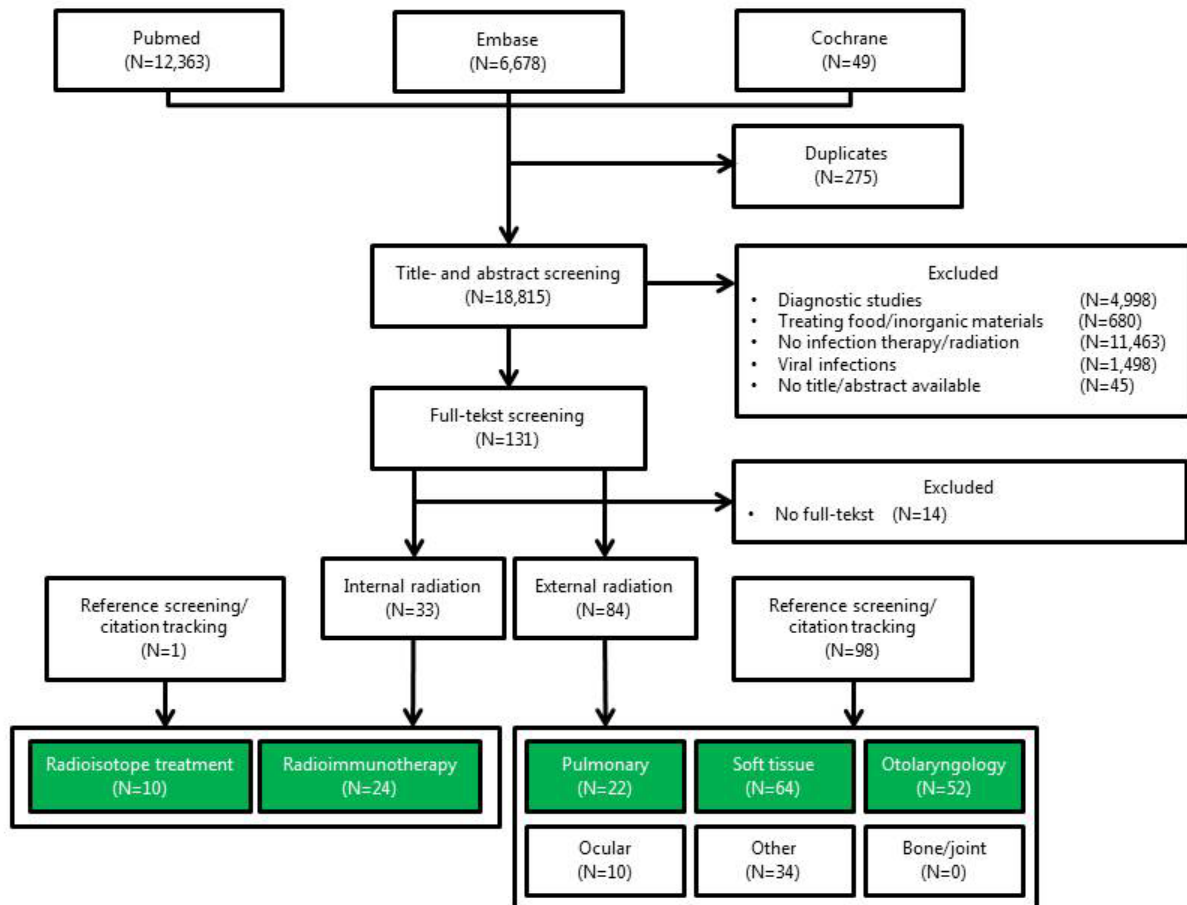


Figure 1: Flowchart of the systematic literature search

External Radiation

Discovery of X-rays

In 1895, Wilhelm Röntgen was the first to describe the existence of X-rays.⁹ Following the publication of a radiograph of his wife's left hand, this new technique was welcomed with great enthusiasm. Already a few years later, the first therapeutic uses were described for infectious diseases.

Pneumonia treated with X-ray

Before the advent of antibiotics, pneumonia was a disease known for its high mortality.¹⁰ Musser and Edsall, performing clinical experiments with x-rays, found that this radiation markedly improved condition and disease progress of leukemia patients, which they hypothesized was due to an increase in metabolic processes in tissues.¹⁰ Unresolved pneumonia was, in their opinion, also a situation in which the body could not adequately metabolize the unresolved exudate that was left in the lungs. Based on this theory, they treated a patient who suffered from a 1 month old unresolved pneumonia with x-ray treatment for 5 minutes daily during 5 days. At the end of the week, the pneumonia had completely resolved.¹⁰ Following this publication, multiple publications were published that also investigated the merits of x-rays in unresolved pneumonia, with good clinical results.^{11,12} Krost et al. then investigated x-ray treatment for pneumonia in 12 children with unresolved pneumonia.¹³ These patients had symptoms for as long as 3-6 weeks before the first x-ray treatment was given. After 1-2 x-ray treatments, (5 mA, 5min, spark gap 7.5 inches, distance 8 inches, 3 mm Al and 4mm leather filter) 11 cases of pneumonia (92%) resolved within several days, the clinical situation often improved after hours. Powell et al. continued research of x-rays in the 1930's, his cohort of



adults showed a decreased mortality of 6.7% (9/134 patients), a sharp improvement from earlier mortality rates for pneumonia.¹⁴ In that study, patients were alternatively included in the x-ray group or the control group, but after seeing the marked reduction in mortality in the x-ray treatment group, all control patients were subsequently treated with x-rays (all patients received 250-350 röntgen). A few years following Powell's research, sulfonamides, the first antibiotics, were used as standard treatment for pneumonia, and use of x-rays fell out of favor. Research, however, was continued for patients who did not respond to, or did not tolerate sulfonamide therapy. In one such study, 22 out of 29 patients (75.9%) who showed no response to sulfonamides, recovered completely with x-ray therapy (120Kv, 40cm distance, 3mm Al filter, 200 röntgen single-dose for a maximum of 3 doses).¹⁵ Some short-term adverse effects were shown by several authors, namely convulsions and cyanosis when the single session radiation dose exceeded 10 Gy.^{16, 17} These complications often resolved, and therapy was still effective in these patients. Unfortunately, none of the authors performed long-term follow-up of their patients, so the long term radiation effects, as well as a potential increased risk of malignancies could not be investigated. For a comprehensive review of the clinical and animal literature on x-ray use in pneumonia, we direct the reader to the comprehensive review by Calabrese and Dhawan.¹⁸

Soft tissue infections treated with X-ray

Different soft tissue infections such as gas gangrene, furuncles and carbuncles were treated with X-rays in the first half of the 20th century and will be discussed in detail below. Gas gangrene, or *Clostridium myonecrosis*, is a destructive soft-tissue infection caused by anaerobic *Clostridium* bacteria. The micro-organisms that are often associated with severe trauma or contaminated wounds thrive in low-oxygen environments and rapidly destroy muscle tissue while producing gas in the tissues. Severe pain, edema and/or bullae, an unusually rapid tachycardia, and palpable soft tissue crepitations are all clinical signs that point to the presence of gas gangrene.¹⁹ Before the antibiotic era, surgery, namely amputation, was the only treatment, and mortality was around 50%.²⁰ Radiologist Kelly reported in 1931 his experience with treating gas gangrene with x-rays and found a mortality of only 2 in 8 patients, without the need for further amputation after x-ray treatment (6-7 doses of 3min; 5-inch spark gap, 5mA, 15 inch distance, 0.5mm Al filter). He described this in his paper in one patient: "*The laboratory cultures were positive for Bacillus welchii, and x-rays films showed considerable gas in the soft tissues. Amputation was advised by consultants, but action was deferred to see the effects of the other treatment. Serum [equine serum containing antibodies against one or more Clostridium species] and x-ray therapy were administered. No amputation was necessary and the patient was dismissed after seven weeks hospitalization*".²¹ Following Kelly's initial success, many studies were performed over the years, with the majority showing excellent results. In a review and meta-analysis of the case series literature, Kelly and Dowell showed that a combination of surgery, serum therapy and x-ray treatment (different radiation regimes were used during this study) resulted in a 11.5% mortality (42/364 patients) compared to a 35-50% mortality rate when only surgery and serum were evaluated together.²⁰ In a subgroup of x-ray patients who received multiple x-ray treatments, mortality was even lower, at 5.9% (17/288 in patients with ≥ 3 x-ray treatments). In a subgroup that underwent only x-ray treatment without serum therapy, mortality was 4.7% (2/42 patients) and no amputations were necessary. How x-rays halted the gas gangrene infection was never elucidated, although it was generally known that the relatively low radiation dose was not able to destroy the bacteria directly. More likely hypotheses that were proposed included the possibility that radiation causes local vessels to dilate, increasing oxygen supply to the infected tissue and thus diminishing the potency of anaerobic bacteria, as well as the possibility that radiation stimulated either the proliferation of immune cells or the release of bactericidal products from lymphocytes.^{22,23} It must be noted that some authors did



not find x-rays to be effective,²⁴ and that the promising mortality figures could have been the result of selection bias as well as an improved standard of care for these infections over time.²⁵

A furuncle, or boil is an infection of the hair follicle and its surrounding tissue caused by *Staphylococcus aureus* or *Staphylococcus epidermidis* which are also the most common pathogens causing PJI today. When multiple furuncles fuse together it is called a carbuncle, both had high mortality rates in the first half of the 20th century, before the use of antibiotics. As early as 1906, Coyle described complete abortion of the carbuncle in 4/5 patients treated with x-rays.²⁶ This result wasn't given much attention until almost a decade later, when Dunham published the results of 67 patients that were treated with a single x-ray dose of 6 Gy and stated that "*nothing in all roentgen therapy gives such positive and uniformly perfect results as the treatment of a carbuncle*".²⁷ In the following years, multiple articles were published about the great and prompt benefit to patients treated with x-rays.²⁸ A lower single therapeutic dose of 0.75-2 Gy showed less radiation-induced side effects and an even greater effect on pain reduction and healing, especially in early stages of the disease.²⁹ In the early 1940's, this x-ray therapy became obsolete due to the introduction of antibiotics. For a more detailed description of the historical role of x-ray treatment for carbuncles and furuncles we direct the reader to the review by Calabrese.²⁹

Otolaryngological applications

Before the advent of tympanostomy tubes, otitis media was a major health problem in school children. Following upper respiratory tract infections, tissue in the nasopharynx swells and blocks the Eustachian tube, thus blocking the outflow of middle ear secretions, which may become infected and cause conductive hearing loss. Blockage of the Eustachian tube may also be caused by swelling of the adenoid tissue of the nasopharynx.³⁰ Treatment in the past consisted of paracentesis, adenoidectomy or surgical removal of tissue surrounding the Eustachian tubes, although these therapies were often ineffective.³¹ The resulting chronic hearing loss had a deleterious effect on the development of normal hearing and speech of children.

Early in the 20th century, x-rays were proposed as a viable treatment to otitis media caused by Eustachian tubes blocked by lymphoid tissue, as it was already known that these tissues were very radiosensitive.³² Beattie et al. found in 1920 that patients suffering from chronic otitis media with symptoms of mastoiditis showed clinical improvement after diagnostic mastoid x-rays. Out of 14 chronic patients, 9 improved after only 1-3 sessions with 180 seconds of x-ray exposure.³³ Similar results were found by other studies over the years.³⁴

Crowe and Baylor, happy with the effect that radiation had in reducing lymphoid tissue around the Eustachian tube, proposed that radiation could be applied much more locally compared to x-ray through nasal application of a small radioactive radium or radon source, which would cause much less systemic radiation.³⁵ Through covering the applicator with brass, all alpha- and most beta-radiation was filtered. Gamma rays were emitted that mimicked the x-ray treatment, but applied only locally, where it was needed. The technique was optimized by Crowe and colleagues, and a nickel-copper alloy was used instead of brass to cover the applicator, so that more beta-radiation was emitted that decreased the necessary application time and reduced the gamma-radiation load on tissues other than the nasopharyngeal lymphoid tissue. The treatment differed between studies but often consisted of 1-4 sessions of application with around 25-50 mg ²²⁶Ra sulphate for 8-15 minutes (~5 Sv at lymphoid tissue over 6 sessions, total dose in



surrounding tissues estimated to be 36-142 Sv).³⁶⁻³⁸ The efficacy of the treatment was excellent, symptoms decreased within days, and the radium treatment was used in many children, but also in thousands of air force pilots and submarine personnel who had undergone baro-trauma.³⁹

The positive results in children were illustrated in a randomized controlled trial by Hardy and Bordley, which consisted of over 1000 school children with conductive hearing loss who were randomized in groups that received three sessions with an applicator containing either radium or a placebo, blinded to patient and physician.⁴⁰ In the subgroup with greatest hearing loss (i.e. the group with large lymphoid tissue overgrowth), hearing improved significantly greater with radium therapy compared to control treatment, and lymphoid tissue was significantly reduced. Interestingly, mild hearing loss in the placebo group improved markedly over the years as well, from which it was concluded that radium therapy should only be performed in cases in which hearing loss is found as a result of Eustachian tube dysfunction, because in most other cases, the condition also improved without treatment.

Over time, physicians became more concerned about the potential long-term health effects. An increase in cancer risk was suggested by some studies that followed children who had received radiation for benign conditions during childhood.^{41,42} However, these increased cancer risks were never unequivocally shown in cohort studies that investigated patients treated with nasopharyngeal radium. A cohort by Ronckers et al. found no increase in head and neck- or thyroid malignancies in a large cohort of over 4000 patients, although the incidence of breast cancer and non-Hodgkin lymphoma was slightly elevated.³⁸ Another study by Yeh et al. found no significant increase in the incidence of malignancies in a cohort of more than 1700 patients with around 40 years of follow-up.⁴³ Loeb et al. performed a literature review of studies on nasal radium therapy that included almost 30,000 patients (of whom a large proportion was treated by Crowe and colleagues). They found no cases of malignancies that could be clearly attributed to radium treatment.⁴⁴

Although an increased incidence of malignancies was never proven, the use of radium was not without risks. Notable was an incident in 1958 at the otolaryngology department of our own institution, the University Medical Center Utrecht, where the tip from a radium capsule broke away from the applicator, and was accidentally swallowed, with the treating physician being unaware. The 5-year old patient returned home, where she threw up the capsule, which was then accidentally deposited into the chimney by her father. The charred (and radioactive) ashes were distributed outside, thus contaminating the entire house and garden with radioactive material. This prompted a citywide emergency, the patient and her family were quarantined, and all persons who had contacted the family during the incident had to be examined both medically, and with Geiger counters. During the first month after the incident, parts of the house were broken down and renovated by army personnel in protective gear. The radioactive waste was dumped in the ocean, some 30 miles from the Dutch coast. A few months after the incident, a new “Radioactive substance decree” was written into Dutch law, detailing “(...) *that sources of Radium could only exceed 1 mCu if, and only if, adequately encapsulated by a shell that cannot be removed without damage (...), which is hermetically sealed and which is created from an indestructible material (...)*”.³¹ Unfortunately, this measure came too late. The incident caused much media publicity, and with increasing fear of radioactive substances, fueled more so by the Cold War, radium therapy was quickly abandoned in the Netherlands, also partly because of the advent of non-radioactive alternatives. An in-depth description of this incident was written by Graamans.⁴⁵ The patient was said to have lived a healthy life, with no radiation-related complications.



Internal Radiation

In this review, internal radiation is defined as a systemic treatment, involving radioisotopes that deliver a cytotoxic level of radiation to a diseased site. The hypothesis of “magic bullets” that could selectively kill pathogens or cells without harming healthy tissue was first described around 1900 by Paul Ehrlich.⁴⁶ The concept of targeted radiation therapy was used from the 1900s for different infectious diseases and is described in detail below.

Thorium X

Starting from around 1912, Thorium X was used in dermatology and as a treatment for rheumatic diseases. Thorium X (Radium-224; ²²⁴Ra) is a short-lived alpha-emitter (half-life of 3.6 days) and was applied topically, intravenously and orally. Around 1940, Peteosthor was developed to treat bone tuberculosis.⁴⁷ The drug contained ²²⁴Ra-chloride (Thorium X), platinum and red dye eosin. The hypothesis was that this short-lived bone-seeking alpha-emitter could selectively target, accumulate, and destroy the infected bone. Between the 1940's, and mid-1950's, primarily children and juveniles were treated with high doses of ²²⁴Ra, receiving repeated injections up to 2 MBq twice a week, often for prolonged periods of time, sometimes totaling up to 140 MBq.⁴⁸ Around 1950, Spiess and Mays questioned the efficacy of Peteosthor and conducted several in vitro and in vivo experiments. They showed that killing of *Mycobacterium tuberculosis* was seen in vitro with high doses of ²²⁴Ra, but no killing was seen in vivo. Objections to the treatment were raised in the early 1950's, the primary one being that ²²⁴Ra deposited in the growing skeleton of children and juveniles would cause severe damage.⁴⁸ Because of the questionable efficacy of the treatment and the introduction of antibiotics like Streptomycin, discovered by Waksman (1943), Peteosthor was abandoned as a treatment for bone tuberculosis in 1956. After 1956, Spiess and Mays followed a cohort of 899 patients treated with high doses of Peteosthor for many years. A significant increase was seen in the incidence of bone tumors (56 cases among 899 patients, 6.2%).⁴⁷

Iodine-131 – helicobacter pylori

Helicobacter pylori (Hp) infection is probably the most common chronic bacterial infection, present in almost half of the world population.⁴⁹ Multiple studies investigated the effect of radioactive iodine-131 (¹³¹I) on Hp. ¹³¹I is a short-lived beta-emitter (half-life 8.4 days) and is an important treatment modality in the management of thyroid cancer and hyperthyroidism. ¹³¹I does not only accumulate in the thyroid, but also in the stomach, and could therefore potentially eradicate Hp infection.⁵⁰ In 71 patients treated for differentiated thyroid carcinoma, a pre-treatment urease breath test was done to diagnose an Hp infection. Twenty-three patients had a negative post-treatment result and thus a significant reduction in Hp.⁵⁰ In another study, 18 of 85 patients infected with Hp who were treated for hyperthyroidism with ¹³¹I showed a negative urease breath test after treatment, which also means a significant reduction in Hp.⁵¹ However, no significant reduction was seen in two other studies, the first with 18 patients treated for differentiated thyroid carcinoma and the second study with 76 patients treated for differentiated thyroid cancer and 11 for primary hyperthyroidism.^{52,53}

Radioimmunotherapy

Currently, RIT is used to treat different types of cancer, but until the 1940's, cancer treatment was exclusively based around the surgical approach. That changed with the advent of molecular medicine, and with the discovery of “chemotherapy” by Louis Goodman and Alfred Gilman.⁵⁴ In the next few decades, multiple chemotherapy agents were discovered that successfully induced remission of multiple types of cancer. However, during the development of these systemic cancer drugs, significant problems, such as acute and long-term toxicities were repeatedly encountered. Therefore, a change of strategy was needed and was found in targeted-



therapy.⁵⁴ The aim of targeted therapy is to specifically target tumor cells with specific antibodies or small molecules that interfere with molecular pathways related to carcinogenesis and tumor growth. In the late 1980's, researchers shifted their focus to unraveling and understanding these molecular pathways and due to innovations in technology more and more antibodies and inhibitors of specific targets were discovered.⁵⁵ While antibodies can directly affect tumor cells, they can also be used as transport vehicles to deliver agents that can destroy tumor cells (e.g. radioisotopes).¹⁷ When antibodies are labeled with radioisotopes, a high dose of ionizing radiation can be delivered directly to the targeted cells. In the past decade, success was seen in treating non-Hodgkin lymphoma with the only two radioimmunoconjugates approved by the FDA, ¹³¹I-tositumomab and ⁹⁰Y-ibritumomab tiuxetan.^{56,57}

Radioimmunotherapy of fungal infections

In vitro experiments showed that both planktonic cells and biofilms of *Cryptococcus neoformans* (CN) are susceptible to RIT. In vitro, CN-specific monoclonal antibodies conjugated to bismuth-213 (²¹³Bi; short-lived alpha-emitter, half-life 45 min.) caused a 50% reduction in metabolic activity of the fungal biofilm and a 70% reduction in metabolic activity of planktonic cells at a dose of 1.11 MBq (30 µCi) when compared to the control non-specific antibody conjugation.⁵⁸ In the same study, 14.8 MBq (400 µCi) rhenium-188 (¹⁸⁸Re; short-lived beta-emitter, half-life 17 h.) conjugated to CN-specific antibodies showed a reduction in metabolic activity of planktonic cells of 83%, but no reduction was seen in the metabolic activity of the biofilm.¹⁹

In an in vivo experiment by Dadachova et al., nine groups of 10 mice were infected with 10⁵ CN cells. Multiple treatment groups were treated with intravenously administered specific antibodies bound to ²¹³Bi and ¹⁸⁸Re, a dose of 3.7 MBq (100 µCi) RIT showed a survival of 60% with ²¹³Bi and 40% with ¹⁸⁸Re on day 75 post-therapy when compared to 0% survival in the 'cold' antibody conjugates (antibodies without radioconjugates) and a saline-treated group.⁵⁹ In another study with the same in vivo CN model, RIT with ²¹³Bi was compared to the antimycotic drug amphotericin. RIT was more effective in reducing fungal burden in lungs and brains, measured by colony forming unit (CFU) count in post mortem organs, where ²¹³Bi conjugates could completely clear the infection, while amphotericin could not reduce that number of fungal cells.⁶⁰

Radioimmunotherapy of bacterial infections

Dadachova et al. also used RIT to combat bacterial infections. In vitro tests with ²¹³Bi radiolabeled antibodies against *Streptococcus pneumoniae* showed minimal but significant killing when doses of 0.11-0.15 MBq (3-4 µCi) were used.⁶¹ A higher dose could potentially have a higher bactericidal effect. Two in vivo experiments were done with C57BL/6 mice infected intra-peritoneally with 1000 CFU of *Streptococcus pneumoniae*. In the first experiment, mice were treated with either ²¹³Bi specific antibodies or "cold" antibodies, one group was left untreated. After 14 days, 87% of the mice treated with ²¹³Bi survived versus 40% in the other two groups. In the second in vivo study, the mice were treated with 2.96 MBq (80 µCi) ²¹³Bi labeled specific and non-specific antibodies. Unlabeled antibodies and an untreated group were used as controls. Mice treated with ²¹³Bi labeled specific antibodies showed a 100% survival after 14 days versus 20% in the Bi²¹³ bound non-specific antibody group and 60% in the unlabeled antibody and untreated group.⁶¹



In another study, RIT with ^{213}Bi showed prolonged survival in mice infected with *Bacillus anthracis* bacterial cells compared to control groups with unlabeled antibodies and phosphate-buffered saline (PBS).⁶² These results showed the therapeutic potential of RIT on infectious diseases.⁸ Until now, there is no literature on using RIT to treat infections in humans.

DISCUSSION

Throughout history, humanity has battled infections and the war is still going on today. With an increasing incidence of antimicrobial-resistant bacteria, finding effective treatments has become increasingly important. In the last century, different treatments have been developed and later abandoned. However, with new techniques, and the need to move away from our dependency to antibiotics, it is not unwise to give older strategies renewed consideration. Also, gathered knowledge on therapies from other fields in healthcare could potentially be used to treat infections. This review aimed to provide a summary of both historical and recent advances in radiation treatment for infections, whilst providing insight in how to proceed forward and learn from mistakes made in the past. Both external and internal radiation has the potential to clear infections as shown in this review. However, collateral damage to healthy tissue is a major concern, especially in external radiation treatment. To treat infections with external gamma-radiation, a high dose is needed to kill the bacteria. As a consequence, the long-term risk of cancer increases in patients who are exposed to these high doses of radiation. Of course, X-ray therapy for infections largely preceded the onset of advances in linear particle accelerators and radiotherapy; therefore, radiotherapy has mostly been ignored as a potential candidate in infection treatment, especially since antibiotics were highly effective and widely available. As we are entering an era in which antibiotics are increasingly failing, a renaissance of external radiation therapy of infections may develop with stereotactic radiation therapy, intensity-modulated radiation therapy and MR guided radiotherapy becoming potential last resort treatments for resistant infections.

In contrary to these therapeutic techniques base on gamma radiation, alpha- and beta emitting radioisotopes can also be used for infection treatment. These radioisotopes have less penetrating power but are much more destructive, especially alpha-radiation. As early as 1950, the bactericidal effect of alpha-emitting radioisotope ^{224}Ra was shown in vitro.⁶³ This makes them particularly interesting to use as Paul Ehrlich's "Magic bullets" that can target bacteria or the biofilm, while minimizing collateral damage to healthy tissue. Key in internal radiation treatment for infections is to bring the radioisotopes in close vicinity to the target. For example, ^{224}Ra has bone-seeking properties as it is a calcimimetic and is therefore incorporated into bone with increased bone-turnover such as bone infections. However, in subsequent clinical studies where ^{224}Ra is used to treat bone tuberculosis, even extremely high doses were not effective and over time, led to a significant increase of bone tumors.⁴⁷ This suggests that a more selective targeting is necessary to utilize the full potential of these alpha- and beta-emitting radionuclides. Dadachova et al. showed that using antibodies as a transport vehicle for delivery of radioisotopes, bacteria and fungi can be targeted with high specificity, comparable to how RIT is used in the field of oncology. RIT relies on the antigen-binding characteristics of the antibodies to deliver cytotoxic radiation to target cells. As microbes express antigens that are unique and different from host antigens, they can be targeted with high specificity and low cross-reactivity. It could especially be of great value in biofilm-related infections where dormant cells are metabolic inactive and therefore not susceptible to most antibiotics because the damaging effects of radiation are independent of the cell's metabolic state. To improve RIT further, smaller vehicles can be used such as nanobodies. These nanobodies are derived from camelids and are ten times smaller than conventional antibodies. Due to their size, nanobodies have increased elimination to get rid of the potential dangerous remaining unbound



radioimmunoconjugates minimizing collateral damage even further. Also, they have considerable better penetration into tissue and presumably the biofilm.⁶⁴ Other advantages include high stability, solubility, expression, and specificity. Theoretically, a patient with a PJI where the hip implant is colonized with bacteria and a biofilm, could be treated with nanobodies labeled with an alpha-emitter like ^{213}Bi or ^{225}Ac that can penetrate deep in the biofilm, destroy the architecture and kill bacteria. (Figure 2) These antibodies could also be a powerful diagnostic tool for positron emission tomography (PET)-imaging when labeled with positron-emitting radioisotopes such as fluorine-18 (^{18}F) or zirconium-89 (^{89}Zr). Due to the high specificity and rapid clearance, low background signal is expected so that even low-grade infections could be detected with high specificity and sensitivity.

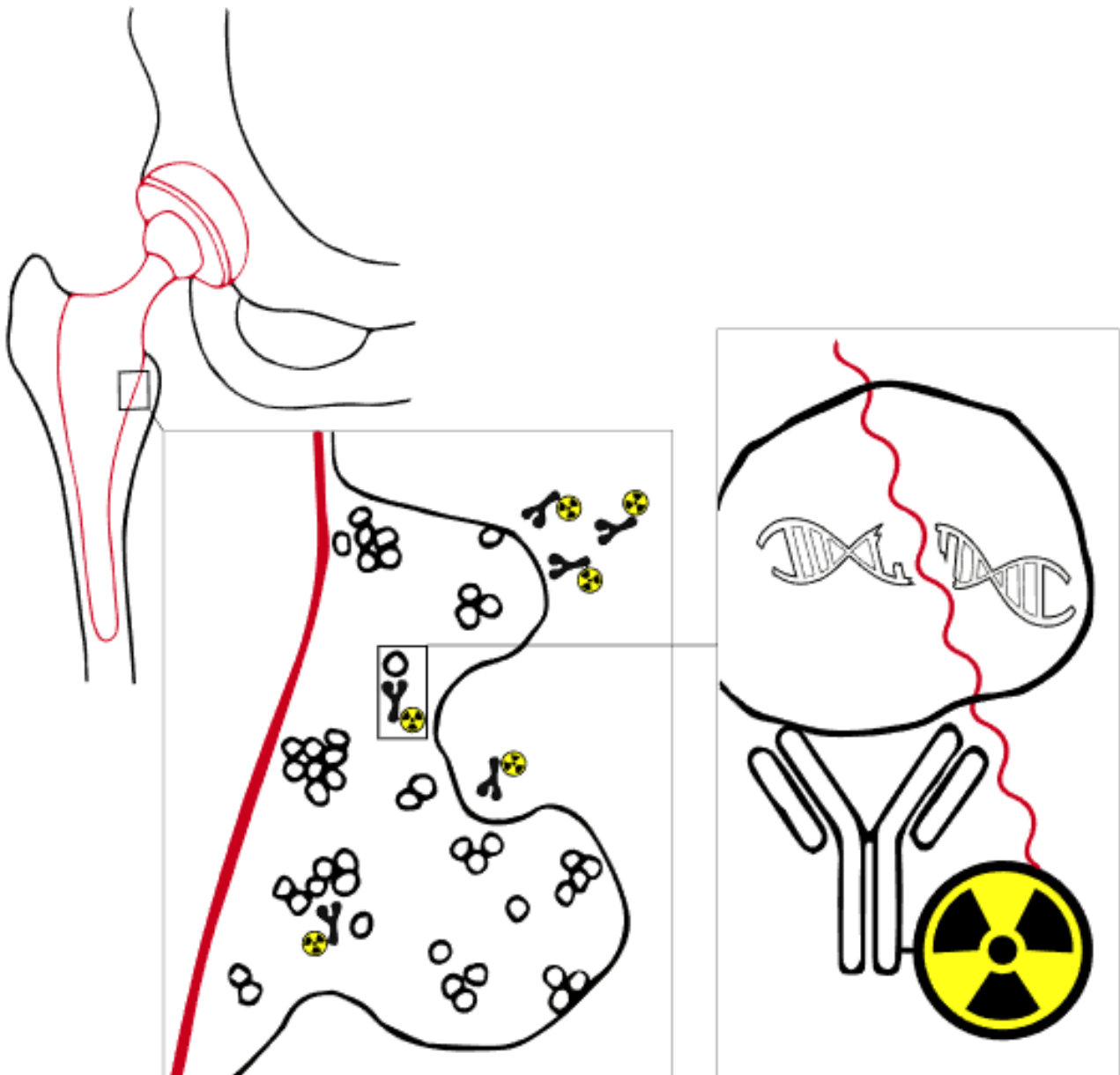


Figure 2. Concept: Radioimmunotherapy for periprosthetic joint infections. Bacteria form a biofilm on the hip prosthesis that protects them from antibiotics and the immune system. Targeted radiation therapy with alpha- or beta-emitting radioisotopes could be able to destroy the structure of the biofilm and kill the bacteria.



Treatment and diagnostics with radiation is always prone to safety concerns. Alpha- and beta-emitting radioisotopes such as ^{223}Ra and ^{188}Re are already used in the clinic for metastatic castration-resistant prostate cancer. Safety studies show that treatment with these radioisotopes is associated with minimal adverse events.^{65,66} Nonetheless, it is important to consider survival time, age, physical and emotional wellbeing and alternative treatment options. As the 5-year survival of PJI patients is lower than the predicted survival for melanoma, prostate and breast cancer, aggressive treatments seem justified. Sometimes, infection surgery yields great risk to the point that only lifetime antibiotics or amputation is an option. Further development of antibiotic resistance due to antibiotic treatment reduces the chance of successful treatment even further. In these cases radiation treatment could be beneficial despite the possible long-term effects although these risks may be limited.

CONCLUSION

The need for alternative treatment options for patients with (implant) infections like PJIs grows every year, not only due to increasing pathogen resistance to antibiotics, but also because biofilm formation obstructs the treatment of these infections with antibiotics. The novel prospects of radiation treatment strategies against planktonic and biofilm-related microbial infections are worth to investigate further.



Appendix 1. Pubmed, Embase and Cochrane search

Pubmed: (((((((Infection[Mesh] OR Infection[tiab] OR Infections[tiab] OR Infective[tiab] OR infectious[tiab]))) OR (((Bacteria[Mesh] OR Bacteria[tiab] OR Bacterial[tiab] OR Bacterium[tiab] OR Fungus[tiab] OR Fungi*[tiab] OR Fungal[tiab] OR Yeast[tiab] OR Yeasts[tiab]))) AND (((((((Radioisotopes[MeSH] OR radionuclide[tiab] OR radionuclides[tiab] OR "Radioactive Isotope"[tiab] OR "Radioactive Isotopes"[tiab] OR radioisotope[tiab] OR radioisotopes[tiab] OR Radiation, Ionizing[MeSH] OR "ionizing radiation"[tiab] OR "alpha ray"[tiab] OR "alpha rays"[tiab] OR "alpha radiation"[tiab] OR "alpha particle"[tiab] OR "alpha particles"[tiab] OR "beta ray"[tiab] OR "beta rays"[tiab] OR "beta particle"[tiab] OR "beta particles"[tiab] OR "beta radiation"[tiab] OR "gamma ray"[tiab] OR "gamma rays"[tiab] OR "gamma radiation"[tiab] OR "roentgen"[tiab] OR "rontgen"[tiab] OR "Elements, Radioactive"[MeSH] OR "radioactive element"[tiab] OR "radioactive elements"[tiab] OR Radiolabel*[tiab]))) AND (((Therapeutics[Mesh] OR therapeutic[tiab] OR therapeutics[tiab] OR therapy[tiab] OR therapies[tiab] OR treatment[tiab] OR treatments[tiab]))) OR (((Radioimmunotherapy[MeSH] OR radioimmunotherap*[tiab] OR immunoradiotherap*[tiab] OR RIT[tiab])))

Embase: (('infection'/exp OR Infection:ab,ti OR Infections:ab,ti OR Infective:ab,ti OR infectious:ab,ti) OR ('bacterium'/exp OR bacteria:ab,ti OR bacterial:ab,ti OR bacterium:ab,ti OR fungus:ab,ti OR fungi*:ab,ti OR fungal:ab,ti OR yeast:ab,ti OR yeasts:ab,ti)) AND (('radioisotope'/exp OR radionuclide:ab,ti OR radionuclides:ab,ti OR 'radioactive isotope':ab,ti OR 'radioactive isotopes':ab,ti OR radioisotope:ab,ti OR radioisotopes:ab,ti OR 'particle radiation'/exp OR 'ionizing radiation':ab,ti OR 'alpha ray':ab,ti OR 'alpha rays':ab,ti OR 'alpha radiation':ab,ti OR 'alpha particle':ab,ti OR 'alpha particles':ab,ti OR 'beta ray':ab,ti OR 'beta rays':ab,ti OR 'beta particle':ab,ti OR 'beta particles':ab,ti OR 'beta radiation':ab,ti OR 'gamma ray':ab,ti OR 'gamma rays':ab,ti OR 'gamma radiation':ab,ti OR 'roentgen':ab,ti OR 'rontgen':ab,ti OR 'radioactive element'/exp OR 'radioactive element':ab,ti OR 'radioactive elements':ab,ti OR radiolabel*:ab,ti) AND ('therapy'/exp OR therapeutic:ab,ti OR therapeutics:ab,ti OR therapy:ab,ti OR therapies:ab,ti OR treatment:ab,ti OR treatments:ab,ti) OR ('radioimmunotherapy'/exp OR radioimmunotherap*:ab,ti OR immunoradiotherap*:ab,ti OR RIT:ab,ti)) AND [embase]/lim NOT [medline]/lim

Conchrane: ((Infection:ab,ti OR Infections:ab,ti OR Infective:ab,ti OR infectious:ab,ti) OR (Bacteria:ab,ti OR Bacterial:ab,ti OR Bacterium:ab,ti OR Fungus:ab,ti OR Fungi*:ab,ti OR Fungal:ab,ti OR Yeast:ab,ti OR Yeasts:ab,ti)) AND (radionuclide:ab,ti OR radionuclides:ab,ti OR Radioactive Isotope:ab,ti OR "Radioactive Isotopes":ab,ti OR radioisotope:ab,ti OR radioisotopes:ab,ti OR "ionizing radiation":ab,ti OR "alpha ray":ab,ti OR "alpha rays":ab,ti OR "alpha radiation":ab,ti OR "alpha particle":ab,ti OR "alpha particles":ab,ti OR "beta ray":ab,ti OR "beta rays":ab,ti OR "beta particle":ab,ti OR "beta particles":ab,ti OR "beta radiation":ab,ti OR "gamma ray":ab,ti OR "gamma rays":ab,ti OR "gamma radiation":ab,ti OR "roentgen":ab,ti OR "rontgen":ab,ti OR "radioactive element":ab,ti OR "radioactive elements":ab,ti OR Radiolabel*:ab,ti) AND ((therapeutic:ab,ti OR therapeutics:ab,ti OR therapy:ab,ti OR therapies:ab,ti OR treatment:ab,ti OR treatments:ab,ti) OR (radioimmunotherap*:ab,ti OR immunoradiotherap*:ab,ti OR RIT:ab,ti))



REFERENCES

1. Levy S.B., Bonnie M. Antibacterial resistance worldwide: Causes, challenges and responses. *Nat Med.* 2004;10(12S):S122-S129.
2. Parvizi J., Bs CJ. Definition of Periprosthetic Joint Infection Is There a Consensus? 2011:3022-3030.
3. Lewis K. Persister Cells. *Annu Rev Microbiol.* 2010;64(1):357-372.
4. Zmistowski B., Karam J.A., Durinka J.B., Casper D.S., Parvizi J. Periprosthetic joint infection increases the risk of one-year mortality. *J Bone Joint Surg Am* 2013;95: 2177-2184
5. Siegel R.L., Miller K.D., Jemal A. Cancer statistics, 2019. *CA Cancer J Clin* 2019;69: 7-34.
6. Lagendijk J.J.W., Raaymakers B.W., Raaijmakers A.J.E., et al. MRI/linac integration. *Radiother Oncol.* 2008;86(1):25-29.
7. Larson S.M., Carrasquillo J.A., Cheung N.K. PO. Radioimmunotherapy of human tumours. *Nat Rev Cancer* 2015 Jun;15(6)347-60.
8. Helal M, Dadachova E. Radioimmunotherapy as a Novel Approach in HIV, Bacterial, and Fungal Infectious Diseases. *Cancer Biother Radiopharm* 2018;33(8):1-6.
9. Rontgen W.C. On a New Kind of Rays. *Science* 3 1896: 227-231
10. Musser J.H., Edsall D.L. A study of metabolism in leukemia, under the influence of the x-ray. With a consideration of the manner of action of the x-ray and of some precautions desirable in its therapeutic use. *Transactions of the Association of American Physicians* 1905;20: 294.
11. Quimby A.J., Quimby W.A. Unresolved Pneumonia: Successful Treatment by Röntgen Ray: AR Elliott. 1916
12. Fried C. Die Röntgentherapie der bronchopneumonia unter besonderer berücksichtigung der bronchopneumonia des kindesalters. *Monatsschrift Kinderheilkunde* 1928;38: 158
13. Krost G.N. Unresolved Pneumonia in Children: Treatment with Roentgen Ray. *American Journal of Diseases of Children* 1925;30: 57-71.
14. Powell E.V. Roentgen therapy of lobar pneumonia. *Journal of the American Medical Association* 1938; 110: 19-22.
15. Rousseau J., Johnson W., Harrell G.T. The value of roentgen therapy in pneumonia which fails to respond to the sulfonamides. *Radiology* 1942;38: 281-289.
16. Oppenheimer A. Roentgen therapy of interstitial pneumonia. *The Journal of Pediatrics* 1943;23: 534-538.
17. Chamberlain W.E. Roentgen Therapy with Very Small Doses: Experience in Lymphadenitis, Leukemia, Hodgkin's Disease and Certain Infections. *Acta Radiologica* 1926;6: 271-280.
18. Calabrese E.J., Dhawan G. How radiotherapy was historically used to treat pneumonia: could it be useful today? *Yale J Biol Med* 2013;86: 555-570.
19. Hart G.B., Lamb R.C., Strauss M.B. Gas gangrene. *J Trauma* 1983;23: 991-1000.
20. Kelly J.F., Dowell D.A. Twelve-year review of x-ray therapy of gas gangrene. *Radiology* 1941;37: 421-439.



21. Kelly J.F. The X-ray as an Aid in the Treatment of Gas Gangrene: *Bacillus welchii* infection—preliminary report. *Radiology* 1933;20: 296-304.
22. Taliaferro W.H., Taliaferro L.G. Effect of x-rays on immunity; a review. *J Immunol* 1951;66: 181-212.
23. Pendergrass E., Hodes P., Griffith J. Effect of roentgen rays on the minute vessels of the skin in man. *Amer J Roent* 1944;52: 123-127.
24. Coleman E., Bennett D. Personal experiences with gas bacillus infection: A report of forty-one cases. *The American Journal of Surgery* 1939;43: 77-80.
25. Calabrese E.J., Dhawan G. The role of x-rays in the treatment of gas gangrene: a historical assessment. *Dose Response* 2012;10: 626-643.
26. Coyle, RR . Odd and ends of x-ray work, including some cases of carbuncle. *Med Electrol Radiol* 1906; 7(1): 39–142.
27. Dunham, K . Treatment of carbuncles by the roentgen ray. *Am J Roentgenol* 1916; 3: 259–260.
28. Desjardins, AU . Radiotherapy for inflammatory conditions. *J Am Med Assoc* 1931; 96: 401–408.
29. Calabrese EJ. X-Ray treatment of carbuncles and furuncles (boils): a historical assessment. *Hum Exp Toxicol.* 2013;32(8):817-827
30. Bluestone C.D. Pathogenesis of otitis media: role of eustachian tube. *Pediatr Infect Dis J* 1996;15: 281-291
31. Radioactieve stoffenbesluit (Warenwet). *Staatsblad van het Koninkrijk der Nederlanden.* 1958. Stb. 1958, 317
32. Heineke H. Experimentelle Untersuchungen über die Einwirkung der Röntgenstrahlen auf innere Organe. *Mitt Grenzgeb Med Chir* 1905;14: 21.
33. Beattie R. Treatment of Subacute and Chronic Otitis Media with Use of X-ray. *J Mich St Med Soc* 1921;20: 449-451.
34. Calabrese E., Dhawan G. Historical use of x-rays: treatment of inner ear infections and prevention of deafness. *Human & experimental toxicology* 2014;33: 542-553.
35. Crowe S.J., Baylor J.W. The prevention of deafness. *Journal of the American Medical Association* 1939;112: 585-590.
36. Crowe S.J., Walzl E.M. Irradiation of Hyperplastic Lymphoid Tissue in the Nasopharynx. *Journal of the American Medical Association* 1947;134: 124-127.
37. Verduijn P.G., Hayes R.B., Looman C., Habbema J.D., van der Maas P.J. Mortality after nasopharyngeal radium irradiation for eustachian tube dysfunction. *Ann Otol Rhinol Laryngol* 1989;98: 839-844.
38. Ronckers C.M., Van Leeuwen F.E., Hayes R.B., Verduijn P.G., Stovall M., et al. Cancer incidence after nasopharyngeal radium irradiation. *Epidemiology* 2002;13: 552-560.
39. Ducatman A.M., Farber S.A. Radium exposure in U.S. military personnel. *N Engl J Med* 1992;326: 71-72.



40. Hardy W.G., Bordley J.E. Observations from a controlled study on the effect of nasopharyngeal irradiation in a group of school age children. *Ann Otol Rhinol Laryngol* 1954;63: 816-826.
41. Schneider A.B., Lubin J., Ron E., Abrahams C., Stovall M., et al. Salivary gland tumors after childhood radiation treatment for benign conditions of the head and neck: dose-response relationships. *Radiat Res* 1998;149: 625-630.
42. Sandler D.P., Comstock G.W., Matanoski G.M. Neoplasms following childhood radium irradiation of the nasopharynx. *J Natl Cancer Inst* 1982;68: 3-8.
43. Yeh H., Matanoski G.M., Wang N., Sandler D.P., Comstock G.W. Cancer incidence after childhood nasopharyngeal radium irradiation: a follow-up study in Washington County, Maryland. *Am J Epidemiol* 2001;153: 749-756.
44. Loeb W.J. Radiation therapy of the nasopharynx: a 30 year view. *Laryngoscope* 1979; 89: 16-21.
45. Graamans K. Nasopharyngeal radium irradiation: The lessons of history. *Int J Pediatr Otorhinolaryngol* 2017;93: 53-62.
46. Strebhardt K., Ullrich A. Strebhardt & Ulrich 2008 Paul Ehrlichs magic bullet concept. 2008;8(june):473-480.
47. Spiess H. Peteosthor – a medical disaster due to Radium-224. 2002:163-172.
48. Wick R.R. DISEASES. 1993;19:467-473.
49. Tomb J.F., White O., Kerlavage A.R., Al. E. Tomb, Jean-F., et al. The complete genome sequence of the gastric pathogen *Helicobacter pylori*. *Nature* 388.6642 (1997): 539-547. *Nature*. 1997;388(September):539-547.
50. Gholamrezanezhad A., Mirpour S., Saghari M., Abdollahzadeh J., Pourmoslemi A., Yarmand S. Radio-iodine therapy and *Helicobacter pylori* infection. *Ann Nucl Med*. 2008;22(10):917-920.
51. Arduc A., Dogan B.A., Ozuguz U., et al. The effect of radioactive iodine treatment on 14C urea breath test results in patients with hyperthyroidism. *Clin Nucl Med*. 2014;39(12):1022-1026.
52. Shmueli H., Friedman M., Aronov I., et al. The effect of radioiodine on eradication of *Helicobacter pylori* infection in patients with thyroid cancer-A pilot study. *Oper Tech Otolaryngol - Head Neck Surg*. 2012;23(3):206-210.
53. Usluogullari C.A., Demir Onal E., Ozdemir E., et al. What is the effect of radioiodine therapy on *Helicobacter pylori* infection? *Turkish J Med Sci*. 2014;44(3):520-523.
54. Chabner B.A., Jr TGR. Chemotherapy and the war on cancer. 2005;5(January).
55. Joo W.D., Visintin I., Mor G., Sciences R., Haven N. Targeted cancer therapy – Are the days of systemic chemotherapy numbered? 2013;76(4):308-314.
56. Adams G.P., Weiner L.M. Monoclonal antibody therapy of cancer. 2005;23(9):1147-1157.
57. Larson S.M., Carrasquillo J.A., Cheung N.K. PO. Radioimmunotherapy of human tumours. *Nat Rev Cancer* 2015 Jun;15(6)347-60.
58. Martinez L.R., Bryan R.A., Apostolidis C., Morgenstern A., Casadevall A., Dadachova E. Antibody-guided alpha radiation effectively damages fungal biofilms. *Antimicrob Agents Chemother*. 2006;50(6):2132-2136.



59. Dadachova E., Nakouzi A., Bryan R.A., Casadevall A. Ionizing radiation delivered by specific antibody is therapeutic against a fungal infection. *Proc Natl Acad Sci U S A*. 2003;100(19):10942-10947.
60. Bryan R.A., Jiang Z., Howell R.C., et al. Radioimmunotherapy Is More Effective than Antifungal Treatment in Experimental Cryptococcal Infection. *J Infect Dis*. 2010;202(4):633-637.
61. Dadachova E., Burns T., Bryan R.A., et al. Feasibility of radioimmunotherapy of experimental pneumococcal infection. *Antimicrob Agents Chemother*. 2004;48(5):1624-1629.
62. Rivera J., Nakouzi A.S., Morgenstern A., Bruchertseifer F., Dadachova E., Casadevall A. Radiolabeled antibodies to Bacillus anthracis toxins are bactericidal and partially therapeutic in experimental murine anthrax. *Antimicrob Agents Chemother*. 2009;53(11):4860-4868.
63. Tietz C.J., Spiess H. Über die Hemmwirkung des Peteosthor und seiner Komponenten auf das Wachstum humaner Tuberkelbakterien in vitro. In: *Klinische Wochenschrift*. 1950
64. Bannas P, Hambach J, Koch-Nolte F. Nanobodies and nanobody-based human heavy chain antibodies as antitumor therapeutics. *Front Immunol*. 2017;8(NOV):1-13.
65. Parker C, Nilsson S, Heinrich D, et al. Alpha emitter radium-223 and survival in metastatic prostate cancer. *N Engl J Med*. 2013;369(3):213-223.
66. Ter Heine R, Lange R, Breukels OB, et al. Bench to bedside development of GMP grade Rhenium-188-HEDP, a radiopharmaceutical for targeted treatment of painful bone metastases. *Int J Pharm*. 2014;465(1-2):317-324.





Radioimmunotherapy of methicillin-resistant *Staphylococcus aureus* in planktonic state and biofilms

Based on: | van Dijk B | Allen KJH | Helal M | Vogely HC | Lam MGEH | de Klerk JMH | Weinans H | van der Wal BCH | Dadachova E. *Radioimmunotherapy of methicillin-resistant Staphylococcus aureus in planktonic state and biofilms*. PLoS ONE. 2020; 15, e0233086.



ABSTRACT

Background

Implant associated infections such as periprosthetic joint infections are difficult to treat as the bacteria form a biofilm on the prosthetic material. This biofilm complicates surgical and antibiotic treatment. With rising antibiotic resistance, alternative treatment options are needed to treat these infections in the future. The aim of this article is to provide proof-of-principle data required for further development of radioimmunotherapy for non-invasive treatment of implant associated infections.

Methods Planktonic cells and biofilms of Methicillin-resistant staphylococcus aureus are grown and treated with radioimmunotherapy. The monoclonal antibodies used, target wall teichoic acids that are cell and biofilm specific. Three different radionuclides in different doses were used. Viability and metabolic activity of the bacterial cells and biofilms were measured by CFU dilution and XTT reduction. **Results** Alpha-RIT with Bismuth-213 showed significant and dose dependent killing in both planktonic MRSA and biofilm. When planktonic bacteria were treated with 370 kBq of ²¹³Bi-RIT 99% of the bacteria were killed. Complete killing of the bacteria in the biofilm was seen at 185 kBq. Beta-RIT with Lutetium-177 and Actinium-225 showed little to no significant killing.

Conclusion Our results demonstrate the ability of specific antibodies loaded with an alpha-emitter Bismuth-213 to selectively kill staphylococcus aureus cells in vitro in both planktonic and biofilm state. RIT could therefore be a potentially alternative treatment modality against planktonic and biofilm-related microbial infections



INTRODUCTION

Introduction Total joint replacement is the last resort treatment for degenerative joint disease. A feared complication is prosthetic joint infection (PJI) with an incidence of 1–2% after primary hip arthroplasty and 1–4% after primary knee arthroplasty¹. PJI is difficult to treat as the bacteria form a biofilm on the prosthetic material. This hinders the host immune system, but more important, the bacteria in a biofilm are mostly in a dormant state and therefore not susceptible to most antibiotics². Alpha or beta radiation could potentially damage or destroy these dormant cells because, in contrary to antibiotics, the damaging effects are independent of the cell's metabolic state. However, due to the limited tissue penetration of both alpha and beta radiation it is crucial to get the radionuclide in close vicinity to the cells. Radioimmunotherapy (RIT) relies on the antigen-binding characteristics of the monoclonal antibodies (mAbs) to deliver cytotoxic radiation to target cells and is successfully used in oncology³. As microbes express antigens that are unique and different from host antigens, they can be targeted with high specificity and low cross-reactivity. In the past we demonstrated that fungal cells could be eliminated *in vitro* and *in vivo* with the radiolabeled microorganism-specific mAbs⁴, and later expanded this approach to other fungal and bacterial pathogens such as *Streptococcus pneumoniae* and *Bacillus anthracis* as well as HIV⁵. This implies that bacterial infections of the prosthetic joints can also, in principle, be treated with RIT. The hypothesis underlying the current study is that radioisotopes Lutetium-177 (¹⁷⁷Lu; a beta-emitter), and Actinium-225 (²²⁵Ac; an alpha-emitter) or Bismuth-213 (²¹³Bi; an alpha-emitter) are able to eradicate *Staphylococcus aureus* using RIT with mAbs directed towards the bacterial cell wall and the biofilm. *S. aureus* is the most common pathogen involved in PJI₆ and therefore this proof-of-principle data is required for further development of RIT for non-invasive treatment of PJIs.

MATERIALS AND METHODS

Growth of bacterial cultures

A methicillin-resistant AH4802-LAC strain of *Staphylococcus aureus* [7] was a kind gift from dr. A.R. Horswill, Professor of Immunology & Microbiology at the University of Colorado, CO, USA. This strain is a known biofilm former on diverse surfaces. For both planktonic growth and biofilm formation, the bacteria were transferred from the frozen stock onto blood agar plates (Tryptic Soy Agar (TSA) with 5% sheep blood) and aerobically cultured overnight at 37°C. After incubation, 3–4 single colonies were emulsified in tryptic soy broth (TSB) and incubated overnight at 37°C with agitation (150–200 RPM).

For planktonic growth, the cultures were vortexed for 30 seconds after incubation and thereafter diluted 1:100 in TSB. Bacteria were grown for 3–4 hours until logarithmic phase was reached. The cultures were vortexed for 1 min and measured on a microplate reader (Spectra MAX 250, Molecular Devices, USA) at 600 nm. The cells were washed twice and re-suspended in sterile phosphate buffered saline (PBS). The diluted bacteria were vortexed for 10 seconds after which 100 µl of this suspension was added to the appropriate number of wells of a sterile flat-bottomed 96-well polystyrene tissue culture-treated microtiter plate with a lid (Fisher Scientific).

Biofilm formation was standardized and based on the recommendations described by Stepanović et al. [8]. After initial incubation, the culture was vortexed for 30 seconds and thereafter diluted 1:100 in TSB supplemented with 1% glucose to reach approximately 10⁶ colony forming units (CFU)/ml, measured at 600 nm. The diluted bacteria were vortexed for 10 seconds after which 100 µl of this suspension was added to the appropriate number of wells of the same type of 96-well plate used for planktonic bacteria. The outer wells were filled with 200 µl of sterile PBS to counter dehydration of the biofilms. The plate was cultured aerobically and under static conditions for 24 hours at 37°C. After incubation the medium was carefully



removed by pipetting and the biofilms were washed twice with sterile PBS to remove nonadherent bacteria. Finally 50 μL of sterile PBS was added to each well containing biofilms. All assays were carried out in duplicate.

Antibodies and radiolabeling

To deliver the radionuclides to the bacteria and biofilms, human mAb anti- β GlcNAc-IgG1 antibody 4497 that targets wall teichoic acids (WTAs) was used [9]. WTAs are cell surface-exposed glycopolymers on *S. aureus* cells that are also found within the extracellular matrix of the biofilm [10]. Thus, this antibody targets both bacteria and biofilm. Human mAb Palivizumab (IgG1) against respiratory syncytial virus (RSV) was acquired from MedImmune and was used as an isotype-matching negative control for non-specific killing of bacteria. Unlabeled 4497 and Palivizumab mAbs were also used as controls. MAb 4497 and Palivizumab were conjugated to bifunctional chelating agents CHXA” or DOTA (Macrocyclics, USA) using a 10- or 20-fold molar excess over mAb as described earlier [11]. Conjugated antibody was radiolabeled with three different radioisotopes, ^{213}Bi , ^{177}Lu and ^{225}Ac . Radiolabeling of the antibody-CHXA” conjugate with ^{177}Lu and ^{213}Bi was performed to achieve a specific activity of 185 kBq/ μg of the antibody whereas for the radiolabeling of antibody-DOTA conjugate with ^{225}Ac a specific activity of 37 kBq/ μg was desired.

^{213}Bi was eluted from the generator with 200 μL of freshly prepared 2% (v/v) HI solution in deionized H₂O followed by 100 μL of deionized H₂O. To facilitate radiolabeling, the pH was adjusted to 7 using 80 μL of 5M ammonium acetate solution and the radioactivity was measured on a dose calibrator. An appropriate amount of Ab-CHXA” was then added to achieve the desired specific activity and the reaction was heated at 37°C for 5 minutes with shaking. The reaction was then quenched by the addition of 3 μL of 0.05 M EDTA solution to bind any free ^{213}Bi . To purify the mixture the solution was then added to an Amicon Ultra 0.5 mL centrifugal filter (30K MW cut off, Fisher Scientific) and spun for 3 minutes at 14 000 g, followed by 300 μL of PBS was and spun again. The purified solution was collected and the percentage of radiolabeling (radiolabeling yield) was measured by instant thin layer chromatography (iTLC) by developing 10 cm silica gel strips (Agilent Technologies, CA, USA) in 0.15 M ammonium acetate buffer. In this system the radiolabeled antibodies stay at the point of application while free ^{213}Bi , in the form of EDTA complexes, moves with the solvent front. The strips were cut in half and each half is counted on a 2470 Wizard2 Gamma counter (Perkin Elmer, MA, USA) that was calibrated for the ^{213}Bi emission spectrum and only emissions in this range were considered in the CPM. The percentage of radiolabeling is calculated by dividing the counts per minute (CPM) at the bottom of the strip (labeled antibody) by the sum of the CPM at the bottom and the top of the strip (total amount of radioactivity) and multiplying the result by 100. Typical yields were greater than 95%.

^{177}Lu chloride was diluted with 0.15 M ammonium acetate buffer and added to a microcentrifuge tube (MCT) containing the mAb-CHXA” conjugate in the 0.15 M ammonium acetate buffer in a reaction volume of ~ 30 μL . The reaction mixture was incubated for 60 min at 37°C. The reaction was then quenched by the addition of 3 μL of 0.05 M EDTA solution to bind any free ^{177}Lu . Labelling efficiency was then measured in the same manner described above using iTLC. Typical yields were greater than 95% and required no further purification.

^{225}Ac labelling was performed similarly to ^{177}Lu , however to accommodate the larger size of ^{225}Ac an antibody-DOTA conjugate had to be used, Three μL of 0.05M Diethylenetriamine pentaacetate (DTPA) solution was used to quench the reaction. iTLC were read 24h after



running to allow for secular equilibrium to be reached. Yields were typically greater than 98% and required no further purification.

Determination of the bactericidal effect of RIT on S. aureus

S. aureus AH4802 planktonic cells and biofilms were treated with three different radionuclides at different doses for 1 hour at 37°C. The doses for ¹⁷⁷Lu were 14.8, 7.4, 3.7 MBq and for ²²⁵Ac 7.4, 3.7 and 1.85 kBq on for both planktonic and biofilm. 370, 185, 111, 74, and 37 kBq of ²¹³Bi was used on planktonic bacteria and 185, 111 and 37 kBq was used on biofilms. Alpha particles have higher (100 keV/μm) linear energy transfer when compared to beta particles (0.8 keV/ μm) and can produce considerably more lethal double strand DNA breaks along their tracks. Therefore, ¹⁷⁷Lu (half-life 6.7 days, 0.5 MeV), being a beta-emitter, needs higher activities to deliver a lethal absorbed dose when compared to alpha-radiation. During its decay, ²²⁵Ac (half-life 10 days, 5.9 MeV) emits four α-particles versus one α-particles emitted by ²¹³Bi (halflife 46 min, 5.9 MeV). Thus, ²²⁵Ac is lethal at lower activities when compared to ²¹³Bi and therefore a lower radiation dose of ²²⁵Ac is used.

After incubation, the 96-wells plates were centrifuged for 7 min at 3,500 RPM, washed twice and the pellets were re-suspended in 100 μl sterile PBS. The biofilms were sonicated for 30 seconds to detach the cells. Viability and metabolic activity of the bacterial cells and biofilms were measured by CFU dilution and XTT reduction. For viability testing, 20 μl of each well was used to make a serial dilution, cultured overnight on blood agar plates and counted for colony forming units (CFU). Metabolic activity was measured by adding 50 μl of freshly mixed 2,3-bis-(2-methoxy-4-nitro-5-sulfophenyl)-2H-tetrazolium-5-carboxanilide (XTT) solution (from XTT cell proliferation kit II, Sigma) to the remaining 80 μl of the bacterial solution in each well. The plates are covered in aluminum foil and incubated for 3 hours at 37°C under static conditions. The colorimetric change was read in an ELISA plate reader (Labsystem Multiskan, Franklin, MA) at 492 nm absorbance. Colorimetric change is the result of mitochondrial dehydrogenase activity that reduced XTT tetrazolium salt to XTT formazan. Thus, the more colorimetric change the more metabolic activity there is. Two wells with sterile PBS were used as blank control. Significant differences between treatment groups and their corresponding controls were calculated using one-way ANOVA with a post-hoc Tukey test.

RESULTS

Multiple experiments were done to assess the efficacy of RIT on planktonic MRSA and biofilms. First, planktonic bacteria were treated with 14,8, 7,4 and 3,7 MBq of beta-emitter ¹⁷⁷Lu bound to the specific WTA-specific mAb 4497 and to the non-specific mAb Palivizumab. XTT results were compared to the unlabeled controls. (Fig 1A and 1B). No significant reduction of cells was seen between treatment groups and their controls ($p = >0,05$). A significant difference in metabolic activity was seen between the specific and non-specific antibodies loaded with 7,4 MBq of ¹⁷⁷Lu ($p = 0.033$). Second, planktonic bacteria were treated with 7,4, 3,7, and 1,85 kBq of alpha-emitter ²²⁵Ac bound to the same antibodies. No significant difference was seen in CFU count between the groups apart from the non-specific treatment group bound to 3.7 kBq of ²²⁵Ac compared to the control. ($p = >0,05$) A significant increase in metabolic activity was seen in all treatment groups compared to both controls and corresponding radiation dose. ($p = > 0,05$) (Fig 1C and 1D). WTA-specific mAb ²²⁵Ac-4497 showed an increase in metabolic activity when compared the labeled non-specific antibodies. Third, planktonic bacteria were treated with 370, 185, 111, 74 and 37 kBq of ²¹³Bi. When treatment groups were compared to their controls, a significant reduction in survival was seen in the WTA-specific mAb 4497 group with 370, 185 and 111 kBq ($p = 0,002$, $p = 0,008$ resp.



$p = 0,032$) when compared to the control. Also, a significant reduction was seen with the non-specific antibodies 370 and 185 kBq compared to the control ($p = 0,003$ resp. $p = 0,036$).

After the planktonic experiments, biofilms were treated with RIT. The WTA-specific mAb 4497 groups with ^{177}Lu , ^{225}Ac and ^{213}Bi showed no significant difference in CFU count compared to the control although there was no bacterial growth with 185 kBq ^{213}Bi bound to WTA and Palivizumab antibodies (Fig 2). There was a significant difference in metabolic activity between ^{177}Lu bound to the non-specific antibodies compared to the control ($p = 0,026$) and a significant difference, in favor of the specific antibody, between the WTA-specific mAb 4497 with a radiation dose of 7.4 MBq when compared to the same dose of the non-specific antibody ($p = 0,011$). In the non-specific antibody group of ^{225}Ac with 1.85 kBq, a significant difference was seen in metabolic activity when compared to the control ($p = 0,029$). A significant difference in metabolic activity was seen in WTA-specific mAb 4497 loaded with 185 and 111 kBq of ^{213}Bi when compared to the control ($p = 0,014$ resp. $p = 0,045$). Also, a significant difference in metabolic activity was seen in the non-specific antibody group loaded with 185 kBq of ^{213}Bi compared to the control ($p = 0,018$). There was a significant difference in metabolic activity between the specific and non-specific antibodies loaded with 111 and 74 kBq of ^{213}Bi ($p = 0,037$ resp. $p = 0,026$). There was no significant difference seen in metabolic activity between the specific and non-specific antibodies loaded with the highest dose of 185 kBq ^{213}Bi because all the plates were sterile.



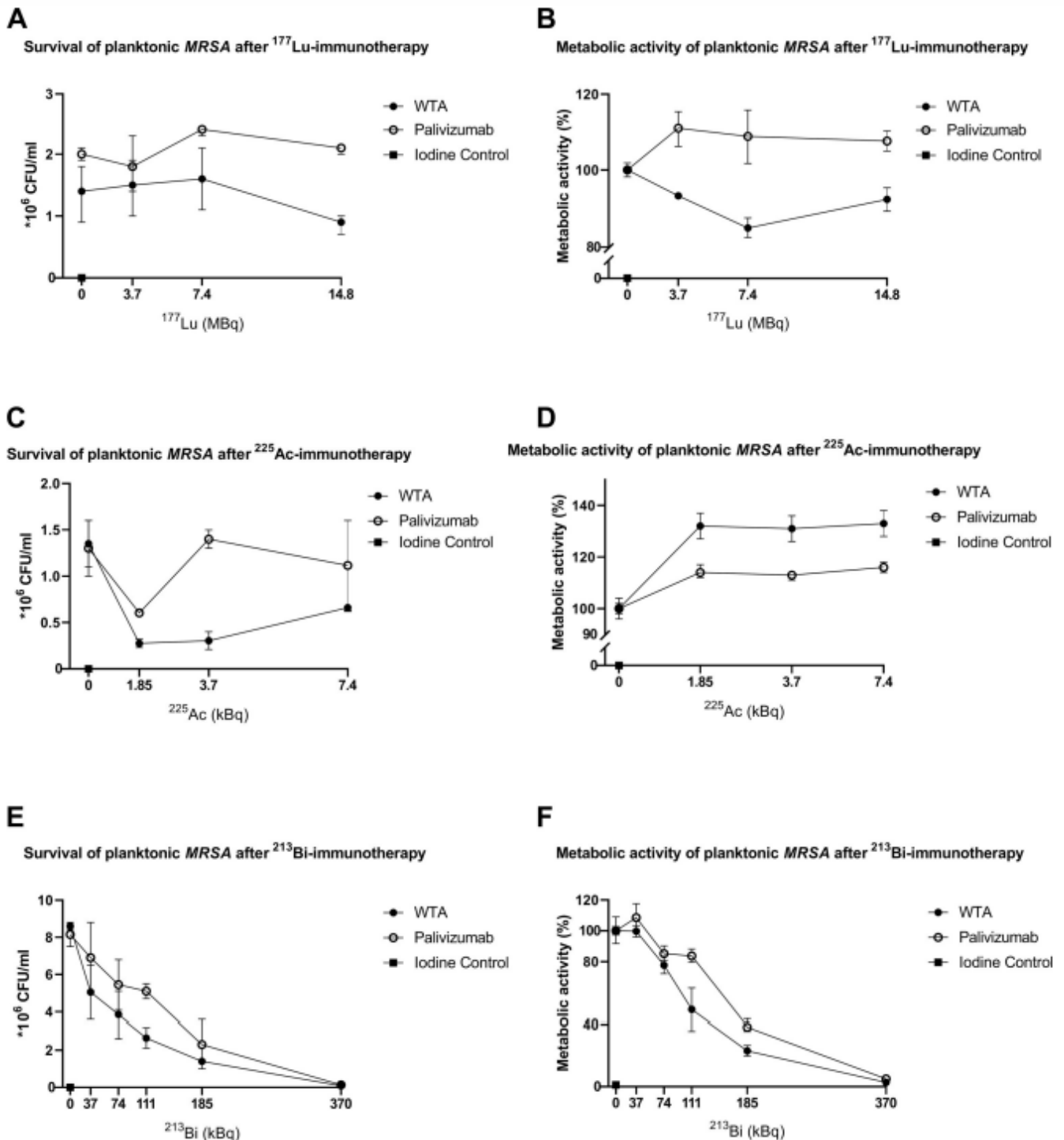


Figure 1. Susceptibility of planktonic *S. aureus* (MRSA) to beta and “short and long-lived” alpha radiation measured by CFU/ml for survivability (A,C,E) and XTT reduction assay for the metabolic activity (B,D,F). Increasing doses of RIT with specific anti-WTA 4497 antibodies and non-specific antibodies Palivizumab labeled with ^{177}Lu (A,B), ^{225}Ac (C,D) and ^{213}Bi (E,F). Treatment results were compared to unlabeled 4497 mAb, Palivizumab, and iodine controls. Each data point represents the average of two measurements



DISCUSSION

The need for alternative treatment options for patients with implant infections like periprosthetic joint infections grows every year, not only due to increasing pathogen resistance to antibiotics, but also because biofilm formation obstructs the treatment of these infections with antibiotics. To the best of our knowledge, this is the first report of RIT treatment of MRSA in particular and of any multidrug resistant bacteria in general in both planktonic and biofilm state. ²¹³Bi-labeled mAb WTA 4497 consistently killed both planktonic bacteria and biofilm as measured by both XTT and CFU assays. A significant decrease in both CFU count and metabolic activity was seen in planktonic bacteria when treated with 370, 185 and 111 kBq ²¹³Bi-WTA-specific mAb 4497 versus 370 and 185 kBq of ²¹³Bi-Palivizumab (Fig 1E and 1F). Although statistically not significant, biofilms treated with specific and non-specific antibodies labeled with 185 kBq of ²¹³Bi showed no residual bacterial growth with the effect being similar to that of Iodine solution, being used as a positive control. (Figs 1 and 2). Also, a significant decrease in metabolic activity was seen in biofilms treated with specific antibodies labeled with 185 and 111 kBq of ²¹³Bi and non-specific antibodies labeled with 185 kBq (Fig 2E and 2F). The decrease in survival and metabolic activity in both planktonic bacteria and biofilms treated with 370 and 185 kBq ²¹³Bi groups was probably due to high levels of radioactivity in a small volume causing non-specific killing. Nonetheless, ²¹³Bi showed a dose dependent killing of planktonic bacteria and biofilms. Interestingly, specific antibodies labeled with 111 kBq showed significantly more killing of planktonic bacteria and biofilms in both CFU count and XTT when compared to non-specific antibodies loaded with the same amount of radiation, suggesting that specific targeting is more effective. This could mean that mAb ²¹³Bi-4497 specifically targets individual cells. In this regard, the non-specific killing by both radiolabeled bacterium-specific and non-specific antibodies results from one or combination of two events: 1) in vitro there is always some non-specific killing of cells by highly destructive alpha and beta particles emitted by the radionuclides in a small volume of an assay; 2) WTA-specific 4497 and RSV mAbs are human monoclonal antibodies which, on average, have much higher isoelectric points (IP) than murine antibodies. Antibodies with higher IPs have a tendency to non-specifically bind to the cells, therefore, both radiolabeled 4497 and RSV mAbs demonstrated some non-specific therapeutic effect towards bacterial cells. However, the killing effect of radiolabeled with ²¹³Bi 4497 mAb was higher than that of radiolabeled RSV mAb under examined conditions, indicating that killing of MRSA by ²¹³Bi-4497 mAb was WTA-specific". This also suggests that α -particles are able to effectively penetrate the architecture of the biofilms to deliver bactericidal radiation to the cells. Encouragingly, the dose required for killing *S. aureus* in a biofilm was of the same order of magnitude as the dose required to kill planktonic cells. ¹⁷⁷Lu-4497 mAb did not have an effect on planktonic bacteria and the biofilm, whereas ²²⁵Ac seemed to even increase metabolic activity in planktonic and biofilm formation. This was probably due to the biofilm matrix release and thus bacterial release, caused by alpha-radiation, which interferes with XTT and gives an increase in CFU when compared to the unlabeled controls. It is possible, that due to the long physical half-lives of ²²⁵Ac (10 days) and ¹⁷⁷Lu (6.7 days) it might take longer than the 1 hour incubation to reveal the full bactericidal potential of these long lived radionuclides but longer incubation time might also improve the damaging effect of ²¹³Bi.

Previously we have performed extensive evaluation of RIT toxicity in mouse models of fungal and bacterial infections using the antibodies labeled with the same ²¹³Bi radionuclide utilized in this work. No systemic toxicity was noted in mice infected with *Streptococcus pneumoniae* and treated with ²¹³Bi-labeled antibody to bacterial polysaccharide [12]. The toxicity evaluation of RIT-treated mice infected intratracheally with *C. neoformans* showed the absence of acute hematologic and long-term pulmonary toxicity [13]. RIT was much better tolerated by the treated mice than Amphoterecin B which is a current standard of care for invasive fungal



infections [14]. In addition, RIT did not adversely affect bystander mammalian cells such as CHO cells and macrophages, with the latter being able to carry out their functions such as nitric oxide production after RIT exposure [15]. As all these observations have been made for systemic administration of the radiolabeled antibodies, the anticipated local application of RIT into the infected joint should be even safer in this regard.

In conclusion, our results demonstrate the ability of specific antibodies loaded with an alpha-emitter ^{213}Bi to selectively kill *S. aureus* cells in vitro in both planktonic and biofilm state. RIT could therefore be a potentially alternative treatment modality against planktonic and biofilm-related microbial infections and can be used with and without conventional therapies such as antibiotics. However, this in vitro observed bactericidal effect of RIT on *S. aureus* must be validated in vivo and the work in the animal models of MRSA infection is currently on-going.



REFERENCES

1. Parvizi J, Jacovides C, Zmistowski B, Jung KA. 2011. Definition of periprosthetic joint infection: Is there a consensus? *Clinical Orthopaedics and Related Research* p. 3022–3030.
2. Zimmerli W, Moser C. 2012. Pathogenesis and treatment concepts of orthopaedic biofilm infections. *FEMS Immunol Med Microbiol* 65:158–168.
3. Larson SM, Carrasquillo JA, Cheung NK PO. Radioimmunotherapy of human tumours. *Nat Rev Cancer* 2015 Jun; 15(6):347–60.
4. Dadachova E., Nakouzi A., Bryan R., and Casadevall A. Ionizing radiation delivered by specific antibody is therapeutic against a fungal infection. *Proc Natl Acad Sci U S A*. 100, p. 10942–10947 (2003).
5. Helal M, Dadachova E. 2018. Radioimmunotherapy as a Novel Approach in HIV, Bacterial, and Fungal Infectious Diseases 33:1–6.
6. Pulido L, Ghanem E, Joshi A, Purtill JJ, Parvizi J. Periprosthetic joint infection: The incidence, timing, and predisposing factors. *Clin Orthop Relat Res*. 2008; 466(7):1710–1715.
7. Boles BR, Thoendel M, Roth AJ, Horswill AR. 2010. Identification of Genes Involved in PolysaccharideIndependent Staphylococcus aureus Biofilm Formation. *PLoS One* 5: e10146.
8. Stepanović S, Vuković D, Hola V, Di Bonaventura G, Djukić S, Cirković I, et al. Quantification of biofilm in microtiter plates: overview of testing conditions and practical recommendations for assessment of biofilm production by staphylococci. *APMIS*. 2007.
9. Brown E.; Darwish M.; Flygare J.; Hazenbos W. et al. Anti-Wall Teichoic Antibodies and Conjugates. Patent WO 2014/194247 A1, 2014.
10. Sadovskaya I, Chaignon P, Kogan G, Chokr A, Vinogradov E. 2006. Carbohydrate-containing components of biofilms produced in vitro by some staphylococcal strains related to orthopaedic prosthesis infections. *FEMS Immunol. Med. Microbiol.* 47:75–82.
11. Allen KJH, Jiao R, Malo ME, Frank C, Dadachova E. 2018. Biodistribution of a Radiolabeled Antibody in Mice as an Approach to Evaluating Antibody Pharmacokinetics. *Pharmaceutics*. 2018 Dec 5; 10(4).
13. Dadachova E, Burns T, Bryan RA, et al. Feasibility of radioimmunotherapy of experimental pneumococcal infection. *Antimicrob Agents Chemother*. 2004 May; 48(5):1624–9.
14. Dadachova E, Bryan RA, Frenkel A, Zhang T, Apostolidis C, Nosanchuk JS, et al. Evaluation of acute hematologic and long-term pulmonary toxicities of radioimmunotherapy of *Cryptococcus neoformans* infection in murine models. *Antimicrob Agents Chemother*. 2004 Mar; 48(3):1004–6.
15. Bryan RA, Jiang Z, Howell RC, Morgenstern A, Bruchertseifer F, Casadevall A, et al. Radioimmunotherapy is more effective than antifungal treatment in experimental cryptococcal infection. *J Infect Dis*. 2010 Aug 15; 202(4):633–7.
16. Bryan RA, Jiang Z, Morgenstern A, Bruchertseifer F, Casadevall A, et al. Radioimmunotherapy of *Cryptococcus neoformans* spares bystander mammalian cells. *Future Microbiol*. 2013 Sep; 8(9):1081–9.





Photoimmuno-antimicrobial therapy for *Staphylococcus aureus* implant infection

Based on: | van Dijk B | Oliveira S | Hooning JFF | Nurmohamed FRHA | Mashayekhi V | Beltrán Hernández I | van Strijp J | de Vor L | Aerts PC | Vogely HC | Weinans H | van der Wal BCH | *Feasibility of photoimmuno-antimicrobial therapy of Staphylococcus aureus implant infection in mice*. PLoS One. 2024 Mar 8;19(3):e0300069.



ABSTRACT

Introduction:

Implant infections caused by *Staphylococcus aureus* are responsible for high mortality and morbidity worldwide. Treatment of these infections can be difficult especially when bacterial biofilms are involved. In this study we investigate the potential of infrared photoimmunotherapy to eradicate staphylococcal infection in a mouse model.

Methods: A monoclonal antibody that targets Wall Teichoic Acid surface components of both *S. aureus* and its biofilm (4497-IgG1) was conjugated to a photosensitizer (IRDye700DX) and used as photoimmunotherapy *in vitro* and *in vivo* in mice with a subcutaneous implant pre-colonized with biofilm of *Staphylococcus aureus*. A dose of 400 µg and 200 µg of antibody-photosensitizer conjugate 4497-IgG-IRDye700DX was administered intravenously to two groups of 5 mice. In addition, multiple control groups (vancomycin treated, unconjugated IRDye700DX and IRDye700DX conjugated to a non-specific antibody) were used to verify anti-microbial effects.

Results: *In vitro* results of 4497-IgG-IRDye700DX on pre-colonized (biofilm) implants showed significant ($p < 0.01$) colony-forming units (CFU) reduction at a concentration of 5 µg of the antibody-photosensitizer conjugate. *In vivo*, treatment with 4497-IgG-IRDye700DX showed no significant CFU reduction at the implant infection. However, tissue around the implant did show a significant CFU reduction with 400 µg 4497-IgG-IRDye700DX compared to control groups ($p = 0.037$).

Conclusion:

This study demonstrated the antimicrobial potential of photoimmunotherapy for selectively eliminating *S. aureus* *in vivo*. However, using a solid implant instead of a catheter could result in an increased bactericidal effect of 4497-IgG-IRDye700DX and administration locally around an implant (per operative) could become valuable applications in patients that are difficult to treat with conventional methods. We conclude that photoimmunotherapy could be a potential additional therapy in the treatment of implant related infections, but requires further improvement.



INTRODUCTION

Implant infections caused by *Staphylococcus aureus* are responsible for high mortality and morbidity worldwide^{1,2}. For example, periprosthetic joint infection is a feared complication in joint replacement surgery and is associated with pain and prolonged hospitalization. As a consequence, multiple surgical interventions are needed to treat these infections³. Implant infections are difficult to treat due to the bacterium's ability to form a biofilm on the foreign device e.g. prosthetic joints made of metal or plastic. Biofilms act as a barrier to the host immune system and antimicrobial agents⁴. Additionally, bacteria in a biofilm can be in a dormant state making them less susceptible to most antibiotics⁵. Next to that, widespread use and misuse of antibiotics have led to the emergence of antibiotic-resistant bacteria and thereby complicates treatment even more⁶. It is therefore critical to explore alternative anti-bacterial therapies in order to complement or enhance current available therapies.

Photoimmuno-antimicrobial therapy (PIAT) could be such an alternative therapy due to the potential strong antimicrobial properties of its photochemical reaction such as release of reactive oxygen species (ROS)⁷ or irreversible cell membrane damage^{8,9} with no bacterial resistance reported. As ROS produced by cellular metabolism are at the heart of innate immunity, copying this phenomenon to battle infections could potentially be of great interest. In principle, the effect of PIAT is based on light-activated non-toxic photosensitizer that is conjugated with an antibody and uses non-thermal near infrared light to activate the photosensitizer. After absorption of photons from a light source, (i). the photosensitizer becomes excited after which it interacts with the surrounding oxygen or biomolecules to form ROS. Once formed, singlet oxygen and ROS induce extensive damage to bacterial cells with minimal effects to surrounding healthy tissue, as the photosensitizers are bound to specific antibodies that target bacteria and ROS have a short diffusion range and are short-lived and (ii) the reaction results in ligand release and greatly affect the shape and solubility of the conjugate or conjugate-antigen complex which causes stress in the cellular membrane compromising its function and resulting in killing of bacterial cells^{8,9}.

Currently in Japan, photoimmunotherapy using IRDye700DX is clinically approved to treat patients with head and neck cancer and has been proven to be safe^{10,10}. Importantly, it has been shown by Mitsunaga et al.¹¹ that PIAT can kill *S. aureus in vitro* and has been successfully used to eradicate *S. aureus* nasal colonization and eliminate MRSA in the deep tissues of mice with MRSA-thigh infections in mice. As a vehicle, they used a commercially available antibody (clone Staph12-569.3, murine IgG3) that targets *S. aureus* peptidoglycan.

Our latest results demonstrated the ability of antibody 4497-IgG1 (anti- β -GlcNAc WTA) to specifically recognize and target clinically relevant *S. aureus* biofilm types *in vitro* and *in vivo*¹². This antibody targets wall teichoic acids (WTA)^{13,14} that are found in both the bacterial cell wall and within the extracellular matrix of the biofilm. Therefore, this antibody may be an ideal carrier for photosensitizer IRDye700DX in a PIAT setting. In this pilot study, the photosensitizer IRDye700DX was conjugated to mAb 4497-IgG1 to treat *S. aureus* implant infections via systemic injection with the conjugate in combination with external near infrared light illumination to excite the photosensitizer (inducing PIAT). We evaluated if PIAT has the potential to kill *S. aureus* bacteria in a biofilm *in vitro* and *in vivo* in a subcutaneous implant infection mice model.



MATERIALS AND METHODS

Biofilm culture

A bioluminescent strain of methicillin-resistant *Staphylococcus aureus*, USA300 LAC (AH4802) was used in this study¹². Biofilms were grown on the implants as described previously¹². Bacteria were grown overnight on sheep blood agar (SBA) at 37°C and cultured overnight in Tryptic Soy Broth (TSB) before each experiment. Overnight cultures were diluted to an OD₆₀₀ of 1 and then diluted 1:1000 in fresh TSB containing 0.5% (wt/vol) glucose and 3% (wt/vol) NaCl. 200 µl was transferred to wells in a flat bottom 96 wells plate (Corning Costar® 3598, Tissue Culture treated) containing 5 mm segment of a 7 French polyurethane catheter (Access Technologies, Chicago, Illinois, USA). Prior to inoculation, the implants were sterilized with 70% ethanol and air dried. The inoculated implants were incubated at 37°C for 48 hours under agitation. Fresh growth medium (200 µl) was added after 24 hours to maintain optimal growing conditions. Implants were washed three times with PBS to remove non-adherent bacteria and great care was taken to unclog every catheter. They were then stored in PBS until *in vitro* treatment or *in vivo* implantation.

Antibodies and photosensitizer immunoconjugates

The antibody 4497-IgG1 (anti-β-GlcNAc WTA) was used to deliver the photosensitizer to the bacteria and biofilm¹². As an isotype-matching negative control, IgG1 (Humanized monoclonal) antibody palivizumab (MedImmune Inc. Synagis) was used. IgG labeling via random NHS-mediated coupling to lysine amino acids was performed by incubation of both antibodies with photosensitizer IRDye700DX (LI-COR, Bad Homburg, Germany). In detail, antibodies were incubated with 10 molar equivalents of the photosensitizer for 2 hours at room temperature and shielded from light. The labelled antibodies were separated from the free IRDye700DX using a Superdex 200 Increase 10/300 GL (GE-Healthcare, 28-9909-44) gel filtration column according to the manufacturer's manual. Subsequently, absorbance was measured at 280 nm for protein and 647 nm for the IRDye700DX using a Nanodrop, to determine the final concentration and degree of conjugation.

PIAT of S. aureus on implants in vitro

S. aureus colonized implants were placed individually in a 48 wells plate and incubated for 1 hour under agitation with 5, 1 and 0,1 µg of 4497-IgG1-IRDye700DX and iso-type matching Palivizumab photosensitizer conjugates. In addition, multiple controls were used: 4497-IgG1 and Palivizumab without photosensitizer conjugates with near infrared illumination, IRDye700DX alone with near infrared illumination, 4497-IgG1-IRDye700DX and Palivizumab-IRDye700DX without near infrared illumination and a control with no treatment at all. After 1 hour, the implants were centrifuged and washed to remove any unbound conjugates before they were illuminated (or no illumination for certain controls) with 50mW·cm⁻² fluence rate using a 690 nm laser (Modulight ML7700, Tampere, Finland) and measured with an Orion/PD optometer (Ophir Optonics, Jerusalem, Israel) for a total light dose of 50J/cm² after which the viability of the bacterial cells were measured by colony-forming units (CFU) dilution. After removal, the colonized implants were sonicated for 10 minutes in a Branson M2800E Ultrasonic Water bath (Branson Ultrasonic Corporation). After sonication, total viable bacterial (CFU) counts per implant were determined by serial dilution and plating.

PIAT of S. aureus implant infection in mice

In this *in vivo* experiment, the effect of antibody-photosensitizer conjugates activated by infrared light was tested in the same mice model with a subcutaneous implant infection, as described previously¹². In short, 25 Balb/cAnNCrl male mice were implanted with a 5 mm segment of a polyurethane catheter colonized with *S. aureus* biofilm. The implants were



completely inserted at distance of >2 cm from the incision of the skin. The implantation side, left or right, was randomized. After 48 hours of implantation, when the infection was established, the mice were intravenously injected with the specific (4497-IgG1-RDye700DX) or non-specific (Palivuzimab) antibody-photosensitizer conjugate. The first (5 mice) and second (5 mice) group received an injected dose of 400 and 200 µg of 4497-IgG-IRDye700DX, respectively. In the control groups, 4 mice (1 mouse was not intravenously injected and therefore excluded) were treated with 400 µg of palivizumab-IgG-IRDye700DX. Five mice were treated with vancomycin. Four mice (1 mouse was wrongfully injected and therefore excluded) were treated with unconjugated photosensitizer (corresponding to that of 400 µg of 4497-IgG-IRDye700DX) and 3 mice were not treated. See the x-axis in figure 2 for an overview of the groups. Mice treated with Vancomycin received an intraperitoneal injection starting with a bolus of 30mg/kg followed by 15mg/kg three times a day for seven days. Mice that received 4497-IgG-IRDye700DX and palivizumab-IgG-IRDye700DX were illuminated with infrared light using a 690 nm laser (Modulight ML7700, Tampere, Finland) 24 hours after injection. Each mouse received a total light dose of 50 J/cm² at a fluence rate of 50mW·cm⁻² measured with an Orion/PD optometer (Ophir Optronics, Jerusalem, Israel). After illumination, the mice were euthanized and frozen at -18 °C before further processing. The viability of the bacterial cells was measured on the implant and the soft tissue (mostly skin) around the implant. First the skin was disinfected using 70% alcohol after which the implants were removed under sterile conditions and stored in PBS. After removal of the implant, a sterile dermal biopsy punch of 8 mm was used to remove the soft tissue and skin around the implant and stored in PBS. Implants were carefully unclogged with a jet of the PBS using a pipette after which the implants were sonicated for 10 minutes in a Branson M2800E Ultrasonic Water bath (Branson Ultrasonic Corporation) and the tissue samples were disrupted by bead beating for 1 minute. The CFU was determined by serial dilution and plating in both implant and tissue samples. Results were calculated in log CFU/mL.

Statistical Analysis

Data management and analysis was performed using the Statistical Package for the Social Sciences (Released 2017. IBM SPSS Statistics for Windows, Version 25.0. IBM Corp, Armonk, NY, USA). One-way ANOVA followed by Bonferroni post hoc test was used to determine the difference between the groups. For the *in vitro* experiment, three experimental replicates were performed to allow statistical analysis. A p-value less than 0.05 was considered significant.

RESULTS

PIAT with IRDye700DX-Labeled mAb 4497 killed S. aureus in a biofilm on implants in vitro
Purity of the photosensitizer-conjugate was >99% as unbound photosensitizer was separated by an exclusion chromatography column. *In vitro* therapeutic efficacy of PIAT with illuminated 4497-IgG-IRDye700DX was studied on polyurethane implants colonized with *S. aureus*. The implants with biofilm without any treatment resulted in 10⁵ to 10⁶ bacterial CFU counts. The dose of 5 µg of 4497-IgG-IRDye700DX immuno-conjugate combined with light showed significant reduction in CFUs, compared to the illumination of the non-specific IRDye700DX-labeled mAb Palivizumab, or IRDye700DX and to the other controls (p=<0.01). Two out of three implants were completely sterile after treatment with this PIAT. A lower dose of 1 µg of 4497-IgG-IRDye700DX, combined with light, provided some reduction *S. aureus* biofilm, whereas 0.1 µg did not result in a significant reduction in CFUs (Figure 1). There were no significant differences between all control groups (Figure 1).



PIAT on implants with *S. aureus* biofilm

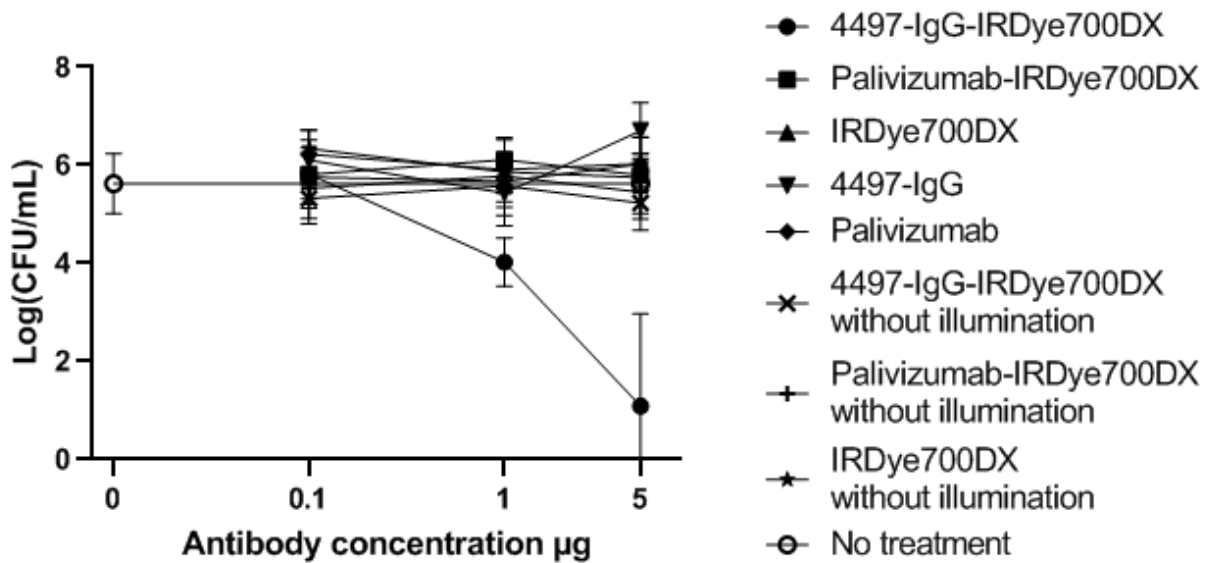


Figure 1. *In vitro* bactericidal effect of 4497-IgG-IRDye700DX on implant colonized with *S. aureus*. Different concentrations of the antibody-photosensitizer conjugate (0.1, 1.0 and 5.0 µg) and controls were used with a no treatment baseline control (black straight line with the 'o' symbol). Biofilms were irradiated with total light dose of 50J/cm² after which Log (CFU/mL) was determined by serial dilution. 4497-IgG-IRDye700DX at 5 µg reduced *S. aureus* biofilm significantly. (CFU, colony-forming units)

PIAT with IRDye700DX-Labeled mAb 4497 kills *S. aureus* in surrounding tissue but not on the implant *in vivo*

Therapeutic efficacy of PIAT with 4497-IgG-IRDye700DX was studied in subcutaneous implant infections in mice. On the implant, no significant difference in CFUs was seen between light activated 4497-IgG-IRDye700DX in both 400 µg (Log CFU/mL 5.6 ± 0.4) and 200 µg (Log CFU/mL 5.8 ± 0.6) and the controls ($p = >0.225$) (Figure 2A). In the tissue samples however, mice treated with PIAT with 400 µg 4497-IgG-IRDye700DX showed significant CFU reduction (Log CFU/mL 2.5 ± 0.9) compared to all other groups of which mice treated with 200 µg 4497-IgG-IRDye700DX (Log CFU/mL 3.8 ± 0.7, $p = 0.037$), 400 µg palivizumab-IgG-IRDye700DX (Log CFU/mL 4 ± 0.5, $p = 0.001$), Vancomycin (Log CFU/mL 4.5 ± 0.4 $p = 0.001$), photosensitizer IRDye700DX (Log CFU/mL 3.8 ± 0.3 $p = 0.044$) and mice that did not receive any treatment (Log CFU/mL 4.5 ± 0.4 $p = 0.002$; Figure 2B).



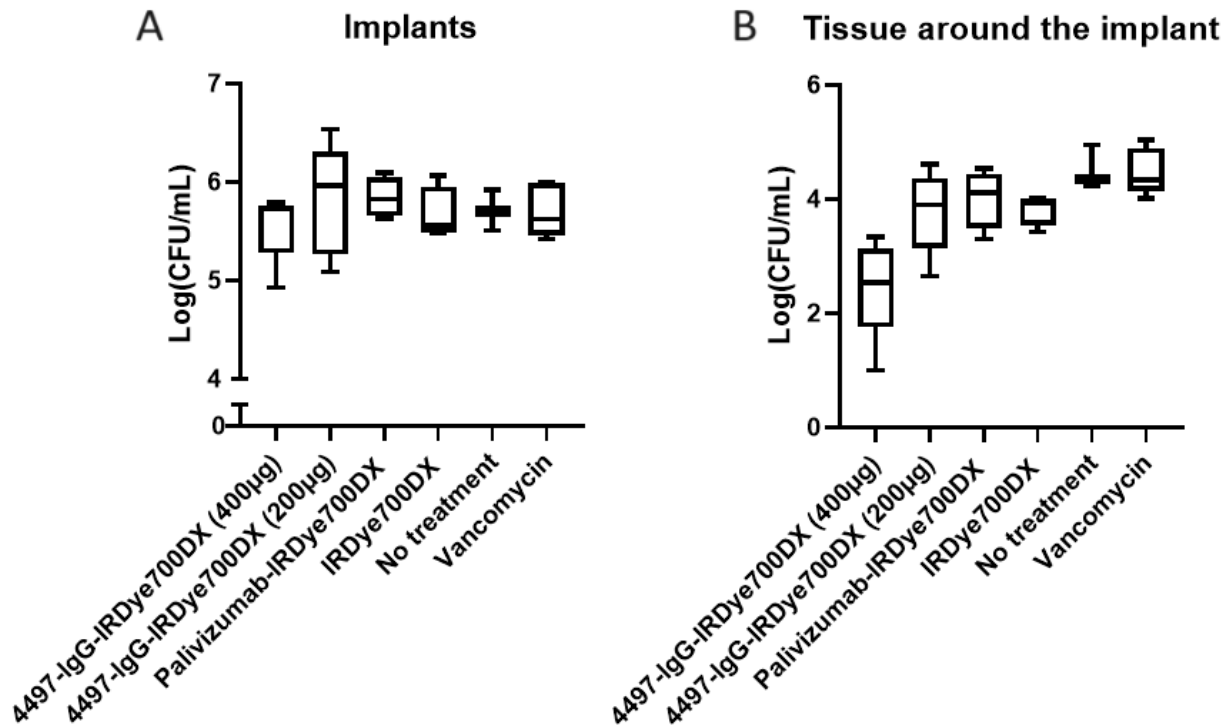


Figure 2. CFU counts from implants and surrounded tissue taken from mice with an implant infection that were treated with 4497-IgG-IRDye700DX at two doses and with various controls, including Vancomycin. The area around the implant was illuminated with a total light dose of 50J/cm² after which CFU (Log) was determined by serial dilution on the implant (A) as well as in the tissue (B) around the implant. No significant difference in CFU was seen at the implants. In the tissue samples surrounding the implant, 4497-IgG-IRDye700DX at the highest dose of 400µg reduced *S. aureus* cells significantly compared to the other (control) groups.

DISCUSSION

This study assessed the therapeutic potential of PIAT with 4497-IgG-IRDye700DX *in vitro* and *in vivo* on subcutaneous implant *S. aureus* infections in mice. *In vitro* results showed that a 5 µg concentration of the antibody-photosensitizer conjugate significantly reduced the CFUs and killed all bacteria (in a biofilm) in 2 out of 3 implants. *In vivo* results showed that PIAT with 4497-IgG-IRDye700DX did not significantly reduce the CFUs in a biofilm at the implant itself, but reduced the (free-floating) CFUs in the tissue around the implant considerably. This occurred only after PIAT at the highest dose with intravenous injection of 400 µg of 4497-IgG-IRDye700DX. This dose also outperformed the vancomycin control group. This result was unexpected as vancomycin has been one of the preferred antibiotic treatments to treat MRSA infections for decades¹⁵. Additionally, non-specific conjugate (palivizumab-IRDye700DX) had no substantial protein A-mediated effect suggesting that non-specific binding did not substantially contribute to antimicrobial activity as also reported previously¹¹. The results of PIAT on bacteria that are not in a biofilm are in concordance with previously described results of eradication of *S. aureus* in nasal colonization rat model and in a murine thigh infection model¹¹. A dose of 5 µg Staph12-569.3-IgG3-IRDye700DX was used to treat *S. aureus* nasally followed by illumination (50J/cm²) at a power density of 330 mW/cm² and eradicated the pathogen without effecting commensal bacteria. Additionally, local administration of 50 µg Staph12-569.3-IgG3-IRDye700DX per mouse in a *S. aureus*-thigh infection mouse model was found to eliminate free-floating bacteria after illumination with 50J/cm². Bispo et al.¹⁶ showed that PIAT with IRDye700DX can kill *S. aureus* in both planktonic state and biofilm *in vitro* as well as in a *Galleria mellonella* larval infection model and postmortem in a human implant model. These results suggest that irradiated photosensitizers can kill free-floating bacteria and



bacteria in a biofilm *in vivo* but specific targeting and precise accumulation is crucial to utilize the full bactericidal effect.

Previously, we showed that antibody 4497-IgG accumulates at the implant and the tissue surrounding the implant *in vitro* and *in vivo*. Up to 9% of the injected dose of 4497-IgG1-CHX-A²-In¹¹¹ In accumulated for at least 5 days at and around the implant infection^{12,17}. It is critical that the photosensitizer is in very close vicinity to the target cells before irradiation and singlet oxygen or ROS is produced or when the reaction affects the shape and solubility of the conjugate to compromise the function of the cellular membrane. For example, the migration distance of hydroxyl radicals is roughly 1 nm before reacting with all neighboring biomolecules¹⁸.

A limitation of treatment with 4497-IgG-IRDye700DX might be the decreased accessibility of the antibodies to the bacteria in the biofilm *in vivo*. This could be due to a limitation in methodology as catheters were all clogged by the abundance of biofilm and bacteria and therefore impede the diffusion of 4497-IgG-IRDye700DX *in vivo* to the center of the clogged implant, limiting the bactericidal effect. This also could explain why the soft tissue around the implant with bacteria that are not in a biofilm are more susceptible to PIAT compared to bacteria on the implant. To counter this effect, solid implants should be used in future studies to investigate the true potential of PIAT on e.g. periprosthetic joint infections.

Another limitation of PIAT is the small penetration depth of infrared light in tissue in order to activate the photosensitizer. However, intraoperative application of photosensitizer to the infected area can bypass this problem to some extent and local (per operative) administration could be of additional value.

Current treatment of implant infections often applies removal of necrotic and debris tissue (debridement) with extensive wound lavage sometimes with removal of the implant. The current study demonstrates the antimicrobial potential of PIAT in the operating theatre as an additional tool. Further improvement of PIAT in the surgical setting could be of value to reduce the reinfection rate in periprosthetic joint infection-related revision arthroplasty. For example, by increasing the availability of the photosensitizer at the implant site and per-operative illumination in the open wound to specifically eradicate remaining bacteria may lower the reinfection rate after reimplantation of a hip or knee prosthesis. Although, reasonably good results are being reported with biofilm-disrupting surgical lavage to reduce bacterial contamination in revision arthroplasty[19], PIAT in its current form may further increase the efficacy of surgical biofilm removal. Additional steps need to be taken to apply PIAT in the operating room such as availability of the laser. Disadvantages might be increased infection risk by changing eye protection and to some extent prolonged open wound time. It's about the balance between benefit and harm.

Although PIAT is proven safe, high circulating concentration of antibodies can theoretically induce non-specific binding and thus could induce side effects. However, due to photosensitizer activation by local light application very limited toxicity elsewhere is expected. Be that as it may, to bypass a high systemic concentration, local administration can be used. As an advantage, this allows the use of much higher concentrations. As mentioned, a drawback to local application is the potential risk of inducing an infection by connecting the infected area to the outside world for a prolonged period. Another way to further improve PIAT is to optimize distribution and penetration by using smaller vehicles such as proteins, nanobodies, peptides or other single domain antibodies as delivery molecules as shown by van Driel et al. where



nanobodies shown to distribute better than antibodies into targeted tumor tissue[20]. Theoretically, smaller antibody-photosensitizer conjugates might have an increased penetration into the biofilm and thereby increase chances of successful treatment[21].

CONCLUSION

In this study, we demonstrated that photoimmuno-antimicrobial therapy has potential as a tool for selectively eliminating *S. aureus in vivo*. The presented study suggests that local per-operative treatment might be the best choice for such treatment. However, using a solid implant instead of a catheter could result in an increased bactericidal effect of 4497-IgG-IRDye700DX as it is reflecting the clinical situation more realistically. These current results trigger further development of next-generation local per-operative PIAT as an additional therapy against staphylococcal bacterial infections.



REFERENCES

- 1 F. D. Lowy, "Medical progress: Staphylococcus aureus infections," *N. Engl. J. Med.*, vol. 339, no. 8, pp. 520–532, Aug. 1998, doi: 10.1056/NEJM199808203390806.
- 2 S. Y. C. Tong, J. S. Davis, E. Eichenberger, T. L. Holland, and V. G. Fowler, "Staphylococcus aureus infections: Epidemiology, pathophysiology, clinical manifestations, and management," *Clin. Microbiol. Rev.*, vol. 28, no. 3, pp. 603–661, 2015, doi: 10.1128/CMR.00134-14.
- 3 M. Cheng Li, MD, Nora Renz, MD, Andrej Trampuz, "Management of Periprosthetic Joint Infection," *Hip Pelvis*, vol. 30, pp. 138–146, 2018, [Online]. Available: <http://www.embase.com/search/results?subaction=viewrecord&from=export&id=L621294862>.
- 4 M. Otto, "Staphylococcal Biofilms," *Microbiol. Spectr.*, vol. 6, no. 4, pp. 1–17, 2018, doi: 10.1128/microbiolspec.gpp3-0023-2018.
- 5 W. Zimmerli and C. Moser, "Pathogenesis and treatment concepts of orthopaedic biofilm infections," *FEMS Immunol. Med. Microbiol.*, vol. 65, no. 2, pp. 158–168, 2012, doi: 10.1111/j.1574-695X.2012.00938.x.
- 6 S. B. Levy and M. Bonnie, "Antibacterial resistance worldwide: Causes, challenges and responses," *Nature Medicine*, vol. 10, no. 12S, pp. S122–S129, 2004, doi: 10.1038/nm1145.
- 7 C. Binding, M. Bispo, and S. B. Santos, "Targeted Antimicrobial Photodynamic Therapy of Biofilm-Embedded and Intracellular Staphylococci with a Phage," vol. 10, no. 1, pp. 1–13.
- 8 K. Sato *et al.*, "Photoinduced Ligand Release from a Silicon Phthalocyanine Dye Conjugated with Monoclonal Antibodies: A Mechanism of Cancer Cell Cytotoxicity after Near-Infrared Photoimmunotherapy," *ACS Cent. Sci.*, vol. 4, no. 11, pp. 1559–1569, 2018, doi: 10.1021/acscentsci.8b00565.
- 9 T. Kato *et al.*, "Electron Donors Rather Than Reactive Oxygen Species Needed for Therapeutic Photochemical Reaction of Near-Infrared Photoimmunotherapy," *ACS Pharmacol. Transl. Sci.*, vol. 4, no. 5, pp. 1689–1701, 2021, doi: 10.1021/acspstsci.1c00184.
- 10 D. M. Cognetti *et al.*, "Phase 1/2a, open-label, multicenter study of RM-1929 photoimmunotherapy in patients with locoregional, recurrent head and neck squamous cell carcinoma," *Head Neck*, vol. 43, no. 12, pp. 3875–3887, 2021, doi: 10.1002/hed.26885.
- 11 M. Mitsunaga *et al.*, "Antimicrobial strategy for targeted elimination of different microbes, including bacterial, fungal and viral pathogens," *Commun Biol* 5, 647 (2022). <https://doi.org/10.1038/s42003-022-03586-4>, doi: 10.1038/s42003-022-03586-4.
- 12 L. de Vor *et al.*, "Human monoclonal antibodies against Staphylococcus aureus surface antigens recognize in vitro and in vivo biofilm," *Elife*, vol. 11, pp. 1–25, 2022, doi: 10.7554/eLife.67301.
- 13 S. M. Lehar *et al.*, "Novel antibody-antibiotic conjugate eliminates intracellular S. aureus," *Nature*, vol. 527, no. 7578, pp. 323–328, 2015, doi: 10.1038/nature16057.
- 14 R. Fong *et al.*, "Structural investigation of human S. aureus-targeting antibodies that bind wall teichoic acid," *MAbs*, vol. 10, no. 7, pp. 979–991, 2018, doi: 10.1080/19420862.2018.1501252.
- 15 Y. Cong, S. Yang, and X. Rao, "Vancomycin resistant Staphylococcus aureus infections: A review of case updating and clinical features," *J. Adv. Res.*, vol. 21, pp. 169–176, 2020, doi: 10.1016/j.jare.2019.10.005.
- 16 M. Bispo *et al.*, "Fighting Staphylococcus aureus infections with light and photoimmunoconjugates," *JCI Insight*, vol. 5, no. 22, pp. 1–16, 2020, doi: 10.1172/jci.insight.139512.
- 17 B. van Dijk *et al.*, "Evaluating the Targeting of a Staphylococcus-aureus-Infected Implant with a



Radiolabeled Antibody In Vivo,” *Int. J. Mol. Sci.*, vol. 24, no. 5, 2023, doi: 10.3390/ijms24054374.

- 18 J. Dumanović, E. Nepovimova, M. Natić, K. Kuča, and V. Jačević, “The Significance of Reactive Oxygen Species and Antioxidant Defense System in Plants: A Concise Overview,” *Front. Plant Sci.*, vol. 11, no. January, 2021, doi: 10.3389/fpls.2020.552969.
- 19 Hunter C, Duncan S. Clinical Effectiveness of a Biofilm Disrupting Surgical Lavage in Reducing Bacterial Contamination in Total Knee Arthroplasty Revision Surgery in Known Cases of Prosthetic Joint Infection. 2019;(Md).
- 20 van Driel PBAA, Boonstra MC, Slooter MD, et al. EGFR targeted nanobody-photosensitizer conjugates for photodynamic therapy in a pre-clinical model of head and neck cancer. *J Control Release*. 2016 May 10;229:93-105.
- 21 Bannas P, Hambach J, Koch-Nolte F. Nanobodies and nanobody-based human heavy chain antibodies as antitumor therapeutics. *Front Immunol*. 2017;8(NOV):1-13.



General discussion and Future Perspectives



GENERAL DISCUSSION

Periprosthetic joint infection (PJI) is a devastating complication after arthroplasty and is a growing problem due to the increasing number of joint replacement procedures and an aging population. The starting point of this thesis was an evaluation of the effectiveness of treatments for PJIs after hip and knee arthroplasty within the UMC Utrecht over the last 13 years. Current treatment such as DAIR (onset <3 months in the UMCU) in an acute phase or after a hematogenous infection showed a failure rate of 31% in our hospital. However, the failure rate of DAIR after prior PJI-related revision arthroplasty was 44% (**See chapter 2**) whereas the more invasive one and two-stage revision showed an overall failure rate of 16% (**See chapter 3**). The infection control rates for DAIR are slightly superior to those found in literature. For example, a meta-analysis by Kunutsor et al. showed an overall pooled failure rate of 38.6 % in patients treated with a DAIR procedure¹. It also showed that a longer duration between onset of symptoms to DAIR (≥ 3 weeks) is associated with lower infection control compared with a shorter duration (< 3 weeks). The pooled failure rates in two meta-analysis of one and two-stage revision procedures was approx. 6% and 8.5%^{2,3}. In this regard, the infection rate of 16% in our hospital is twice as high. This, however, can be explained by the complex patient population in the UMC Utrecht as it is a tertiary referral center. No large patient population studies have been done into these complex patients but the success rates in tertiary referral centers are lower as these patients have undergone previous infection surgery or have multiple comorbidities. For example, Kildow et al.⁴ reported a failure rate of 12% in a multicenter study where patients (n=221) were treated at three large tertiary referral centers. Previous failed PJI treatment drastically reduces the chance of successful infection eradication with failure rates of 58% and 69%^{5,6}. A systematic review of Maden et al. showed failure rates of 22 to 48% after failure of two-stage revision knee arthroplasty⁷.

This population of patients with previous failed infection treatment and/or multiple comorbidities and are not able to undergo intensive surgery or do not have other curative PJI treatment options left, resort to either lifelong antibiotics, a Girdlestone procedure or amputation in the event of an infected knee prosthesis. This greatly reduces their quality of life.^{8,9} In addition, PJI is accompanied by high mortality rates that can even surpasses the mortality rates of multiple types of cancer^{10,11,12}. A 5 and 10 years' survival of respectively 21% and 44%^{11,13} shows that PJI patient are not dissimilar to oncology patients in terms of mortality and are in dire need of alternative treatment options. In this thesis both radioimmunotherapy and photoimmunotherapy have been explored as treatment options for PJI using *in vitro* and *in vivo* (animal) experiments.

It all starts with the right antibody

To enable the use of photo or radioimmunotherapy for PJI, finding the right antibody as a vehicle for bactericidal molecules is crucial for a successful therapy. In this thesis the antibody 4497-IgG1 was used as it targets WTA that is abundant in both the bacterial cell wall as well as the biofilm of *Staphylococcus aureus*. We showed that 4497-IgG1 is specific to planktonic *S. aureus* and its biofilm by performing *in vitro* experiments and proof-of-principle in *in vivo* (mice) experiments (**see chapter 4**). High uptake (8.34 ± 2.25 %ID/cm³ at 24 h. and up to 9.22 ± 2.86 %ID/cm³ after 120 h.) of 4497-IgG1 was continuously seen for 5 days at the implant infection site in mice and was significantly higher compared to a non-infected negative control implant. Long retention time of the antibody conjugate at the infection site was found and therefore could benefit bactericidal molecules as there is more time to have an eradicating effect on the bacterial cells. Further evaluation of the biodistribution of 4497-IgG1 showed uptake in



blood rich organs such as heart, liver, lungs and kidneys and decreased gradually over time (**see chapter 5**). Although a decrease in uptake over time was seen at the heart, it still showed relative high uptake at 5 days. This indicates a slow elimination of the antibody 4497-IgG1-¹¹¹In-conjugate. Slow pharmacokinetics have benefits as well as limitations, as it could pose a toxicity risk when prolonged exposure of potential harmful radionuclides to healthy tissue. On the other hand, initially harmless molecules such as photosensitizers could benefit from slow pharmacokinetics as there is more time to accumulate at the infection site and therefore enable better irradiation at the infected site with multiple illumination times. It can be concluded that the long retention time and slow pharmacokinetics and relative low uptake in vital organs indicates that 4497-IgG1 antibody holds promise as a vehicle to deliver bactericidal molecules to the infection site cells.

Radioimmunotherapy

Ionizing radiation has had the capability of treating infections and killing bacteria for over 100 years but acute and long-term health risks are major drawbacks (**see chapter 6**). Technology has advanced and since the early 2000s FDA has approved targeted therapy in the form of radioimmunotherapy for treating non-Hodgkin lymphoma with great success and very acceptable toxicity profiles^{14,15}. RIT for infections was first described by Dadachova as treatment for HIV, bacterial, and fungal infectious diseases¹⁶. Subsequently, we investigated the possibility of treating PJI with RIT. As shown in this thesis, ²¹³Bi-labeled mAb 4497-IgG1 consistently killed both planktonic *S. aureus* and in a biofilm *in vitro* with an incubation time of only an hour (**see chapter 7**). Other radionuclides such as ¹⁷⁷Lutetium and low doses of ²²⁵Actinium did not show robust bactericidal properties *in vitro* after an incubation time of an hour. However, long physical half-lives of ¹⁷⁷Lu (6.7 days) and ²²⁵Ac (10 days) suggests that a longer incubation time can be applied to reveal the full bactericidal potential. Therefore, ²²⁵Ac could potentially be as or more destructive to bacteria and the biofilm compared to its daughter molecule ²¹³Bi. The toxicity profile and half-life of ²²⁵Ac makes it one of the most preferable alpha emitters. As with other alpha emitters, a significant disadvantage of using ²²⁵Ac is its scarcity. There are only a few locations globally with thorium generators to produce ²²⁵Ac in research-scale quantities. Recent new production methods such as the use of high accelerator irradiation of Thorium-232 can boost production significantly and could meet production demand for clinical use¹⁷.

Treatment with radiation is always prone to safety concerns. Radioisotopes such as ²²³Ra and ¹⁸⁸Re are already clinically used and their safety profiles are well known. Treatments with these radioisotopes are associated with minimal adverse events^{18,19}. Nonetheless, one must strive to reduce radiation damage to non-target tissues. For example, instead of direct conjugation of the radionuclide to the antibody, pre-targeting could be used²⁰. Pre-targeting involves the concept of coupling radioactive isotopes to the antibody *in vivo*. For example, a dose of *S. aureus* targeting antibodies coupled to a chelator specific for radioactive isotopes are given to the patient so that the antibodies can accumulate at the infection site and unbound antibodies are excreted. The second stage of the therapy is the administration of radioactive isotopes that can bind to the antibodies. This decreases circulation time of the radioactive isotopes in the body and therefore reduce uptake in healthy tissue, minimizing collateral damage. In this regard, pre-targeting allows the use of multiple injections of (harmless) antibody vehicles improving the targeting of the infection by fully saturating the infection site and increase the therapeutic effect of RIT. Additionally, administration of different antibodies could be used to treat mixed infections in case a patient is infected with two or more pathogens.



Photoimmuno-antimicrobial therapy (PIAT)

The medical application of a fluorescent compound activated by light has been available for a century. It has been proven to be effective and safe in a range of medical applications but it is mostly applied in dermatology.²¹ Lately there has been an increased interest in photodynamic therapy used as a treatment for bacterial, fungal and viral infections²²⁻²⁴ due to it being harmless before illumination and it has a low probability of developing therapeutical resistance. Bispo et al.²³ showed that PIAT with IRDye700DX can kill *S. aureus* in planktonic state as well as in a biofilm *in vitro*, in a *G. mellonella* larval infection model and postmortem in a human implant model. Additionally, Mitsunaga et al.²⁵ showed that antibody-IRDye700DX conjugates were able to eradicate *S. aureus* nasal colonization in rats and eliminate MRSA in the deep tissues of mice with MRSA-thigh infections. We showed that PIAF (mAb 4497-IgG1-IRDye700DX) can indeed kill *S. aureus* in a biofilm *in vitro* and free-floating bacteria in a subcutaneous implant infection model (**see chapter 8**). However, PIAF could not kill bacteria in a biofilm on an implant *in vivo* (mice). In addition, limitations of PIAT such as the limited tissue penetration of NIR are a problem as this therapy is unable to penetrate the deeper infected tissues. Therefore, systemic application of PIAF to combat PJI in this form might not be a suitable therapy. However, there could be a place for it in perioperative treatment. For example, in a one or two-stage revision procedure where antibody-photosensitizer conjugates are administered systemically preoperatively or locally perioperatively. After removal of the implant, the surgical site is irradiated with NIR light to eliminate remaining bacteria. This might reduce the reinfection rate of PJI in patients.

FUTURE PERSPECTIVES

The perfect transport vehicle

A general limitation of using antibodies as a vehicle is the lack in versatility as antibodies are often specific to a typical bacterial strain. *S. aureus* (and *S. epidermidis*) is the most common pathogen in PJI but other species are surfacing progressively (**see chapter 3**). Bacteria specific antibodies need to be developed for each type of bacteria. This involves tedious and extensive research but such research is unfortunately inevitable in the development of immunotherapy for PJI. Another hurdle is that bacteria not only reside in a biofilm but they can also be internalized in other cells such as osteoclasts²⁶, osteoblasts²⁷, osteocytes²⁸ or immune cells²⁹ thus complicating specific targeting even more. Therefore, the perfect vehicle that serves as transport for bactericidal molecules need to fulfill certain properties such as high specificity and affinity to the bacterial cells, strong biofilm penetration, high metabolic stability, fast clearance, low immunogenicity and toxicity. One of the first steps to improve accessibility to the bacteria in a biofilm is to find molecules that are smaller than monoclonal antibodies as the penetration would be improved. For example, nanobodies such as heavy chain (VHH) or other single domain antibodies or peptides combine the beneficial properties of small molecules and monoclonal antibodies^{30,31}. Their small size makes them useful for targeting bacteria residing in the biofilm which are poorly accessible. Additionally, smaller size leads to increased elimination which could be beneficial as remaining unbound conjugates carrying potentially dangerous therapeutical molecules are excreted more quickly, minimizing collateral damage. Other advantageous features of small vehicles are high stability, good solubility, high thermostability and low immunogenicity^{32,33}.



The perfect radionuclide

The success of RIT depends on the selective accumulation of cytotoxic radioisotopes at affected areas. In a theragnostic approach diagnostic and therapeutic radionuclides are delivered in the same agent by a target specific vehicle. A combination of alpha, beta and gamma emitting radionuclides is ideal as a small amount of gamma emission could be beneficial for diagnostic purposes while alpha and beta emitters provide their destructive effect. Beta emission is less damaging to bacterial cells but have increased tissue penetration depth so, theoretically, it could reach bacteria buried deep in the biofilm. When combined with the close vicinity destruction of the alpha-emitters, therapeutic effect is maximized. A wide range diagnostic radionuclides can be used, but preferably one with a short half-life and extensive clinical experience such as non-metallic positron emitter fluorine-18 or zirconium-89 (PET) or gamma emitting ^{99m}Tc (SPECT). Subsequently, a combination of alpha and beta emitting radionuclides might increase their bactericidal effect. However this bactericidal effect should be studied separately. ^{225}Ac as an alpha emitter has great potential but the limited availability poses a problem. Alternatively, astatine-211, bismuth-212, Bi-213, lead-212, radium-223, terbium-149 and thorium-227 could be investigated for PJI as they are considered the most suitable therapeutic alpha emitters in cancer therapy³⁴. To study the effect of beta radiation on bacteria, strong beta-emitting radioisotopes such as ^{188}Re and ^{177}Lu could be used. These have the advantage of being readily available and their toxicity profiles have been studied extensively. For all radionuclides it is important that they are readily available, cheap to manufacture, environmentally friendly and safe. In this regard, we can look at other radionuclides used in oncology where the possibilities seem endless as researchers continue to develop new therapies and find uses for all different kinds of radionuclides. All of these radionuclides, with their own positive and negative properties, can be adapted to each individual situation. Therefore, pathogen specific therapy might be the future.

The perfect therapy for PJI patients

Hypothetically, a patient with PJI is seen at the outpatient clinic (Figure 1). When a patient is suspected of having PJI a diagnostic puncture is taken and afterwards a pathogen specific treatment is offered with a drug delivery system targeting bacteria by bringing antimicrobial molecules to the infected tissue on and around the infected prosthesis and thus curing the infection. However surgery might still be needed to irrigate and debride the infected area with adjuvant antibiotic and radioimmunotherapy to treat the infection and reduce re-infection rates. Additionally, PJI patients with multimorbidity and in poor health and who are not fit for surgery, would be the first group of patients that could benefit from prolonged antibiotic and radioimmunotherapy.



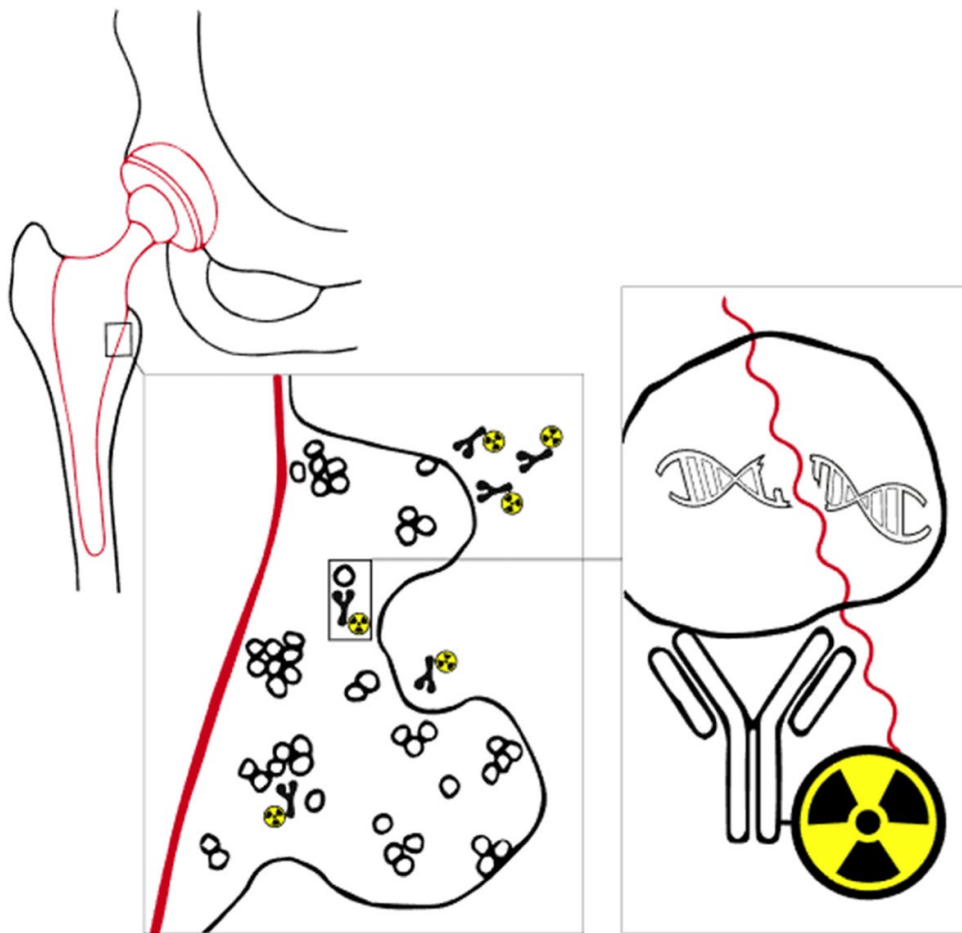


Figure 1. Image copied from van Dijk et al.³⁵ Concept: Radioimmunotherapy for a patient with PJI. The biofilm on the hip prosthesis protects the bacteria from antibiotics and the immune system. RIT with alpha or beta-emitting radioisotopes might be able to destroy the structure of the biofilm and kill the bacteria.

CONCLUSION

We identified a group of PJI patients with previous failed infection treatment and/or multiple comorbidities that do not have other curative PJI treatment options left and who resort to either lifelong antibiotics, a Girdlestone situation or amputation. Alternative treatment options must be explored and rigorous therapy might be justified in patients with PJI considering the high mortality rates. In this thesis we explored both radioimmunotherapy and photoimmunotherapy as a treatment option for PJI using *in vivo* models in mice. We showed that *S. aureus* targeting antibody 4497-IgG1 holds promise as a drug delivery system for diagnostic and bactericidal agents. Unfortunately, PIAT seem to have limited therapeutic effect in this form. However, the bactericidal effect of radioimmunotherapy, despite its disadvantages, might give patients another chance to recover fully from a bacterial infection. An example of this is adjuvant therapy after one and two stage revision in combination with prolonged antibiotic therapy. The current results described in this thesis may trigger the development of a preclinical treatment study to establish therapeutic efficacy for PJI and thereby pave the way for subsequent clinical trials.



REFERENCES

1. Kunutsor SK, Beswick AD, Whitehouse MR, Wylde V, Blom AW. Debridement, antibiotics and implant retention for periprosthetic joint infections: A systematic review and meta-analysis of treatment outcomes. *J Infect.* 2018;77(6):479-488.
2. Kunutsor SK, Whitehouse MR, Lenguerrand E, Blom AW, Beswick AD; INFORM Team. Re-Infection Outcomes Following One- And Two-Stage Surgical Revision of Infected Knee Prosthesis: A Systematic Review and Meta-Analysis. *PLoS One.* 2016 Mar 11;11(3):e0151537.
3. Goud AL, Harlianto NI, Ezzafzafi S, Veltman ES, Bekkers JEJ, van der Wal BCH. Reinfection rates after one- and two-stage revision surgery for hip and knee arthroplasty: a systematic review and meta-analysis. *Arch Orthop Trauma Surg.* 2021;143(2):829-838.
4. Kildow BJ, Springer BD, Brown TS, Lyden E, Fehring TK, Garvin KL. Long Term Results of Two-Stage Revision for Chronic Periprosthetic Hip Infection: A Multicenter Study. *J Clin Med.* 2022;11(6).
5. Stammers J, Kahane S, Ranawat V, Miles J, Pollock R, Carrington RW, Briggs T, Skinner JA. Outcomes of infected revision knee arthroplasty managed by two-stage revision in a tertiary referral centre. *Knee.* 2015 Jan;22(1):56-62.
6. Shichman I, Ward SA, Lu L, Garceau S, Piuze NS, Seyler TM, Schwarzkopf R. Failed 2-Stage Revision Knee Arthroplasty for Periprosthetic Joint Infection-Patient Characteristics and Outcomes. *J Arthroplasty.* 2023 May 12:S0883-5403(23)00465-5.
7. Maden C, Jaibaji M, Konan S, Zagra L, Borella M, Harvey A, Volpin A. The outcomes of surgical management of failed two-stage revision knee arthroplasty. *Acta Biomed.* 2021 Jul 1;92(3):e2021197.
8. Vincenten CM, Den Oudsten BL, Bos PK, Bolder SBT, Gosens T. Quality of life and health status after Girdlestone resection arthroplasty in patients with an infected total hip prosthesis. *J Bone Jt Infect.* 2019;4(1):10-15.
9. Akyol Y, Tander B, Goktepe AS, Safaz I, Kuru O, Tan AK. Quality of life in patients with lower limb amputation: Does it affect post-amputation pain, functional status, emotional status and perception of body image? *J Musculoskelet Pain.* 2013;21(4):334-340.
10. Natsuhara KM, Shelton TJ, Meehan JP, Lum ZC. Mortality During Total Hip Periprosthetic Joint Infection. *J Arthroplasty.* 2019 Jul;34(7S):S337-S342.
11. Wildeman P, Rolfson O, Söderquist B, Wretenberg P, Lindgren V. What Are the Long-term Outcomes of Mortality, Quality of Life, and Hip Function after Prosthetic Joint Infection of the Hip? A 10-year Follow-up from Sweden. *Clin Orthop Relat Res.* 2021;479(10):2203-2213.
12. Zmistowski B, Karam JA, Durinka JB, Casper DS, Parvizi J. Periprosthetic joint infection increases the risk of one-year mortality. *J Bone Joint Surg Am.* 2013 Dec 18;95(24):2177-84.
13. Natsuhara KM, Shelton TJ, Meehan JP, Lum ZC. Mortality During Total Hip Periprosthetic Joint Infection. *J Arthroplasty.* 2019;34(7S):S337-S342.
14. Larson SM, Carrasquillo JA, Cheung NK PO. Radioimmunotherapy of human tumours. *Nat Rev Cancer* 2015 Jun;15(6)347-60.
15. Adams GP, Weiner LM. Monoclonal antibody therapy of cancer. *Nat Biotechnol.* 2005 Sep;23(9):1147-57.
16. Helal M, Dadachova E. Radioimmunotherapy as a Novel Approach in HIV, Bacterial, and Fungal Infectious Diseases. *Cancer Biother Radiopharm.* 2018 Oct;33(8):330-335.
17. Hatcher-Lamarre JL, Sanders VA, Rahman M, Cutler CS, Francesconi LC. Alpha emitting nuclides for targeted therapy. *Nucl Med Biol.* 2021;92:228-240.
18. Parker C, Nilsson S, Heinrich D, et al. Alpha emitter radium-223 and survival in metastatic prostate cancer. *N Engl J Med.* 2013;369(3):213-223.
19. Lepareur N, Lacœuille F, Bouvry C, et al. Rhenium-188 labeled radiopharmaceuticals: Current clinical applications in oncology and promising perspectives. *Front Med.* 2019;6(June):1-19.



20. Zeglis BM, Sevak KK, Reiner T, et al. A pretargeted PET imaging strategy based on bioorthogonal diels-alder click chemistry. *J Nucl Med.* 2013;54(8):1389-1396.
21. Ackroyd R, Kelty C, Brown N, Reed M. The history of photodetection and photodynamic therapy. *Photochem Photobiol.* 2001 Nov;74(5):656-69.
22. Sadraeian M, Bahou C, da Cruz EF, Janini LMR, Sobhie Diaz R, Boyle RW, Chudasama V, Eduardo Gontijo Guimarães F. Photoimmunotherapy Using Cationic and Anionic Photosensitizer-Antibody Conjugates against HIV Env-Expressing Cells. *Int J Mol Sci.* 2020 Dec 1;21(23):9151.
23. Bispo M, Anaya-Sanchez A, Suhani S, Raineri EJM, López-Álvarez M, Heuker M, Szymański W, Romero Pastrana F, Buist G, Horswill AR, Francis KP, van Dam GM, van Oosten M, van Dijk JM. Fighting Staphylococcus aureus infections with light and photoimmunoconjugates. *JCI Insight.* 2020 Nov 19;5(22):e139512.
24. Yasui H, Takahashi K, Taki S, Shimizu M, Koike C, Umeda K, Rahman S, Akashi T, Nguyen VS, Nakagawa Y, Sato K. Near Infrared Photo-Antimicrobial Targeting Therapy for Candida albicans. *Adv Ther.* 2021;4(2):1-12.
25. Mitsunaga M, Ito K, Nishimura T, et al. Antimicrobial strategy for targeted elimination of different microbes, including bacterial, fungal and viral pathogens. *Commun Biol* 5, 647 (2022)
26. Raynaud-Messina B, Verollet C, Maridonneau-Parini I. The osteoclast, a target cell for microorganisms. *Bone.* 2019;127:315-323.
27. Josse J, Velard F, Gangloff SC. Staphylococcus aureus vs. Osteoblast: Relationship and Consequences in Osteomyelitis. *Front Cell Infect Microbiol.* 2015;5(November):1-17.
28. de Mesy Bentley KL, Trombetta R, Nishitani K, et al. Evidence of Staphylococcus Aureus Deformation, Proliferation, and Migration in Canaliculi of Live Cortical Bone in Murine Models of Osteomyelitis. *J Bone Miner Res.* 2017;32(5):985-990.
29. Voza EG, Mulcahy ME, McLoughlin RM. Making the Most of the Host; Targeting the Autophagy Pathway Facilitates Staphylococcus aureus Intracellular Survival in Neutrophils. *Front Immunol.* 2021;12(June):1-16.
30. Muyldermans S. Nanobodies: Natural single-domain antibodies. *Annu Rev Biochem.* 2013;82(March):775-797.
31. Vargason AM, Anselmo AC, Mitragotri S. The evolution of commercial drug delivery technologies. *Nat Biomed Eng.* 2021;5(9):951-967.
32. Bannas P, Hambach J, Koch-Nolte F. Nanobodies and nanobody-based human heavy chain antibodies as antitumor therapeutics. *Front Immunol.* 2017;8(NOV):1-13.
33. Arbabi-Ghahroudi M. Camelid single-domain antibodies: Historical perspective and future outlook. *Front Immunol.* 2017;8(NOV):1-8.
34. Eychenne R, Chérel M, Haddad F, Guérard F, Gestin JF. Overview of the most promising radionuclides for targeted alpha therapy: The “hopeful eight.” *Pharmaceutics.* 2021;13(6).
35. van Dijk B, Lemans JVC, Hoogendoorn RM, Dadachova E, de Klerk JMH, Vogely HC, Weinans H, Lam MGEH, van der Wal BCH. Treating infections with ionizing radiation: a historical perspective and emerging techniques. *Antimicrob Resist Infect Control.* 2020 Jul 31;9(1):121.





Nederlandse samenvatting/Dutch summary



SAMENVATTING

Implantaten zoals heup- en knieprothesen hebben de kwaliteit van leven aanzienlijk verbeterd, maar ze brengen ook risico's op infecties met zich mee. Bacteriën kunnen deze implantaten koloniseren, wat tot ernstige gevolgen kan leiden. Periprosthetische gewrichtsinfecties (PJI) komen voor bij 1% tot 2,5% van de primaire gewrichtsvervangingen. Bij revisieprothesen kan dit percentage oplopen tot 16%. In 2019 werden in Nederland ongeveer 60.000 heup- en knieprothesen uitgevoerd, en dit aantal zal in de toekomst alleen maar toenemen. In de Verenigde Staten bijvoorbeeld, wordt verwacht dat het aantal heup- en knieprothesen zal stijgen tot 2,8 miljoen in 2030 en 4,8 miljoen in 2040. Door de toenemende levensverwachting stijgt ook het risico op late periprosthetische gewrichtsinfecties en daarmee ook op invasieve revisieprocedures.

Staphylococcus aureus is een van de meest voorkomende bacteriën die infecties veroorzaken bij implantaten zoals heup- en knieprothesen. Deze bacteriën vormen een biofilm op het prothesemateriaal, wat de antimicrobiële behandeling bemoeilijkt. Bacteriën in een biofilm zijn vaak metabool inactief (slapend), waardoor ze resistent kunnen worden tegen veelgebruikte antibiotica. Ze kunnen zich ook schuilhouden in botweefsel en in een latente toestand blijven voordat ze actief worden en een (her)infectie veroorzaken. Het behandelen van dergelijke infecties is complex; zelfs na 'succesvolle' behandeling kan een infectie na vele jaren opnieuw optreden, wat de antibioticaresistentie verder vergroot.

Behandelingsopties variëren per land en ziekenhuis maar omvatten meestal toediening van antibiotica en chirurgische ingrepen zoals debridement, antibiotica en implantaatbehoud (DAIR), eventueel gevolgd door revisie van implantaten in één of twee fasen. Ondanks deze behandelingen varieert de mortaliteit binnen één jaar van 2,6% tot 10,6%, en na vijf jaar stijgt dit percentage tot ongeveer 21%. De behandeling wordt bemoeilijk door toename van resistente bacteriën, hogere leeftijd en multimorbiditeit van patiënten. Om deze redenen moeten alternatieve behandelopties worden overwogen.

Een eeuw geleden beschreef Paul Ehrlich een theorie over een 'magische kogel' die pathogenen of cellen selectief zou kunnen doden zonder gezond weefsel te beschadigen. In de moderne tijd zouden deze magische kogels kunnen verwijzen naar monoklonale antilichamen (mAbs), die specifieke cellen kunnen targeten en kunnen worden gebruikt om het immuunsysteem te activeren of om andere moleculen zoals radionucliden, fotosensibilisatoren of enzymen naar het doelwit te brengen. Dergelijke benaderingen worden al gebruikt in de oncologie, met name in radio-immuuntherapie en foto-immuuntherapie voor de behandeling van verschillende vormen van kanker. Deze strategieën zouden mogelijk ook effectief kunnen zijn bij de behandeling van PJI, vooral bij patiënten waarbij conventionele behandelingen niet succesvol zijn gebleken.

Radio-immuuntherapie maakt gebruik van antilichamen gekoppeld aan radionucliden die ioniserende straling uitzenden. Deze radioantilichamen worden intraveneus toegediend en richten zich specifiek op de doelcellen of weefsels. De doelcellen worden op basis van ioniserende straling vernietigd door aantasting van de DNA-structuur. Dit gebeurt met beperkte schade aan omliggend (gezond) weefsel vanwege de beperkte doordringingsdiepte van specifieke radionucliden.

Een andere alternatieve therapie is foto-immuuntherapie. Hierbij worden antilichamen gekoppeld aan fotosensibilisatoren; deze niet-giftige kleurstoffen kunnen onder invloed van nabij-infrarood licht grote hoeveelheden reactieve zuurstofsoorten (ROS) vrijgeven. ROS kunnen pathogenen rechtstreeks doden door oxidatieve schade aan het DNA te veroorzaken.



Dit proces van oxidatieve schade wordt ook gebruikt door verschillende cellen van het immuunsysteem, zoals fagocyten, als een dodelijk wapen tegen bacteriën.

In theorie zouden infecties bij implantaten, zoals PJI, kunnen worden behandeld met antilichamen die specifiek gericht zijn op *S. aureus* om bacteriën rechtstreeks te elimineren door antibacteriële moleculen aan de antilichamen te koppelen. Radio-immuuntherapie of foto-immuun-antibacteriële therapie in combinatie met antibiotica kunnen een krachtige combinatie vormen voor de behandeling van PJI.

In dit proefschrift is de effectiviteit geëvalueerd van PJI-behandelingen na heup- en knieervanging in het UMC Utrecht over de afgelopen 13 jaar. De huidige behandeling, zoals DAIR, toonde in de acute fase of na een hematogene infectie een faalpercentage van 31%. Wanneer er eerder PJI-gerelateerde revisiechirurgie had plaatsgevonden, nam dit percentage toe tot 44%. Invasievere één- en twee-staps revisieprocedures toonden een algemeen faalpercentage van 16%. De succespercentages van DAIR in het UMCU zijn beter dan die in de literatuur, maar het faalpercentage bij een één- en twee-staps revisieprocedure in het UMCU was tweemaal zo hoog als het gemiddelde in de literatuur, wat kan worden verklaard door de complexe patiëntpopulatie. Patiënten met eerdere mislukte infectiebehandelingen of meerdere comorbiditeiten hebben vaak lagere succespercentages, met faalpercentages variërend van 22% tot 48%. Uit deze cijfers blijkt dat er een groep patiënten is zonder verdere curatieve behandelingsopties. Deze patiënten krijgen vaak levenslange antibiotica, een Girdlestone-procedure of amputatie aanbevolen, wat hun kwaliteit van leven aanzienlijk vermindert. PJI gaat gepaard met hoge sterftcijfers, en om die reden wordt er in dit proefschrift onderzoek gedaan naar alternatieve behandelingen zoals radio-immunotherapie en foto-immunotherapie voor PJI, met behulp van *in vitro* en *in vivo* experimenten.

Het juiste antilichaam is cruciaal voor succesvolle therapie. In dit proefschrift werd 4497-IgG1 gebruikt, gericht op WTA in de bacteriële celwand en biofilm van *S. aureus*. *In vitro* experimenten en *in vivo* muizenexperimenten toonden aan dat 4497-IgG1 specifiek was voor *S. aureus* en zijn biofilm, met hoge opname en lange retentietijd op de plaats van infectie.

Radio-immunotherapie (RIT) maakt gebruik van ioniserende straling om bacteriën te doden. Het ²¹³Bi-gelabelde 4497-IgG1-antilichaam doodde effectief *S. aureus* en zijn biofilm *in vitro*. Andere radionucliden zoals ¹⁷⁷Lutetium en lage doses ²²⁵Actinium vertoonden minder robuuste bacteriedodende eigenschappen, maar kunnen potentieel effectief zijn bij langere incubatietijden. Veiligheidszorgen blijven bestaan, maar technieken zoals pre-targeting kunnen de blootstelling van gezond weefsel aan straling minimaliseren.

Foto-immuno-antimicrobiële therapie (PIAT) maakt gebruik van lichtgeactiveerde fluorescerende (kleur)stoffen om bacteriën te doden. PIAT met mAb 4497-IgG1-IRDye700DX doodde effectief *S. aureus* *in vitro* en *in vivo* in een subcutaan implantaatinfectiemodel. Echter, systemische toepassing van deze therapie voor PJI is gelimiteerd door de beperkte weefselpenetratie van NIR-licht. PIAT kan echter nuttig zijn in perioperatieve behandelingen om resterende bacteriën na verwijdering van geïnfecteerde implantaten te elimineren.

TOEKOMSTPERSPECTIEF

Het perfecte transportmiddel moet specifieke bacteriële cellen en biofilm kunnen bereiken, hoge stabiliteit en lage immunogeniciteit hebben, en een snelle klaring hebben. Nanobodies en peptiden bieden voordelen vanwege hun kleine formaat en hoge stabiliteit.



De perfecte radionuclide voor RIT combineert diagnostische en therapeutische eigenschappen, bij voorkeur met alfa- en beta-emitters voor maximale bacteriedodende effecten. Radionucliden zoals ^{225}Ac , ^{177}Lu en ^{188}Re hebben veelbelovende eigenschappen, maar de beschikbaarheid van ^{225}Ac is beperkt. Een combinatie van alfa-, beta- en gamma-emitters kan het therapeutische effect maximaliseren.

De perfecte therapie voor PJI-patiënten omvat diagnostische puncties en pathogeen specifieke behandelingen met bacteriedodende moleculen. Chirurgie blijft hoogstwaarschijnlijk noodzakelijk voor debridement waarna gecombineerd met adjuvante antibiotica en radio-immunotherapie om infecties optimaal te behandelen en re-infectie te voorkomen. Patiënten met multimorbiditeit en slechte gezondheid kunnen baat hebben bij een combinatie van langdurige antibiotica en radio-immunotherapie.





List of Publications and Manuscripts



This thesis is based upon the following publications and manuscripts:

Chapter 2:

Nurmohamed FRHA, van Dijk B, Veltman ES, Hoekstra M, Rentenaar RJ, Weinans, Vogely HC, van der Wal BCH. *One-year infection control rates of a DAIR (debridement, antibiotics and implant retention) procedure after primary and prosthetic-joint-infection-related revision arthroplasty – a retrospective cohort study*. J. Bone Joint Infect., 6, 91–97, 2021.

Chapter 3:

van Dijk B, Nurmohamed, FRHA, Hooning van Duijvenbode JFF, Veltman ES, Rentenaar R J, Weinans, H, Vogely HC, van der Wal BCH. *A mean 4-year evaluation of infection control rates of hip and knee prosthetic joint infection-related revision arthroplasty: an observational study*. Acta Orthopaedica, 93, 652–657, 2021.

Chapter 4:

de Vor L*, van Dijk B*, van Kessel K, Kavanaugh JS, de Haas C, Aerts PC, Viveen MC, Boel EC, Fluit AC, Kwiecinski JM, Krijger GC, Ramakers RM, Beekman FJ, Dadachova E, Lam MGEH, Vogely HC, van der Wal BCH, van Strijp JA, Horswill AR, Weinans H, Rooijackers SH. *Human monoclonal antibodies against Staphylococcus aureus surface antigens recognize in vitro and in vivo biofilm*. Elife. 2022 Jan 6;11:e67301. *authors contributed equally

Chapter 5:

van Dijk B, Hooning van Duijvenbode JFF, de Vor L, Nurmohamed, FRHA, Lam MGEH, Poot AJ, Ramakers RM, Koustoulidou S, Beekman FJ, van Strijp J, Rooijackers SHM, Dadachova E, Vogely HC, Weinans H, van der Wal BCH. *Evaluating the Targeting of a Staphylococcus-aureus-Infected Implant with a Radiolabeled Antibody In Vivo*. Int J Mol Sci. 2023 Feb 22;24(5):4374

Chapter 6:

van Dijk B*, Lemans JVC*, Hoogendoorn RM, Dadachova E, de Klerk JMH, Vogely, HC, Weinans H, Lam MGEH, van der Wal BCH. (2020) *Treating Infections with Ionizing Radiation: A Historical Perspective and Emerging Techniques*. Antimicrob Resist Infect Control 9, 121 (2020). *authors contributed equally

Chapter 7:

Van Dijk B, Allen KJH, Helal M, Vogely HC, Lam MGEH, de Klerk JMH, Weinans H, van der Wal BCH, Dadachova E. *Radioimmunotherapy of methicillin-resistant Staphylococcus aureus in planktonic state and biofilms*. PLoS ONE 2020, 15, e0233086.

Chapter 8:

Van Dijk B, Oliveira S, Hooning van Duijvenbode JFF, Nurmohamed FRHA, Mashayekhi V, Beltrán Hernández I, van Strijp J, de Vor L, Aerts PC, Vogely HC, Weinans H, van der Wal BCH. *Photoimmuno-antimicrobial therapy for Staphylococcus aureus implant infection*, PLoS One. 2024 Mar 8;19(3):e0300069.



Other papers:

van Hengel, I, van Dijk B, Modaresifar K, Hooning van Duyvenbode JFF, Nurmohamed, FRHA, Leeftang MA, Fluit A, Fratila-Apachitei LE, Apachitei I, Weinans H, Zadpoor A. *In vivo prevention of implant-associated infections caused by antibiotic resistant bacteria through biofunctionalization of additively manufactured porous titanium*. J. Funct. Biomater. 2023, 14, 520.

Bourgonjen YP, Hooning van Duyvenbode JFF, van Dijk B, Nurmohamed FRHA, Veltman ES, Vogely CH, van der Wal BCH (2021) *Outcome Of Two-stage Revision Surgery After Hip And Knee Prosthetic Joint Infections In A Tertiary Referral Center: An Observational Study*, J Bone Jt Infect. 2021; 6(8): 379–387.

Helal M, Allen KJH, van Dijk B, Nosanchuk JD, Snead E, Dadachova E, *Radioimmunotherapy of Blastomycosis in a Mouse Model With a (1→3)-β-Glucans Targeting Antibody*. Front. Microbiol. 2020, 11, 147.

Hoekstra M, Veltman ES, Nurmohamed RFRH, van Dijk B, Rentenaar RJ, Vogely HC & van der Wal BCH. *Sonication Leads to Clinically Relevant Changes in Treatment of Periprosthetic Hip or Knee Joint Infection*. Journal of Bone and Joint Infection, 2020, 5(3), 128–132.





Acknowledgements



Acknowledgements

Het begon met een idee (dank je wel, Bart) dat uitgroeide tot een onderzoekslijn, dit proefschrift en verder. Onderzoek doen doe je samen en de volgende mensen wil ik in het bijzonder bedanken voor het direct en indirect tot stand brengen van dit proefschrift.

Bart van der Wal, dank voor je vertrouwen, je eerlijkheid, eeuwige optimisme en strakke deadlines. Hoewel dat laatste menig slaapgebrek heeft veroorzaakt, is dit boekje daardoor wel tijdig tot stand gekomen. Als mentor heb je mij veel geleerd, vooral jouw adviezen m.b.t. een tactische aanpak zal ik blijven toepassen.

Harrie Weinans, ik had maar een half woord nodig en je begreep wat ik bedoelde. Met wat sturing konden we snel starten met menig experiment. Dank voor de vrijheid en ruimte die ik kreeg om onderzoek te doen, het vertrouwen en de uitstekende begeleiding.

Charles Vogely, dank voor jouw kennis, klinische blik, ideeën, aanpassingen en toevoegingen. Jouw deur stond altijd open.

Ruben, van student tot arts tot Phd'er. Ik heb het allemaal mogen meemaken. Dank voor de fijne samenwerking, je harde werk, tomeloze inzet en natuurlijk het voortzetten van het onderzoek.

Paranimfen: Austin en Fred. Austin dank voor al die pagina's aan Engelse tekst die je door hebt genomen en hebt gecorrigeerd. Fred, dank voor al die uren in het lab, je punctualiteit, nauwkeurigheid en goede gesprekken.

Zonder de afdeling microbiologie was dit onderzoek niet mogelijk geweest, met in het bijzonder de begeleiding van Jos en Suzan en de samenwerking met Lisette. Daarnaast wil ik ook Carla en Piet bedanken voor het maken van alle antilichamen (en voor alle hulp).

Afdeling nucleaire geneeskunde, met in het bijzonder Marnix Lam, Gerard Krijger en Alex Poot. Mede dankzij jullie is dit proefschrift geworden tot wat het nu is.

Veel dank aan MiLabs (Ruud, Behdad, Sofia en Freek) voor jullie kennis en voor de mogelijkheid om altijd bij jullie binnen te lopen met een vraag. Ruud, misschien ben ik jou nog wel het meest dankbaar voor die keer dat je mijn ontsnapte radioactieve muis had teruggevonden in de bioluminescentiescanner.

Geachte leden van de leescommissie, Prof. dr. P.A. de Jong, Prof. dr. M.G.J. de Boer, Prof. dr. L.C. Heyligers, Prof. dr. J.A.J.W. Kluijtmans en Prof. dr. J.J. Verlaan, hartelijk dank voor het lezen en beoordelen van mijn proefschrift.

Bedankt alle collega's van Q, Hubrecht en de staf(gang): dank voor alle lunches, borrels, weekenden en natuurlijk bijna Nederlands kampioen Kubb geworden!

Thank you, Kate Dadachova, for the wonderful collaboration and the warm welcome from you and your team (in a very cold time of year) in Saskatoon.

Dank aan alle co-auteurs voor jullie bijdrage.

Ook wil ik mijn ouders, broers, familie, schoonfamilie en vrienden bedanken voor alle onvoorwaardelijke steun tijdens dit traject.



Mijn lieve vrouw Claire, nu dan de afsluiting van wat toch wel wat langer heeft geduurd dan gedacht, het proefschrift. Dank voor al je steun, advies en het doorlezen van zoveel pagina's. Wat hebben we toch prachtige herinneringen gemaakt en blijven maken, met als hoogtepunt het krijgen van onze Lily en Neil. Ik kijk uit naar de toekomst om deze samen met ons gezin te delen.





Curriculum Vitae

Bruce van Dijk was born on October 6th 1986 in Soest, the Netherlands. He began at Griffland College in Soest where he got his mavo diploma in 2003 following a diploma of intermediate laboratory education (MLO) in 2007. After multiple jobs he decided to become a medical doctor and passed the colloquium doctum to study



Medicine at the University of Utrecht. In 2012, Bruce obtained his Bachelor's degree, followed by the completion of his master's degree in 2016. Subsequently, he started as a full-time PhD candidate at the department of Orthopedics at the University Medical Center Utrecht. He undertook a research initiative with the objective of investigating alternative treatment modalities for *Staphylococcus Aureus* periprosthetic joint infections under supervision of prof. dr. ir. H. Weinans, prof. dr. S.H.M. Rooijackers, dr. B.C.H. van der Wal and dr. H.C. Vogely. In this process he went to Canada to collaborate with Prof. Dr. E. Dadachova and her team at the University of Saskatchewan in Saskatoon. The primary discoveries of this research focused on radio-immunotherapy and photo-immunotherapy for PJI are outlined in this thesis, have been showcased at various international scientific conferences and have been published in multiple peer-reviewed journals.